ISSN: 2008-2010; eISSN: 2008-322X

JAN 2022
VOLUME 17
NUMBER 1

JOURNAL OF OPHTHALMIC & VISION RESEARCH

Official Publication of the Ophthalmic Research Center
Affiliated to Shahid Beheshti University of Medical Sciences

Editorial

- Improving Intravitreal Drug Bioavailability

Original Articles

- Conjunctival Autograft versus AMT and Mini-SLET for Pterygium Excision
- Inferior Spear-Like Lens Opacities in KCN
- Quality of Life with Monofocal vs Multifocal IOLs
- Peak IOP Time during Water Drinking Test and Glaucoma Severity
- Virtual Reality VF Analyzer for Identification and Classification of Glaucoma
- Lamellar MH with or without Epimacular Proliferations
- ABCA4 Mutations in Stargardt Disease
- Biodistribution of Nanoparticles in an Animal Model of Retinoblastoma
- Development of a Spatio-temporal Contrast Sensitivity Test
- Prevalence and Burden of Refractive Errors in Iran

Review Articles

- PK versus DALK for KCN: A Systematic Review and Meta-analysis
- Management of NPDR without DME; a Paradigm Shift?
- Orbital Inflammation Caused by Aminobisphosphonates

Perspective

- HZO: Coming Back with Vengeance or Finding Its Nemesis?

Case Reports

- Choroidal Metastasis from Lung Cancer Responding to Osimertinib
- Coats'-like Response in Linear Scleroderma
- Peripapillary Circulation in Methanol Toxicity
- Tubercular Osteomyelitis Presenting as Cellulitis

Photo Essays

- Iatrogenic PVD Following Dilated Examination?
- Pigmentary Retinopathy and Chronic SRF in Angioid Streaks

Letter

- Toxic Intraocular Syndrome

Erratum

- Erratum to Side Effects of Brolucizumab

KnowledgeE
enriching | engaging | empowering

Print ISSN 2008-2010;
E-ISSN 2008-322X

JOURNAL OF OPHTHALMIC AND VISION RESEARCH

Official Publication of the Ophthalmic Research Center

Print ISSN 2008-2010;
E-ISSN 2008-322X

JOURNAL OF
OPHTHALMIC AND VISION RESEARCH

Official Publication of the Ophthalmic Research Center

General Information

The journal

The Journal of Ophthalmic and Vision Research is a peer-reviewed, open-access journal published quarterly on behalf of the Ophthalmic Research Center, Shahid Beheshti University of Medical Sciences with the mission to disseminate information, viewpoints and questions about eye diseases, research, clinical and laboratory science, and education. The journal aims to advance the science, technology, ethics and art of ophthalmology through research and education worldwide. The scope of the journal is intended to include not only clinical ophthalmology, but related disciplines in basic sciences that contribute to the knowledge and science of vision.

Abstracting and indexing information

The journal is registered with the following abstracting partners:
Baidu Scholar, CNKI (China National Knowledge Infrastructure), EBSCO Publishing's Electronic Databases, Exlibris - Primo Central, Google Scholar, Hinari, Infotrieve, National Science Library, ProQuest, TdNet.
The journal is indexed with, or included in, the following: DOAJ, Emerging Sources Citation Index, Index Copernicus, Index Medicus for the Eastern Mediterranean Region (IMEMR), PubMed Central, Scimago Journal Ranking, SCOPUS, Web of Science.

Information for Authors

There are no page charges for submissions to the journal. Please check https://knepublishing.com/index.php/JOVR/authorguidelines for details. All manuscripts must be submitted online at https://knepublishing.com/index.php/JOVR/about/submissions

Advertising policies

The journal accepts display and classified advertising. Frequency discounts and special positions are available. Inquiries about advertising should be sent to Knowledge E. The journal reserves the right to reject any advertisement considered unsuitable according to the set policies of the journal. The appearance of advertising or product information in the various sections in the journal does not constitute an endorsement or approval by the journal and/or its publisher of the quality or value of the said product or of claims made for it by its manufacturer.

Copyright

Permissions

For information on how to request permissions to reproduce articles/information from this journal, please visit https://knepublishing.com/index.php/JOVR/authorguidelines

Disclaimer

The information and opinions presented in the Journal reflect the views of the authors and not of the Journal or its Editorial Board or the Society of the Publisher. Publication does not constitute endorsement by the journal. Neither the Journal of Ophthalmic and Vision Research nor its publishers nor anyone else involved in creating, producing or delivering the Journal of Ophthalmic and Vision Research or the materials contained therein, assumes any liability or responsibility for the accuracy, completeness, or usefulness of any information provided in the Journal of Ophthalmic and Vision Research, nor shall they be liable for any direct, indirect, incidental, special, consequential or punitive damages arising out of the use of the Journal of Ophthalmic and Vision Research. The Journal of Ophthalmic and Vision Research, nor its publishers, nor any other party involved in the preparation of material contained in the Journal of Ophthalmic and Vision Research represents or warrants that the information contained herein is in every respect accurate or complete, and they are not responsible for any errors or omissions or for the results obtained from the use of such material. Readers are encouraged to confirm the information contained herein with other sources.

Addresses

Editorial Office
Journal of Ophthalmic and Vision Research
Ophthalmic Research Center, #23, Paidarfard St., Boostan 9 St., Pasdaran Ave., Tehran, Iran
Postal code: 1666673111
Phone: +98 21 2277 0957
Fax: +98 21 2259 0607
E-mail: labbafi@gmail.com & jovrjournal@gmail.com
Website: https://knepublishing.com/index.php/JOVR

Published by

Knowledge E Office 4401–02 ,4404
Jumeirah Bay X2 Tower
Jumeirah Lakes Towers (JLT)
P.O. Box 488239
Dubai, UAE
Website: www.knowledgee.com

Print ISSN 2008-2010;
E-ISSN 2008-322X

JOURNAL OF
OPHTHALMIC AND VISION RESEARCH

Official Publication of the Ophthalmic Research Center

VOLUME 17, ISSUE 1, JANUARY 2022

Contents

EDITORIAL

Thiolated Chitosan-carboxymethyl Dextran Nanoparticles: Improving Intravitreal Drug Bioavailability for Retinoblastoma
Dalvin LA 1

ORIGINAL ARTICLES

Conjunctival Autograft versus Combined Amniotic Membrane and Mini-Simple Limbal Epithelial Transplant for Primary Pterygium Excision
Jha A, AbhaySimba. 4

Inferior Spear-like Lens Opacity as a Sign of Keratoconus
Salouti R, Khosravi A, Fardaei M, Zamani M, Nejabat M, Ghoreyshi M, Yazdanpanah M, Salouti S, Nowroozzadeh MH 12

Vision-related Quality of Life after Bilateral Implantation of Monofocal and Multifocal Intraocular Lenses
Bamdad S, Razavizadegan SA, Farvardin M, Mohaghegh S 19

Peak Intraocular Pressure Time during Water Drinking Test and Its Relationship with Glaucoma Severity
Susanna CN, Susanna BN, Susanna R, De Moraes CG 27

Diagnostic Performance of the PalmScan VF2000 Virtual Reality Visual Field Analyzer for Identification and Classification of Glaucoma
Shetty V, Sankhe P, Haldipurkar SS, Haldipurkar T, Dhamankar R, Kashelkar P, Shah D, Mhatre P, Setia S 33

Structural and Functional Outcomes of Surgery for Lamellar Macular Holes with or without Epimacular Proliferations
Venkatesh R, Pereira A, Jain K, Yadav NK 43

Mutation Screening of Six Exons of *ABCA4* in Iranian Stargardt Disease Patients
Darbari E, Ahmadieh H, Daftarian N, Kanavi MR, Suri F, Sabbaghi H, Elahi E 51

Biodistribution of CY5-labeled Thiolated and Methylated Chitosan-Carboxymethyl Dextran Nanoparticles in an Animal Model of Retinoblastoma
Delrish E, Ghassemi F, Jabbarvand M, Lashay A, Atyabi F, Soleimani M, Dinarvand R 59

Development of a Spatio-temporal Contrast Sensitivity Test for Clinical Use
Costa MF, Henriques LD, Pinho OC 70

Prevalence and Burden of Refractive Errors at National and Sub-national Levels in Iran
Mohammadi SF, Farzadfar F, Pour PM, Ashrafi E, Lashay A, Mohajer B, Lari MA 78

Contents Contd...

REVIEW ARTICLES

Penetrating Keratoplasty versus Deep Anterior Lamellar Keratoplasty for Keratoconus: A Systematic Review and Meta-analysis
Shams M, Sharifi A, Akbari Z, Maghsoudlou A, Tajali MR 89

Update on Management of Non-proliferative Diabetic Retinopathy without Diabetic Macular Edema; Is There a Paradigm Shift?
Arabi A, Tadayoni R, Ahmadieh H, Shahraki T, Nikkhah H 108

Orbital Inflammation Caused by Aminobisphosphonates
Barlatay JG, Boza CP, Gauna GVH, Premoli JE 118

PERSPECTIVE

Herpes Zoster Ophthalmicus: A Devastating Disease Coming Back with Vengeance or Finding Its Nemesis?
Torabi R, Harris A, Siesky B, Zukerman R, Oddone F, Mathew S, Januleviciene I, Verticchio Vercellin AC 123

CASE REPORTS

Treatment of Choroidal Metastasis from Epidermal Growth Factor Mutant Non-Small Cell Lung Cancer with First-line Osimertinib Therapy
Vu AN, Mehta UV, Israelsen P, Ignatius Ou AH, Browne AW 130

Coats'-like Response Associated with Linear Scleroderma
Behboudi H, Zayeni H, Haji-Abbasi A, Moravvej Z, Azaripour E, Alizadeh Y, Soltani-Moghadam R 135

Peripapillary Capillary Network in Methanol Induced Optic Neuropathy
Hassanpour K, Mohammadi N, Sabbaghi H, Amirabdi A, Pakravan M 140

Tubercular Osteomyelitis of the Orbit Presenting as Periorbital Cellulitis
Bhattacharya S, Raina UK, Gupta SK, Mishra M, Saini V, Kumar B 146

PHOTO ESSAYS

Iatrogenic PVD Following Dilated Fundus Examination: A New Diagnosis or Fluke?
Commiskey PW, Kalra G, Chhablani J 150

Pigmentary Retinopathy and Chronic Subretinal Fluid Associated with Pseudoxanthoma Elasticum and Angioid Streaks
Starr and Bakri 152

LETTER

Toxic Intraocular Syndrome
Amigó A, Martinez-Sorribes P 155

ERRATUM

Erratum: Side Effects of Brolucizumab
..... 157

Editorial

Thiolated Chitosan-carboxymethyl Dextran Nanoparticles: Improving Intravitreal Drug Bioavailability for Retinoblastoma

Lauren A Dalvin, MD

Department of Ophthalmology, Mayo Clinic, Rochester, Minnesota, USA

ORCID:
Lauren A Dalvin: http://orcid.org/0000-0001-9710-4284

J Ophthalmic Vis Res 2022; 17 (1): 1–3

In the current issue of *Journal of Ophthalmic and Vision Research* (*JOVR*), Delrish et al discuss the use of modified nanoparticles for intravitreal drug delivery in a rat model of retinoblastoma.[1] Retinoblastoma is the most common intraocular malignancy of childhood, with an incidence of 11.8 cases per million children aged 0–4 years in the US and with recent increase in incidence reported in Europe.[2, 3] While developing countries often face more advanced disease and worse survival prognosis, retinoblastoma is considered curable, and mortality is rare in well-developed nations.[4] Although the primary goal of retinoblastoma treatment is to protect the child's life, secondary and tertiary goals of globe salvage and visual acuity preservation have become more achievable with treatment advances, particularly the combination of intra-arterial and intravitreal chemotherapy. With current standard of care therapy, globe salvage can be achieved even for the most advanced group E eyes in about 50% of cases.[5]

Delrish et al describe what may be the next frontier in intravitreal chemotherapy delivery, with improved drug bioavailability using thiolated chitosan-carboxymethyl dextran nanoparticles (CMD-TCs-NPs). Although intravitreal injection offers direct drug access to the vitreous cavity and retina, it can take several hours for drug to diffuse across the entire vitreous cavity.[6, 7] Moreover, *in vitro* experiments show that drug dispersion in the vitreous cavity is driven by advective mass transport rather than molecular diffusion, relying on natural saccadic movements to distribute the drug.[8, 9] Drug distribution may be especially challenging in more formed pediatric vitreous, and speed of dispersion could be important to achieve tumor control in the setting of drugs such as melphalan, which have a short half-life.[10] Thus, improved bioavailability of intravitreal chemotherapy agents could decrease injection burden and retinal toxicity, improve overall tumor control rates, and improve globe salvage for retinoblastoma with vitreous seeding.

Chitosan is a semi-synthetic cationic polysaccharide produced by partial or complete deacetylation of the naturally occurring polymer chitin, which can be harvested from crustacean shells or fungal cell walls.[11, 12] Chitosan is highly biocompatible, nontoxic, and mucoadhesive; has favorable enzymatic biodegradability, low immunogenicity, and inherent antibacterial properties; and can disrupt epithelial tight junctions to enhance permeability.[13] Given these favorable properties, combined with easy accessibility, chitosan has become a popular candidate for pharmaceutical development, and the US Food and Drug Administration has already approved several chitosan-containing products.[13]

Mucoadhesive polymers like chitosan contain numerous charged molecular groups that can form non-covalent bonds with mucin, allowing bioadhesion to mucosal surfaces.[13] Numerous factors can influence mucoadhesion, including pH, concentration, ionic strength, temperature, incubation time, surface charges, molecular weight, degree of deacetylation, and hydrophilicity, among others.[13] Chitosan, in particular, has pH-dependent mucoadhesion, and certain modifications have been employed to improve the polymer's mucoadhesive properties at physiologic pH relevant to ophthalmic drug delivery. Trimethyl chitosan has been extensively studied and has

strong mucoadhesive properties due to its high cationic charge. Thiolated chitosan derivatives have also been studied, which have free thiol groups to form covalent bonds with cysteine-rich subdomains of mucus glycoproteins.[13] Compared to unmodified chitosan, thiolated chitosan has several advantages, including 6- to 100-fold improved mucoadhesion, 1.6- to 3-fold enhanced permeability, and *in situ* gelling properties at physiologic pH.[14, 15] Together, these properties improve drug residence time and increase bioavailability. Thiolated derivatives require sulfhydryl groups to react, limiting use to cysteine-rich tissues,[13] but secreted protein acidic and rich in cysteine (SPARC) has demonstrated localization to Muller and ganglion cells in the retina, making the retina a reasonable target tissue.[16]

In ophthalmology, initial interests aligned with the use of chitosan to improve bioavailability of topically administered medications, but there is a growing body of literature on possible intravitreal applications.[11] Previous studies have demonstrated that nanoparticle surface properties are a key factor determining distribution in the retina and vitreous following intravitreal injection, and although glycosylated chitosan polymers maintained a positive charge and could reach the retina, these particles were not able to penetrate the internal limiting membrane.[17] Thiolated derivatives, on the other hand, may have improved penetration due to their interaction with cysteine-rich SPARC localized to Muller cells. In this issue of *JOVR*, Delrish et al specifically compare the biodistribution of thiolated versus methylated chitosan-carboxymethyl dextran nanoparticles (CMD-TCs-NPs vs CMD-TMC-NPs) following an intravitreal injection in a rat model of retinoblastoma.[1] The authors found improved uptake of CMD-TCs-NPs in retinoblastoma cell culture, and in the rat model, 24 hr after injection; the CMD-TCs-NPs demonstrated diffusion throughout the vitreous cavity and retinal penetration, while the CMD-TMC-NPs were immobilized in the vitreous.[1] The authors attributed these differences to improved bioadhesion of thiolated chitosan and prohibitive effects on vitreous diffusion of the greater positive charge of methylated chitosan (zeta potential +29mV) compared with the thiolated counterparts (+11mV).[1]

Although this was a small study with 10 rats, Delrish et al concluded that surface charge is a key factor determining vitreous diffusion and retinal penetration for chitosan-derived intraocular drug-delivery mechanisms, and they propose future use of thiolated chitosan derivatives for intravitreal chemotherapy delivery aimed at retinoblastoma treatment.[1] Of relevance to the article at hand, Delrish et al recently reported improved efficacy and tumor control using thiolated chitosan nanoparticles containing topotecan compared to free topotecan in a rat model of retinoblastoma.[18] These early studies indicate feasibility and potential benefit of the application of thiolated chitosan derivatives in retinoblastoma treatment. Although further study is required to investigate the safety and reproducibility prior to human trials, there are potential exciting applications of these biocompatible nanoparticles to improve treatment outcomes for retinoblastoma in the future, and this technology could also be applied to a wide variety of other retinal diseases which have traditionally been managed with intravitreal injections.

Financial Support and Sponsorship

This publication was supported by Grant No. P30 CA015083 from the National Cancer Institute. Its contents are solely the responsibility of the authors and do not necessarily represent the official view of the National Institutes of Health.

Conflicts of Interest

There are no conflicts of interest.

REFERENCES

1. Delrish E, Ghasemi F, Jabbarvand M, Lashay A, Atyabi F, Soleimani M, et al. Comparative biodistribution properties of CY5-labeled thiolated and methylated chitosan-carboxymethyl dextran nanoparticles intended for designing ideal drug delivery system for retinoblastoma treatment. *J Ophthalmic Vis Res* 2022 .....
2. Broaddus E, Topham A, Singh AD. Incidence of retinoblastoma in the USA: 1975–2004. *Br J Ophthalmol* 2009;93:21–23.
3. Stacey AW, Bowman R, Foster A, Kivelä TT, Munier FL, Cassoux N, et al. Incidence of retinoblastoma has increased: results from 40 European countries. *Ophthalmology* 2021;128:1369–1371.
4. Fabian ID, Abdallah E, Abdullahi SU, Abdulqader RA, Boubacar SA, Ademola-Popoola DS, et al. Global retinoblastoma presentation and analysis by national income level. *JAMA Oncol* 2020;6:685–695.
5. Dalvin LA, Kumari M, Essuman VA, Shipa SS, Ancona-Lezama D, Lucio-Alvarez JA, et al. Primary intra-arterial

chemotherapy for retinoblastoma in the intravitreal chemotherapy era: five years of experience. *Ocul Oncol Pathol* 2019;5:139–146.

6. Agrahari V, Mandal A, Agrahari V, Trinh HM, Joseph M, Ray A, et al. A comprehensive insight on ocular pharmacokinetics. *Drug Deliv Transl Res* 2016;6:735–754.
7. Willekens K, Reyns G, Diricx M, Vanhove M, Noppen B, Coudyzer W, et al. Intravitreally injected fluid dispersion: importance of injection technique. *Invest Ophthalmol Vis Sci* 2017;58:1434–1441.
8. Bonfiglio A, Repetto R, Siggers JH, Stocchino A. Investigation of the motion of a viscous fluid in the vitreous cavity induced by eye rotations and implications for drug delivery. *Phys Med Biol* 2013;58:1969–1982.
9. Modareszadeh A, Abouali O, Ghaffarieh A, Ahmadi G. Saccade movements effect on the intravitreal drug delivery in vitreous substitutes: a numerical study. *Biomech Model Mechanobiol* 2013;12:281–290.
10. Buitrago E, Winter U, Williams G, Asprea M, Chantada G, Schaiquevich P. Pharmacokinetics of melphalan after intravitreal injection in a rabbit model. *J Ocul Pharmacol Ther* 2016;32:230–235.
11. Ilochonwu BC, Urtti A, Hennink WE, Vermonden T. Intravitreal hydrogels for sustained release of therapeutic proteins. *J Control Release* 2020;326:419–441.
12. Mohammed MA, Syeda JTM, Wasan KM, Wasan EK. An overview of chitosan nanoparticles and its application in non-parenteral drug delivery. *Pharmaceutics* 2017;9:53.
13. Zamboulis A, Nanaki S, Michailidou G, Koumentakou I, Lazaridou M, Ainali NM, et al. Chitosan and its derivatives for ocular delivery formulations: recent advances and developments. *Polymers* 2020;12:1519.
14. Liu D, Li J, Pan H, He F, Liu Z, Wu Q, et al. Potential advantages of a novel chitosan-N-acetylcysteine surface modified nanostructured lipid carrier on the performance of ophthalmic delivery of curcumin. *Sci Rep* 2016;6:28796.
15. Bernkop-Schnürch A, Hornof M, Guggi D. Thiolated chitosans. *Eur J Pharm Biopharm* 2004;57:9–17.
16. Gilbert RE, Cox AJ, Kelly DJ, Wilkinson-Berka JL, Sage EH, Jerums G, et al. Localization of secreted protein acidic and rich in cysteine (SPARC) expression in the rat eye. *Connect Tissue Res* 1999;40:295–303.
17. Koo H, Moon H, Han H, Na JH, Huh MS, Park JH, et al. The movement of self-assembled amphiphilic polymeric nanoparticles in the vitreous and retina after intravitreal injection. *Biomaterials* 2012;33:3485–3493.
18. Delrish E, Jabbarvand M, Ghassemi F, Amoli FA, Atyabi F, Lashay A, et al. Efficacy of topotecan nanoparticles for intravitreal chemotherapy of retinoblastoma. *Exp Eye Res* 2021;204:108423.

Correspondence to:

Lauren A Dalvin, MD. Department of Ophthalmology, Mayo Clinic, 200 1st St. SW, Rochester, MN 55905, USA. Email: dalvin.lauren@mayo.edu

Received: 28-08-2021 Accepted: 12-11-2021

Access this article online

Website: https://knepublishing.com/index.php/JOVR

DOI: 10.18502/jovr.v17i1.10163

How to cite this article: Dalvin LA. Thiolated Chitosan-carboxymethyl Dextran Nanoparticles: Improving Intravitreal Drug Bioavailability for Retinoblastoma. J Ophthalmic Vis Res 2022;17:1–3.

Original Article

Conjunctival Autograft versus Combined Amniotic Membrane and Mini-Simple Limbal Epithelial Transplant for Primary Pterygium Excision

Ashok Jha[1], MS; Abhay Simba[2], MS

[1]*Department of Ophthalmology, Military Hospital Gaya, Gaya, India*
[2]*Department of Ophthalmology, Anugrah Narayan Medical College, Gaya, India*

ORCID:
Ashok Jha: https://orcid.org/0000-0001-7072-4168

Abstract

Purpose: To compare outcomes of conjunctival autograft (CAG) and combined amniotic membrane with mini-simple limbal epithelial transplant (mini-SLET) after primary pterygium excision.

Methods: All consenting adults with primary pterygium were included in this study. After pterygium excision, patients were randomized to receive either CAG or mini-SLET and both grafts were held in place with fibrin glue. The patients were followed-up at days 1, 3, 7, 14, and 30 and subsequently at the third, sixth, and ninth months. The recurrence rate was considered as the primary outcome measure whereas the operating time, postoperative symptoms, and surgical complications were considered the secondary outcome measures.

Results: The study comprised of 264 eyes of 264 patients, of which 233 (88%) completed the nine months of follow-up. Of these, 118 (51%) received CAG and 115 (49%) received mini-SLET. The groups were comparable at baseline. Recurrence of pterygium was seen in two (1.6%) eyes in the CAG group and three (2.6%) eyes in the mini-SLET group ($P = 0.68$). Operative time for mini-SLET (20.33 ± 1.28 min) was significantly higher than that for CAG (12.01 ± 1.26 min) ($P < 0.001$). Graft displacement was observed in one case in group II ($P = 0.999$). The Lim Bon Siong (foreign body sensation, lacrimation, pain, and irritation) score in the CAG group was statistically significant for all four symptoms at days 1 and 3; however, at day 7, foreign body sensation, pain, and irritation scores were significantly higher for the CAG group.

Conclusion: In this study, the overall recurrence rate was very low and comparable between mini-SLET and the established technique of CAG after performing the primary pterygium excision. Despite a longer surgical time, mini-SLET appears to be a viable option for the management of primary pterygium.

Keywords: Conjunctival Autograft (CAG); Mini-simple Limbal Epithelial Transplant (mini-SLET); Pterygium

J Ophthalmic Vis Res 2022; 17 (1): 4–11

INTRODUCTION

Pterygium is a benign, fleshy triangular ocular lesion that can cross the limbus and encroach on the cornea, with subsequent visual impairment.[1] It most often involves nasal conjunctiva and may necessitate surgical removal if associated with visual impairment, astigmatic refractive errors, or cosmetic concerns. Postoperative recurrence is not uncommon, hence surgical excision has been coupled with various adjunctive measures like beta irradiation[2] and anti-metabolites such as Mitomycin C.[3, 4] Although these methods are relatively safe, complications such as secondary bacterial infection, punctate keratitis, scleral melting, and raised intraocular pressure (IOP) have been reported. To prevent these side effects and achieve superior results in terms of graft stability and potentially lower recurrence rates, human amniotic membrane grafting (AMG)[5] and conjunctival autografting (CAG)[6] were introduced to cover the bare sclera after pterygium excision. Of these, ipsilateral CAG is now the surgical procedure of choice, owing to the ease of the procedure and the difficulties in procuring AMG. Additionally, the efficacy and low recurrence rate of the CAG method has been corroborated by many authors.[6–9]

Tissue adhesives like fibrin glue[10] which are used to secure the grafts in place after pterygium excision present many benefits such as lesser operating time, reduced discomfort during the postoperative period, and reduced complications associated with sutures.[11, 12] Alternatively, the CAG can be secured using autologous in situ blood coagulum.[13–15]

More recently, Hernández-Bogantes et al have described a technique of using a combination of AMG and small pieces of autologous limbal epithelial cells (mini-simple limbal epithelial transplant [SLET])[16] to cover the bare sclera using tissue adhesive. Authors reported excellent outcomes with this new technique, albeit in only 10 eyes. Given these encouraging results, we believe that this may be an alternative technique to CAG for surgical management of pterygium. At present there are very few head to head studies comparing outcomes of the well-established CAG with the relatively new mini-SLET after primary pterygium excision. Hence, this study was performed to assess the efficacy and recurrence rate after the two aforementioned procedures.

METHODS

This prospective, randomized, interventional study was duly approved by the local Institutional Ethics Committee (Ethical clearance certificate no. 29/MH/2015 dated Aug 11, 2015). This study was conducted in accordance with the tenets of the Declaration of Helsinki. Patient enrollment occurred between August 2015 and January 2019.

All consecutive adult patients visiting the outpatient department of our hospital with primary pterygium and requiring surgical excision for cosmesis, intense foreign body sensation, and reduced vision either due to induced astigmatism or encroachment on the visual axis were invited to participate in the study. Patients who agreed to follow-up for nine months after surgery were recruited after their informed consent. Patients with other ocular surface disorders, hypersensitivity to blood constituents, and seropositivity to Hepatitis B, Hepatitis C, and HIV were excluded from the study.

Sample size calculation was based on presumed differences in the recurrence rates of pterygium in the two groups. Given 1:1 randomization, 90% power, and a precision error of 5% to detect a difference of 10% or more in proportion of patients experiencing recurrent pterygium, a required minimum sample size of 230 eyes (115 in each group) was obtained. To account for a 15% loss to follow-up, we recruited 264 patients for the study.

Using simple randomization, the patients were divided into two groups: one received

Correspondence to:

Ashok Jha, MS. Department of Ophthalmology, Military Hospital Gaya, Bihar 823005, India.
E-mail: ashokjha1025@gmail.com

Received 04-05-2020; Accepted 12-02-2021

Access this article online

Website: https://knepublishing.com/index.php/JOVR

DOI: 10.18502/jovr.v17i1.10164

How to cite this article: Jha A, AbhaySimba. Conjunctival Autograft versus Combined Amniotic Membrane and Mini-Simple Limbal Epithelial Transplant for Primary Pterygium Excision. J Ophthalmic Vis Res 2022;17:4–11.

the CAG and the other received the mini-SLET treatment. This simple randomization utilized serially generated computer codes along with allocation concealment. A parallel allocation strategy was used in a 1:1 allocation. The evaluating ophthalmologist (AS) was masked to the type of graft used. The operating surgeon (AJ) and patients were masked to the procedural details and the type of graft used. The sealed envelopes for the type of graft were opened just before the completion of the pterygium excision. The graft status was masked in all cases at every follow-up visit during the clinical testing.

Thorough medical and ocular history and demographic details such as age and gender of the participants were obtained. Thereafter, a comprehensive examination of the eyes included best-corrected visual acuity assessment, slit-lamp evaluation of the pterygium, and the anterior and posterior segment evaluation using a +90D lens. Pterygia were divided into three grades based on the classification proposed by Tan and coworkers:[17] T1 = unobscured and distinguished episcleral vessels underneath the body of the pterygium; T2 = partially obscured or indistinct episcleral vessels; and T3 = completely obscured episcleral vessels by fibrovascular tissue. Serial clinical photographs of patients were taken preoperatively, per-operatively, and postoperatively on days 1 and 30 in addition to the sixth and ninth months for both cohorts [Figure 1].

Peribulbar anesthesia (2% lidocaine hydrochloride) was used for all of the surgeries, which were performed by a single surgeon (AJ). Westcott scissors were used to draw horizontal incisions along the superior and inferior borders of the body of pterygium. Subsequently, using Moorefield's conjunctival forceps, the pterygium was reflected toward the limbus making another peripheral incision parallel to the limbus. The remaining fibrovascular tissues underneath the bulbar conjunctiva were dissected and excised to the maximum possible extent.

The bare sclera was then measured by a caliper. In the CAG group, a near tenon-free CAG, which was 1 mm larger in area than the bare sclera was harvested from the supero-temporal region. This thin graft was stuck to the exposed sclera using fibrin glue (Baxter, TISSEEL) with correct orientation. The angled flat part of two iris spatulas was maneuvered horizontally and vertically utilized to expand the graft to its maximum possible size besides removing excess glue from the sclera bed.

In the mini-SLET cohort, after an initial one clock hour (10–11 o'clock for right eye and 1–2 o'clock for left eye) peritomy performed with Westcott scissors, a limbal tissue 2 × 2 mm in size was excised with the help of a crescent blade. Using Vannas scissors, this strip was then sliced into six to eight pieces under increased magnification. These pieces were then affixed on the inlay AMG closer to the limbus using fibrin glue. Thereafter, an AMG overlay was used to maintain graft pieces in the exact position. Freeze-dried AMG (Amnio-care, Biocover Labs, India), available in 3 × 3 cm size was used for the study. A bandage contact lens was placed on the cornea at the end of the procedure.

Using a patented fibrinotherm device, the fibrin glue (TISSEEL VH, Baxter AG) used in the above described procedures was prepared by reconstituting thrombin and freeze-dried protein concentrate in calcium chloride and fibrinolysis inhibitor solutions, respectively. Both thrombin and fibrin were suctioned into separate syringes, which were mounted with a 27G canula. To use the glue, almost an equal number of drops of fibrin and thrombin were utilized for both the cohorts. Total operating time was noted for both the groups. Mitomycin C was not used in either group.

In the first week of the postoperative period, patients received 1% prednisolone acetate and 0.5% moxifloxacin eye drops every 4 and 6 hr, respectively, followed by tapering dosages of topical steroid, which continued for one month. The patients were reviewed on postoperative days 1, 3, 7, 14, and subsequently at months 1, 3, 6, and 9.

While early postoperative visits involved the assessment of graft positioning, later visits included reporting of the recurrence and disintegration of limbal pieces on the slit lamp by a masked investigator. Recurrence was considered the primary outcome measure, which was defined as any fibrovascular growth that occurred at the surgical site at any time during the follow-up period. Operating time and surgical complications were considered the secondary outcome measures. Four symptoms (foreign body sensation, epiphora [watering], pain and irritation) were evaluated, based on a 5-point scale adapted from Lim Bon Siong R et al. The patients were asked to complete a questionnaire in which 0 meant no pain, 1 meant presence of easily tolerable pain, 2 meant pain

causing some discomfort, 3 meant presence of pain partially interfering with sleep or usual activity, and 4 meant pain completely interfering with usual activity or sleep.

Statistical Analysis

The statistical analysis was performed using SPSS (Statistical Package for the Social Sciences) software version 20. A *P*-value < 0.05 was considered statistically significant. Comparison of continuous variables such as age, preoperative BCVA, operative time, and the dimensions of graft between the two groups was done using the parametric unpaired *t*-test. Pearson's Chi-square test or the Fisher's exact test were used for comparative analysis of categorical variables like gender, laterality, grades of pterygium, and indication of surgery between the two groups.

RESULTS

A total of 264 consecutive eyes of 264 patients were enrolled in the study, of which 31 eyes (15 in CAG and 16 in mini-SLET groups) were ruled out due to inadequate follow-up. Hence, data from 233 eyes (*n* = 118 CAG and 115 in mini-SLET) that finished nine months of follow-up was included in the final analysis. Table 1 depicts the baseline characteristics of CAG and mini-SLET groups. Baseline characteristics were statistically insignificant between the two groups. The comparative analysis of graft size and the operating time has been summarized in Table 2. The mean operative time for mini-SLET group (20.33 ± 1.28 min) was significantly higher (*P* < 0.001) than the CAG group (12.01 ± 1.26 min). Four postoperative symptoms have been compared in Table 3 using the nonparametric Mann–Whitney U-test. Both groups exhibited foreign body sensation until day 7. A statistically significant difference in the median score of foreign body sensation was noted on day 1 (*P* < 0.001), day 3 (*P* < 0.001), and day 7 (*P* < 0.001) between the CAG and mini-SLET groups. This symptom improved significantly between days 1 and 7 in both group I (*P* < 0.001) and group II (*P* < 0.001) as demonstrated by the Wilcoxon signed-rank test. Both groups showed persistence of epiphora (watering) till day 7. A statistically significant difference in the median score of epiphora (watering) was observed on day 1 (*P* < 0.001) and day 3 (*P* < 0.001) between the two groups. It was noted that this symptom, too, showed significant improvement at days 1 and 7 in both group I (*P* < 0.001) and group II (*P* < 0.001). Pain persisted until days 7 and 3 in groups I and II, respectively. Both the study and control groups exhibited significant difference in the median score of pain on day 1 (*P* < 0.001), day 3 (*P* <0.001), and day 7 (*P* = 0.008). Despite a median score of 6 and 0, the significant difference at days 1 and day 7, respectively, is ascribed to the variance in the distribution of pain score between the two groups. A significant improvement in this symptom was observed between day 1 and day 7 in both the groups (*P* < 0.001). Irritation in the operated eye persisted until day 7 in both the groups. The median score for irritation was noted to be statistically significant on day 1 (*P* < 0.001), day 3 (*P* < 0.001), and day 7 (*P* < 0.001) between the two groups. Both the study and control groups showed significant improvement in this symptom between day 1 and day 7 (*P* < 0.001), and between day 1 and day 14, respectively.

Recurrence was observed at the first, third, sixth, and ninth months. Two (1.6%) eyes in the CAG group exhibited recurrence whereas three (2.6%) had recurrence in mini-SLET group (*P* = 0.681). Two patients in the CAG group and one in the mini-SLET group showed recurrence within three months. Recurrence in the remaining two patients in the mini-SLET group was observed between the third and sixth months. Two cases in each group underwent revision surgery whereas one patient in the mini-SLET group refused surgery. Within the six months follow-up period, no recurrence was observed in any of the patients who underwent revision surgery.

One eye (0.87%) in the mini-SLET group exhibited AMG displacement on the first postoperative day, which was repositioned on the very same day. None of the eyes in the study experienced any other adverse effects related to the grafts.

DISCUSSION

In this randomized study, we found a very low rate of recurrence in eyes that received CAG versus mini-SLET, with statistically insignificant difference in the recurrence rates between the two groups. The operating time was significantly higher in

Table 1. Comparison of baseline characteristics between the CAG Group and the mini-SLET group

Characteristics	CAG group (*n* = 118)	Mini-SLET group (*n* = 115)	*P*-value
Age (yr)	53.81 ± 14.28 (range = 22–80)	52.38 ± 14.62 (range = 26–78)	0.446*
Sex	F = 49.15% (*n* = 58)	F = 44.35% (*n* = 51)	0.437†
	M = 50.85% (*n* = 60)	M = 55.65% (*n* = 64)	
Laterality	Right eye = 57.6% (*n* = 68)	Right eye = 53.9% (*n* = 62)	0.696†
	Left eye = 42.4% (*n* = 50)	Left eye = 46.1% (*n* = 53)	
Grade			
I	13.5% (*n* = 16)	12.2% (*n* = 14)	0.920†
II	61.9% (*n* = 73)	61.7% (*n* = 71)	
III	24.6% (*n* = 29)	26.1% (*n* = 30)	
Occupation	Outdoor = 61.1% (*n* = 72)	Outdoor = 67.8% (*n* = 78)	0.282†
	Indoor = 38.9% (*n* = 46)	Indoor = 32.2% (*n* = 37)	
Indications for surgery			0.895†
Cosmesis	40.7% (*n* = 48)	40% (*n* = 46)	
Foreign body sensation	29.7% (*n* = 35)	26.1% (*n* = 30)	
Reduced VA due to Astigmatism	16.1% (*n* = 19)	22.6% (*n* = 26)	
Threatening Visual Axis	13.5% (*n* = 16)	11.3% (*n* = 13)	
Preoperative BCVA (LogMar)	0.46 ± 0.38 (range = 0–1.46)	0.43 ± 0.26 (range = 0.16–1.18)	0.476*

*Unpaired *t*-test; †χ^2test

Table 2. Comparison of the size of the graft and operative time between the CAG group and mini-SLET group

Measures	CAG group (*n* = 118)	Mini-SLET group (*n* = 115)	*P*-value
Dimensions of the graft (mm)			
Horizontal	5.10 ± 0.41 (range = 4.2–6.5)	5.14 ± 0.45 (range = 4.5–6.8)	0.448*
Vertical	6 ± 0.32 (range = 5.5–8.0)	6.09 ± 0.54 (range = 5.5–8.0)	0.097*
Operative time (min)	12.01 ± 1.26 (range = 10.1–14.0)	20.33 ± 1.28 (range = 18–22)	<0.001*

*Unpaired *t*-test

the mini-SLET group, however, none of the eyes experienced intra- or postoperative complications attributable to the surgery.

Pterygium is postulated to occur due to localized dysfunction of nasal limbal stem cells consequential to exposure to UVB light.[18] This theory forms the basis of the incorporation of limbal stem cells in the surgical treatment of pterygium. Of all the techniques described in literature,[3–6] CAG modality has been found to be associated with the lowest recurrence rate.[7, 8, 10] The CAG can be attached to the bare sclera by sutures, fibrin glue, or autologous in situ blood coagulum. Amongst the three techniques of fixing CAG, fibrin glue definitely scores over others with the least operative time.[19]

Use of SLET for the treatment of limbal stem cell deficiency was first advocated by Sangwan et al.[20] Subsequently, mini-SLET[16] was innovatively used for treating 10 patients suffering with primary pterygium. The basis of using mini-SLET for pterygium surgery was localized deficiency or dysfunction of limbal stem cells.[21, 22] The AMG acts as a basement membrane and a substrate supporting the growth of epithelial progenitor cells.[23] AMG is also endowed with anti-inflammatory properties owing to the presence of protease inhibitors.[24] However, AMG itself is

Table 3. Comparative outcome of the postoperative symptom score between the CAG group and mini-SLET group

	CAG group (*n* = 118)			Mini-SLET group (*n* = 115)			*P*-value*
	Min	Max	Median	Min	Max	Median	
Foreign body sensation							
Day 1	3	9	9	0	9	6	**<0.001**
Day 3	0	9	6	0	6	3	**<0.001**
Day 7	0	6	3	0	3	0	**<0.001**
Day 14	0	6	0	0	0	0	0.255
Day 30	0	0	0	0	0	0	0.999
Epiphora (watering)							
Day 1	0	9	6	0	9	6	**<0.001**
Day 3	0	6	3	0	6	3	**<0.001**
Day 7	0	6	0	0	6	0	0.511
Day 14	0	0	0	0	0	0	0.999
Day 30	0	0	0	0	0	0	0.999
Pain							
Day 1	0	9	6	0	6	3	**<0.001**
Day 3	0	9	3	0	6	0	**<0.001**
Day 7	0	6	0	0	6	0	**0.008**
Day 14	0	6	0	0	0	0	0.089
Day 30	0	0	0	0	0	0	0.999
Irritation							
Day 1	3	9	9	0	9	6	**<0.001**
Day 3	0	9	6	0	6	3	**<0.001**
Day 7	0	6	3	0	3	0	**<0.001**
Day 14	0	6	0	0	6	0	0.183
Day 30	0	0	0	0	0	0	0.999

Statistically significant values are in boldface after *Mann–Whitney U-test

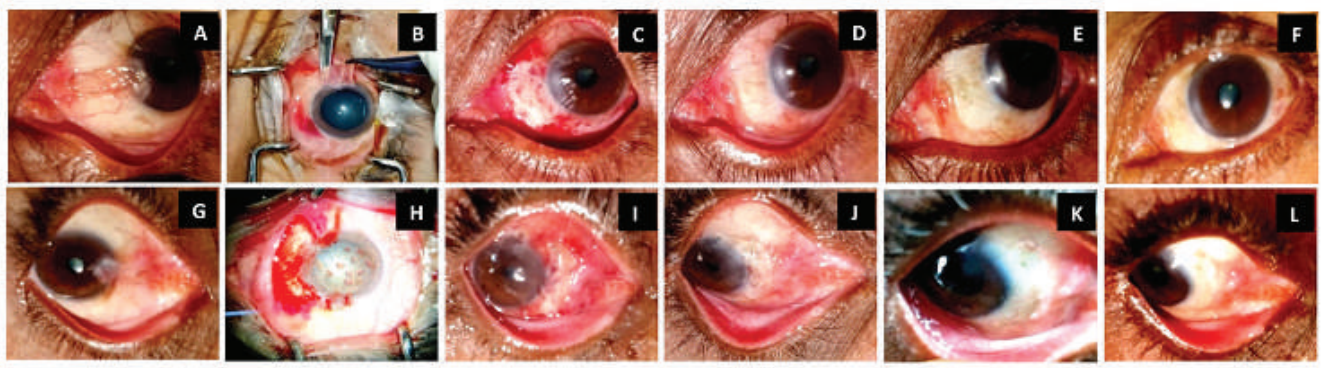

Figure 1. Serial clinical photographs of two patients of primary pterygium: (Patient 1 [A~F]; Patient 2 [G~L]): preoperative, intraoperative, and postoperative. Pterygium excision with CAG with fibrin glue (A–F) and pterygium excision with mini-SLET (G–L). (A) A case of primary nasal pterygium (left eye[LE]) before pterygium excision with CAG. (B) Dissection of pterygium. (C) POD 1. (D) POD 30 graft well taken. (E & F) Postoperative months 6 and 9, respectively: restoration of near normal anatomy without any recurrence. (G) A case of primary nasal pterygium (Right eye [RE]) before pterygium excision with mini-SLET. (H) Intraoperative photograph showing dissected pterygium with eight limbal pieces. (I) POD 1. (J) POD 30: well-settled graft. (K & L) Postoperative months 6 and 9, respectively: restoration of near normal anatomy without any signs of recurrence.

devoid of limbal stem cells, hence its solitary use to cover the bare sclera after pterygium excision, despite providing a mechanical barrier, does not address the underlying pathology of limbal stem cell deficiency. As a result, this may in turn lead to potentially more recurrences and tilt the balance toward CAG in terms of beneficial outcomes.

An extensive MEDLINE search did not reveal any similar study of this magnitude; hence we undertook a randomized trial to compare the aforementioned two techniques as mini-SLET appeared to be a viable prospect for the treatment of pterygium.[16] In 2015, Hernández-Bogantes E et al,[16] elicited this interesting innovation in 10 patients with primary pterygium without any recurrence after eight months of follow-up. Sati et al[25] reported a randomized control trial, comparing the outcomes between 42 cases of CAG and 40 cases of mini-SLET. The study reported a 9.5% recurrence in the CAG group and 2.5% recurrence in the mini-SLET group. Although clinically meaningful, these differences were not found to be statistically significant. We experienced much lower rates of recurrence in the CAG group and almost similar in the mini-SLET group. Mini-SLET incorporates the use of AMG and limbal stem cells, which could lower recurrence rates as is evident in our study. Mini-SLET is a miniaturized modification of the original SLET technique first described by Sangwan et al.[20] However, mini-SLET technique scores over SLET in terms of placing the limbal stem cells' pieces over amniotic membrane in proximity to the limbus. In our opinion, mini-SLET offers an alternative solution to patients with insufficient conjunctiva due to prior surgeries or those suspected of suffering with glaucoma. Additionally, it is more likely to restore the normal anatomy of the limbus.

There were a few limitations of the study such as the relatively low overall numbers of recurrences, which made it difficult to make robust conclusions while using statistical tools. Follow-up of <12 months and the considerable number of excluded eyes (12%) also contributed toward limiting our evaluations. The strength of this study included its randomized and masked study design, the relatively large sample size, and the longer follow-up period, which exceeded that of other similar studies.

In summary, the overall recurrence rate was very low in this study and comparable between mini-SLET and the established technique of CAG for primary pterygium excision. Despite a longer surgical time, mini-SLET appears to be a viable alternative to CAG in the management of primary pterygium. The mini-SLET may be considered as the procedure of choice for all cases of primary pterygium surgery, especially, if cost and availability are not an issue. Also, mini-SLET is more likely to replace the abnormal limbal stem cells compared to CAG. In particular, this should be adopted as the procedure of choice as conjunctival-sparing surgery (especially in young patients, glaucoma, and cicatrizing conjunctivitis).

Acknowledgements

The authors would like to thank Dr. Charima Priya for excellent counselling and follow-up of patients.

Financial Support and Sponsorship

The authors did not receive any financial support for the research, authorship, and/or publication of this article.

Conflicts of Interest

The authors report no conflict of interest.

REFERENCES

1. Jaros PA, DeLuise VP. Pingueculae and pterygia. *Surv Ophthalmol* 1988;33:41–49.
2. Viani GA, Fonseca EC, De Fendi LI, Rocha EM. Conjunctival autograft alone or combined with adjuvant beta-radiation? A randomized clinical trial. *Int J Radiat Oncol Bio Phys* 2012;82:507–511.
3. Donnenfeld ED, Perry HD, Fromer S, Doshi S, Solomon R, Biser S. Subconjunctival mitomycin C as adjunctive therapy before pterygium excision. *Ophthalmology* 2003;110:1012–1016.
4. Rubinfeld RS, Pfister RR, Stein RM. Serious complications of topical mitomycin-C after pterygium surgery. *Ophthalmology* 1992;99:1647–1654.
5. Yu CM, Liang WL, Huang YY, Guan W. Comparison of clinical efficacy of three surgical methods in the treatment of pterygium. *Eye Sci* 2011;26:193–196.
6. Kenyon KR, Wagoner MD, Hettinger ME. Conjunctival autograft transplantation for advanced and recurrent pterygium. *Ophthalmology* 1995;92:1461–1470.
7. Chen PP, Ariyasu RG, Kaza V. A randomized trial comparing mitomycin C and conjunctival autograft after excision of primary pterygium. *Am J Ophthalmol* 1995;120:151–160.
8. Prabhasawat P, Barton K, Burkett G, Tseng SC. Comparison of conjunctival autografts, amniotic membrane grafts and primary closure for pterygium excision. *Ophthalmology* 1997;104:974–985.

9. Al Fayez MF. Limbal versus conjunctival autograft transplantation for advanced and recurrent pterygium. *Ophthalmology* 2002;109:1752–1755.
10. Marticorena J, Rodriguez-Ares MT, Tourino R. Pterygium surgery; conjunctival autograft using fibrin adhesive. *Cornea* 2006;25:34–36.
11. Uy HS, Reyes JMG, Flores JDG. Comparison of fibrin glue and sutures for attaching conjunctival autografts after pterygium excision. *Ophthalmology* 2005;112:667–671.
12. Bahar I, Weinberger D, Dan G. Pterygium surgery: fibrin glue versus vicryl sutures for conjunctival closure. *Cornea* 2006;25:1168–1172.
13. Wit D, Athanasiadis I, Sharma A. Sutureless and glue free conjunctival autograft in pterygium surgery: a case series. *Eye* 2010;24:1474–1477.
14. Malik KPS, Goel R, Gupta A. Efficacy of sutureless and glue free limbal conjunctival autograft for primary pterygium surgery. *Nepal J Ophthalmol* 2012;24:230–235.
15. Singh PK, Singh S, Vyas C, Singh M. Conjunctival autografting without Fibrin Glue or sutures for Pterygium Surgery. *Cornea* 2013;32:104–107.
16. Hernández-Bogantes E, Amescua G, Navas A. Minor ipsilateral simple limbal epithelial transplantation (mini-SLET) for pterygium treatment *Br J Ophthalmol* 2015;99:1598–1600.
17. Tan DT, Chee SP, Dear KB, Lim AS. Effect of pterygium morphology on pterygium recurrence in a controlled trial comparing conjunctival autografting with bare sclera excision. *Arch Ophthalmol* 1997;115:1235–1240.
18. Aletras AJ, Trilivas I, Christopulou ME. UVB-mediated down regulation of proteasome in cultured human primary pterygium fibroblasts *BMC Ophthalmol* 2018;18:328.
19. Sati A, Shankar S, Jha A. Comparison of efficacy of three surgical methods of conjunctival autograft fixation in treatment of pterygium. *Int Ophthalmol* 2014;34:1233–1239.
20. Sangwan VS, Basu S, MacNeil S. Simple limbal epithelial transplantation (SLET): a novel surgical technique for the treatment of unilateral limbal stem cell deficiency. *Br J Ophthalmol* 2012;96:931–934.
21. Cardenas-Cantu E,Zavala J,Valenzuela J. Molecular Basis of Pterygium Development. *Semin Ophthalmol* 2014:1–17.
22. Chui J, Coroneo MT, Tat LT. Ophthalmic pterygium: a stem cell disorder with premalignant features. *Am J Pathol* 2011;178:817–827.
23. Grueterich M, Tseng SC. Human limbal progenitor cells expanded on intact amniotic membrane ex-vivo. *Arch Ophthalmol* 2002;120:783–790.
24. Shimmura S, Shimazaki J, Ohashi Y, Tsubota K. Anti-inflammatory effects of amniotic membrane transplantation in ocular surface disorders. *Cornea* 2001;20:408–413.
25. Sati A, Banerjee S, Kumar P. Mini-simple limbal epithelial transplantation versus conjunctival autograft fixation with fibrin glue after primary pterygium excision: a randomized controlled trial. *Cornea* 2019;38;1345–1350.

Original Article

Inferior Spear-like Lens Opacity as a Sign of Keratoconus

Ramin Salouti[1,2], MD; Amir Khosravi[1], MD; Majid Fardaei[3], PhD; Mohammad Zamani[2], MD Mahmoud Nejabat[1], MD; Maryam Ghoreyshi[2,4], MD; Mahboobeh Yazdanpanah[3], MS; Kia Salouti[5], BD; M. Hossein Nowroozzadeh, MD[1]

[1]Department of Ophthalmology, School of Medicine, Shiraz University of Medical Sciences, Shiraz, Iran
[2]Salouti Cornea Research Center, Salouti Eye Clinic, Shiraz, Iran
[3]Department of Medical Genetics, Shiraz University of Medical Sciences, Shiraz, Iran
[4]Health Policy Research Center, Shiraz University of Medical Sciences, Shiraz, Iran
[5]Science Department, The university of British Columbia, Vancouver, Canada

ORCID:
Ramin Salouti: https://orcid.org/0000-0002-5853-4799
M. Hossein Nowroozzadeh: https://orcid.org/0000-0002-7412-1900

Abstract

Purpose: To report 21 cases of typical inferior feather-shape lens opacity associated with keratoconus.

Methods: In this cross-sectional study, we evaluated the association of keratoconus with inferior feather-shape lens opacity in refractive surgery candidates. Visual acuity, demographic, refractive, and topographic characteristics of 26 eyes of 21 patients with inferior feather-shape lens opacity were evaluated in detail. Pedigree analysis was also performed to assess possible inheritance.

Results: Overall, 2122 out of 33,368 cases (6.4%) without lens opacity had keratoconus, while 20 out of 21 patients (95.2%) with peculiar lens opacity had definite keratoconus ($P < 0.001$). Lens opacity was bilateral in 5 cases (24%), and keratoconus was bilateral in all 20 patients with lens opacity. Nine eyes out of thirty-six with a complete data record (25%) had a severe keratoconus and underwent deep lamellar keratoplasty, while 11 (31%) had forme fruste keratoconus. Pedigrees were drawn for eight patients, most families of whom suggested an X-linked recessive inheritance.

Conclusion: The present study was the first to investigate patients with a peculiar inferior feather-shape lens opacity accompanied by bilateral keratoconus, which was observed in 95% of the patients. This finding should raise awareness as to the possibility of diagnosing keratoconus in the eyes of the patients with these characteristics.

Keywords: Cataract; Feather-shape; Keratoconus; Lens Opacity; Sectoral

J Ophthalmic Vis Res 2022; 17 (1): 12–18

INTRODUCTION

Keratoconus is a noninflammatory, often bilateral, and asymmetric corneal disorder[1] in which the progressive central or paracentral corneal thinning leads to the bulging of the thinned cornea.[2] Keratoconus often occurs as an isolated disorder.[3, 4] Despite the extensive studies carried out over the recent decades on the etiology and pathogenesis of keratoconus, the exact pathophysiology and biochemical mechanisms of keratoconus is yet to be fully understood. However, several environmental (such as eye rubbing, atopy, sun exposure, and geography), genetic (i.e., familial inheritance, association with other known genetic disorders, and predisposing mutations), and biomechanical mechanisms have been proposed to contribute to this ectatic disorder.[5] Investigating the possible association of keratoconus with other diseases requires understanding of the pathogenesis and biochemical mechanisms of this condition.

Since keratoconus is a progressive disorder, an early diagnosis to save uncorrected visual performance is of utmost importance. Unfortunately, certain detection of early keratoconus in refractive surgery candidates is impossible, even with the help of the latest corneal imaging technologies. Extra-corneal clues such as genetic susceptibility might help to spot early keratoconus in uncertain situations. In our current study, we report 21 patients with an inferior feather-shape lens opacity accompanied by bilateral keratoconus at different stages in almost all of the cases.

METHODS

From January 2010 to July 2017, all refractive surgery candidates who were referred to *Salouti Eye Clinic* were evaluated for inferior feather-shape lens opacity by using slit-lamp examinations with dilated pupils. Pentacam HR (Oculus Optikgeräte GmbH) was also obtained for all of these patients, where any grade of keratoconus could be detected.

We also collected and analyzed all relevant data from these 21 patients who were diagnosed with typical feather-shape lens opacity. They underwent a complete ophthalmic examination including visual acuity, refraction, slit-lamp biomicroscopy, and fundus examination. The recorded data comprised of the corrected distance visual acuity, spherical equivalent refraction, Pentacam keratometric, pachymetric and keratoconus indices (Topographic Keratoconus Classification [TKC]). The Pentacam keratoconus indices consisted of the index of surface variance (ISV), index of vertical asymmetry (IVA), keratoconus index (KI), center keratoconus index (CKI), index of height asymmetry (IHA), index of height decentration (IHD), and minimum sagittal curvature (Rmin).

Clinical evaluations were followed by a detailed interview, which included questions about demographics, the assessment of the presence or absence of other diseases, drug intake, etc. Pedigrees were drawn up to three generations in order to evaluate the keratoconus mode of inheritance. Informed consent was obtained from the 21 participants who had cataract. The study protocol was approved by the Ethics Committee at Shiraz University of Medical Sciences and adhered to the principles of the Declaration of Helsinki.

All statistical analyses were performed using SPSS for Windows (Version 22 SPSS Inc., Chicago, IL, USA). Numerical variables were described as median (minimum to maximum).

RESULTS

We assessed the medical charts of 33,389 refractive surgery candidates, of whom 21 patients had the typical feather-shape lens opacity. Overall, 2122 out of 33,368 cases (6.4%) without lens opacity had keratoconus, while 20 out of 21

Correspondence to:

M. Hossein Nowroozzadeh, MD. Poostchi Ophthalmology Research Center, Poostchi Clinic, Zand Street, Shiraz 7134997446, Iran.
E-mail: nowroozzadeh@hotmail.com

Received 30-05-2020; Accepted 11-03-2021

Access this article online

Website: https://knepublishing.com/index.php/JOVR

DOI: 10.18502/jovr.v17i1.10165

How to cite this article: Salouti R, Khosravi A, Fardaei M, Zamani M, Nejabat M, Ghoreyshi M, Yazdanpanah M, Salouti S, Nowroozzadeh MH. Inferior Spear-like Lens Opacity as a Sign of Keratoconus. J Ophthalmic Vis Res 2022;17:12–18.

patients (95.2%) with lens opacity had definite keratoconus ($P < 0.001$).

All lens opacities were inferior sectoral and triangular in shape, with bases toward the equator. Although the width of the opacities varied among the patients, most had a width of about one clock hour or less. Densities of the opacities were also different among the patients, some of whom had a central dense line. The borders of the cataracts were fluffy, and most of them resembled a feather [Figure 1]. The opacities were bilateral in 5 cases (24%), and keratoconus was bilateral in all 20 cases who had the ectatic disorder. No patients had Down syndrome, atopic disease, or history of corticosteroid use. Nine out of thirty-six eyes with complete data (25%) recorded had a severe keratoconus and underwent deep lamellar keratoplasty, and 11 (31%) had forme fruste keratoconus (grade 1 in Pentacam). All diagnoses of combined lens-opacity/keratoconus were made before any intervention for treating keratoconus. Only one female patient with this characteristic form of lens opacity had no corneal finding in favor of keratoconus in her prior frequent examinations. However, her first-degree relatives had a positive history of keratoc. The other three patients did not agree to be interviewed/re-examined, so their detailed data are unavailable.

As a result, a total of 18 patients, 14 males and 4 females, were evaluated in detail. The median age was 27.5 years, ranging from 13 to 52 years. The median of the visual acuities of the patients with combined keratoconus/lens-opacity was 20/50 ranging from 20/20 to 20/200. The median of patient's spherical equivalent refraction was –4.00 D (range, –13.25 to –0.50). The medians (ranges) of the keratometric and pachymetric indices were as follows: mean keratometry, 48.8 D (44.1 to 55.1); maximum keratometry, 54.6 D (45.3 to 63.9); astigmatic keratometry, 3.3 D (1.0 to 7.6); and thinnest point, 475 µm (362 to 558). Tables 1 and 2 summarize the patients' demographic, refractive, and topographic information. Of the nine eyes with more advanced keratoconus that had undergone the graft procedure, eight belonged to men (28.6% of male's eyes) and only one to a woman (12.5% of female's eyes), suggesting a more severe phenotype in males. This is further corroborated by the lower median of TKC in females as compared to males (1.5 vs 2.0). However, due to the limited number of patients, we were not able to perform a complete statistical analysis on the patients.

None of the 18 patients interviewed declared any family relationship with one another. According to the information accessed, eight patients reported to have at least one other person with keratoconus among their family members [Table 1]. We were able to draw the pedigrees of all these patients, which were more suggestive of an X-linked recessive inheritance in most cases [Figure 2]. As an ongoing project, we will try to elucidate the genetic basis of combined keratoconus/feather-shape lens opacity in future studies.

DISCUSSION

In this study, we introduced a novel association between inferior feather-shape lens opacities and keratoconus. This type of lens opacity is more easily visualized when the pupils are dilated; however, they could still be detected in most eyes with undilated pupils.

Keratoconus is a multifactorial disorder, originating from complex interaction between many genetic and environmental factors. In this regard, previous studies have reported that 0.5 to 15.0% of individuals with Down syndrome are also affected by keratoconus. This association is 10–300 times higher as compared with a normal population.[6–8] It has been suggested that the primary cause of this association is eye rubbing due to the increased rate of blepharitis observed in about 46% of patients with Down syndrome.[8] Other studies have reported a higher incidence or a more severe form of keratoconus in subjects with vernal keratoconjunctivitis.[9, 10] About 40% of patients with Leber's congenital amaurosis are affected by keratoconus;[11, 12] genetic factors and eye rubbing have been suggested as possible mechanisms.[12] There are also possible associations reported between keratoconus and advanced mitral valve prolapse,[13, 14] and certain connective tissue disorders such as Osteogenesis Imperfecta[15] and Ehlers-Danlos syndrome subtype VI.[16]

A few studies have found this association between keratoconus and lens opacities. A family affected with keratoconus and anterior polar cataract was reported back in 1931.[17] The same phenotype with a supposed genetic association was reported in a large Northern Irish family.[18–20] Co-incidence of cataract and

Table 1. Demographic, refractive, and keratometric characteristics of cases

Case	Age	Sex	Keratoconus in family	Eye	SE	CDVA	K_{mean}	K_{max}	K_{astig}	P_{min}
	(yr)				(D)		(D)	(D)	(D)	(μm)
1	24	M	Cousin	OD	–6.25	20/25	49.7	54.5	3.1	452
				OS	–6.5	20/30	49.7	55.9	3.6	422
2	16	M	Cousin	OD	–3.75	20/200	48	53.9	4.2	459
				OS	–9.75	20/60	44.9	51.2	2.8	572
3	25	M	Sister; Cousin; Two first cousins once removed	OD	–2.25	20/40	46.8	49.5	2.1	516
				OS	–5.75	20/200	51.1	55.3	2.8	498
4	52	M	–	OD	–9	20/100	45.3	53.9	4.2	558
				OS	–0.5	20/50	45.5	53.9	4	545
5	13	M	–	OD	–1.5	20/20	47.7	54.6	2	517
				OS	–1	20/25	47.9	53.2	1.9	451
6	26	M	–	OD	–3	20/20	46.8	57.6	7.6	478
				OS	–0.5	20/200	54.2	59.5	6.6	475
7	33	M	Two uncles	OD	–3.75	20/50	42.9	50.7	4.2	687
				OS	–1.25	20/50	49.3	52.1	1.3	410
8	24	M	–	OD	–2.5	20/30	51.2	55.2	3.2	391
				OS	–1.5	20/30	52	55.9	3	362
9	32	M	Sister	OD	–3.75	20/40	42.6	50.1	8.2	541
				OS	–10	20/60	48.8	58.5	5.7	495
10	29	F	–	OD	–5.25	20/60	49.4	63.9	3.9	548
				OS	–4	20/40	44.3	52	4.5	492
11	27	F	Sister	OD	–4	20/30	44.1	45.3	1.4	530
				OS	–3	20/30	43.5	45.5	2	543
12	29	M	Cousin	OD	–1.5	20/20	44.1	45.3	1.4	530
				OS	–0.5	20/20	47.3	56.1	3.6	523
13	43	M	–	OD	–3.25	20/40	47.4	48.4	0.9	530
				OS	–2.75	20/30	47.8	48.6	1	522
14	26	M	Cousin	OD	–3.25	20/40	45.3	50	1.7	519
				OS	–2.75	20/30	45.2	48.3	0.7	516
15	35	F	Mother and brother	OD	–3.25	20/40	45.7	48.5	3.3	486
				OS	–6.75	20/50	47.6	48.5	4.2	480
16	37	M	–	OD	–9.25	20/50	47.8	54	3.5	455
				OS	–9.75	20/50	47.9	54	4.8	449
17	27	F	–	OD	–11.25	20/50	52	54.6	4.1	397
				OS	–11.25	20/40	51.9	54.6	3.3	408
18	28	M	–	OD	–13.25	20/80	53.4	55.2	3.7	445
				OS	–13	20/80	55.1	55.2	2.9	421

CDVA, corrected distance visual acuity; D, diopter; F, female; K_{astig}, astigmatic keratometry; K_{mean}, mean keratometry; K_{max}, maximum keratometry; M, male; OD, right eye; OS, left eye; P_{min}, minimum pachymetry; Y, year.

Table 2. Pentacam keratoconus indices and feather-shape lens opacity in reported cases

Case	Eye	Lens opacity	TKC*	ISV†	IVA†	KI†	CKI†	IHA†	IHD†	R_{min} †
1	OD	+	1	50	0.38	1.08	1.02	33.8	0.048	6.2
	OS		1	60	0.56	1.02	*1.03*	40.1	0.066	6.03
2	OD	+	2–3	98	1.15	1.3	1.04	27.2	0.089	6.27
	OS		Post-graft	50	0.45	0.92	0.97	5.2	0.047	6.59
3	OD		1	44	0.46	1.1	*1.03*	15.3	0.028	6.82
	OS	+	2	83	0.82	1.16	1.07	15.6	0.06	6.11
4	OD	+	Post-graft	57	0.42	0.88	0.96	12.1	0.054	6.26
	OS		Post-graft	57	0.42	0.88	0.96	12.1	0.054	6.26
5	OD		Post-graft	48	0.43	1.08	0.97	26	0.038	6.19
	OS	+	2–3	94	1.12	1.24	1.05	4.6	0.103	6.34
6	OD	+	2	76	0.64	1.09	0.97	37.6	0.069	5.86
	OS	+	Post-graft	80	0.8	0.88	1.01	*20.1*	0.125	5.67
7	OD		Post-graft	47	*0.31*	0.96	0.96	9.9	0.024	6.65
	OS	+	2	74	0.74	1.23	1.04	5.9	0.05	6.47
8	OD	+	2	76	0.77	1.24	1.05	1	0.076	6.12
	OS	+	2	83	0.81	1.24	1.05	2.6	0.078	6.03
9	OD		1	52	0.24	0.94	0.99	16.4	0.017	6.73
	OS	+	1	63	0.55	1.09	0.97	7.3	0.047	5.76
10	OD	+	Post-graft	18	0.1	1.08	0.97	26	0.038	6.2
	OS		1	44	0.5	1.1	*1.03*	15.1	0.028	6.82
11‡	OD	+	0	14	0.03	1.01	1.01	0.2	0.001	7.45
	OS		0	18	0.07	1.02	1.01	5.1	0.005	7.42
12	OD		Post-graft	14	0.03	1.01	1.01	0.2	0.001	7.45
	OS	+	Post-graft	51	0.25	0.97	0.97	23.5	0.024	6.02
13	OD		1	23	0.12	1.04	1.01	5.5	0.01	6.97
	OS	+	1	24	0.13	1.09	1.01	5.6	0.01	6.95
14	OD	+	1–2	44	0.5	1.1	1.03	15.1	0.028	6.82
	OS		1	45	0.52	1.3	1.03	16.3	0.032	6.7
15	OD	+	1	42	0.47	1.1	1.01	25.6	0.035	6.78
	OS	+	2	60	0.66	1.15	1.04	21	0.05	6.48
16	OD		1	42	*0.31*	1.03	1.02	26.8	0.05	6.57
	OS	+	1–2	51	0.45	1.09	1.02	*20*	0.055	6.49
17	OD	+	2	77	0.61	1.25	1.06	34	0.053	5.99
	OS	+	2–3	87	0.76	1.3	1.06	21	0.058	6.08
18	OD	+	3	115	1.1	1.31	1.12	61.1	0.124	5.56
	OS	+	3	98	0.76	1.24	1.1	35	0.081	5.6

*The cases that are marked as "Post-graft" are those that had undergone lamellar keratoplasty for advanced keratoconus †The typographical coding of Pentacam keratoconus indices are based on the Pentacam definition, in which plain text refers to normal index, underlined letters to abnormal, and *italic* letters to suspicious values ‡This case had typical cataract but no sign of keratoconus CKI, center keratoconus index; IHA, index of height asymmetry; IHD, index of height decentration; ISV, index of surface variance; IVA, index of vertical asymmetry; KI, keratoconus index; R_{min}, minimum sagittal curvature; TKC, topographic keratoconus classification

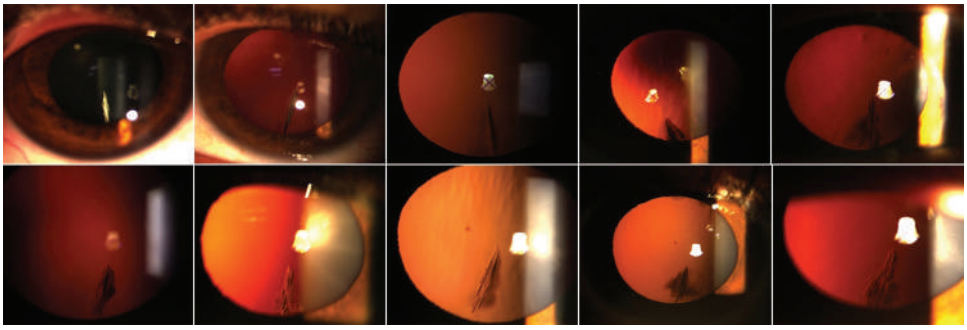

Figure 1. The typical inferior feather-shape lens opacity in 10 eyes of 10 cases from the cohort.

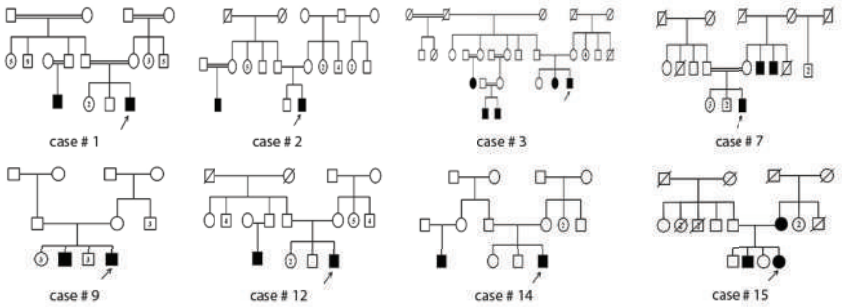

Figure 2. The pedigree drawings of eight cases with combined inferior feather-shape lens opacity and keratoconus. The number assigned to each case corresponds to the patients' numbers provided in Tables 1 and 2.

keratoconus has also been reported in patients with atopic dermatitis.[21, 22]

This is the first study to report a combination of keratoconus with a peculiar feather-shape lens opacity in a series of patients. We are not sure about the pattern of inheritance; however, the absence of male-to-male transmission, the lower number of affected females, and the milder phenotype in females are mostly suggestive of an X-linked inheritance in most pedigrees. In addition, the penetrance of the lens opacity was varied in the keratoconus cases of the index patients' families. Intuitively, the inferior location of both the lens opacity and the keratoconus cone might suggest a developmental error in the early fetal development of the eye, where the lens and cornea must be precisely separated from each other. Since some cases with bilateral keratoconus (which is usually asymmetric) have unilateral feather-shape lens opacity, the proposed developmental error might present in different severities with resultant phenotypes of various origins. It is logical to suppose that the keratoconus and the related lens opacity have the same genetic basis but with different degrees of penetrance and expressivity. In other words, the background lens abnormality probably involves both eyes; however, the visible lens opacity may be present in one or both eyes. Whether or not there exists a single gene basis for such an association is the subject of our future investigation.

Among the limitations of our study, mention can be made of the retrospective nature in the primary collection of data for all of the cases. However, all patients who were willing to participate were re-examined and interviewed prospectively, and the nature of the findings was not subject to classic biases posed by retrospective design (such as inadequate recording, misclassification, etc.). In addition, although we amassed detailed information on our patients, there was an inability to exact genetic evidence for the observed association, which would be the subject of future investigation for this cohort of patients.

In summary, our study revealed that the typical inferior feather-shape lens opacity is suggestive of an associated keratoconus, particularly in cases who might not show the clinical signs

of keratoconus. Therefore, we recommend an appropriate workup to diagnose keratoconus in patients with such type of cataract.

Financial Support and Sponsorship

None.

Conflicts of Interest

None declared.

REFERENCES

1. Zadnik K, Steger-May K, Fink BA, Joslin CE, Nichols JJ, Rosenstiel CE, et al. Between-eye asymmetry in keratoconus. *Cornea* 2002;21:671–679.
2. Auffarth GU, Wang L, Volcker HE. Keratoconus evaluation using the Orbscan Topography System. *J Cataract Refract Surg* 2000;26:222–228.
3. Rabinowitz YS. Keratoconus. *Surv Ophthalmol* 1998;42:297–319.
4. Li X, Rabinowitz YS, Rasheed K, Yang H. Longitudinal study of the normal eyes in unilateral keratoconus patients. *Ophthalmology* 2004;111:440–446.
5. Gordon-Shaag A, Millodot M, Shneor E, Liu Y. The genetic and environmental factors for keratoconus. *Biomed Res Int* 2015;2015:795738.
6. Cullen JF, Butler HG. Mongolism (down's syndrome) and keratoconus. *Br J Ophthalmol* 1963;47:321–330.
7. Krachmer JH, Feder RS, Belin MW. Keratoconus and related noninflammatory corneal thinning disorders. *Surv Ophthalmol* 1984;28:293–322.
8. Shapiro MB, France TD. The ocular features of Down's syndrome. *Am J Ophthalmol* 1985;99:659–663.
9. Totan Y, Hepsen IF, Cekic O, Gunduz A, Aydin E. Incidence of keratoconus in subjects with vernal keratoconjunctivitis: a videokeratographic study. *Ophthalmology* 2001;108:824–827.
10. Cingu AK, Cinar Y, Turkcu FM, Sahin A, Ari S, Yuksel H, et al. Effects of vernal and allergic conjunctivitis on severity of keratoconus. *Int J Ophthalmol* 2013;6:370–374.
11. Damji KF, Sohocki MM, Khan R, Gupta SK, Rahim M, Loyer M, et al. Leber's congenital amaurosis with anterior keratoconus in Pakistani families is caused by the Trp278X mutation in the AIPL1 gene on 17p. *Can J Ophthalmol* 2001;36:252–259.
12. Elder MJ. Leber congenital amaurosis and its association with keratoconus and keratoglobus. *J Pediatr Ophthalmol Strabismus* 1994;31:38–40.
13. Lichter H, Loya N, Sagie A, Cohen N, Muzmacher L, Yassur Y, et al. Keratoconus and mitral valve prolapse. *Am J Ophthalmol* 2000;129:667–668.
14. Sharif KW, Casey TA, Coltart J. Prevalence of mitral valve prolapse in keratoconus patients. *J R Soc Med* 1992;85:446–448.
15. Beckh U, Schonherr U, Naumann GO. [Autosomal dominant keratoconus as the chief ocular symptom in Lobstein osteogenesis imperfecta tarda]. *Klin Monbl Augenheilkd* 1995;206:268–272.
16. Robertson I. Keratoconus and the Ehlers-Danlos syndrome: a new aspect of keratoconus. *Med J Aust* 1975;1:571–573.
17. Sander P. A family affected with keratoconus and anterior polar cataract. *Br J Ophthalmol* 1931;15:23–25.
18. Hughes AE, Dash DP, Jackson AJ, Frazer DG, Silvestri G. Familial keratoconus with cataract: linkage to the long arm of chromosome 15 and exclusion of candidate genes. *Invest Ophthalmol Vis Sci* 2003;44:5063–5066.
19. Dash DP, Silvestri G, Hughes AE. Fine mapping of the keratoconus with cataract locus on chromosome 15q and candidate gene analysis. *Mol Vis* 2006;12:499–505.
20. Hughes AE, Bradley DT, Campbell M, Lechner J, Dash DP, Simpson DA, et al. Mutation altering the miR-184 seed region causes familial keratoconus with cataract. *Am J Hum Genet* 2011;89:628–633.
21. Longmore L. Atopic dermatitis cataract and keratoconus. *Australas J Dermatol* 1970;11:139–141.
22. Brunsting LA, Reed WB, Bair HL. Occurrence of cataracts and keratoconus with atopic dermatitis. *AMA Arch Derm* 1955;72:237–241.

Original Article

Knowledge E
enriching | engaging | empowering
Check for updates

Vision-related Quality of Life after Bilateral Implantation of Monofocal and Multifocal Intraocular Lenses

Shahram Bamdad[1], MD; Seyyed Ahmad Razavizadegan[1], MD; Mohsen Farvardin[1], MD; Sahar Mohaghegh[2], MS

[1]Poostchi ophthalmology research center, Department of Ophthalmology, School of Medicine, Shiraz University of Medical Sciences, Shiraz, Iran
[2]Department of Optometry, School of rehabilitation, Shahid Beheshti University of Medical Sciences, Tehran, Iran

ORCID:
Shahram Bamdad: https://orcid.org/0000-0002-5609-016X
Sahar Mohaghegh: https://orcid.org/0000-0002-5953-3085

Abstract

Purpose: To evaluate vision-related quality of life in two sets of patients after routine cataract surgery implanting with traditional versus multifocal intraocular lens (IOLs).

Methods: In a cross-sectional prospective study, 58 and 33 candidates for cataract surgery were divided into traditional (Acrysof SN60WF, Alcon Laboratories, Inc) and multifocal IOL (AcrySof IQ PanOptix IOL TFNT00, Alcon Laboratories, Inc.) groups, respectively. The primary outcome was VFQ-25 scores. The secondary outcomes were making comparisons between the two IOL types in the near vision and the driving items.

Results: The mean patients' age in traditional and multifocal IOL groups was 60.85 ± 7.40 (55% female) and 59.85 ± 8.95 (36% female) years, respectively. The mean VFQ-25 total scores in traditional and multifocal IOL groups before and after surgery were 63.69 ± 4.95 and 72.15 ± 9.66, and 98.08 ± 0.70 and 95.70 ± 1.30, respectively (P = 0.001 & 0.001). The mean scores of night driving in traditional and multifocal IOL groups were 38.79 ± 20.50 and 44.35 ± 21.12 (P = 0.1) before surgery which improved to 97.41 ± 7.68 and 56.45 ± 11.12 after surgery, respectively (P = 0.001). The mean scores of near vision in traditional and multifocal IOL groups were 46.83 ± 10.56 and 50.53 ± 8.58 (P = 0.2) before surgery which improved to 89.94 ± 4.87 and 100.00 ± 0.00 after surgery, respectively (P = 0.001).

Conclusion: Vision-related quality of life after cataract surgery with either type of traditional or multifocal (PanOptix) IOLs improved to an excellent level. Traditional IOLs provided more satisfaction in nighttime driving while multifocal IOLs provided increased satisfaction in near and intermediate vision.

Keywords: Cataract Surgery; Multifocal IOL; Quality of Life; Presbyopia; Vision-related Quality of Life

J Ophthalmic Vis Res 2022; 17 (1): 19–26

INTRODUCTION

Cataract is amongst the most prevalent causes of visual impairment in the world.[1] The prevalence of senile cataract increases with age during the years of presbyopia.[2] Cataract surgery with an intraocular lens (IOL) implantation is one of the most common and thought to be one of the most effective surgical procedures in any field of medicine.[1, 2] Monofocal lens as the first generation and most common type of intraocular lenses brings far distance into clear focus.[2] However, the ideas of accommodative[3] and multifocal intraocular lenses[4] developed due to increasing demand for activities that require near sight adjustment in the modern life style. Although the progress in the area of accommodative intraocular lenses did not advance as quickly as its counterparts,[3] the multifocal intraocular lenses progressed to a clinically satisfactory level and spectacle independency.[4–11]

The trifocal intraocular lenses are the most recent type of multifocal intraocular lenses that provide clear vision not only for far and near distances but also for intermediate distances that facilitate vision for electronic devices and automobile dashboards.[10] Trifocal intraocular lenses that are mostly pupil independent, designed to encompass the refractive–diffractive functionality in addition to extended depth of focus optics[8] which are mostly pupil independent, provide highly successful clinical outcomes,[5–11] increased visual satisfaction,[10–12] and improved quality of life as a result of enhanced vision.[11–15] The trifocal intraocular lens of PanOptix (AcrySof IQ PanOptix intraocular lens TFNT00, Alcon Laboratories, Inc.) is a noble diffractive non-apodized pupil independent aspheric intraocular lens that provides clear vision in 40 cm, 60 cm, 120 cm, 4 m, and optical infinity distances.[10] Some of the previous studies showed that PanOptix provides increased satisfaction for near and intermediate vision patients as compared to other competing tri-focal intraocular lens brands.[8, 10, 11]

Photic phenomena which is defined as light scattering, halos and glare, presents itself when positioned in poor lighting environments. They are known to be the source of minor visual dissatisfaction that may occur after tri-focal intraocular lens implantation.[14–16] Photic phenomena occurs as a result of multiple diffraction of the light beam due to the optics of the intraocular lenses. While present in an environment of glare lighting, the optical bench evaluation revealed a decrease in the image quality of the multifocal when compared to the monofocal intraocular lens.[16] Hence, it is of critical importance to evaluate the extent of the effect of these photic phenomena on the patient's vision in order to present a more complete judgement about the patient's state of vision after multifocal intraocular lens implantation.

Since patient-reported outcomes are of paramount importance when evaluating the success of treatments,[17] the first aim of the current study was to evaluate changes in vision as it related to the quality of life after bilateral traditional (monofocal) and multifocal (PanOptix) intraocular lenses implantation in the Iranian population. In this study, we used the Persian-version of the visual function questionnaire-25 (VFQ-25) which had been previously validated in the Persian population.[18] This questionnaire has been widely utilized for evaluating the quality of life in cataractous patients.[14, 19, 20] Quality of life measurements evaluates the level of improvement that a specific treatment may bring about in various life dimensions beyond the clinical evaluations. The second and third aims of the current study were to compare the near vision and driving items scores cumulated from the questionnaire between the two intraocular lens types.

Correspondence to:

Sahar Mohaghegh, MS. Rehabilitation Faculty, Shahid Beheshti University of Medical Sciences, Damavand Street, Imam Hossein Square, Tehran, Iran.
E-mail: saharmohaghegh79@gmail.com

Received 28-01-2019; Accepted 14-09-2021

Access this article online

Website: https://knepublishing.com/index.php/JOVR

DOI: 10.18502/jovr.v17i1.10166

How to cite this article: Bamdad S, Razavizadegan SA, Farvardin M, Mohaghegh S. Vision-related Quality of Life after Bilateral Implantation of Monofocal and Multifocal Intraocular Lenses. J Ophthalmic Vis Res 2022;17:19–26.

METHODS

This cross-sectional prospective study was conducted at Khalili Eye Hospital, Shiraz, Iran. The study protocol followed the tenets of the Helsinki and was approved by the local ethics committee of Shiraz University of Medical Sciences. Informed consent was obtained from all patients. Inclusion criteria were patients with bilateral cataract and corneal astigmatism <1.25 diopter power. In addition, patients who routinely drive were included. Exclusion criteria were prior history of refractive surgery, and other ocular conditions that may affect the vision such as glaucoma, age-related macular degeneration, and diabetic retinopathy. Prior to the surgery, optical coherence tomography was performed to exclude patients with any impairment in the macular area such as age-related macular degeneration disease, drusen, and diabetic exudate. Corneal topography was also assessed for all patients to exclude patients with irregular or skewed astigmatism. The excluded patients were not good candidates for multifocal intraocular lens implantation. Uncorrected distance visual acuity, best-corrected distance visual acuity, refraction, slit-lamp bio-microscopy and fundoscopy were performed at baseline and two months after surgery. The postsurgical examinations were performed for all patients in each follow-up session.

Keratometry and axial length measurements with intraocular lens Master 500 (Carl Zeiss Meditec, Germany) was performed prior to the surgery for all patients. The intraocular lens dioptric power was selected to target emmetropia using the intraocular lens power that corresponded to the negative (myopic) predicted refractive outcome closest to zero. The appropriate formulas that corresponded to axial length were used for the intraocular lens power calculation. Patients underwent the intracapsular cataract extraction for the first eye. Two months after the first eye healed, the second eye surgery was performed. All surgical procedures were performed by the same surgeon (FM). According to the patients' visual demand and desire expressed in the consultation session, either the monofocal intraocular lens with the double haptic aspheric design (Acrysof SN60WF, Alcon Laboratories, Inc.) or the multifocal intraocular lens (AcrySof IQ PanOptix intraocular lens TFNT00, Alcon Laboratories, Inc.) was chosen for implantation. It was impossible to randomize patients between these two groups because of the differences in the costs of the intraocular lens and the lifestyle of the patients.

PanOptix Intraocular Lens

The multifocal intraocular lens of PanOptix is an aspheric, hydrophobic intraocular lens with a blue filter and a 6.0-mm optical zone composed of a 4.5-mm large diffractive area with 15 diffractive zones and an outer refractive rim. It has three focal points from distance to intermediate and near ranges, dividing the incoming light to create intermediate and near add powers of 2.17 diopters (D) and 3.25 D, respectively. Therefore, it provides optimal close reading distances at 60 cm and 42 cm. This novel diffractive structure provides high light utilization transmitting 88% of light at the simulated 3.0 mm pupil size to the retina. This light energy is distributed 25% each for near and intermediate and 50% for distance vision.

The Persian-Version-VFQ-25

We used the 25-item Persian-version-VFQ, short-form version of 51-item VFQ. It was divided into 12 subscales including general health (two items), general vision (two items), ocular pain (two items), near vision (six items), distance vision (six items), vision-specific social functioning (three items), vision-specific mental health (five items), vision-specific role difficulties (four items), vision-specific dependency (four items), driving (three items), color vision (one item), and peripheral vision (one item). Subscale responses were graded 0 to 100, higher VFQ scores represent a better quality of life. The items were averaged to form subscales, and the sum of averages resulted in the total score. The Persian-version-VFQ-25 questionnaire, as determined in the Iranian population, has been shown to be valid and reliable. Through face-to-face interview by an ophthalmic technician the Persian-version-VFQ-25 results were obtained from all patients at baseline and two months after the cataract surgery of the second eye. For further comparison, we matched the groups of the monofocal and PanOptix intraocular lenses according to the scores of the near vision and driving items at baseline.

Statistical Analysis

Statistical analysis was performed using SPSS 18.0 for Windows (SPSS Inc., Chicago, Illinois, USA). We used descriptive statistics to illustrate the future of the data. The nonparametric test of Wilcoxon and Mann–Whitney U-test were used to make a comparison between the before and after data within the two groups. $P < 0.05$ was considered as statistically significant.

RESULTS

Fifty-eight patients (55% female [32 out of 58]) with the mean age 60.85 ± 7.40 years and 33 patients (36% female [12 out of 33]) with the mean age 59.85 ± 8.95 years were included in the monofocal and PanOptix intraocular lenses groups, respectively. The mean binocular uncorrected distance visual acuity in the monofocal intraocular lens group was 1.24 ± 1.89 and 0.07 ± 0.04 before and after surgery, respectively, ($P = 0.00$) and in the PanOptix group was 0.79 ± 1.08 and 0.00 ± 0.00 before and after surgery, respectively ($P = 0.00$). The mean scores of the Persian-version-VFQ-25 in the monofocal and PanOptix intraocular lens groups before and after the cataract surgery are presented in Tables 1 and 2.

The mean scores of near vision and driving references in both groups are presented in Graph 1. The driving reference is evaluated in the categories of day and nighttime driving and vision in driving in adverse conditions. Two groups were matched in the mean scores of near vision driving references before surgery ($P > 0.05$). The differences in the references of near vision, nighttime driving, and vision in driving in adverse conditions were statistically significant between the two groups ($P = 0.001$).

There were no intra- or postoperative complications or adverse effects in the study population in the two groups.

DISCUSSION

Nowadays, cataract surgery has the potential to provide excellent visual rehabilitation for all of the far, intermediate, and near distances by implanting multifocal intraocular lenses. However, monofocal intraocular lenses are still the most commonly used types of intraocular lenses across the world. Multifocal intraocular lenses have the potential to provide spectacle independency for pan-distances while they may increase the possibility of minor photic phenomena occurring due to their optical designs. Previous clinical evaluations revealed that a high level of visual acuity and contrast sensitivity after multifocal intraocular lens implantation is obtainable. However, the mesopic contrast sensitivity in patients with multifocal intraocular lenses has been reported to be less than monofocal.[16] In the current study using the Persian-version-VFQ-25, we evaluated the state of improvement that cataract surgery by implanting monofocal and multifocal (PanOptix) intraocular lenses may bring about in the patients' quality of life.

Our data analysis shows that the vision-related quality of life improved to an excellent level after cataract surgery with either type of monofocal or PanOptix intraocular lenses. For both groups, the mean score values in all dimensions were approximately >90, except for the driving reference in the PanOptix group (=75) that is discussed thoroughly in the paragraphs below. The prominent improvements observed in the dimensions of general and mental health, social function, dependency, and role limitation reveal that cataract surgery with either type of intraocular lenses improves both vision and sense of well-being. Cataract surgery with either lenses reduces the patients' stress level, and improves the patients' social relationships and activities. Our results are in agreement with the results of previous studies.[11, 13, 14, 21] Akman et al[13]utilized the VF-14 quality-of-life questionnaire and evaluated the vision-related quality of life in 48 patients after PanOptix implantation. Similarly, they reported an overall high level of satisfaction and a high quality of life among these patients. In another study, Carneros-Llorente et al[11] compared the visual acuity, contrast sensitivity, and quality of life scores among three trifocal designs. They reported high satisfaction levels with all of the designs and a slightly improved intermediate vision with PanOptix. Hamidi et al[21] reported highly satisfactory results with the toric PanOptix intraocular lens model in the eyes with longer or shorter axial length.

The novelty of the PanOptix intraocular lens is the provision of clear images at near and intermediate distances. Since the PanOptix group obtained the maximum score in the "near &

Table 1. Vison-related quality of life in patients with monofocal intraocular lens

	Mean ± Std. Deviation N = 58	Mean ± Std. Deviation N = 58	P-value
General health	47.84 ± 17.69	100.00 ± 0.00	0.001
General vision	54.31 ± 14.91	88.91 ± 12.47	0.001
Peripheral vision	50.43 ± 12.81	100.00 ± 0.00	0.001
Color vision	65.08 ± 12.33	100.00 ± 0.00	0.001
Mental health	77.58 ± 7.68	100.00 ± 0.00	0.001
Ocular pain	71.87 ± 15.23	88.36 ± 8.06	.001
Near vision	46.83 ± 10.56	89.94 ± 4.87	0.001
Distance vision	55.02 ± 7.47	100.00 ± 0.00	0.001
Social function	70.47 ± 13.18	100.00 ± 0.00	0.001
Role limitation	86.63 ± 8.71	100.00 ± 0.00	0.001
Dependency	91.66 ± 6.24	100.00 ± 0.00	0.001
Driving	47.27 ± 15.48	98.27 ± 4.05	0.001
Total Score	63.69 ± 4.95	98.08 ± 0.70	0.001

Table 2. Vison-related quality of life in patients with PanOptix intraocular lens

	Mean ± Std. Deviation (before) N = 33	Mean ± Std. Deviation (after) N = 33	P-value
General health	74.24 ± 14.63	96.96 ± 8.28	0.001
General vision	69.69 ± 14.99	93.18 ± 11.30	0.001
Peripheral vision	64.39 ± 12.54	94.69 ± 10.37	0.001
Color vision	100.00 ± 0.00	100.00 ± 0.00	>0.99
Mental health	69.69 ± 14.58	89.77 ± 9.08	0.001
Ocular pain	94.50 ± 6.00	100.00 ± 0.00	0.01
Near vision	51.01 ± 9.02	100.00 ± 0.00	0.001
Distance vision	77.02 ± 12.50	100.00 ± 0.00	0.001
Social function	88.25 ± 10.33	96.59 ± 3.16	0.001
Role limitation	68.56 ± 20.99	100.00 ± 0.00	0.001
Dependency	69.69 ±17.77	100.00 ± 0.00	0.001
Driving	44.08 ± 21.10	77.15 ± 3.70	0.001
Total	72.15 ± 9.66	95.70 ± 1.30	0.001

intermediate fine works" category, it is evident that the PanOptix design from the patients' viewpoint was very successful in achieving its aim. Although patients with a monofocal intraocular lens may take advantage of near glasses and obtain a good score the spectacle independency that PanOptix provides has resulted in a prominently higher score in these patients. Our results are in agreement with the results of previous studies.[22–24] Chichester et al reported spectacle independence in 90% of patients with trifocal intraocular lenses, and all patients stated that they would be willing to repeat surgery with the same intraocular lens type.[22] Akman et al[13]reported no difficulty

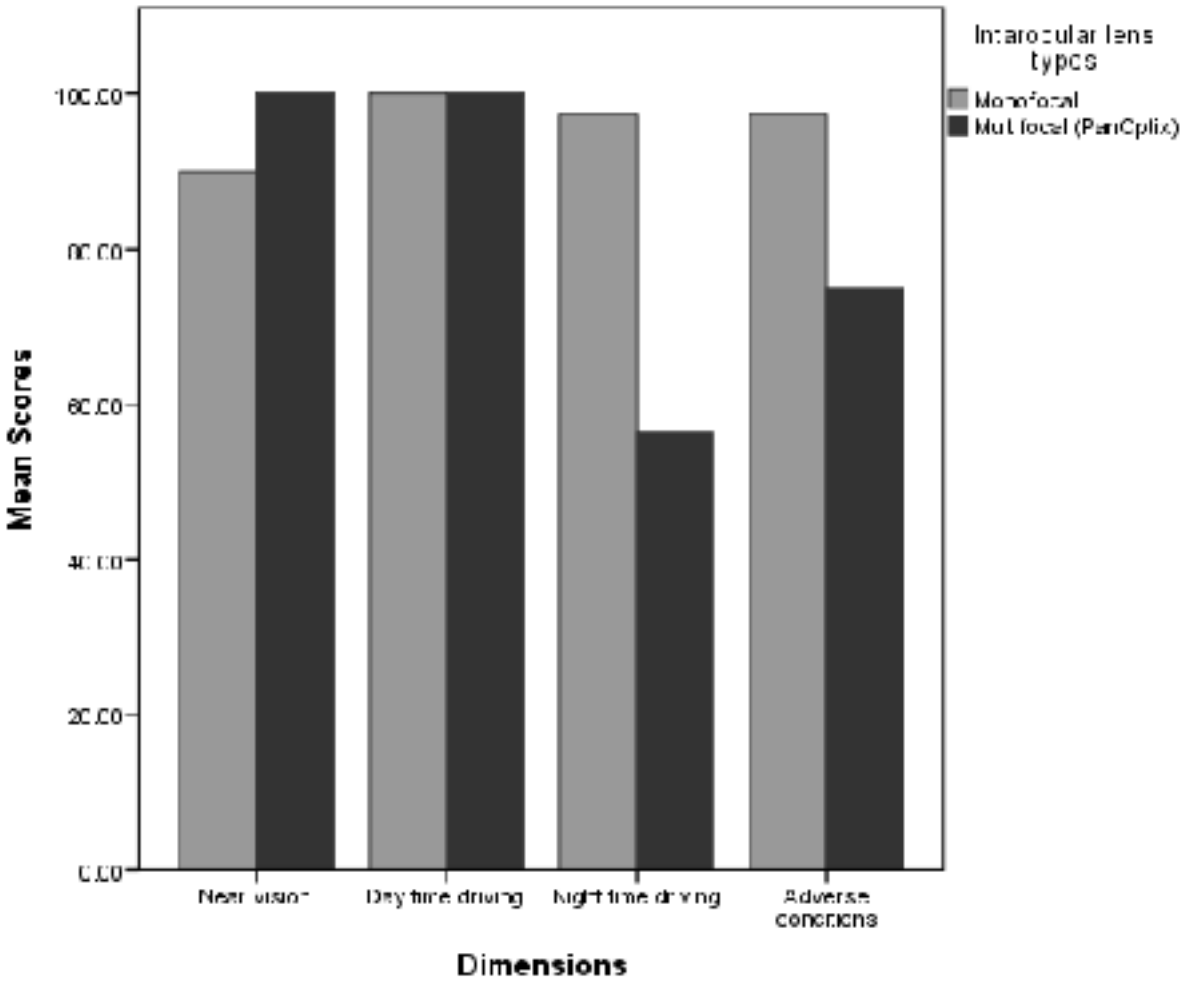

Figure 1. A comparison between monofocal and PanOptix intraocular lenses.

in near activities such as reading books and phone numbers, writing checks, performing computer tasks, wearing make-up, and cooking with PanOptix. However, they reported a little difficulty in reading very small print sizes and sewing. Rementería-Capelo et al[15] reported high scores in near activities such as reading newspapers, viewing prices on goods, and doing handcrafts.

Our findings revealed that nighttime driving and driving in adverse conditions had a moderate improvement in the PanOptix group. Albeit the daytime driving reached the maximum level of improvement in this group. We relate that to the diffractive design of the PanOptix lens and the light halos that appears in the field.[16, 25] Trifocal PanOptix intraocular lens provides three images simultaneously, so in poor lighting conditions, the multiple images' shadows disturb the vision. It seems that the effect of shadows is significant in nighttime driving and is reflected in the patient's reported outcome. Moreover, the higher-order aberrations amount increases at nights due to the larger pupil size, that superimposes the previous problems of halos and glare with this design. Although the results of our study were in agreement with previous studies,[12, 13] it has been reported that as a result of neural adaptation this problem described above decreases with time.[26] Previous studies revealed that resolving the remaining uncorrected refractive errors with wavefront-guided lasers in situ keratomileuses can prominently enhance the satisfaction level of patients after multifocal lens implantation.[27] Moreover, performing the incision after the corneal steep axis in surgery results in astigmatism

reduction in the corneal, <1D power. Consequently, this consideration with PanOptix design improves the quality of vision and the satisfaction of the patients.[28]

As expected, postoperative uncorrected visual acuity prominently improved after cataract surgery with both lens types and no adverse effects were observed in both groups. Previous studies revealed that presurgical visual acuity should not be considered as the only indicator when performing cataract surgery. Rather, vision-related quality of life measurements with validated questionnaires is recommended as a necessary additional tool for making decisions about surgery.[29] These tools are necessary because there might be high visual demands present in some patients' lifestyles where even early stage cataract can profoundly degrade their quality of life and vision satisfaction. In choosing the intraocular lens design patients who are more demanding and are perfectionists may request multifocal lenses while the more easygoing patients may choose the traditional design. Therefore, the personality of the patient itself may affect postoperative acceptance. In our study, we observed increased satisfaction from patients in near vision with PanOptix. However, if the traditional group were served by PanOptix, this resultant satisfaction may not be obtained, as PanOptix intraocular lens requires making an adjustment for the near vison which easygoing patients may find inconvenient.

The strength of our study was utilizing the Persian-version VFQ-25 as a validated questionnaire which is widely used in cataract evaluations[14, 19, 20] in global populations.[30–32] Thus, it makes comparisons in future studies more convenient than using self-designed questionnaires. The study's limitation was the short follow-up time. A longer follow-up period is recommended when considering the probability of neural adaptation in evaluating the state of nighttime driving after PanOptix intraocular lens implantation. Another limitation was not measuring and comparing the contrast sensitivity between the two groups. In addition, our study does not cover the high myopic and extremely hyperopic eyes. Previous studies show satisfactory clinical outcomes in such cases, however less successful results when compared to patients with more normal refractive errors.[33, 34] Therefore, in order to properly address these limitations that exist, more resources are required in determining the patients' vision satisfaction and reported outcomes in such cases.

In conclusion, we discovered that in all aspects of life both monofocal and PanOptix intraocular lens provide patients with a substantial level of vision-related quality of life and visual satisfaction. The monofocal intraocular lenses enhanced the vision of the patient during nighttime driving as compared to that of the PanOptix multifocal intraocular lens. In addition, the PanOptix intraocular lens improved the quality of the vision of the patients in the near and intermediate categories as a result of its optical design. Therefore, it is recommended in order to adequately assess choosing the suitable option it is mandatory to consider the patient's visual demand prior to the cataract surgery and inform the patient about the probability of visual dissatisfaction occurring with nighttime driving if multifocal intraocular lenses are the chosen option.

Financial Support and Sponsorship

Nil.

Conflicts of Interest

None declared.

REFERENCES

1. Thompson J, Lakhani N. Cataracts. *Prim Care* 2015;42:409–423.
2. Asbell PA, Dualan I, Mindel J, Brocks D, Ahmad M, Epstein S. Age-related cataract. *Lancet* 2005;365:599–609.
3. Pepose JS, Burke J, Qazi MA. Benefits and barriers of accommodating intraocular lenses. *Curr Opin Ophthalmol* 2017;28:3–8.
4. Kohnen T. First implantation of a diffractive quadrafocal (trifocal) intraocular lens. *J Cataract Refract Surg* 2015;41:2330–2332.
5. Kohnen T, Titke C, Böhm M. Trifocal intraocular lens implantation to treat visual demands in various distances following lens removal. *Am J Ophthalmol* 2016;161:71–77. e1.
6. Alfonso JF, Fernández-Vega-Cueto L, Fernández-Vega L, Montés-Micó R. Visual function after implantation of a presbyopia-correcting trifocal intraocular lens. *Ophthalmic Res* 2020;63:152–164.
7. Rodov L, Reitblat O, Levy A, Assia EI, Kleinmann G. Visual outcomes and patient satisfaction for trifocal, extended depth of focus and monofocal intraocular lenses. *J Refract Surg* 2019;35:434–440.

8. Yoon CH, Shin I-S, Kim MK. Trifocal versus bifocal diffractive intraocular lens implantation after cataract surgery or refractive lens exchange: a meta-analysis. *J Korean Med Sci* 2018;33:e275.
9. Mencucci R, Favuzza E, Caporossi O, Savastano A, Rizzo S. Comparative analysis of visual outcomes, reading skills, contrast sensitivity, and patient satisfaction with two models of trifocal diffractive intraocular lenses and an extended range of vision intraocular lens. *Graefes Arch Clin Exp Ophthalmol* 2018;256:1913–1922.
10. Ruiz-Mesa R, Abengózar-Vela A, Ruiz-Santos M. A comparative study of the visual outcomes between a new trifocal and an extended depth of focus intraocular lens. *Eur J Ophthalmol* 2018;28:182–187.
11. de Carneros-Llorente AM, de Carneros AM, de Carneros-Llorente PM, Jiménez-Alfaro I. Comparison of visual quality and subjective outcomes among 3 trifocal intraocular lenses and 1 bifocal intraocular lens. *J Cataract Refract Surg* 2019;45:587–594.
12. Kohnen T, Herzog M, Hemkeppler E, Schönbrunn S, De Lorenzo N, Petermann K, et al. Visual performance of a quadrifocal (trifocal) intraocular lens following removal of the crystalline lens. *Am J Ophthalmol* 2017;184:52–62.
13. Akman A, Asena L, Ozturk C, Güngör SG. Evaluation of quality of life after implantation of a new trifocal intraocular lens. *J Cataract Refract Surg* 2019;45:130–134.
14. Zhang F, Sugar A, Jacobsen G, Collins M. Visual function and spectacle independence after cataract surgery: bilateral diffractive multifocal intraocular lenses versus monovision pseudophakia. *J Cataract Refract Surg* 2011;37:853–858.
15. Rementería-Capelo LA, Contreras I, García-Pérez JL, Blázquez V, Ruiz-Alcocer J. Visual quality and patient satisfaction with a trifocal intraocular lens and its new toric version. *J Cataract Refract Surg* 2019;45:1584–1590.
16. Lee S, Choi M, Xu Z, Zhao Z, Alexander E, Liu Y. Optical bench performance of a novel trifocal intraocular lens compared with a multifocal intraocular lens. *Clin Ophthalmol* 2016;10:1031–1038.
17. Lamoureux E, Pesudovs K. Vision-specific quality-of-life research: a need to improve the quality. *Am J Ophthalmol* 2011;151:195–197. e2.
18. Asgari S, Hashemi H, Nedjat S, Shahnazi A, Fotouhi A. Persian version of the 25-Item National Eye Institute Visual Functioning Questionnaire (NEI-VFQ 39): a validation study. *J Curr Ophthalmol* 2011;23:5–14.
19. Kirwan C, Lanigan B, O'Keefe M. Vision-related quality of life assessment using the NEI-VFQ-25 in adolescents and young adults with a history of congenital cataract. *J Pediatr Ophthalmol Strabismus* 2012;49:26–31.
20. Zhu M, Yu J, Zhang J, Yan Q, Liu Y. Evaluating vision-related quality of life in preoperative age-related cataract patients and analyzing its influencing factors in China: a cross-sectional study. *BMC Ophthalmol* 2015;15:160.
21. Hamdi IM. Subjective perception of trifocal IOL performance, including toric models. *Clin Ophthalmol* 2019;13:1955–1961.
22. Cochener B, Boutillier G, Lamard M, Auberger-Zagnoli C. A comparative evaluation of a new generation of diffractive trifocal and extended depth of focus intraocular lenses. *J Refract Surg* 2018;34:507–514.
23. Alió JL, Plaza-Puche AB, Alió Del Barrio JL, Amat-Peral P, Ortuño V, Yébana P, et al. Clinical outcomes with a diffractive trifocal intraocular lens. *Eur J Ophthalmol* 2018;28:419–424.
24. García-Pérez JL, Gros-Otero J, Sánchez-Ramos C, Blázquez V, Contreras I. Short term visual outcomes of a new trifocal intraocular lens. *BMC Ophthalmol* 2017;17:72.
25. Monaco G, Gari M, Di Censo F, Poscia A, Ruggi G, Scialdone A. Visual performance after bilateral implantation of 2 new presbyopia-correcting intraocular lenses: trifocal versus extended range of vision. *J Cataract Refract Surg* 2017;43:737–747.
26. Rosa AM, Miranda ÂC, Patrício M, McAlinden C, Silva FL, Murta JN, et al. Functional magnetic resonance imaging to assess the neurobehavioral impact of dysphotopsia with multifocal intraocular lenses. *Ophthalmology* 2017;124:1280–1289.
27. Seiler TG, Wegner A, Senfft T, Seiler T. Dissatisfaction after trifocal IOL implantation and its improvement by selective wavefront-guided Lasik. *J Refract Surg* 2019;35:346–352.
28. Xue S, Zhao G, Yin X, Lin J, Li C, Hu L, et al. Effect of incision on visual outcomes after implantation of a trifocal diffractive IOL. *BMC Ophthalmol* 2018;18:171.
29. Date RC, Al-Mohtaseb ZN. Advances in preoperative testing for cataract surgery. *Int Ophthalmol Clin* 2017;57:99–114.
30. Suzukamo Y, Oshika T, Yuzawa M, Tokuda Y, Tomidokoro A, Oki K, et al. Psychometric properties of the 25-Item National Eye Institute Visual Function Questionnaire (NEI VFQ-25), Japanese version. *Health Qual Life Outcomes* 2005;3:65.
31. Broman AT, Munoz B, West SK, Rodriguez J, Sanchez R, Snyder R, et al. Psychometric properties of the 25-Item NEI-VFQ in a Hispanic population: Proyecto ver. *Invest Ophthalmol Vis Sci* 2001;42:606–613.
32. Labiris G, Katsanos A, Fanariotis M, Tsirouki T, Pefkianaki M, Chatzoulis D, et al. Psychometric properties of the Greek version of the NEI-VFQ 25. *BMC Ophthalmol* 2008;8:4.
33. Steinwender G, Schwarz L, Böhm M, Slavík-Lencová A, Hemkeppler E, Shajari M, et al. Visual results after implantation of a trifocal intraocular lens in high myopes. *J Cataract Refract Surg* 2018;44:680–685.
34. Alfonso JF, Fernández-Vega-Cueto A, Alfonso-Bartolozzi B, Rodríguez-Uña I, Montés-Micó R. Visual and refractive outcomes in hyperopic pseudophakic Patients implanted with a trifocal intraocular lens. *Clin Ophthalmol* 2019;13:2261–2268.
35. García-Pérez JL, Gros-Otero J, Sánchez-Ramos C, Blázquez V, Contreras I. Short term visual outcomes of a new trifocal intraocular lens. *BMC Ophthalmol* 2017;17:72.

Original Article

Peak Intraocular Pressure Time during Water Drinking Test and Its Relationship with Glaucoma Severity

Carolina Nicolela Susanna[1], MD; Bianca Nicolela Susanna[1], MD; Fernanda Nicolela Susanna[2], MS
Remo Susanna Jr[2], MD, PhD; Carlos Gustavo De Moraes[3], MD, PhD

[1]Department of Ophthalmology, ABC Foundation School of Medicine, Santo André, Brazil
[2]Department of Ophthalmology, University of Sao Paulo School of Medicine, Sao Paulo, Brazil
[3]Department of Ophthalmology, Columbia University Irving Medical Center, New York, United States

ORCID:
Carolina Nicolela Susanna: https://orcid.org/0000-0003-1341-6112
Remo Susanna Jr: https://orcid.org/0000-0001-9147-9528

Abstract

Purpose: To investigate the association between the time of occurrence of intraocular pressure (IOP) peaks during the water-drinking test (WDT) and visual field damage in a cohort of primary open-angle glaucoma (POAG) patients.
Methods: In this retrospective, cross-sectional study, 98 eyes from 49 consecutive POAG patients were followed in a referral clinical practice. The relationship between the time when IOP peaks occurred during the WDT and the visual field mean deviation (MD) assessed with 24-2 visual field was tested with mixed-effects models.
Results: MD value was significantly associated with the time of IOP peak occurrence (P = 0.020) when adjusting for the number of medications, but not with the IOP peak values (P = 0.238).
Conclusion: The time of IOP peaks occurrence during the WDT was associated with glaucoma severity among treated POAG patients.

Keywords: Glaucoma Severity; IOP Peak Time; Primary Open-angle Glaucoma; Water Drinking Test

J Ophthalmic Vis Res 2022; 17 (1): 27–32

INTRODUCTION

Provocative tests have been widely employed in medicine to assess changes in physiological systems when stressed under strenuous conditions. For instance, coronary ischemia, not usually noted in physiologic conditions, may become evident when the subject undergoes a treadmill provocative test or following intravenous pharmacological stimulation. Depending on the magnitude of the change, treatment may be required to prevent long-term complications.

Correspondence to:
Remo Susanna Jr. MD, PhD. Department of Ophthalmology, University of Sao Paulo School of Medicine, Av. Dr. Arnaldo, 455, Sao Paulo, 01246-903, Brazil.
E-mail: rsusannajr@gmail.com

Received 07-04-2021; Accepted 01-08-2021

Access this article online

Website: https://knepublishing.com/index.php/JOVR

DOI: 10.18502/jovr.v17i1.10167

How to cite this article: Susanna CN, Susanna BN, Susanna R, De Moraes CG. Peak Intraocular Pressure Time during Water Drinking Test and Its Relationship with Glaucoma Severity. J Ophthalmic Vis Res 2022;17:27–32.

Similarly, the water-drinking test (WDT) is a stress test used to assess intraocular pressure (IOP) behavior and indirectly evaluate the outflow facility of the eye.[1] Glaucoma progression in patients whose IOP is apparently well-controlled during clinic visits maintain a challenge. A satisfactory correlation between clinic-based IOP measurements and mean circadian IOP have been shown, even though not predictive of the peak IOP.[2] In fact, more than 70% of IOP peaks occur at night or in the early morning hours.[3–6] However, monitoring IOP 24 hr is not practical in routine glaucoma practice. Diurnal tension curves (DTC) misses IOP peaks occurring overnight.[7] The WDT is a reliable and feasible means to estimate peak IOP.

While many glaucomatous eyes may have seemingly controlled IOP during office hours or usual steady-state conditions, IOP peaks triggered by this test may reveal pressure measurements inconsistent with controlled disease and which could yield to disease progression in the long run. In fact, the peak IOP elicited during the WDT has been shown to correlate with the IOP peak that occurs during the day[8–12] and is highly reproducible.[9, 13, 14] More importantly, it has been shown to be associated with the risk of visual field (VF) progression of glaucoma and disease severity.[15–18] Recently, it has also been suggested that the WDT could be used to evaluate retinal ganglion cell function and hence have potential application for risk assessment.[18] In addition, the WDT is an indicator of treatment efficacy, assessing the effect of hypotensive drugs as well as surgeries.[9, 19–22]

The mechanism of IOP elevation remains unclear, but there are some postulates, such as limited outflow facility, increased episcleral venous pressure (EVP), increased IOP mediated by the autonomic nervous system, and choroidal expansion.[23–25] Eyes with lower outflow facility should experience higher IOP peaks after ingestion of water than eyes with normal outflow function, thus being a surrogate measure of the outflow system of the eye and its ability to respond to transient IOP elevation.[26] The time interval in which peak IOP occurs after the ingestion of water can also be related to the ability of the drainage system to maintain IOP homeostasis. Eyes with worse outflow facility may experience continued IOP rise during the WDT, and as so, later IOP peaks than eyes with better outflow facility.

This study aims to investigate the association between severity of glaucomatous VF loss, the magnitude, and the time of IOP peaks during the WDT in a group of treated primary open-angle glaucoma (POAG) patients.

METHODS

This retrospective, cross-sectional study included 98 eyes from 49 consecutive POAG patients followed in a referral glaucoma center. The study protocol adhered to the tenets of the Declaration of Helsinki[27] and was approved by the committee of ethics. Informed consent for the research was obtained from all the patients. Consecutive patients that met the inclusion and exclusion criteria were selected for the present study.

A review of medical history, IOP measurement with Goldmann applanation tonometry, best-corrected visual acuity, and slit-lamp biomicroscopy was performed in these patients. Patients were included if they had a glaucomatous appearing optic disc during disc photograph evaluation defined by a senior glaucoma specialist associated with glaucomatous VF loss on 24-2 standard automated perimetry. VF loss was defined according to the modified Anderson's criteria. These results were confirmed on at least two consecutive examinations.

Included eyes had a best-corrected visual acuity of at least 20/40, spherical refraction better than ±5.00 diopters, and cylinder correction within 3.00 diopters. We excluded participants with non-glaucomatous optic neuropathy, closed or narrow angle assessed by gonioscopic examination, retinal disease, secondary glaucoma, or any other abnormality that could interfere with VF testing. None of the patients had undergone trabeculectomy or laser trabeculoplasty and none had cataract surgery within the last six months before enrollment.

The water-drinking test (WDT) consists of one baseline IOP measurement, followed by ingestion of 800 mL of water in 5 min and three more IOP measurements taken at 15-min intervals.[28] All participants were required to stop liquid ingestion 2 hr before the test. Intraocular pressure measurements were performed with a Goldmann applanation tonometer (Haag-Streit, GmbH, Switzerland). The maximum value of the three measurements was considered as the IOP

Table 1. Baseline characteristics

Variables	Data
Number of eyes	98
Age	60 ±12 (range: 33–95)
Race Caucasian Asian	88% 12%
Sex Female Male	54% 46%
Number of medications	of 2 ± 1 (range: 0–5)
Latanoprost use	76 (77.5%)
Mean baseline MD	–8.23 ± 7.94 dB (range: –31.19 to 2.38 dB)
Mean baseline IOP	14 ± 3 mmHg (range: 8 to 22 mmHg)
Mean peak IOP	18 ± 4 mmHg (range: 10 to 30 mmHg)

*Presented mean ± standard deviation, calculated using summary statistics. MD, mean deviation; IOP, intraocular pressure

Table 2. Distribution of number of eyes, mean MD, and mean IOP peak value of eyes according to the time of IOP peak in the WDT

Time of IOP peak	Number of eyes	MD value (dB)†	IOP peak (mmHg)†
15	20 (20.4%)	–4.36 ± 5.51	17 ± 4
30	42 (42.9%)	–9.35 ± 7.98	19 ± 3
45	36 (36.7%)	–9.13 ± 8.56	19 ± 5

†Presented as mean ± standard deviation, calculated using summary statistics. MD, mean deviation; IOP, intraocular pressure; WDT, water-drinking test.

peak during the WDT.[9] The time of the peak was defined as the time when the maximum IOP was measured. To minimize the effect of the IOP circadian rhythm, all WDT were performed between 4:00 PM and 5:00 PM.

Standard achromatic perimetry was performed with the Humphrey VF Analyzer (24-2 SITA-Standard; Carl Zeiss Meditec Inc., Dublin, CA). All patients underwent VF testing and reliable exams (<20% fixation losses, <33% false-positive and false-negative rates) were analyzed. Visual field tests and WDT were performed up to four months apart.

Statistical Analyses

Statistical comparisons were performed between patients with mixed-effects models, which considers the correlation between both eyes of the same patient.

Statistical analysis was performed using Stata Version 14 (StataCorp LP, College Station, TX). Statistical significance was reached at $P < 5\%$.

RESULTS

Ninety-eight eyes from 49 POAG patients were analyzed. The mean age of patients was 60 ± 12 years (range, 33–95) and 54% were women. Patients were on a mean of 2 ± 1 (range, 0–5) IOP lowering medications. The mean of mean deviation values (MD) was –8.23 ± 7.94 dB (range, –31.19 to 2.38 dB). Baseline characteristics are described in Table 1.

Table 2 depicts the distribution of the number of eyes, mean MD values (dB), and mean IOP peak according to the time point of the WDT in which the IOP peak occurred. The mean IOP peak and the mean MD values (17 ± 4 mmHg and 4.36 ± 5.51 dB, respectively) were lower at 15 min compared to 30 min (19 ± 3 mmHg and –9.35 ± 7.98 dB) and 45 min (19 ± 5 mmHg and –9.13 ± 8.56 dB) in the WDT.

The box plot of the distribution of MD value in each time IOP peak occurrence (Figure 1) shows lower MD values in the later time points (30 and 45 min) compared to 15 min.

Table 3. Results of the mixed model evaluating the association between the MD and time of IOP peak, IOP peak value, and number of medications.

Parameter	Coefficient	95% CI	P-value
Time of IOP peak	–0.155	–0.284 to –0.025	0.020
Peak value	– 0.237	–0.630 to 0.156	0.238
Number of medications	–1.137	–2.899 to 0.625	0.206
Constant	3.859	–4.691 to 12.411	0.376

†Calculated using mixed effect model. CI, confidence interval

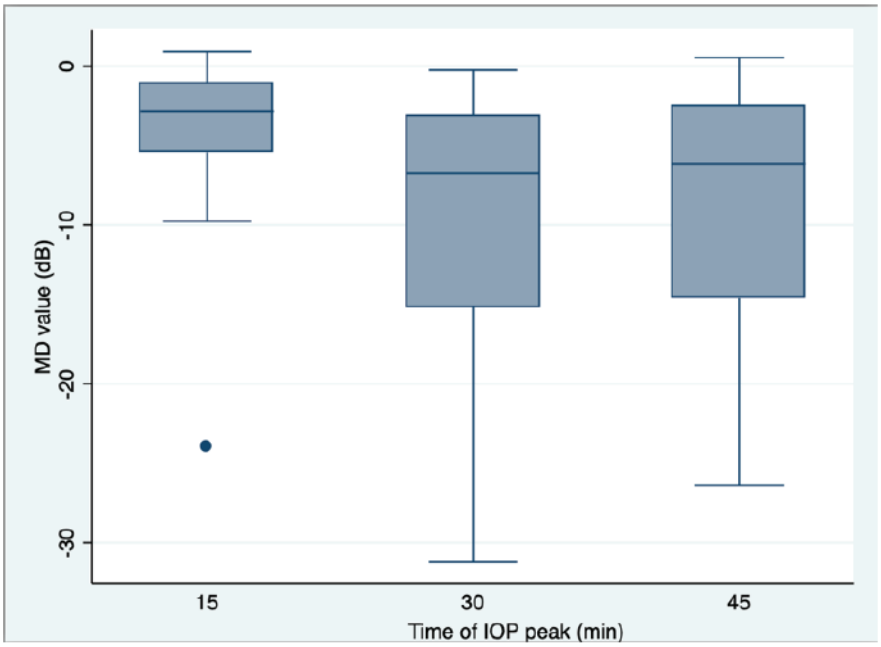

Figure 1. Distribution of mean deviation value at each time point of the WDT. †Boxplot depicting the MD distribution. MD, mean deviation; IOP, intraocular pressure; WDT, water-drinking test; min, minutes.

Separate multivariable models showed a statistically significant relationship between the time of IOP peak and MD values (P = 0.010) adjusting for number of medications. However, peak value was not associated with MD values when adjusting for number of medications (P = 0.117).

The results of the mixed-effect model relating MD values to the time of IOP peak, IOP peak value, and number of medications together are presented in Table 3. Eyes with more damage in VFs had later IOP peaks during WDT (P = 0.020). Neither number of medications nor IOP peak value were significantly related to MD values (P = 0.238 and P = 0.206, respectively).

DISCUSSION

Intraocular pressure peak is a key risk factor for glaucoma progression.[29–31] To better investigate other parameters obtained from the WDT, we tested whether the IOP peak time was related to the level of glaucomatous functional damage, which might reflect the eye's outflow system status of a given eye. Therefore, it is expected that in eyes with worse outflow facility, IOP elevation may remain rising for longer time, leading to later IOP peaks during the WDT.

Razeghinejad et al[32] investigated the effect of WDT after tube shunt surgery and trabeculectomy and showed that 30 min after the WDT, IOP in the trabeculectomy group initiated to decline, whereas for the tube shunt group it remained increasing

up to 60 min, which might have implications on tubes' efficacy in advanced glaucoma patients. Additionally, Waisbourd et al[22] investigated the effect of the WDT on the IOP of patients with angle-closure glaucoma and demonstrated that after peripheral iridotomy was performed, patients had a more pronounced IOP recovery, probably due to an increased trabecular meshwork area exposure following treatment. This corroborates the reasoning that eyes with impaired outflow have different time responses during the WDT.

We found that the time during WDT of IOP peaks' occurrence was associated with glaucoma severity in a population with treated POAG. Specifically, eyes with more severe disease had a later IOP peak than eyes with less severe disease (P = 0.020). In other words, eyes with later IOP peaks experienced continued IOP rise during the WDT until the maximum IOP was reached (IOP peak) and as so, a longer period of IOP elevation than eyes with earlier IOP peaks, possibly reflecting a better ability of these eyes to handle transient IOP elevation.

Accordantly, De Moraes et al[33] showed that the number of long peaks assessed with contact lens sensor (CLS) was the best predictors of faster progression in treated glaucoma patients.[33]

In contrast with results found by other authors,[15–17] there was no association between peak IOP value and MD (P = 0.238) in our study. Probably because patients were under treatment based on physician's discretion, which was adjusted to reduce IOP peaks elicited by the WDT. Therefore, patients showing more advanced glaucoma were likely prone to receive aggressive therapy in both eyes to achieve lower target IOP peaks.

One limitation is that this was a retrospective study. In order to reduce selection bias, we consecutively selected patients from a cohort in which all patients had routinely been submitted to the WDT.

Further prospective studies evaluating these WDT parameters, preferably with patients free of topical treatment, should be done to better understand the relationship between the peak time and VF defect.

In conclusion, this study demonstrated that the time of occurrence of IOP peak measured with the WDT was associated with glaucoma severity and might be an additional tool to evaluate glaucomatous patients.

Financial Support and Sponsorship

Nil.

Conflicts of Interest

There are no conflicts of interest.

REFERENCES

1. Kronfeld C. Water drinking and outflow facility. *Invest Ophthalmol* 1975;14:49–52.
2. Nakakura S, Nomura Y, Ataka S, Shiraki K. Relation between office intraocular pressure and 24-hour intraocular pressure in patients with primary open-angle glaucoma treated with a combination of topical antiglaucoma eye drops. *J Glaucoma* 2007;16:201–204.
3. Barkana Y, Anis S, Liebmann J, Tello C, Ritch R. Clinical utility of intraocular pressure monitoring outside of normal office hours in patients with glaucoma. *Arch Ophthalmol* 2006;124:793–797.
4. Liu JHK, Zhang X, Kripke DF, Weinreb RN. Twenty-four-hour intraocular pressure pattern associated with early glaucomatous changes. *Invest Opthalmol Vis Sci* 2003;44:1586.
5. Liu JHK, Kripke DF, Hoffman RE, Twa MD, Loving RT, Rex KM, et al. Nocturnal elevation of intraocular pressure in young adults. *Invest Ophthalmol Vis Sci* 1998;39:2707–2712.
6. Liu JHK, Kripke DF, Twa MD, Hoffman RE, Mansberger SL, Rex KM, et al. Twenty-four-hour pattern of intraocular pressure in the aging population. *Invest Ophthalmol Vis Sci* 1999;40:2912–2917.
7. Goldberg I, Clement CI. The water drinking test. *Am J Ophthalmol* 2010;150:447–449.
8. Kumar RS, De Guzman MHP, Ong PY, Goldberg I. Does peak intraocular pressure measured by water drinking test reflect peak circadian levels? A pilot study. *Clin Exp Ophthalmol* 2008;36:312–315.
9. Susanna R, Clement C, Goldberg I, Hatanaka M. Applications of the water drinking test in glaucoma management. *Clin Exp Ophthalmol* 2017;45:625–631.
10. Olatunji O, Olawoye O, Ajayi BGK. Correlation and agreement between water drinking test and modified diurnal tension curve in untreated glaucoma patients in Nigeria. *J Glaucoma* 2020;29:498–503.
11. V De Moraes CG, Furlanetto RL, Reis ASC, Vegini F, Cavalcanti NF, Susanna R Jr. Agreement between stress intraocular pressure and long-term intraocular pressure measurements in primary open-angle glaucoma. *Clin Exp Ophthalmol* 2009;37:270–274.
12. Vasconcelos-Moraes CG, Susanna R. Correlation between the water drinking test and modified diurnal tension curve in untreated glaucomatous eyes. *Clinics* 2008;63:433–436.
13. Hatanaka M, Alencar LM, De Moraes CG, Susanna R. Reproducibility of intraocular pressure peak and fluctuation of the water-drinking test. *Clin Exp Ophthalmol* 2013;41:355–359.

14. Babic M, De Moraes CG, Hatanaka M, Ju G, Susanna R. Reproducibility of the water drinking test in treated glaucomatous patients. *Clin Exp Ophthalmol* 2015;43:228–233.
15. Susanna R, Hatanaka M, Vessani RM, Pinheiro A, Morita C. Correlation of asymmetric glaucomatous visual field damage and water-drinking test response. *Invest Ophthalmol Vis Sci* 2006;47:641–644.
16. De Moraes CG, Susanna R, Sakata LM, Hatanaka M. Predictive value of the water drinking test and the risk of glaucomatous visual field progression. *J Glaucoma* 2017;26:767–773.
17. Susanna R, Vessani RM, Sakata L, Zacarias LC, Hatanaka M. The relation between intraocular pressure peak in the water drinking test and visual field progression in glaucoma. *Br J Ophthalmol* 2005;89:1298–1301.
18. Gameiro G, Monsalve P, Golubev I, Ventura L, Porciatti V. Neurovascular changes associated with the water drinking test. *J Glaucoma* 2018;27:429–432.
19. Kerr NM, Lew HR, Skalicky SE. Selective laser trabeculoplasty reduces intraocular pressure peak in response to the water drinking test. *J Glaucoma* 2016;25:727–731.
20. Martinez P, Trubnik V, Leiby BE, Hegarty SE, Razeghinejad R, Savant S, et al. A comparative study of the water drinking test in eyes with open-angle glaucoma and prior trabeculectomy or tube shunt. *J Glaucoma* 2017;26:119–125.
21. Germano RAS, Susanna R, De Moraes CG, Susanna BN, Susanna CN, Chibana MN. Effect of switching from latanoprost to bimatoprost in primary open-angle glaucoma patients who experienced intraocular pressure elevation during treatment. *J Glaucoma* 2016;25:e359–e366.
22. Waisbourd M, Savant SV, Sun Y, Martinez P, Myers JS. Water-drinking test in primary angle-closure suspect before and after laser peripheral iridotomy. *Clin Exp Ophthalmol* 2016;44:89–94.
23. Spaeth GL, Vacharat N. Provocative tests and chronic simple glaucoma. I. Effect of atropine on the water-drinking test: intimations of central regulatory control. II. Fluorescein angiography provocative test: a new approach to separation of the normal from the pathological. *Br J Ophthalmol* 1972;56:205–216.
24. Diestelhorst M, Krieglstein GK. The effect of the water-drinking test on aqueous humor dynamics in healthy volunteers. *Graefes Arch Clin Exp Ophthalmol* 1994;232:145–147.
25. De Moraes CGV, Reis ASC, Cavalcante AF de S, Sano ME, Susanna R. Choroidal expansion during the water drinking test. *Graefes Arch Clin Exp Ophthalmol* 2009;247:385–389.
26. Bhartiya S, Ichhpujani P. Water drinking test: the second innings scorecard. *Clin Exp Vis Eye Res* 2020;3:1–3.
27. World Medical Association. World Medical Association declaration of Helsinki: ethical principles for medical research involving human subjects. *JAMA* 2013;310:2191–2194.
28. Susanna CN, Susanna R, Hatanaka M, Susanna BN, Susanna FN, De Moraes CG. Comparison of intraocular pressure changes during the water drinking test between different fluid volumes in patients with primary open-angle glaucoma. *J Glaucoma* 2018;27:950–956.
29. Konstas AGP, Quaranta L, Mikropoulos DG, Nasr MB, Russo A, Jaffee HA, et al. Peak intraocular pressure and glaucomatous progression in primary open-angle glaucoma. *J Ocul Pharmacol Ther* 2012;28:26–32.
30. De Moraes CG, Liebmann JM, Greenfield DS, Gardiner SK, Ritch R, Krupin T. Risk factors for visual field progression in the low-pressure glaucoma treatment study. *Am J Ophthalmol* 2012;154:702–711.
31. V De Moraes CG, Juthani VJ, Liebmann JM, Teng CC, Tello C, Susanna R Jr, et al. Risk factors for visual field progression in treated glaucoma. *Arch Ophthalmol* 2011;129:562–568.
32. Razeghinejad M, Tajbakhsh Z, Nowroozzadeh M, Masoumpour M. Water drinking test: intraocular pressure changes after tube surgery and trabeculectomy. *J Ophthalmic Vis Res* 2017;12:390.
33. De Moraes CG, Jasien JV, Simon-Zoula S, Liebmann JM, Ritch R. Visual field change and 24-hour IOP-related profile with a contact lens sensor in treated glaucoma patients. *Ophthalmology* 2016;123:744–753.

Article Type

Diagnostic Performance of the PalmScan VF2000 Virtual Reality Visual Field Analyzer for Identification and Classification of Glaucoma

Vijay Shetty, MS, DNB, FRCS, FAICO; Prachi Sankhe, DNB; Suhas S Haldipurkar, DOMS, FAICO Tanvi Haldipurkar, MS; Rita Dhamankar, DOMS, MS; Priyanka Kashelkar, DNB; Dhruven Shah, DO, DNB Paresh Mhatre, MOptom; Maninder Singh Setia, MD, PhD

Laxmi Eye Institute, Panvel, Maharashtra, India

ORCID:
Vijay Shetty: http://orcid.org/0000-0003-0544-0200
Maninder Singh Setia: http://orcid.org/0000-0003-1291-9033

Abstract

Purpose: To evaluate the diagnostic test properties of the Palm Scan VF2000® Virtual Reality Visual Field Analyzer for diagnosis and classification of the severity of glaucoma.

Methods: This study was a prospective cross-sectional analysis of 166 eyes from 97 participants. All of them were examined by the Humphrey® Field Analyzer (used as the gold standard) and the Palm Scan VF 2000® Virtual Reality Visual Field Analyzer on the same day by the same examiner. We estimated the kappa statistic (including 95% confidence interval [CI]) as a measure of agreement between these two methods. The diagnostic test properties were assessed using sensitivity, specificity, positive predictive value (PPV), and negative predictive value (NPV).

Results: The sensitivity, specificity, PPV, and NPV for the Virtual Reality Visual Field Analyzer for the classification of individuals as glaucoma/non-glaucoma was 100%. The general agreement for the classification of glaucoma between these two instruments was 0.63 (95% CI: 0.56-0.78). The agreement for mild glaucoma was 0.76 (95% CI: 0.61-0.92), for moderate glaucoma was 0.37 (0.14-0.60), and for severe glaucoma was 0.70 (95% CI: 0.55-0.85). About 28% of moderate glaucoma cases were misclassified as mild and 17% were misclassified as severe by the virtual reality visual field analyzer. Furthermore, 20% of severe cases were misclassified as moderate by this instrument.

Conclusion: The instrument is 100% sensitive and specific in detection of glaucoma. However, among patients with glaucoma, there is a relatively high proportion of misclassification of severity of glaucoma. Thus, although useful for screening of glaucoma, it cannot replace the Humphrey® Field Analyzer for the clinical management in its current form.

Keywords: Glaucoma; Sensitivity; Specificity; Test Properties; Virtual Reality Perimetry

J Ophthalmic Vis Res 2022; 17 (1): 33–41

INTRODUCTION

Glaucoma, the second most common cause of vision loss in the world, is an important cause of blindness in India.[1–3] About 6.48 million people were estimated to have primary open-angle glaucoma in India.[3] It may be rightly termed as "the silent disease", as it causes bilateral, painless, and progressive vision loss.[4] One of the instruments used for the diagnosis and management of glaucoma, the Humphrey® Field Analyzer (Zeiss/USA) (HFA), is an automated perimeter and is well-known to ophthalmologists and optometrists. It is considered to be accurate, reliable, and a trusted method to detect the visual field defects of patients.[5] However, like other devices, HFA also has certain disadvantages and limitations. It is big and bulky, non-portable, demands a dark room, time-consuming, and may be difficult for patients with neck problems, old age, children, or those with any disability where it is difficult to keep their heads in a fixed slot to maintain good fixation.[6]

The Palm Scan VF2000® (MMD/USA) is a virtual reality (VR)-based visual field analyzer developed to measure the patient's visual field defect. It is a battery-operated portable device. The VF2000 consists of a system with three main sections connected to each other by a wireless mechanism. These three major components are: (1) the VR goggles worn by the patients; (2) the controller device operated by the healthcare staff who sets the testing strategy, technical parameters, and monitors the entire test; and (3) the clicker, which will be clicked by the patient when visualizing the stimulus.[6] There is a classic perimeter bowl in HFA whereas the Palm Scan VF 2000® VR Visual Field Analyzer has VR goggles. However, the VR perimetry has algorithms in place to make the stimuli appear on the retina as if they have been projected from the classic perimeter bowl.[7] The entire VR perimetry system fits in a small portable unit and it does not require a dedicated dark room or the fellow eye to be occluded. Furthermore, the VF2000 perimeter may be a more practical device for examining the visual fields in children, as well as in patients who are unable to perform HFA testing such as those with disabilities, those in nursing homes, and those who are hospitalized.[7]

Although, there are apparent advantages of the VF2000, it is also important to evaluate its accuracy in diagnosis and classification of glaucoma. Previous studies have shown that there is a correlation between the tablet-based visual field assessment and HFA; however, they have not discussed the performance of these instruments in the classification of the severity of glaucoma.[7, 8] With this background, we designed the present study to evaluate the diagnostic test properties of the Palm Scan VF2000® VR visual field analyzer for the diagnosis of glaucoma and the classification of the severity of glaucoma. We compared the agreement for diagnosis and classification of glaucoma between VR perimetry and HFA.

METHODS

The present study was a prospective cross-sectional analysis of 166 eyes from 97 participants.

Study Site

The study was conducted at the Laxmi Eye Hospital, a tertiary eye care center situated at a distance of about 50 km from Mumbai, India. The study was approved by the Ethics Committee at LEI for primary data analysis.

Study Population

We recruited 97 consenting patients who presented to the center. Of these, 57 individuals (86 eyes) had glaucoma and 40 (80 eyes) did not. The inclusion criteria for the glaucoma group

Correspondence to:

Maninder Singh Setia, MD, PhD. Laxmi Eye Institute, Panvel, Maharashtra 410206, India.
E-mail: maninder.setia@karanamconsultancy.in

Received 24-04-2020; Accepted 11-11-2021

Access this article online

Website: https://knepublishing.com/index.php/JOVR

DOI: 10.18502/jovr.v17i1.10168

How to cite this article: Shetty V, Sankhe P, Haldipurkar SS, Haldipurkar T, Dhamankar R, Kashelkar P, Shah D, Mhatre P, Setia S. Diagnostic Performance of the PalmScan VF2000 Virtual Reality Visual Field Analyzer for Identification and Classification of Glaucoma. J Ophthalmic Vis Res 2022;17:33–41.

were: (1) aged between 20 and 65 years; (2) those classified as glaucoma based on the Anderson criteria[9] – three non-edge points on the pattern deviation map, pattern standard deviation (PSD), and glaucoma hemifield test along with an intraocular pressure (IOP) of ≥20; and (3) those consenting for the study. The inclusion criteria for the non-glaucoma group were: (1) aged between 20 and 65 years; (2) those who were negative for all three parameters in the aforementioned criteria with an IOP of <20; and (3) those consenting for the study. The exclusion criteria were: (1) those with visual acuity <6/60 and (2) any other coexisting ocular comorbidities that are likely to affect the test like corneal or macular pathology (such as any corneal opacity or any macular scar). We used the following reliability indices for glaucoma cases: fixation losses (0.2); the fraction was converted to a decimal number form; <20% for false-positive and false-negative errors.

Study Procedures

All the study participants were examined with the HFA (Zeiss/USA) and the VF 2000® VR Visual Field Analyzer (MMD/USA) on the same day by the same examiner. We had performed perimetry on all these patients previously at least twice using the HFA; the criteria for fixation losses, false positive, and false negative were based on the acceptable and standard cut-off values.

HFA (Zeiss/USA): The participant sat in a comfortable (rested forehead and chin) position in front of the HFA (Zeiss/USA) bowl in a semi-dark room. The patient was told to look at the central fixation target and click the buzzer whenever the light stimulus was visualized. The lens power and type were provided by the HFA (Zeiss/USA) analyzer in patients with refractive errors. In these cases, wire-rimmed full aperture lenses were used. We tested one eye at a time and the eye which was not being tested was occluded with a patch. We used the Swedish Interactive Thresholding Algorithm (SITA) Standard 24-2 for these cases.

Palm Scan VF2000® Virtual reality (VR) Visual Field Analyzer (MMD/USA): Participants wore the VR glasses; these glasses are fitted with a strap and adjusted to avoid any tilt. The participant was told to look at the central fixation target and click the buzzer whenever the light stimulus was visualized. The examiner adjusted the focus using two rotating knobs present on the instrument; this was to correct the refractive errors. The Palm Scan VF 2000® VR Visual Field Analyzer (MMD/USA) has an occluder within the system. Thus, even though the eyes were tested alternatively, no external occlusion patch is required [Figure 1a]. All participants underwent the HFA test followed by the Palm Scan VF2000® VR Visual Field Analyzer. They were given a rest of 1 hr at least between the tests on these two machines.

We used the central 24-2 threshold test with a stimulus size of three and a presentation time of 200 ms for both these perimeters. The background illumination was 31.5 apostilb for HFA (Zeiss/USA) and 36 decibels for Palm Scan VF 2000® VR Visual Field Analyzer (MMD/USA). The software measured fixation losses by the Heijl–Krakau blind spot method. The false positives were events in which the participant responded only to audible stimulus (not visual stimulus) and false negatives were events in which participant failed to respond to supra threshold stimuli.[10]

For each test type, we extracted the following data; Mean Deviation (MD), Pattern Standard Deviation (PSD), and Visual Field Index (VFI). Those with an MD of <6 were classified as mild, with 2–12 as moderate, and with values >12 as severe glaucoma; this categorization was done according to the Hoddap Classification.[11]

Statistical Analysis

Data were entered in MS Excel (©Microsoft, USA) and analyzed using Stata Version 15.1 (©StataCorp, College Station, Texas, USA). We estimated the means and standard deviation (SD) or median and interquartile range (IQR) for continuous variables, and proportions for categorical variables. The means were compared using *t*-tests and the medians were compared using the Mann–Whitney test. The proportions were compared using the Chi-square test or Fisher's exact test for low expected cell counts.

We estimated the kappa statistic and its 95% confidence interval (CI) as a measure of agreement between the two methods. The diagnostic test properties of Palm Scan VF 2000® VR Visual Field Analyzer (MMD/USA) was assessed using sensitivity, specificity, positive predictive value (PPV), and negative predictive value (NPV); HFA (Zeiss/USA) was considered as the gold standard

Figure 1. Figure showing the use of the instrument in a participant.

for this analysis. The following analyses were done: (1) comparison of glaucomatous versus non-glaucomatous eyes and (2) severity of glaucoma (mild/moderate/severe) in eyes that were classified as glaucomatous.

We used intraclass correlation coefficient (ICC) as a measure of reliability for continuous variables (MD, PSD, and VFI). These paired values were also visualized using the Bland Altman Plot. A *p*-value of < 0.05 was considered statistically significant.

All procedures performed in studies involving human participants were in accordance with the ethical standards of the institutional and/or national research committee and with the 1964 Helsinki Declaration and its later amendments or comparable ethical standards.

RESULTS

The mean age (SD) of individuals was 51.3 (14.9) years. About 62% of participants in the study were males and 38% were females. Of the 86 glaucomatous eyes, 22 (26%) had mild, 18 (21%) had moderate, and 46 (53%) had severe glaucoma (based on the gold standard – HFA [Zeiss/USA]).

Comparison of Glaucomatous and Non-glaucomatous Eyes

In these analyses, the agreement between Palm Scan VF 2000® VR Visual Field Analyzer and HFA for diagnosis of glaucoma was 1.00 (95% CI: 1.00-1.00). According to Palm Scan VF 2000® VR Visual Field Analyzer, the proportion for true positives and true negatives was 100% respectively. Thus, the sensitivity and specificity for Palm Scan VF 2000® VR Visual Field Analyzer for classifying individuals as glaucoma/non-glaucoma was 100%. The PPV and NPV were both 100%.

Glaucomatous Eyes

We initially classified these individuals into mild vs moderate/severe glaucoma. The true positive proportion for moderate/severe glaucoma was 92% and the true negative proportion was 86%. Thus, sensitivity and specificity of Palm Scan VF 2000® VR Visual Field Analyzer for the detection of moderate/severe glaucoma was 92.2% and 86.4%, respectively. The PPV was 95.2% and the NPV was 79.2%. Detailed estimates and their 95% CI are presented in Table 1.

We also classified the eyes mild/moderate vs severe glaucoma. The true positive proportion

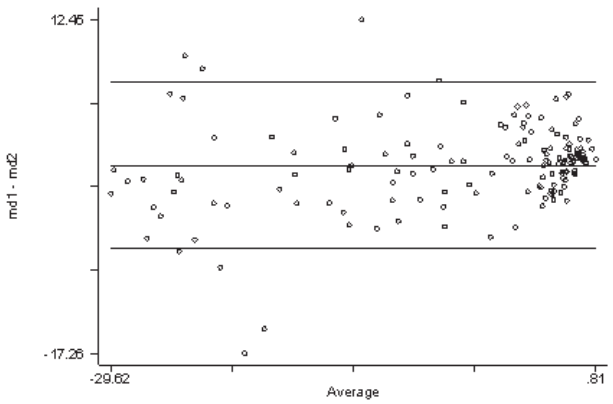

a)

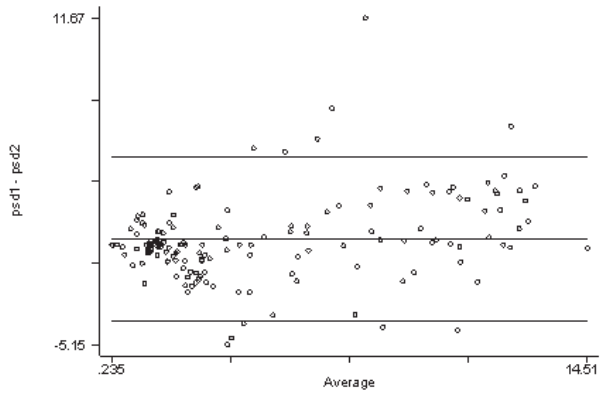

b)

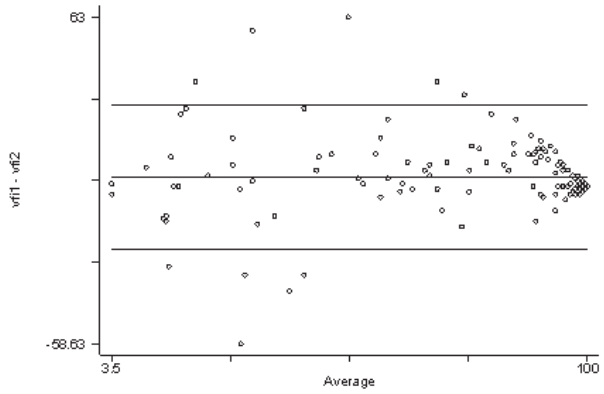

c)

Figure 2. a) Bland Altman plot of the mean deviation values from both the instruments, b) Bland Altman plot of the pattern standard deviation values from both the instruments, c) Bland Altman plot of Visual Field Index values from both the instruments.

for mild/moderate glaucoma was 90% and the true negative proportion for severe was 80%. The sensitivity of Palm Scan VF 2000® VR Visual Field Analyzer for identification of mild/moderate glaucoma was 90.0%, and the specificity was 80.4%. The PPV was 80% and the NPV was 90.2%. We have presented all the diagnostic test properties (estimates and 95% CI) in Table 1.

We also tested the kappa agreement between these two instruments for severity of glaucoma. The overall agreement for severity of glaucoma between these two instruments was 0.63 (95% CI: 0.56-0.78). We have presented kappa values and their 95% CI in Table 2. For classification of glaucoma as moderate or severe, the kappa value was 0.43 (95% CI: 0.22-0.65). The agreement was

Table 1. Table showing the diagnostic test properties (including the Area Under the Curve) of the Palm Scan VF2000® Virtual Reality Visual Field Analyzer in 166 eyes.

	Estimate	95% Confidence Intervals
Glaucoma vs non-glaucoma		
Sensitivity	100%	95.7%-100%
Specificity	100%	95.5%-100%
Positive Predictive Value	100%	95.7%-100%
Negative Predictive Value	100%	95.5%-100%
ROC Area Under the Curve	1.00	1.00-1.00
Type of glaucoma		
Mild/moderate vs severe		
Sensitivity	80.4%	66.1%-90.6%
Specificity	90.0%	76.3%-97.2%
Positive Predictive Value	90.2%	76.9%-97.3%
Negative Predictive Value	80.0%	65.4%-90.4%
ROC Area Under the Curve	0.85	0.78-0.93
Mild vs moderate/severe		
Sensitivity	92.2%	82.7%-97.4%
Specificity	86.4%	65.1%-97.1%
Positive Predictive Value	95.2%	86.5%-99.0%
Negative Predictive Value	79.2%	57.8%-92.9%
ROC Area Under the Curve	0.89	0.81-0.97

Table 2. Table showing the kappa agreement and 95% confidence intervals between Palm Scan VF2000® Virtual Reality Visual Field Analyzer and Humphrey Field Analyzer

	Kappa estimate	95% Confidence Intervals
Glaucoma vs non-glaucoma	1.00	1.00-1.00
Classification of glaucoma		
Mild glaucoma	0.76	0.61-0.92
Moderate glaucoma	0.37	0.14-0.60
Severe glaucoma	0.70	0.55-0.85
Group of glaucoma included		
Mild or moderate	0.49	0.20-0.78
Moderate or severe	0.43	0.22-0.65
Mild or severe	0.67	0.39-0.95

best for classification of glaucoma as mild or severe (kappa: 0.67-95% CI: 0.39-0.94) [Table 2]. We found that the highest proportion of misclassification was in the moderate group; they were classified as mild (28%) or severe (17%). Furthermore, about 20% of severe cases were misclassified as moderate by the VR Visual Field Analyzer [Table 3].

Other Parameters

The ICC for MD was 0.96 (95% CI: 0.94-0.97), for PSD was 0.93 (95% CI: 0.92-0.95), and for VFI was 0.92 (95% CI: 0.90-0.95). The Bland Altman plots for these three parameters are presented in Figures 2a–2c. The median (IQR) fixation loss in

Table 3. Table showing the classification of severity of glaucoma according to Palm Scan VF2000® Virtual Reality Visual Field Analyzer and Humphrey Field Analyzer in 86 glaucomatous eyes.

Humphrey	VR Perimetry			Total
	Mild	**Moderate**	**Severe**	
Mild	1986.36 %	29.09 %	14.55 %	22100 %
Moderate	527.78 %	1055.56 %	316.67 %	18100 %
Severe	00 %	919.57 %	3780.43 %	46100 %
Total	2427.91 %	2124.42 %	4147.67 %	86100 %

χ^2 = 72.053; df = 4; Cramer's V = 0.647; Fisher's $p < 0.001$

the HFA group was 0.45 (0-13.3) and in the Palm Scan VF 2000® VR Visual Field Analyzer group was 0 (0-18.2); the difference was not statistically significant (p = 0.89). Similarly, the median (IQR) difference for false negative responses was not significantly different in both these methods (HFA (Zeiss/USA): 0 [0, 6] vs Palm Scan VF 2000® VR Visual Field Analyzer (MMD/USA): 0 [0, 18]; p = 0.07). However, we found the median (IQR) false positives were significantly higher in the HFA (0 [0, 2]) compared with that of the Palm Scan VF 2000® VR Visual Field Analyzer (0 [0, 0]); the difference was statistically significant (p = 0.0003).

DISCUSSION

This study showed that Palm Scan VF2000® VR Visual Field Analyzer had a perfect agreement with HFA for the detection of glaucoma. The sensitivity and PPV for identifying glaucoma were 100%; however, the sensitivity, specificity, PPV, and NPV was lower for the severity of glaucoma. The agreement was best for the classification of glaucoma as mild or severe; however, the agreement was not good for classification cut-off at mild or moderate, and moderate or severe.

Glaucoma may go unnoticed in the early stages as it starts with loss of peripheral vision. The patient may not realize the loss and hence may not seek any medical advice.[12] Hence, it is important to have screening tools for this disease so that patients in initial stages can be identified because in glaucoma, optic nerve damage is irreversible and it may progress in most cases without appropriate treatment.[13] As seen in our study, the VR Visual Field Analyzer had perfect agreement[14] with the HFA for classification of eyes as glaucomatous or non-glaucomatous; the diagnostic test properties were also good. In fact, the sensitivity and specificity observed in our study was better compared with that of the optical coherence tomography (OCT) for classification of eyes as glaucomatous or non-glaucomatous.[15] Tpaskis and colleagues, and Mees and coworkers found an excellent correlation between these two methods in detecting glaucoma.[7, 16] The main advantage of the HFA is the current gold standard. However, the disadvantages are that it cannot be used in community screenings due to the difficulty in transportation of the instrument or for patients who are unable to sit or are immobile (due to any reason such as post-surgery). The main advantage of the VR perimetry is that it can be used for community- and clinic-based screenings. It can also be used with patients with back pain who have difficulty to sit for perimetry or those who are immobile or confined to the bed.[6, 7] However, it cannot be used to identify the severity of glaucoma and hence is not very useful in the management of the condition in the present form.

It has been suggested that due to the subjectivity in visual filed testing, the variability in examination recorded is likely to be higher when the damage is greater.[7, 17, 18] In general, portable and/or tablet based, or online perimeters have shown to be reliable and assess the visual fields fairly accurately,[8, 19–22] however , a recently published report found that a VR head-mounted device did not identify the deficits reliably.[16] As seen in our study, the agreement between these two instruments was best when the glaucoma was classified as either mild or severe. Furthermore, we did find that a large proportion of moderate glaucoma cases were misclassified as mild. Thus, the present algorithm is not able to classify the glaucoma appropriately.

The study was conducted in a clinic-based setting; this is a more controlled setting with better co-operation by patients. Hence, we may have overestimated some of the diagnostic test properties. For example, patients who came to the clinic were more likely to be aware of glaucoma and its importance for vision. Thus, they are more likely to adhere to all the instructions during these tests. This may influence the test results. It will be appropriate to test the properties of this instrument in community settings as well. Although, we would like to suggest the use of this instrument as a screening tool for glaucoma, a community-based study will provide additional evidence to this effect.

This study is an important contribution to the literature. We went beyond the glaucoma/non-glaucoma differentiation and evaluated the instrument for classification of glaucoma. We did find that the instrument in its current form is able to differentiate between glaucomatous and non-glaucomatous eyes. However, among patients with glaucoma, the instrument is not able to correctly classify the stage of glaucoma. Particularly, moderate glaucoma is more likely to be misclassified as mild or severe. Hence, it cannot replace the HFA in clinical settings in its current form for the management of glaucoma. The algorithm needs to be refined to account for this discrepancy. The instrument may be used in screening of individuals for the presence/absence of glaucoma in community settings, health camps, and clinical practices. It is also useful for those patients who are unable to come to the examination room or sit in the examination chair due to back problems/surgeries, old age, neck problems, and disabilities. However, based on the evidence generated from this study, in the current form, the instrument may only be used as a screening tool for identification of glaucoma.

Financial Support and Sponsorship

Nil.

Conflicts of Interest

There are no conflicts of interest.

REFERENCES

1. Cook C, Foster P. Epidemiology of glaucoma: what's new? *Can J Ophthalmol* 2012;47:223–226.
2. World Health Organization. Blindness and vision impairment [Internet]. WHO; 2019 [cited 2020 February 27]. Available from: https://www.who.int/news-room/fact-sheets/detail/blindness-and-visual-impairment.
3. George R, Ve RS, Vijaya L. Glaucoma in India: estimated burden of disease. *J Glaucoma* 2010;19:391–397.
4. Kulkarni U. Early detection of primary open angle glaucoma: Is it happening? *J Clin Diagn Res* 2012;6:667–670.
5. Alencar LM, Medeiros FA. The role of standard automated perimetry and newer functional methods for glaucoma diagnosis and follow-up. *Indian J Ophthalmol* 2011;59:S53–S58.
6. Wroblewski D, Francis BA, Sadun A, Vakili G, Chopra V. Testing of visual field with virtual reality goggles in manual and visual grasp modes. *Biomed Res Int* 2014;2014:206082.
7. Tsapakis S, Papaconstantinou D, Diagourtas A, Droutsas K, Andreanos K, Moschos MM, et al. Visual field examination method using virtual reality glasses compared with the Humphrey perimeter. *Clin Ophthalmol* 2017;11:1431–1443.
8. Kong YX, He M, Crowston JG, Vingrys AJ. A comparison of perimetric results from a tablet perimeter and humphrey field analyzer in glaucoma patients. *Transl Vis Sci Technol* 2016;5:2.
9. Anderson DR, Drance SM, Schulzer M, Collaborative Normal-Tension Glaucoma Study Group. Natural history of normal-tension glaucoma. *Ophthalmology* 2001;108:247–253.
10. Nayak B, Dharwadkar S. Interpretation of autoperimetry. *J Clin Ophthalmol Res* 2014;2:31–59.
11. Hodapp E, Parrish RI, Anderson D. Clinical decisions in glaucoma. St. Louis, Mo: Mosby; 1993.
12. Cioffi G. Glaucoma. Basic and clinical science course (Book 10). USA: American Academy of Ophthalmology; 2011.
13. McManus JR, Netland PA. Screening for glaucoma: rationale and strategies. *Curr Opin Ophthalmol* 2013;24:144–149.
14. McHugh ML. Interrater reliability: the kappa statistic. *Biochem Med* 2012;22:276–282.
15. Brusini P. OCT Glaucoma Staging System: a new method for retinal nerve fiber layer damage classification using spectral-domain OCT. *Eye* 2018;32:113–119.
16. Mees L, Upadhyaya S, Kumar P, Kotawala S, Haran S, S Rajasekar, et al. Validation of a head mounted virtual reality visual field screening device. *J Glaucoma* 2020;29:86–91.
17. Wall M, Wild J. Perimetry Update 1998/1999: Repeatability of abnormality and progression in glaucomatous standard and SWAP visual fields. Proceedings of the XIIIth International Perimetric Society Meeting; 1998. Gardone Riveira (BS), Italy: Kugler Publications.
18. Wall M, Woodward KR, Doyle CK, Artes PH. Repeatability of automated perimetry: a comparison between standard automated perimetry with stimulus size III and V, matrix, and motion perimetry. *Invest Ophthalmol Vis Sci* 2009;50:974–979.

19. 19. Prea SM, Kong YXG, Mehta A, He M, Crowston JG, Gupta V. Six-month longitudinal comparison of a portable tablet perimeter with the humphrey field analyzer. *Am J Ophthalmol* 2018;190:9–16.

20. Schulz AM, Graham EC, You Y-Y, Klistorner A, Graham SL. Performance of iPad-based threshold perimetry in glaucoma and controls. *Clin Exp Ophthalmol* 2018;46:346–355.

21. Ianchulev T, Pham P, Makarov V, Francis B, Minckler D. Peristat: a computer-based perimetry self-test for cost-effective population screening of glaucoma. *Curr Eye Res* 2005;30:1–6.

22. Lowry EA, Hou J, Hennein L, Chang RT, Lin S, J Keenan, et al. Comparison of peristat online perimetry with the humphrey perimetry in a clinic-based setting. *Transl Vis Sci Technol* 2016;5:4.

Original Article

Structural and Functional Outcomes of Surgery for Lamellar Macular Holes with or without Epimacular Proliferations

Ramesh Venkatesh, MS; Arpitha Pereira, DO, DNB; Kushagra Jain, MS; Naresh Kumar Yadav, DO, FMRF

Department of Retina-Vitreous, Narayana Nethralaya Eye Hospital, Rajaji Nagar, Benguluru, India

ORCID:

Ramesh Venkatesh: https://orcid.org/0000-0002-4479-9390

Abstract

Purpose: To compare the clinical, optical coherence tomography (OCT) features, and surgical outcomes of lamellar macular hole (LMH) depending on the presence of epimacular membrane proliferation (EMPF).

Methods: This retrospective chart review included 112 eyes with LMH. The patients were divided into two groups depending on the presence of EMPF. Group 1 had LMH without EMPF and Group 2 had LMH with EMPF. The best-corrected visual acuity was recorded and OCT scans were obtained.

Results: Lamellar macular hole without and with EMPF was noted in 62 (55%) and 50 (45%) eyes, respectively. The presence of EMPF was associated with lower presenting visual acuity ($P = 0.049$), wider LMH size at the largest diameter on the horizontal scan ($P = 0.001$), thinner residual retinal tissue ($P = <0.0001$), and larger IS-OS defects ($P = <0.0001$) as compared to the non-EMPF group. Of the 112 eyes, 18 eyes underwent surgery for LMH. Seven eyes had EMPF and the remaining eleven did not have EMPF. The average follow-up time for patients post-surgery and under observation was 16.8 and 24.1 weeks, respectively. A significant improvement in visual acuity was noted in the operated eyes with no EMPF as compared to the eyes with EMPF ($P = 0.008$). Worsening visual acuity ($P = 0.021$) was noted in eyes with LMH associated with EMPF which did not undergo surgery. Eyes with LMH and no EMPF, which were not operated on showed a minimal negative change in visual acuity.

Conclusion: LMH with EMPF showed a higher association with accompanying ellipsoid zone disruption. Better anatomical and functional outcomes were achieved in those eyes that underwent surgery for LMH with no presence of EMPF and ellipsoid zone defect.

Keywords: Epimacular Membrane Proliferation; Full-Thickness Macular Hole; Lamellar Hole Epithelial Proliferation; Lamellar Macular Hole; Surgery

J Ophthalmic Vis Res 2022; 17 (1): 42–50

INTRODUCTION

Epimacular membrane proliferation (EMPF) was previously described as a "thick" epiretinal membrane (ERM) by Witkin et al in 2006, "dense non-tractional membrane" by Parolini et al in 2011, and then more commonly as the lamellar hole epithelial proliferation (LHEP) by Pang and associates in 2014.[1–3] This different type of ERM seen in cases of lamellar macular holes (LMH) on high-resolution optical coherence tomography (OCT) was identified as a homogenous mass of medium reflectivity lying over the retinal surface.[3] In 2015, Schumann et al renamed this phenomenon as "atypical epiretinal tissue", because it occurred in conditions other than LMH, such as in a full-thickness macular hole (FTMH) condition.[4] The commonly accepted hypothesis for the formation of LMH is that it arises from the ERM contraction, which then results in a tear in the inner retinal layers.[2, 5] During clinical examination, EMPF is identified as a yellow elastic jelly lying over the epiretinal surface and commonly associated with a thick non-contractile ERM. Its yellowish color is likely due to the xanthophyll pigment identified in histological analysis.[2, 6] Despite the absence of a clear mechanism for EMPF formation, the most likely theory is that it results from the migration of the retinal Muller glial cell.[3] The association of the EMPF with higher rates of ellipsoid disruption and positivity to pan-keratin created another theory of the retinal pigment epithelial origin of the disease.[4, 7–10] It has been reported that patients with EMPF tend to have lower baseline visual acuities, greater external MH diameters, thinner residual retinal tissue, and higher rates of inner segment-outer segment (IS-OS) band disruption when compared to non-EMPF eyes.[4, 7, 9] Visual acuity in eyes with LMH varies from having baseline normal vision to having lower visual acuities depending upon the integrity of the ellipsoid zone. A wide variety of anatomic and visual outcomes has been reported after the performance of vitrectomy for macular holes with and without EMPF presence. Marques et al reported no differences in visual performance or closure rates between the EMPF group and non-EMPF group after surgery or in the subset of patients who did not undergo treatment.[11] One paper reported a significantly poor visual outcome for patients with LMH and EMPF after surgery,[6] while another study showed an increase in area of EMPF and a decline in the visual function in eyes who were managed conservatively.[12] The majority of retinal specialists in the Indian subcontinent tend to manage the cases of LMH conservatively either because of underlying ellipsoid layer integrity, better presenting visual acuity, or associated poor visual prognosis. Given the variable characteristics in the physical and structural properties of EMPF, there are no clear guidelines currently available regarding patient selection and timing of surgery in such eyes with LMHs. In addition, to the best of our knowledge, there is no reported literature from the Indian subcontinent describing this clinical entity in these eyes or discussing the treatment outcomes either from surgery or through conservative management. In this report, we intend to analyze the morphological changes and visual outcomes of the LMH cases that presented with EMPF, and describe the surgical outcomes. By comparing the clinical and surgical data from the LMH cases with and without EMPF, we intend to appreciate and understand better the significance of this unique epimacular proliferation. The objective of this study is also to make the readers aware of this clinical entity in clinical/OCT examinations and to encourage them to understand the relevance and impact it can have on the final outcome of the disease.

METHODS

This study was approved by Narayana Nethralaya institutional review board and ethics committee

Correspondence to:

Ramesh Venkatesh, MS. Vitreo Retina consultant, Narayana Nethralaya Eye Hospital, 121/C, Chord Road, 1st 'R' Block, Rajaji Nagar, Benguluru 560010, India.
Email: vramesh80@yahoo.com

Received 05-12-2019; Accepted 22-11-2021

Access this article online

Website: https://knepublishing.com/index.php/JOVR

DOI: 10.18502/jovr.v17i1.10169

How to cite this article: Venkatesh R, Pereira A, Jain K, Yadav NK. Structural and Functional Outcomes of Surgery for Lamellar Macular Holes with or without Epimacular Proliferations. J Ophthalmic Vis Res 2022;17:42–50.

(C-2019/01/003). This retrospective study was conducted at the retina clinic of a tertiary eye hospital in Southern India. In this study, a single observer (RV) reviewed the SD-OCT images acquired by the Spectralis, Heidelberg machine, which were saved in the folders labelled as lamellar macular hole and epiretinal membrane between the January 2011 and December 2018. The diagnosis of LMH was based on the updated criteria proposed by the International Vitreomacular Traction Study Group.[13] According to the group, LMH is a non-full-thickness retinal defect seen at the macula. This defect is characterized by the presence of the following features on the SD-OCT: (1) an irregular foveal contour; (2) inner foveal defect; (3) intraretinal splitting, typically between the outer plexiform and outer nuclear layers; and (4) presence of a photoreceptor layer at the base of the hole. The OCT images were viewed to identify the presence or absence of EMPF in these eyes. EMPF was identified on the OCT imaging as a homogenous material of medium reflectivity arising from the outer retinal layers, crawling along the walls of the macular hole and lying on the epiretinal surface. The eyes were categorized into two groups for further analysis: (1) LMH with no EMPF and (2) LMH with EMPF. Demographic data records included age, gender, laterality, and Snellen visual acuity (VA) at presentation. Features on OCT which were recorded included presence of LMH, EMPF, IS-OS defect, and ERM. The macular hole size in LMH was measured as the widest horizontal diameter at the level of the middle retinal layers at the foveal center. The length of the IS-OS defect and thickness of residual retinal tissue in LMH were manually measured at the fovea using the calipers provided with the software. The LMHs observed on the OCT were further divided into tractional or degenerative types based on the classification proposed by Govetto et al.[14] The tractional type was characterized by the schitic separation of neurosensory retina between outer plexiform and outer nuclear layers with an intact ellipsoid layer and was associated with tractional epiretinal membranes and/or vitreomacular traction at the fovea. The degenerative type was characterized by the presence of intraretinal cavitation, non-tractional epiretinal proliferation, a retinal ”bump” and with an early ellipsoidal zone defect. In addition, other documented data included treatment and outcome of surgery for the LMH, postoperative VA, and anatomic status of the macular hole. The indications to operate in the LMH group were visual acuity < 6/12, patient who complained of metamorphopsia and had a presence of an epiretinal membrane. In the present study, we looked at patients with a minimum follow-up of eight weeks following surgery to analyze the outcomes. Successful macular hole closure was defined as the collapse of the excavation between the outer nuclear and outer plexiform layers while achieving a normal foveal contour.

Surgical Technique

All the surgeries were performed by a single surgeon (NKY). A three-port 23- or 25-gauge pars plana vitrectomy was performed. After core vitrectomy, intravitreal triamcinolone acetonide was injected to stain the posterior cortical vitreous and the posterior vitreous detachment was then induced. In cases where epimacular membrane was present, removal was performed. Care was taken to not forcibly peel the ERM from the edge of the LMH. A vitrectomy cutter was used to trim and leave the adherent epiretinal tissue at the margin of the hole. An attempt was made to remove the EMPF that was lying over the internal limiting membrane (ILM). A 0.1–0.2 cc of Brilliant Blue Green (BBG) dye was injected to stain the ILM to facilitate its removal from the macular area. If the ERM was difficult to identify, BBG-assisted ILM peeling was done from outside the ERM-covered area that was not stained. The ERM was then removed along with the ILM. Again, care was taken to not forcibly peel the ERM/ILM from the edge of the hole. Finally, air–fluid exchange was done and 15 % perfluoropropane (C3F8) or 20% Sulphur hexafluoride (SF6) gas was used for an endotamponade procedure. A minimum of seven days of prone positioning was recommended.

Statistical Analysis

Normal distribution of quantitative variables was checked using the Kolmogorov–Smirnov test. Snellen’s vision data were converted to logarithm of minimum angle of resolution (logMAR) vision for statistical analysis. Categorical variables were labelled as numerical for easy analysis as in identification of the IS-OS defects, the ERM, and

the hole closures. Value 1 indicated presence and value 0 absence of these findings. Categorical variables between the two groups were compared using the Chi-square test. The Mann–Whitney U-test was used to compare quantitative data between the two groups. Correlations between the presence of EMPF and other variables were determined using the Spearman correlation test. A correlation (*r*) value of 0 means no correlation between the two variables while values closer to –1 indicate strong negative correlation and values closer to +1 indicate strong positive correlation. For the analysis of surgical outcomes, the eyes were divided into two groups: (1) eyes with EMPF and (2) eyes without EMPF. Wilcoxon signed-rank test was applied for the comparison of VA changes in the two groups. All data were analyzed with GraphPad Prism software (version 8.1.1). *P*-values < 0.05 were considered statistically significant.

RESULTS

During the study period, a total of 112 eyes with LMHs were included. The number of eyes included in each group were: (1) Group 1 – Eyes with LMH and no EMPF (62, 55%); (2) Group 2 – Eyes with LMH and EMPF (50, 45%).

The comparison of clinical and OCT findings of patients with lamellar macular hole presenting with and without EMPF is described in Table 1 and depicted in Figure 1.

Tractional types of LMH were identified in 25 (22%) eyes, the degenerative types of LMH in 81 (72%) eyes, and mixed variety in 6 (6%) eyes. EMPF was most commonly seen with the degenerative type of LMH (45/50, 90%) followed by the mixed type (5/50, 10%). ERM was absent in eight eyes with EPMF and LMH. Analysis of presence of EMPF with different OCT features showed strong positive correlations with the presence (r = 0.742) and size (r = 0.743) of IS-OS defects while strong negative correlation was noted with thickness of the residual retinal tissue (r = –0.641) present within the MH [Table 2].

Moreover, 18 of the 112 (16%) cases with LMH were treated surgically using the pars plana vitrectomy procedure. The remainder of the cases were managed conservatively. Of the 18 eyes which underwent surgery, 7 eyes had EMPF. Table 3 compares the clinical and OCT features of eyes with and without EMPF that were operated on. The width of the LMH (p = 0.027), size of the IS-OS defect (p = 0.002), and residual retinal tissue thickness (p = 0.000) showed statistically significant correlation between the two groups. The average follow-up period for patients post-surgery was 16.8 weeks. Single surgery hole closure was achieved in 4 (57%) eyes and 11 (100%) eyes in cases with and without EMPF, respectively. Of the remaining three eyes where surgical success was not achieved due to the development of a full-thickness macular hole, repeat surgery introducing a fluid-air exchange and silicone oil/intraocular gas tamponade was performed in all the eyes. In two eyes the hole closed while in one eye the hole remained open despite the second surgery. In the observation group, 43 of the 94 (46%) eyes, which were managed by observation, showed EMPF on the SD-OCT scans. However, by the end of the final follow-up visit, an additional 16 eyes showed development of EMPF, thus increasing the number to 59 (63%) eyes for those who were managed conservatively. The average follow-up period for patients under observation was 24.1 weeks.

The mean preoperative visual acuity in eyes with EMPF and without EMPF was 0.5 (20/63) and 0.592 (20/78) (p = 0.052), respectively. The eyes in the EMPF group showed a mean decrease of –0.312 logMAR units (p = 0.797) in visual acuity following surgery while eyes in the non-EMPF group showed a mean of 0.272 logMAR units' improvement (p = 0.008) following surgery. By the end of the final follow-up visit, a significant decrease in visual acuity was noted in eyes with LMH and EMPF who were managed conservatively (p = 0.021). Eyes with LMH and no EMPF who were managed conservatively showed a minimal worsening in visual acuity.

Changes in the visual acuity in the two groups before and after surgery is described in Table 4.

DISCUSSION

The use of spectral domain OCT has allowed us to visualize the presence of substantive material on the epiretinal surface in the LMH and the FTMH which we describe as EMPF or LHEP as described by Pang et al.[3] In this article, we studied the clinical and OCT features and surgical outcomes of LMHs with and without EMPF.

The findings in this study suggest that in LMHs, EMPF formation was accompanied by

ellipsoid layer loss, a wider than normal macular hole diameter, deep retinal defects, and the presence of IS-OS defects in large-sized MHs. The ERM was not present in all the cases of EMPF. The EMPF was yellowish in color and connected to the retinal tissue within the hole. Taken together, these findings suggested that EMPF could be a secondary event following LMH formation and is usually accompanied with deep outer retina involvement. Also, histological studies have shown absence of the inner retinal tissue within the epiretinal tissue.[2] Many theories were proposed for the development of EMPF in LMH; however, none are conclusive.[3, 4, 10] The findings of this study reinforce an alternate theory for the EMPF formation. According to this theory, EMPF originates secondary to the defects in the ellipsoid zone which then allows the retinal pigment epithelial cells to migrate along the walls of the MH and then onto the retinal surface and finally leading to EMPF and ERM formation.

The prevalence of EMPF in LMH has ranged from 20.5% to 44% in previous studies.[3, 7, 8, 16] In our study, EMPF was noted in 44% of eyes with LMH. This is comparable to that observed with other studies. EMPF was seen more commonly with the degenerative variety of LMH (90%) as compared to the mixed or tractional variety. The presence of EMPF was associated with lower presenting visual acuity, larger MH size, thinner residual retinal tissue, and larger IS-OS defects before operation. As a result, the visual and anatomical outcomes following surgery in these eyes were significantly different from those with no EMPF. Eyes with LMH with EMPF showed no visual acuity gain following surgery. Also, successful anatomic closure of the MH was achieved in only four of the seven (57%) eyes following surgery compared to that of the non-EMPF group where the MH closed in all cases (100%). Similar observations were also noted by Choi et al and Ko et al where the visual outcomes in LHEP group was poorer as compared to the eyes with no LHEP.[7, 16] However, Lai et al reported no difference in the visual and anatomic outcomes between the LHEP group and non-LHEP group following surgery.[8] In their study, the largest mean diameter on the horizontal scan of the LMH in eyes with LHEP (98.4 μ) was less than the eyes with no LHEP (146.9 μ). While in our study, eyes with LMH with EMPF (1282 μ) had wider large mean diameters on the horizontal scan as compared to eyes with no EMPF (715 μ). Also, the IS-OS defects were much larger in eyes with EMPF (808 μ) than in eyes with no EMPF (54.4 μ). This would explain the poor visual and anatomic outcomes following surgery in our study.

The recommendations for the surgical repair of eyes with LMH remain controversial.[15, 16] While there have been reports with good surgical outcomes,[17, 18] there have also been reports that have advised caution with performing vitrectomy in these cases.[1, 2] In our series, only 18 of the 112 (16%) eyes with LMH underwent surgery. The rest of the eyes were managed conservatively through observation. In the observation group, 43 of the 94 (46%) eyes, which were managed by observation, showed EMPF on the SD-OCT scans, this category further increased to 63% by the end of the final follow-up visit. Thus, suggesting that solely observing such cases may lead to progression of the outer retinal defects and EMPF formation, ultimately leading to decrease in vision. Consequently, we recommend surgery for eyes with LMH when visual acuity is 6/18 or less, there is the presence of epiretinal membrane causing retinal traction, presence of an intact ellipsoid zone, progression in the size of LMH on follow-up visits or progression to full-thickness within the macular hole.

During surgery in cases that possess LMH with EMPF, it is recommended to peel the proliferative tissue while peeling the ERM. The cellular composition of the EMPF may lead to the recurrence of the ERM formation if not removed completely. However, aggressive peeling of the EMPF may lead to the conversion of the LMH to FTMH as seen in three cases in this study. Care should be taken to not forcibly pull the ERM from the edge of the hole. Applying the least amount of traction as possible may theoretically reduce the possibility of retinal tissue damage or the formation of FTMH. In fact, a few studies have reported a high incidence of FTMH formation after the LHEP was peeled in surgeries for LMH.[2, 3] Shiraga et al recommended inversion of the pigment containing proliferative tissue into the LMH to facilitate normalization of the foveal contour;[21] however, we did not practice this technique in any of our cases. We did a conventional ILM peeling extending from arcade to arcade in all our cases with the intention of removing the cellular proliferative tissue where possible without much damage to the retina. In some cases, it is sometimes easier to start peeling

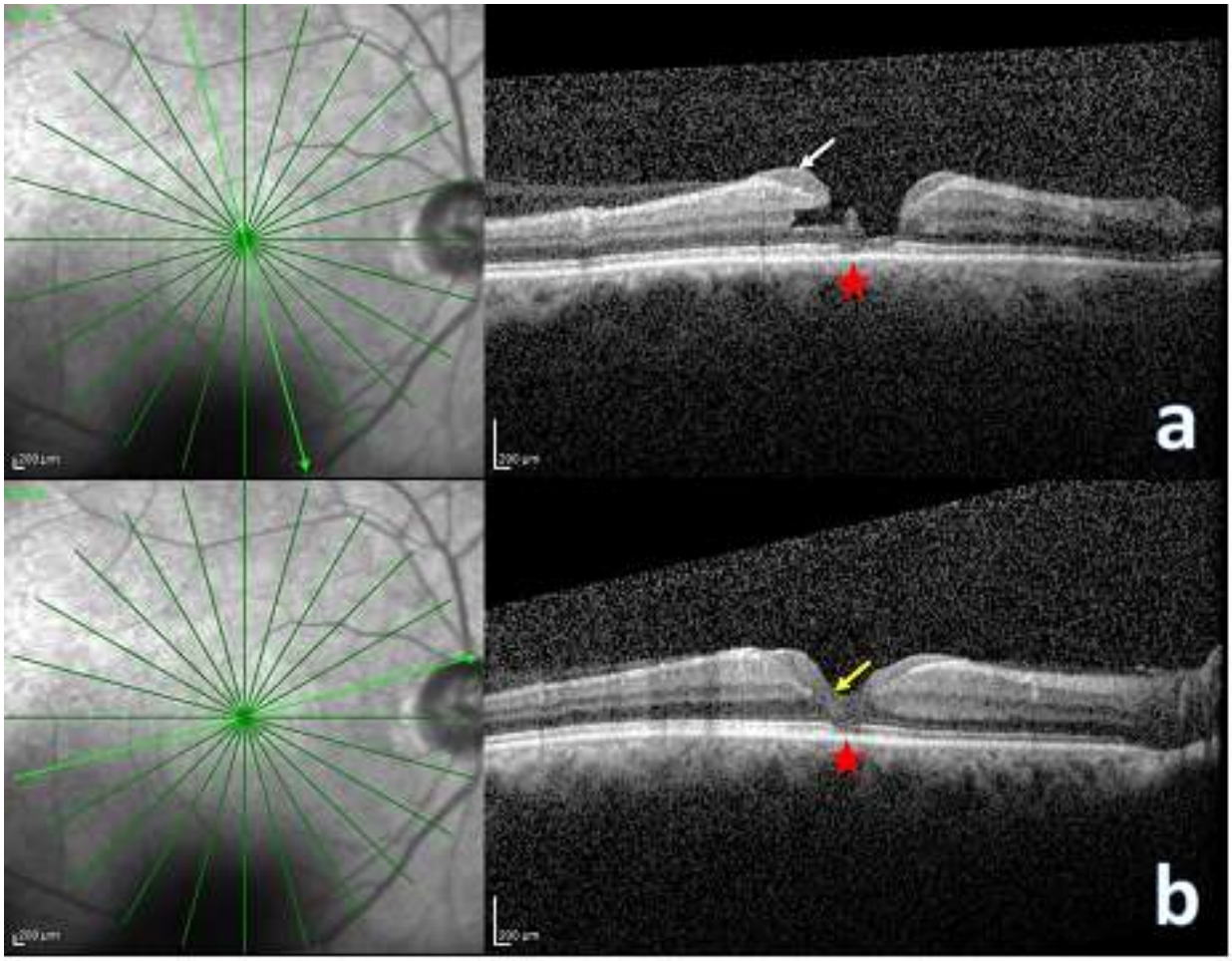

Figure 1. Lamellar macular hole (LMH) with EMPF. (a) Optical coherence tomography (OCT) image of a patient with LMH in right eye showing the presence of epiretinal proliferative tissue at the margin of the hole (white arrow) with presence of ellipsoid zone defect (red star). (b) Another OCT scan passing through a different section acquired on the same day demonstrating the extension of the proliferative tissue (yellow arrow) from the ellipsoid zone defect (red star) and then crawling along the walls of the macular hole to lie over the retinal surface.

Table 1. Clinical and optical coherence tomography findings of patients with and without EMPF in eyes with LMH

Variable	LMH without EMPF (n = 62)	LMH with EMPF (n = 50)	P-value
Mean age (yr)	72.6 ± 8.25	69.9 ± 13.0	0.316[#]
Sex (M:F)	26:36	33:17	0.667[#]
Laterality (RE:LE)	35:27	31:19	0.667[*]
Mean presenting logMAR VA (Snellen equivalent)	0.396 (20/50)	0.518 (20/66)	0.05[#]
Size of LMH (µm)	715 ± 305	986 ± 471	0.001[#]
Residual retinal thickness (µm)	144 ± 28.1	102 ± 33.7	<0.001[#]
Presence of IS-OS defect (*n*, %)	8 (13)	42 (84)	>0.999[*]
Size of IS-OS defect (µm)	32.8 ± 101	401 ± 389	<0.001[#]
Presence of ERM (*n*, %)	52 (84)	42 (84)	0.667[*]
Eyes undergoing surgery (*n*, %)	11 (18)	7 (14)	0.667[*]

LMH, lamellar macular hole; EMPF, epimacular proliferative tissue; VA, visual acuity; ETDRS, Early Treatment Diabetic Retinopathy Study; IS–OS, inner segment–outer segment; ERM, epiretinal membrane [#]*P*-value calculated using the Mann–Whitney U-test; [*]*P*-value calculated using the Chi-square test

Table 2. Correlation of EMPF with different clinical and OCT variables

		Age	Sex	Pre-op log MAR VA	Type of LMH	Width of LMH	Thickness of residual retinal tissue	IS–OS defect	Size of the IS–OS defect	ERM	Post op logMAR VA	LMH closure
EMPF	*r* value	–0.145	–0.243	–0.257	0.327	0.233	–0.641	0.742	0.743	–0.082	–0.641	–0.665
	p-value[#]	0.107	0.007	0.004	0.000	0.009	0.000	0.000	0.000	0.367	0.001	0.000

EMPF, epimacular proliferative tissue; VA, visual acuity; LMH, lamellar macular hole; IS–OS, inner segment–outer segment; ERM, epiretinal membrane [#]*P*-value calculated using Spearman' correlation test

Table 3. Surgical outcomes in eyes with and without EMPF

Variable	Surgery in EMPF cases (n = 7)	Surgery without EMPF cases (n = 11)	P-value
Pre-op mean logMAR VA (Snellen equivalent)	0.5 (20/63)	0.592 (20/78)	0.052#
MH width (μm)	1232 ± 528	795 ± 252	0.027#
Residual retinal thickness (μm)	82.1 ± 16.3	143 ± 30	0.0004#
Presence of IS–OS defect (*n*, %)	6(86)	2(18)	0.013*
Size of IS–OS defect (μm)	808 ± 757	54.4 ± 128	0.002#
Presence of ERM (*n*, %)	6(86)	10(91)	>0.999*
Hole closure achieved (*n*, %)	4(57)	11(100)	0.043*
Post op mean logMAR VA (Snellen equivalent)	0.518 (20/130)	0.32 (20/42)	0.001#

VA, visual acuity; EMPF, epimacular proliferative tissue; MH, macular hole; IS–OS, inner segment–outer segment; ERM, epiretinal membrane #*P*-value calculated using the Mann–Whitney U-test; **P*-value calculated using the Chi-square test

Table 4. Visual acuity changes before and after surgery in eyes with and without EMPF

	Mean Pre-op logMAR VA (Snellen equivalent)	Mean Post-op logMAR VA (Snellen equivalent)	P-value#
Surgery in EMPF	0.5 (20/63)	0.812 (20/130)	0.797
Surgery in no EMPF	0.592 (20/78)	0.32 (20/42)	0.008

EMPF, epimacular proliferative tissue; VA, visual acuity; ETDRS, Early Treatment Diabetic Retinopathy Study; MH, macular hole #*P*-value calculated using the Wilcoxon signed rank test

by first engaging the ILM not occupied by the ERM, and then removing the ILM along with the ERM.

Our study has several clinical implications. Our study suggests that surgery in eyes with LMH with EMPF have both poor anatomic and visual prognosis. Intervention in eyes with LMH without EMPF/LHEP and without ellipsoid zone disruption can have better visual and surgical prognosis.

Our study has the advantage of having an adequate number of eyes both with and without EMPF in LMHs for evaluation. The descriptive features of eyes with EMPF on OCT confirms the outer retinal damage theory of EMPF origin. The study also describes the surgical outcomes of patients operated for LMH with EMPF. The most significant limitation of our study is its retrospective design in accessing pertinent data for evaluation. Our study was further limited as there was only a single observer evaluating the OCT scans, in addition, only a small number of eyes underwent surgery for management of LMH . Extensive clinical and pathological studies may be required to complement our observations and to provide answers to the questions of the cellular origin of EMPF and the reason for its recurrence following surgery.

From this study, we can conclude that EMPF in LMH has a poor visual prognosis when accompanied with ellipsoid zone disruption. Better functional and anatomical outcomes can be achieved following surgery when LMH are not associated with EMPF and/or ellipsoid zone disruption.

Financial Support and Sponsorship

Nil.

Conflicts of Interest

There are no conflicts of interest.

REFERENCES

1. Witkin AJ, Ko TH, Fujimoto JG, Schuman JS, Baumal CR, Rogers AH, et al. Redefining lamellar holes and

the vitreomacular interface: an ultrahigh-resolution optical coherence tomography study. *Ophthalmology* 2006;113:388–397.

2. Parolini B, Schumann RG, Cereda MG, Haritoglou C, Pertile G. Lamellar macular hole: a clinicopathologic correlation of surgically excised epiretinal membranes. *Invest Ophthalmol Vis Sci* 2011;52:9074–9083.
3. Pang CE, Spaide RF, Freund KB. Epiretinal proliferation seen in association with lamellar macular holes: a distinct clinical entity. *Retina* 2014;34:1513–1523.
4. Schumann RG, Compera D, Schaumberger MM, Wolf A, Fazekas C, Mayer WJ, et al. Epiretinal membrane characteristics correlate with photoreceptor layer defects in lamellar macular holes and macular pseudoholes. *Retina* 2015;35:727–735.
5. Gass JD. Lamellar macular hole: a complication of cystoid macular edema after cataract extraction. *Arch Ophthalmol* 1976;94:793–800.
6. Obana A, Sasano H, Okazaki S, Otsuki Y, Seto T, Gohto Y. Evidence of carotenoid in surgically removed lamellar hole-associated epiretinal proliferation. *Invest Ophthalmol Vis Sci* 2017;58:5157–5163.
7. Choi WS, Merlau DJ, Chang S. Vitrectomy for macular disorders associated with lamellar macular hole epiretinal proliferation. *Retina* 2018;38:664–669.
8. Lai TT, Chen SN, Yang CM. Epiretinal proliferation in lamellar macular holes and fullthickness macular holes: clinical and surgical findings. *Graefes Arch Clin Exp Ophthalmol* 2016;254:629–638.
9. dell'Omo R, Virgili G, Rizzo S, De Turris S, Coclite G, Giorgio D, et al. Role of lamellar hole-associated epiretinal proliferation in lamellar macular holes. *Am J Ophthalmol* 2017;175:16–29.
10. Son G, Lee JS, Lee S, Sohn J. Epiretinal proliferation associated with macular hole and intraoperative perifoveal crown phenomenon. *Korean J Ophthalmol* 2016;30:399–409.
11. Marques MF, Rodrigues S, Raimundo M, Costa J, Marques JP, Alfaiate M, et al. Epiretinal proliferations associated with lamellar macular holes: clinical and surgical implications. *Ophthalmologica* 2018;240:8–13.
12. Compera D, Schumann RG, Cereda MG, Acquistapace A, Lita V, Priglinger SG, et al. Progression of lamellar hole-associated epiretinal proliferation and retinal changes during long-term follow-up. *Br J Ophthalmol* 2018;102:84–90.
13. Duker JS, Kaiser PK, Binder S, de Smet MD, Gaudric A, Reichel E, et al. The International Vitreomacular Traction Study Group classification of vitreomacular adhesion, traction, and macular hole. *Ophthalmology* 2013;120:2611–2619.
14. Govetto A, Dacquay Y, Farajzadeh M, Platner E, Hirabayashi K, Hosseini H, et al. Lamellar macular hole: two distinct clinical entities? *Am J Ophthalmol* 2016;164:99–109.
15. Ko J, Kim GA, Lee SC, Lee J, Koh HJ, Kim SS, et al. Surgical outcomes of lamellar macular holes with and without lamellar hole-associated epiretinal proliferation. *Acta Ophthalmol* 2017;95:e221–e226.
16. Kokame GT, Tokuhara KG. Surgical management of inner lamellar macular holes. *Ophthalmic Surg Lasers Imaging* 2010;41:418–424.
17. Witkin AJ, Castro LC, Reichel E, Rogers AH, Baumal CR, Duker JS, et al. Anatomic and visual outcome of vitrectomy for lamellar macular holes. *Ophthalmic Surg Lasers Imaging* 2010;5:1–7.
18. Garrettson BR, Pollack JS, Ruby AJ, Drenser KA, Williams GA, Sarrafizadeh R, et al. Vitrectomy for a symptomatic lamellar macular hole. *Ophthalmology* 2008;115:884–886.
19. Sun JP, Chen SN, Chuang CC, Lin CW, Lin CJ, Huang JY, et al. Surgical treatment of lamellar macular hole secondary to epiretinal membrane. *Graefes Arch Clin Exp Ophthalmol* 2013;251:2681–2688.
20. Ubukata Y, Imai H, Otsuka K, Nishizaki M, Hara R, Uenishi M, et al. The comparison of the surgical outcome for the full-thickness macular hole with/without lamellar hole-associated epiretinal proliferation. *J Ophthalmol* 2017;2017:9640756.
21. Shiraga F, Takasu I, Fukuda K, Fujita T, Yamashita A, Hirooka K, et al. Modified vitreous surgery for symptomatic lamellar macular hole with epiretinal membrane containing macular pigment. *Retina* 2013;33:1263–1269.

Original Article

Mutation Screening of Six Exons of *ABCA4* in Iranian Stargardt Disease Patients

Ensieh Darbari[1], PhD; Hamid Ahmadieh[2,3], MD; Narsis Daftarian[2,3], MD; Mozhgan Rezaei Kanavi[2,3], PhD; Fatemeh Suri[2], PhD; Hamideh Sabbaghi[4,5], PhD; Elahe Elahi[1*], PhD

[1]*School of Biology, College of Science, University of Tehran, Tehran, Iran*
[2]*Opthalmic Research Center, Research Institute for Ophthalmology and Vision Science, Shahid University of Medical Sciences, Tehran, Iran*
[3]*Ocular Tissue Engineering Research Center, Research Institute for Ophthalmology and Vision Science, Shahid Beheshti University of Medical Sciences, Tehran, Iran*
[4]*Ophthalmic Epidemiology Research Center, Research Institute for ophthalmology and Vision Science, Shahid Beheshti University of Medical Sciences, Tehran, Iran*
[5]*Department of Optometry, School of Rehabilitation, Shahid Beheshti University of Medical Sciences, Tehran, Iran*

ORCID:
Ensieh Darbari: https://orcid.org/0000-0003-1050-6999
Elahe Elahi: https://orcid.org/0000-0002-6897-2223

Abstract

Purpose: Stargardt disease type 1 (STGD1) is a recessively inherited retinal disorder that can cause severe visual impairment. *ABCA4* mutations are the usual cause of STGD1. *ABCA4* codes a transporter protein exclusively expressed in retinal photoreceptor cells. The gene contains 50 exons. Mutations are most frequent in exons 3, 6, 12, and 13, and exons 10 and 42 each contain two common variations. We aimed to screen these exons for mutations in Iranian STGD1 patients.
Methods: Eighteen STGD1 patients were recruited for genetic analysis. Diagnosis by retina specialists was based on standard criteria, including accumulation of lipofuscin. The six *ABCA4* exons were PCR amplified and sequenced by the Sanger method.
Results: One or more *ABCA4*-mutated alleles were identified in 5 of the 18 patients (27.8%). Five different mutations including two splice site (c.1356+1G>A and c.5836-2A>G) and three missense mutations (p.Gly1961Glu, p.Gly1961Arg, and p.Gly550Arg) were found. The p.Gly1961Glu mutation was the only mutation observed in two patients.
Conclusion: As *ABCA4* mutations in exons 6, 12, 10, and 42 were identified in approximately 25% of the patients studied, these may be appropriate exons for screening projects. As in other populations, STDG1 causative *ABCA4* mutations are heterogeneous among Iranian patients, and p.Gly1961Glu may be relatively frequent.

Keywords: *ABCA4*; Mutation Screening; Retinal Dystrophy; Stargardt Disease; STGD1

J Ophthalmic Vis Res 2022; 17 (1): 51–58

INTRODUCTION

Stargardt disease type 1 (STGD1: OMIM No. 248200) is a relatively common form of macular dystrophy with a prevalence of 1 in 8000 to 1 in 10,000.[1, 2] It is a genetic disease with an autosomal recessive pattern of inheritance. Stargardt disease begins in childhood or young adulthood, and causes progressive bilateral loss of central vision,

Correspondence to:
Elahe Elahi, PhD. College of Science, University of Tehran, Tehran, Iran.
Email: elaheelahi@ut.ac.ir, elahe.elahi@gmail.com

Received 19-11-2020; Accepted 21-05-2021

Access this article online

Website: https://knepublishing.com/index.php/JOVR

DOI: 10.18502/jovr.v17i1.10170

How to cite this article: Darbari E, Ahmadieh H, Daftarian N, Kanavi MR, Suri F, Sabbaghi H, Elahi E. Mutation Screening of Six Exons of *ABCA4* in Iranian Stargardt Disease Patients. J Ophthalmic Vis Res 2022;17:51–58.

impairment of color vision, and degeneration of retinal pigment epithelium (RPE) cells.[2, 3] Accumulation of orange–yellow flecks in the macula is often observed during ophthalmoscopic examination. *ATP-binding cassette sub-family A member 4* (*ABCA4*, OMIM: 601691; also known as ABCR) is the most important Stargardt disease-causing gene.[4–10] This gene is positioned on chromosome 1p21-p22, contains 50 exons, and encodes a 2273 amino acid protein that belongs to ABC transporter protein family. ABC transporter proteins have four essential domains, including two transmembrane domains (TMDs) and two cytoplasmic nucleotide-binding domains (NBDs). TMDs are responsible for translocation of substrates, and NBDs bind to ATP and hydrolyze ATP to ADP to produce energy for the translocation. *ABCA4* expression is specific to the retina and its protein product is responsible for the transport of vitamin A derivatives in the outer segment disc membranes of photoreceptors.[11, 12] Mutations in the gene result in accumulation of toxic bisretinoid adducts in RPE cells, eventually leading to RPE cell death and macular degeneration.[13]

In addition to STGD1, mutations in *ABCA4* can cause several other types of retinal degenerative diseases.[14–16] This suggests a complex genotype/phenotype relationship between mutations in the gene and the consequent phenotypes. Additionally, the number of sequence variations and disease-associated variations in *ABCA4* is astounding. Variability in frequencies of the variations in different populations is also notable. The Human Genome Mutation Database (HGMD, http://www.hgmd.cf.ac.uk) reports 1467 mutations in the *ABCA4* gene as cause of various retinal degenerative diseases; 629 of the mutations are associated with STGD1. The Genome Aggregation Database (gnomAD v2.1.1; https://gnomad.broadinstitute.org) reports 3979 sequence variations for *ABCA4*, including exonic, intronic, UTR, splicing, and INDEL variations; the frequency of 3930 of these is <0.01. The Iranome database (http://www.iranome.ir) which comprises exome sequence data on 800 healthy Iranians reports 389 *ABCA4* sequence variations, and the frequency of 301 of these is <0.01. Clearly, common sequence variations are unlikely to contribute to disease status, but rare variations may have deleterious effects.

Here, we report the results of mutation screening of six exons of the *ABCA4* gene in 18 unrelated Iranian Stargardt disease patients. To the best of our knowledge, mutation screening of this gene in Iranians has not been previously reported. Among the 50 exons of *ABCA4*, exons that were more likely to contain mutations were screened. Based on the HGMD database, more mutations have been reported in exons 3, 6, 12, and 13 than in other exons. These exons of *ABCA4* have, respectively, 33, 33, 39, and 45 reported mutations. In addition to these, exons 10 and 42 were also screened. A common nucleotide sequence variation that causes p.His432Arg is positioned in exon 10. Although now considered a polymorphism, this variation was earlier thought to contribute to disease status. Exon 42 was screened because the most frequent disease-associated variation in various populations is positioned within this exon. This variation causes p.Gly1961Glu.

METHODS

This research was performed in accordance with the Declaration of Helsinki, with informed consent of participants or responsible guardians, and with the approval of the Ethics Board of the University of Tehran. Eighteen unrelated Stargardt patients were sequentially recruited from the Retina Clinic of Labbafinejad Medical Center affiliated to Shahid Beheshti University of Medical Sciences, Tehran, Iran. Ophthalmic examinations included visual acuity assessment, fundus photographs (color, infrared, and autofluorescence) and fluorescein angiography (FA) for accumulation of lipofuscin in the retina, measurement of macular thickness by optical coherence tomography (OCT), visual field (VF) testing, and electroretinography (ERG). A combination of clinical presentations and progression, decreased visual acuity, fundus photographs, FA, VF, OCT, and ERG results were considered for the diagnosis of Stargardt disease.[17]

For genetic analysis, genomic DNA was isolated from the white blood cells of the peripheral blood of the patients. Exons 3, 6, 10, 12, 13, 42, and flanking intronic regions of *ABCA4* were amplified by the polymerase chain reaction (PCR). Primer sequences are available upon request. The amplified PCR products were sequenced using the Sanger sequencing protocol. Sequences were analyzed using the Sequencher Software (Gene Codes Corporation, Ann Arbor, MI). Variations were assessed by comparison with *ABCA4* reference

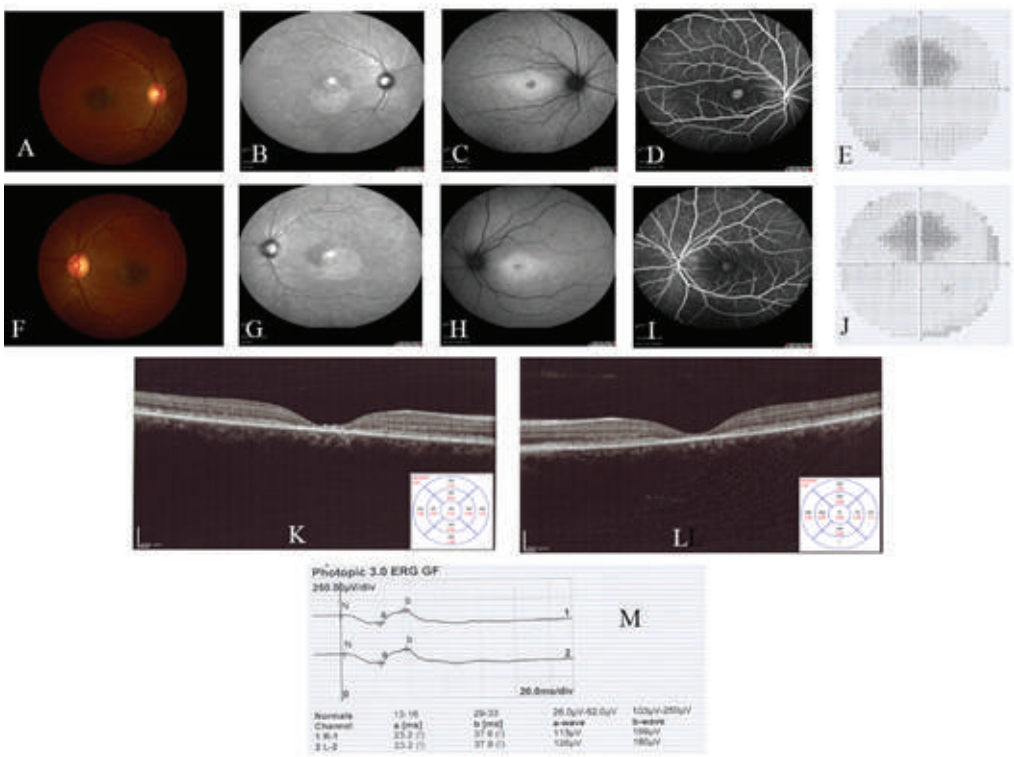

Figure 1. Fundus photographs (color, infrared, and autofluorescence), fluorescein angiography (FA), visual field (VF), optical coherence tomography (OCT), and electroretinography (ERG) findings in a representative patient (STG-5). (A–D) and (F–I) represent color (A & F), infrared (B & G), autofluorescence (C & H), and fluorescein angiographic (D & I) fundus photographs of the patient's right and left eyes, respectively, and demonstrate the lipofuscin accumulation in the macula. VF defects are evident in the right (E) and left eyes (J). Reduced central macular thicknesses were illustrated in the OCT images of the right (K) and left (L) eyes. Note the abnormal photopic ERG graphs and values for both eyes in (M).

sequence available at NCBI (NC_000001.10, NM_000350.3, NP_000341.2).

RESULTS

The average age of patients at the disease onset was 17 years (range 6–41 years). Of the 18 included patients, 11 (61%) were male. The average age at the examination was 26 years (range 8–45 years). All investigated patients demonstrated decreased best-corrected visual acuity and evidence of lipofuscin accumulation in the macula, decreased central macular thickness, constricted visual fields, and variable degrees of ERG abnormalities [Figure 1].

Of the 18 patients screened, three (STG-2, STG-6, and STG-18) had two definitive disease-causing mutated *ABCA4* alleles [Table 1]. Of these, two patients had homozygous mutations (p.Gly1961Arg and p.Gly550Arg), consistent with them having been born to consanguineous parents. The third patient had compound heterozygous mutations; one was the very common p.Gly1961Glu-causing mutation in exon 42 that was noted above, and the other was a donor splice site mutation in intron 10 (c.1356+1G>A). Patient STG-1 harbored a splice site mutation (c.5836-2A>G) in intron 41 and a variation in exon 6 that causes p.Arg212His [Table 1]. The intronic mutation is a known STGD1-causing mutation. As the p.Arg212His-causing variation was observed in the homozygous state, the allele with the c.5836-2A>G intronic mutation must be in cis with a c.635G>A variation that causes p.Arg212His. Although the p.Arg212His-causing variation has sometimes been considered a polymorphism because of its relatively high allele frequency (0.052720), it was reported to contribute to STGD1 status in a Turkish patient.[4, 7, 18, 19] It is possible that in an individual with a clearly disease-causing mutation such as the splice site mutation of patient STG-1, the presence of p.Arg212His will result in disease presentation.

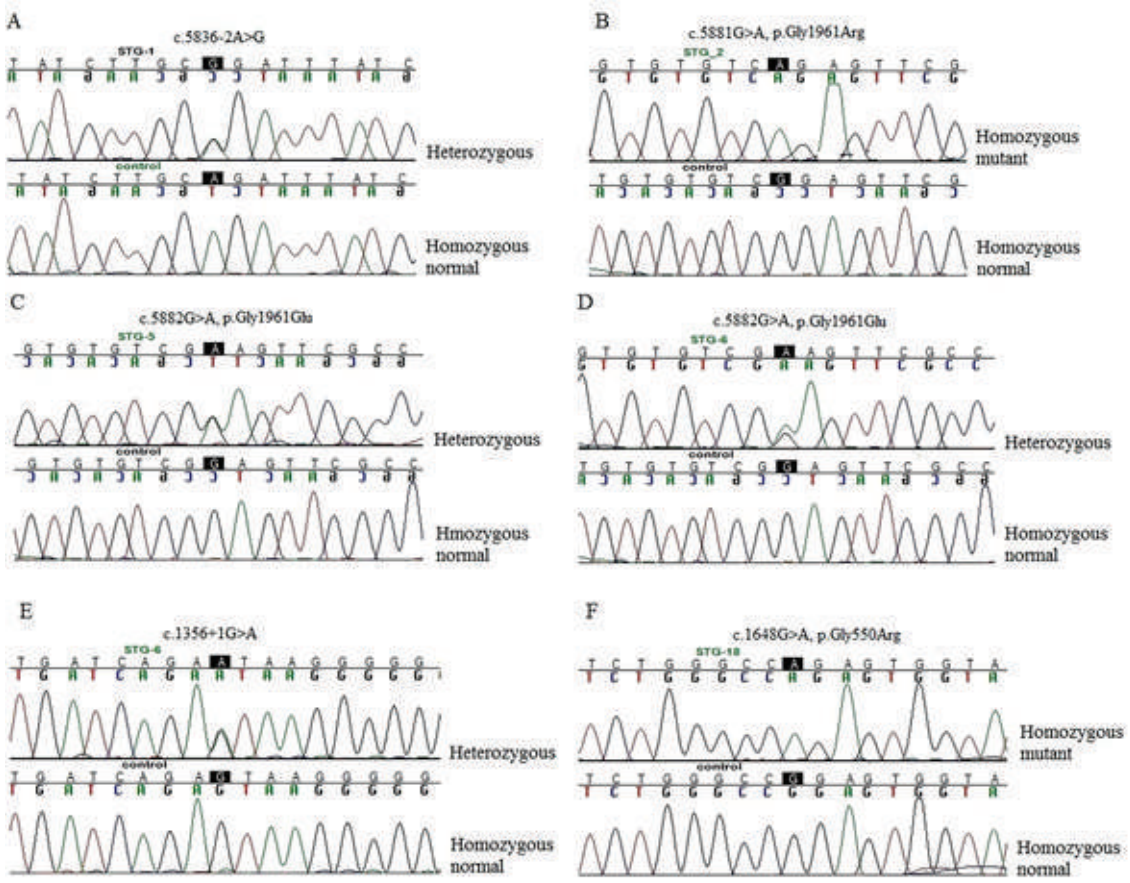

Figure 2. Sequence chromatograms of five mutations observed among the Stargardt disease-affected patients studied. (A) c.5836-2A>G in patient STG-1; (B) c.5881G>A mutation in patient STG-2; (C) c.5882G>A mutation in patient STG-5 and STG-6; (D) mutation c.1356+1G>A in patient STG-6; and (E) mutation c.1648G>A in patient STG-18.

Alternatively, the second mutated *ABCA4* allele in patient STG-1 may be positioned in one of the many exons not screened in this study. Patient STG-5 also harbored two variations in *ABCD4*, a variation that causes p.Gly1961Glu and the intronic variation c.1356+11T>G. Although the intronic mutation is rare (0.0001), bioinformatics tools including Human Splice Finder (http://umd.be/Redirect.html) and NNsplice (https://www.fruitfly.org/seq_tools/splice.html) predict that it would not affect splicing. Therefore, the second mutated *ABCA4* allele in patient STG-5 is likely positioned in one of the exons not screened. The presence of a shared haplotype between the two mutated alleles that cause p.Gly1961Glu cannot be ascertained because of phase issues in the two heterozygous carriers, STG-5 and STG-6. Sequence chromatographs of the reported STGD1-associated mutations are shown in Figure 2.

DISCUSSION

All diseases associated with *ABCA4* are progressive retinopathies accompanied by degeneration of photoreceptor cells that can lead to blindness. There is a significant association between the severity of phenotype and the nature of the *ABCA4* mutations. Stargardt disease is generally considered to be less severe than cone-rod dystrophy (CRD) or retinitis pigmentosa (RP).[20, 21] Deletions, nonsense mutations, and INDELs are usually associated with severe phenotypes.[5] Missense mutations are more commonly found in less severely affected patients. It is interesting that the pathogenicity of some missense mutations, such as p.His432Arg and p.Arg212His discussed above, and even of p.Gly1961Glu that is described below, remains controversial.

Table 1. Data on patients with at least one candidate Stargardt disease-causing mutation in ABCA4

Patient ID	Sex	Consan-guinoeus parents	AOS	AAE	Visual acuity		Candidate disease-causing variations							Non-disease associated variations				
					OD	OS	Variation	Homo/ Het	Exon/ Intron	Effect	MAF gnomAD	ACMG annnotation	Variation ID	Variation	Homo/ Het	MAF gnomAD	ACMG annnotation	Variation ID
STG-2	F	+	6	8	20/200	20/200	c.5881G>A	Homo	Exon 42	p.Gly1961Arg	0.0001	Likely pathogenic	rs142253670					
STG-6	F	–	29	31	1/10	1/10	c. 1356+1G>A	Het	Intron 10	Splicing		No data	Novel	c.302+26A>G	Het	0.49537	No data	rs2297634
							c.5882G>A	Het	Exon42	p.Gly1961Glu	0.0035	Likely pathogenic	rs1800553	c.5836 -11G>A	Het	0.2035	No data	rs1800739
														c.5844A>G	Homo	0.1978	Benign	rs2275029
STG-18	M	+	6	37	20/150	20/200	c.1648G>A	Homo	Exon 12	p.Gly550Arg	0.000004	Uncertain significance	rs61748558					
STG-1	F	–	12	20	20/160	20/160	c.635G>A*	Homo	Exon 6	p.Arg212His*	0.05272	Benign	rs6657239					
							c.5836-2A>G	Het	Intron 41	Splicing		No data	CS161784					
STG-5	F	–	16	17	CF at 500 cm	CF at 400 cm	c.5882G>A	Het	Exon42	p.Gly1961Glu	0.0035	Likely pathogenic	rs1800553	c.1356+11T>G	Het	0.000137	No data	rs113055350

*Considered to possibly contribute to disease status as described in the text

F, female; M, male; AOS, age at onset; AAE, age at examination; OD, right eye; OS, left eye; CF, counting finger; Homo, homozygous; Het, heterozygous; MAF, minor allele frequency

One or more *ABCA4*-mutated alleles were identified in 5 of the 18 Iranian STGD1 patients (27.8%) in whom only six of the gene's 50 exons were screened. No variant nucleotide was found in exons 3 and 13, and the single variation found by screening exon 10 was in fact in intron 10. Without considering p.Arg212His as a mutation that affects disease status, five different mutations were observed. Three of the mutations were missense mutations. P.Gly1961Glu and p.Gly1961Arg affect an amino acid that is localized in the second NBD domain. Although p.Gly1961Glu has been reported as one of the most frequent mutations in Stargardt patients of various populations, its pathogenicity has been questioned largely because of the relatively high frequency of its coding allele in some populations.[22] For example, its frequencies in the Somalian, Ashkenazi, Qatar, and Iranian populations are reported to be 0.10,[22] 0.024 (gnomAD), 0.023,[23] and 0.026 (Iranome), respectively. The consensus appears to be that p.Gly1961Glu is a moderate mutation.[5, 24] In the homozygous state, it presents a mild form of STGD1; in the compound heterozygous state with a more deleterious mutation, it can contribute to a severe form of Stargardt disease.[5] As in other populations, p.Gly1961Glu may be relatively common among Iranian STGD1 patients, as it was observed in two patients of the relatively small cohort studied here. P.Gly1961Arg is found less frequently than p.Gly1961Glu in retinal dystrophy patients. The frequency of the allele that causes p.Gly1961Arg among Iranians is 0.0025, and the frequency is <0.01 in most other populations as well (Iranome, gnomeAD). P.Gly550Arg, that has been reported as a Stargardt disease-causative mutation, was the third missense mutation found in the Iranian cohort.[25] P.Gly550 is localized in the extracytosolic domain 1 (ECD1) of the protein encoded by *ABCA4*.

The molecular consequences of two observed splice site mutations were not critically investigated. C.5836-2A> G that abolishes the acceptor splice site in intron 41 was previously reported in a CRD patient of a Chinese cohort.[6] C.1356+1G>A is being reported for the first time in a Stargardt disease-affected patient, although c.1356+1G>T was previously reported in age-related macular degeneration patients.[26] This signifies potential variability of phenotypic features associated with any *ABCA4* mutation.

To the best of our knowledge, this is the first report of the *ABCA4* mutation screening of the Iranian patients affected by Stargardt disease. Of course, more patients need to be screened in order to achieve a representative profile of *ABCA4* mutation in this population. This knowledge will be needed for various purposes, including possible initiatives for gene therapy.

Acknowledgments

Some of patients in the current article are provided by the disease registry, titled "The Iranian National Registry of Inherited Retinal Dystrophy (IRDReg®)" and code number of IR.SBMU.ORC.REC.1396.15 from the ethic committee, that was supported by the deputy of research and technology in Shahid Beheshti University of medical sciences. (http://dregistry.sbmu.ac.ir).

Financial Support and Sponsorship

Nil.

Conflicts of Interest

There are no conflicts of interest.

REFERENCES

1. Blacharski PA. Fundus flavimaculatus. In: Newsome DA, editor. Retinal dystrophies and degenerations. New York, NY: Raven Press; 1988. 135–159p.
2. Tombran-Tink J, Barnstable CJ. Retinal degenerations: biology, diagnostics, and therapeutics. Totowa, NJ: Humana Press; 2007.
3. North V, Gelman R, Tsang SH. Juvenile-onset macular degeneration and allied disorders. *Dev Ophthalmol* 2014;53:44–52.
4. Rivera A, White K, Stöhr H, Steiner K, Hemmrich N, Grimm T, et al. A comprehensive survey of sequence variation in the ABCA4 (ABCR) gene in Stargardt disease and age-related macular degeneration. *Am J Hum Genet* 2000;67:800–813.
5. Simonelli F, Testa F, Zernant J, Nesti A, Rossi S, Allikmets R, et al. Genotype-phenotype correlation in Italian families with Stargardt disease. *Ophthalmic Res* 2005;37:159–167.
6. Jiang F, Pan Z, Xu K, Tian L, Xie Y, Zhang X, et al. Screening of ABCA4 gene in a Chinese cohort with Stargardt disease or cone-rod dystrophy with a report on 85 novel mutations. *Invest Ophthalmol Vis Sci* 2016;57:145–152.
7. Riveiro-Alvarez R, Aguirre-Lamban J, Lopez-Martinez MA, Trujillo-Tiebas MJ, Cantalapiedra D, Vallespin E, et al. Frequency of ABCA4 mutations in 278 Spanish controls: an insight into the prevalence of autosomal recessive Stargardt disease. *Br J Ophthalmol* 2009;93:1359–1364.

8. Garces F, Jiang K, Molday LL, Stöhr H, Weber BH, Lyons CJ, et al. Correlating the expression and functional activity of ABCA4 disease variants with the phenotype of patients with Stargardt disease. *Invest Ophthalmol Vis Sci* 2018;59:2305–2315.
9. Nassisi M, Mohand-Saïd S, Dhaenens CM, Boyard F, Démontant V, Andrieu C, et al. Expanding the Mutation spectrum in *ABCA4*: sixty novel disease causing variants and their associated phenotype in a large French Stargardt cohort. *Int J Mol Sci* 2018;19:2196.
10. Salles MV, Motta FL, Martin R, Filippelli-Silva R, Dias da Silva E, Varela P, et al. Variants in the ABCA4 gene in a Brazilian population with Stargardt disease. *Mol Vis* 2018;24:546–559.
11. Illing M, Molday LL, Molday RS. The 220-kDa rim protein of retinal rod outer segments is a member of the ABC transporter superfamily. *J Biol Chem* 1997;272:10303–10310.
12. Sun H, Nathans J. Stargardt's ABCR is localized to the disc membrane of retinal rod outer segments. *Nat Genet* 1997;17:15–16.
13. Quazi F, Molday RS. ATP-binding cassette transporter ABCA4 and chemical isomerization protect photoreceptor cells from the toxic accumulation of excess 11-cis-retinal. *Proc Natl Acad Sci USA* 2014;111:5024–5029.
14. Klevering BJ, Deutman AF, Maugeri A, Cremers FP, Hoyng CB. The spectrum of retinal phenotypes caused by mutations in the ABCA4 gene. *Graefes Arch Clin Exp Ophthalmol* 2005;243:90–100.
15. Rong WN, Wang XG, Sheng XL. [ABCA4 mutations and phenotype of different hereditary retinopathies in 3 pedigrees]. *Zhonghua yan ke za zhi [Chinese J Ophthalmol]* 2018;54:775–781.
16. Allikmets R, Shroyer NF, Singh N, Seddon JM, Lewis RA, Bernstein PS, et al. Mutation of the Stargardt disease gene (ABCR) in age-related macular degeneration. *Science* 1997;277:1805–1807.
17. Tanna P, Strauss RW, Fujinami K, Michaelides M. Stargardt disease: clinical features, molecular genetics, animal models and therapeutic options. *Br J Ophthalmol* 2017;101:25–30.
18. Briggs CE, Rucinski D, Rosenfeld PJ, Hirose T, Berson EL, Dryja TP. Mutations in ABCR (ABCA4) in patients with Stargardt macular degeneration or cone-rod degeneration. *Invest Ophthalmol Vis Sci* 2001;42:2229–2236.
19. Ozgül RK, Durukan H, Turan A, Oner C, Ogüs A, Farber DB. Molecular analysis of the ABCA4 gene in Turkish patients with Stargardt disease and retinitis pigmentosa. *Hum Mutat* 2004;23:523.
20. Cideciyan AV, Swider M, Aleman TS, Tsybovsky Y, Schwartz SB, Windsor EA, et al. ABCA4 disease progression and a proposed strategy for gene therapy. *Hum Mol Genet* 2009;18:931–941.
21. Gerth C, Andrassi-Darida M, Bock M, Preising MN, Weber BH, Lorenz B. Phenotypes of 16 Stargardt macular dystrophy/fundus flavimaculatus patients with known ABCA4 mutations and evaluation of genotype-phenotype correlation. *Graefes Arch Clin Exp Ophthalmol* 2002;240:628–638.
22. Guymer RH, Héon E, Lotery AJ, Munier FL, Schorderet DF, Baird PN, et al. Variation of codons 1961 and 2177 of the Stargardt disease gene is not associated with age-related macular degeneration. *Arch Ophthalmol* 2001;119:745–751.
23. Rodriguez-Flores JL, Fakhro K, Agosto-Perez F, Ramstetter MD, Arbiza L, Vincent TL, et al. Indigenous Arabs are descendants of the earliest split from ancient Eurasian populations. *Genome Res* 2016;26:151–162.
24. Fakin A, Robson AG, Fujinami K, Moore AT, Michaelides M, Pei-Wen Chiang J, et al. Phenotype and progression of retinal degeneration associated with nullizigosity of ABCA4. *Invest Ophthalmol Vis Sci* 2016;57:4668–4678.
25. Shroyer NF, Lewis RA, Yatsenko AN, Wensel TG, Lupski JR. Cosegregation and functional analysis of mutant ABCR (ABCA4) alleles in families that manifest both Stargardt disease and age-related macular degeneration. *Hum Mol Genet* 2001;10:2671–2678.
26. Fritsche LG, Fleckenstein M, Fiebig BS, Schmitz-Valckenberg S, Bindewald-Wittich A, Keilhauer CN, et al. A subgroup of age-related macular degeneration is associated with mono-allelic sequence variants in the ABCA4 gene. *Invest Ophthalmol Vis Sci* 2012;53:2112–2118.

Original Article

Knowledge E
enriching | engaging | empowering
Check for updates

Biodistribution of Cy5-labeled Thiolated and Methylated Chitosan-Carboxymethyl Dextran Nanoparticles in an Animal Model of Retinoblastoma

Elham Delrish[1], PhD; Fariba Ghassemi[1,2], MD; Mahmoud Jabbarvand[1], MD; Alireza Lashay[1], MD
Fatemeh Atyabi[3,4], PhD; Masoud Soleimani[5], PhD; Rassoul Dinarvand[3,4], PhD

[1]Translational Ophthalmology Research Centre, Farabi Eye Hospital, Tehran University of Medical Sciences, Tehran, Iran
[2]Retina & Vitreous Service, Farabi Eye Hospital, Tehran University of Medical Sciences, Tehran, Iran
[3]Nanotechnology Research Centre, Faculty of Pharmacy, Tehran University of Medical Sciences, Tehran, Iran
[4]Department of Pharmaceutics, Faculty of Pharmacy, Tehran University of Medical Sciences, Tehran, Iran
[5]Department of Hematology, School of Medical Sciences, Tarbiat Modares University, Tehran, Iran

ORCID:
Elham Delrish: https://orcid.org/0000-0003-4993-7593

Abstract

Purpose: The use of more potent medicine for local chemotherapy of retinoblastoma in order to minimize local and systemic adverse effects is essential. The main goal of this investigation was to assess the biodistribution of thiolated and methylated chitosan-carboxymethyl dextran nanoparticles (CMD-TCs-NPs and CMD-TMC-NPs) following intravitreal (IVT) injection into rat eyes with retinoblastoma.

Methods: An ionic gelation method was used to fabricate Cy5-labelled CMD-TCs-NPs and CMD-TMC-NPs. The NPs were characterized. Cellular internalization of Cy5-labelled NPs was investigated using confocal microscopy and the absorption of labeled NPs was quantified by flow cytometry in human retinoblastoma (Y79) cells. In addition, the Cy5-labeled distribution of nanoparticles in the posterior segment of the eye was histologically imaged by confocal microscopy after IVT injection of NPs into the eyes of rats with retinoblastoma.

Results: CMD-TCs-NPs and CMD-TMC-NPs showed a mean diameter of 34 $\pm$ 3.78 nm and 42 $\pm$ 4.23 nm and zeta potential of +11 $\pm$ 2.27 mV and +29 $\pm$ 4.31mV, respectively. The in vivo study of intraocular biodistribution of Cy5-labeled CMD-TCs-NPs and CMD-TMC-NPs revealed that there is more affinity of CMD-TCs-NPs to the retina and retinoblastoma tumor after IVT administration while methylated chitosan nanoparticles are immobilized in the vitreous and are not able to reach the retina even after 24 hr.

Conclusion: The ionic gelation technique was efficient in synthesizing a biocompatible polymeric nanosystem for drug delivery into the posterior segment of the eye. The current study demonstrated increased ocular bioavailability of CMD-TCs-NPs relative to CMD-TMC-NPs in retinoblastoma induced rat eyes.

Keywords: Biodistribution; Carboxymethyl Dextran; Chitosan; Cy5-Labeled; Nanoparticles; Retinoblastoma

J Ophthalmic Vis Res 2022; 17 (1): 58–68

INTRODUCTION

The blood–retinal barrier prevents large molecules from passing into the retina from the blood and choriocapillaris.[1] The presence of efflux transporters and the pigmented structure of the choroid are the major limiting factors affecting therapeutic molecule penetration from the choroid to the retina and subsequently into the vitreous.[2, 3] Sclera mainly limits the delivery of lipophilic drugs. The effect of the molecular radius however is greater than that of lipophilicity, which affects the scleral permeability of the drug.[1] Vitreous, which consists mostly of 99% water, also contains only a few solid components, such as collagen and glycosaminoglycans.[4] The vitreous poses a substantial barrier to injectable therapeutic molecules, especially to the diffusion of suspended solids or combinations of high molecular weight.[5]

Intravitreal (IVT) injection is the most popular method for delivering drugs into the posterior portion of the eye. It delivers the needed therapeutic concentration of the drug to the posterior segment with minimal but considerable hazards.[6–8] With recent developments in nanocarriers, polymeric carriers are being employed in facilitating drug delivery to the eye to improve the drug's bioavailability.[9–12] Natural polysaccharides are attractive for the formulation of ocular medications because they are nontoxic, economical, available, generally biodegradable and biocompatible, and usually amenable to chemical modification to fabricate new derivatives.[13–18] Chemical modifications have been recently used to fabricate derivatives with improved properties in terms of mucoadhesion, increased ocular bioavailability, and drug solubilization.[19–23]

The bioavailability of NPs in the retina can be enhanced using this technique. It is proven that PEG-coated polystyrene NPs with neutral surface charge up to the size of 750 nm could freely diffuse through bovine vitreous to reach the retina. Diffusion coefficients in nanoparticles were found to be greater at 100–500 nm rather than at 750 nm. Carboxylic groups coating was used to fabricate negatively charged beads, which were able to readily diffuse through the vitreous. Negatively charged nanoparticles, on the other hand, are more impacted by size than neutrally charged NPs, as a negative-500nm-particle was unable to efficiently disperse through vitreous fluid.[26] When nanoparticles made of human serum albumin (HSA), hyaluronic acid, or a combination of the two are injected intravitreally, they can reach the retina. Polyethylene imine nanoparticles with positive surface charge cannot spread through the vitreous when intravitreally injected and are therefore not beneficial for IVT route. Nanoparticles fabricated from glycosylated chitosan (200–500 nm) can reach the retina when intravitreally injected but are not able to penetrate inner limiting membrane.[27]

To the best of our knowledge, no study has been performed to investigate the bioavailability of Cy5 fluorescent dye oligonucleotide labeled thiolated and methylated chitosan nanoparticles following IVT injection in the eyes of rats with retinoblastoma. Therefore, in this investigation, we characterized the effects of the surface charge of thiolated and methylated chitosan NPs on the diffusion and tissue distribution after a single IVT injection into the retinoblastoma bearing rat eyes.

METHODS

Materials

Medium-molecular-weight chitosan (Cs) with a degree of deacetylation of about 89% was purchased from Primex (Karmoy, Norway). N-ethylcarbodiimide hydrochloride (EDC), N-hydroxysuccinimide (NHS), carboxymethyl dextran (CMD) sodium salt (10–20 KD, 1.1–1.5 mmol carboxyl/g), Ellman's reagent, RPMI-1640 tissue

Correspondence to:

Mahmoud Jabbarvand, MD. Translational Ophthalmology Research Centre, Farabi Eye Hospital, Tehran University of Medical Sciences, Tehran 1336616351, Iran.
Email: ma.jabarvand@gmail.com

Received 21-12-2020; Accepted 11-08-2021

Access this article online

Website: https://knepublishing.com/index.php/JOVR

DOI: 10.18502/jovr.v17i1.10171

How to cite this article: Delrish E, Ghassemi F, Jabbarvand M, Lashay A, Atyabi F, Soleimani M, Dinarvand R. Biodistribution of Cy5-labeled Thiolated and Methylated Chitosan-Carboxymethyl Dextran Nanoparticles in an Animal Model of Retinoblastoma . J Ophthalmic Vis Res 2022;17:58–68.

culture medium, fetal bovine serum (FBS), and dialysis tubing (molecular weight cut-off 2, and 12 kDa)'1 were purchased from Sigma-Aldrich (Missouri, USA). N-Methyl-2-pyrrolidone (NMP), sodium chloride, hydrochloric acid, and sodium hydroxide (NaOH) were all purchased from Merck (Darmstadt, Germany). The human retinoblastoma cell line (Y79). All chemicals were of analytical grade.

Synthesis and Characterization of TMC

TMC was synthesized according to the method reported by Sieval et al.[28] The degree of quaternization (% DQ) was distinguished using ^{1}H NMR spectrum of TMC which was prepared by a 600 MHz spectrometer (Bruker-Biospin, Germany). The %DQ was estimated by the following formula:

$$DQ = [[(CH3)3 / [H] \times 1/9] \times 100,$$

where DQ is the level of quaternization; [(CH3)3] is the integral of chemical shift of the hydrogens of N+(CH3)3 groups at 3.4 ppm; and [H] is the integral of H-1 peaks between 4.7 and 5.7 ppm.[29]

Synthesis and Characterization of TMC-Cysteine Conjugates:

The method of synthesis was according to Margit et al.[30] In the first step, 100 milligrams (mgr) of synthesized TMC was dissolved in 5 ml of distilled water (DI) and then 200 mgr of cysteine was added and then mixed until dissolved. In the second stage, EDC and NHS were added. The mixture was then incubated for 3 hr in the dark under continuous stirring at room temperature and the pH was balanced to 5. Afterward, the solution was dialyzed (membrane dialysis MW cut-off = 2 kDa) using 1 mM HCl for three days at 4°C. Eventually, the solution was lyophilized to obtain a powdery substance (TMC-cys) and stored at 4°C. The amount of free thiol groups attached on the TMC backbone was determined by photometry with Ellman's reagent. The thioglycolic acid standards curve was used to determine the quantitative amount of thiol groups.[31] FT-IR spectra of TCs were prepared with an FTIR spectrophotometer (Vectore 22, Germany).

Preparation of CMD-TCs Nanoparticles

The nanoparticles were fabricated by a simple coacervation technique.[32] Carboxymethyl dextran (CMD) was used as the cross-linking agent. Nanoparticles were prepared by adding CMD solutions to TCs or TMC solutions. Then, an instant vortex stirring was executed and samples were incubated at room temperature for 2 hr.

Nanoparticles Characteristics

The particle size of the nanoparticles was distinguished by applying dynamic light scattering on a Malvern Zetasizer Nano-ZS (Worcestershire, United Kingdom). A Zetasizer Nano series (Malvern Instruments) was performed to determine the surface charge of the NPs. Field emission scanning electron microscopy (FESEM; ZEISS) and transmission electron microscopy (TEM, Zeiss, EM 900) were used to study the morphology of nanoparticles.

In Vitro Cellular Uptake of Nanoparticles

Qualitative cellular uptake of Cy5-loaded NPs was investigated with a confocal laser scanning microscope (Nikon, Eclipse).[33] For this purpose, the Y79 cells were cultured in 6-wells at the density of 2×10^5 cells per well. When the cells reached confluence, the cells were then incubated with Cy5-labeled TMC-CMD-NPs and TMC-cys-CMD-NPs suspension to track their uptake in Y79 cells. As a result of this procedure, the nanoparticles were well-dispersed in the culture medium at concentrations of 100 µg/ml. Nanoparticle dispersions were incubated at 37°C in a 5% CO_2 atmosphere for 2 hr. After aspiration of the medium, the cells were rinsed with 10 ml of cold phosphate buffered saline (PBS) (pH7.4) to eliminate any traces of nanoparticles remaining in the medium. Then, the cells were fixed with 2% paraformaldehyde for 10 min at room temperature and stained with DAPI (4',6-Diamidino-2-phenylindole dihydrochloride). The fluorescence of the Cy5-labeled nanoparticles was monitored applying a confocal microscope (excitation 640.8 nm/emission 662–737 nm).

Quantifying Level of NPs Cellular Uptake By Flow Cytometry

The cellular internalization of Cy5-labeled CMD-TMC-NPs and CMD-TCs-NPs were reconfirmed and compared by flow cytometric analysis in the Y79 cells. To execute, the cells were cultured in a 6-well plate at a density of 250×10^4 cells/well. After 24 hr of incubation, the cells were treated with Cy5-labeled NPs at 37°C for 2 hr. After the incubation, cells were washed with PBS and analyzed for intracellular fluorescence of Cy5-labeled NPs using BD FACS Calibur flow cytometer (BD Biosciences, San Jose, CA, USA).[34]

Rat Xenograft Model of Retinoblastoma

For this study, 10 Wistar albino rats (male, two months old, purchased from Pasteur Institute, Karaj, Iran) were used. All rats were treated in accordance with the ARVO (Association for Vision and Ophthalmology Research) Declaration on the Procedure of Animals in Ophthalmic and Vision Research, approved by the University of Medical Sciences of Tehran. Surgeries were performed by the same surgeon (FG). The rats were immunosuppressed with daily injections of Cyclosporin A (CsA) (Sandimmun®; Novartis). Approximately 1×10^6 Y79 cells were intravitreally injected to the rat eyes.[35] After retinoblastoma tumor formation, Cy5-labeled TMC-CMD-NPs and TMC-cys-CMD-NPs (100 µg/ml) was intravitreally injected. The control eyes received IVT normal saline as same concentration. All the animals were euthanized 24 hr after the IVT injection of Cy5-labeled nanoparticles and enucleation was performed on them. Afterward, tissues were cut into 5-µm thick layers using a microtome for investigation of qualitative ocular uptake and biodistribution of Cy5-labeled NPs, which was done with a confocal laser scanning microscope (Nikon, Eclipse).

RESULTS

Nanoparticles Characteristics

The ^{1}H NMR spectrum of TMC is shown in Figure 1. In the ^{1}H NMR spectrum of TMC, the signals at 3.3 to 3.8 ppm were attributed to the methyl group at the N,N,N-trimethylated site ([H3]–[H6]).[36]

FTIR spectroscopy is an efficient tool for the investigation of the physicochemical attributes of polysaccharide. In this study, the syntheses of TMC and TCs were corroborated by the FTIR spectra illustrated in Figure 2. The TMC-cys conjugate was synthesized by the development of amide bonds between the amino group of methylated chitosan and carboxylic acid group of cysteine. Meanwhile, for TMC the peak at 1470 cm^{-1} corresponded to the characteristic absorption of N–CH3. The peak at around 1250 cm^{-1} in the spectra of compound was accredited to the C–SH stretching band. Also, the spectra of thiolated-chitosan displayed two powerful characteristic absorptions at 1641 cm^{-1} and 2500 cm^{-1} which were attributed to the C = O double bonds of the amido group and stretching vibration of –SH, respectively [Figure 2].[37, 38] Furthermore, the degree of substitution of thiols using Ellman's protocol was determined as 11%. In addition, CMD-TCs-NPs and CMD-TCs-NPs had diameters of 34 ± 3.78 and 42 ± 4.23and zeta potentials of 11 ± 2.27 and 29 ± 4.31 (mV), respectively. The polydispersity index (PI) is a parameter used to investigate the homogeneity in the particle size distribution of synthesized NPs, PI values <0.3 guarantees the stability of colloidal dispersion.[39] The size distributions of the CMD-TCs-NPs and CMD-TCs-NPs were 0.27 ± 0.05 and 0.21 ± 0.05, respectively. As demonstrated by the SEM images [Figures 3A & 3B], CMD-TMC-NPs and CMD-TCs-NPs were spherical in shape.

Uptake of Cy5-Labeled Nanoparticles By Y79 Cells

The cellular uptake of Cy5-labeled CMD-TCs-NPs and CMD-TMC-NPs by Y79 cells was visualized using a confocal microscope after 2 hr of exposure [Figure 4]. Meanwhile, the nuclei of the Y79 cells were stained by DAPI (blue fluorescence) in order to ascertain the location of internalized NPs. A direct indicator of uptake enhancement by the Y79 cells could be increasing the number of uptakes of NPs, which was documented by the increase in the intensity of the red color as seen in Figure 4. In the Cy5-labeled NPs groups, the red signal that appeared, was mostly located in cytoplasm. Contrastingly, a stronger red signal was discovered to be distributed inside the cells treated with CMD-TCs-NPs. Compared with CMD-TMC-NPs, more bioadhesive CMD-TCs-NPs were better adsorbed by cell membrane, resulting in

improved endocytosis of Y79 cells and efficacious cellular uptake [Figure 4].

Uptake with Flow Cytometry

A rapid method for the determination of the absorption of nanoparticles in Y79 cells using flow cytometry has been used in this research. The cellular uptake of Cy5-labeled CMD-TCs-NPs and CMD-TMC-NPs by Y79 cells was further investigated by flow cytometry analysis. The fluorescence intensity of cell emission determined by flow cytometry can be a good marker of the amount of NPs internalized by Y79 cells. As shown in Figure 5, the peak of the fluorescence intensity shifted to a higher level when the CMD-TCs-NPs were used, suggesting the promoted Cy5-labeled CMD-TCs-NPs internalization by Y79.

Animal Model Diffusion Study

Within the first 24 hr after the IVT injection, the eyes were enucleated and severed into 5 μm thick sections. The NPs distribution was investigated by taking confocal images after the IVT injection of the Cy5-labeled NPs [Figure 6]. The two chitosan compositions showed various diffusion rates in the vitreous. After the injection, only Cy5-labeled CMD-TCs-NPs freely disseminated all over the vitreous cavity; 24 hr after the IVT injection, confocal microscopy demonstrated that the Cy5-labeled CMD-TCs-NPs had accumulated throughout the different retinal layers [Figure 6]. Also, it showed that cationic CMD-TCs-NPs with Zeta potentials +11 ± 2.27 mV were able to penetrate efficiently into the rat retina, while CMD-TMC-NPs with zeta potential value of +29 mV were trapped in the vitreous. The distinguished diffusion rate between the groups receiving CMD-TMC-NPs versus CMD-TCs-NPs might be due to the difference in surface charges of NPs.

DISCUSSION

Chemotherapy by nanoparticles has been an effective approach in ophthalmic research in overcoming poor intraocular bioavailability of drugs due to the presence of anatomical barriers and it has also contributed toward improving therapeutic efficiency. The main purpose in the engineering of nano-carriers in this investigation was to develop a promising vehicle via biopolymers to transport drugs to the posterior part of the eye. Chitosan is a polymer that has been discovered by researchers for the application of ophthalmic drug delivery systems. Mucoadhesive chitosan formulations were also considered as an effective strategy in overcoming the rapid elimination of topical ophthalmic drugs.[40, 41]

Due to its solubility in acidic solutions (pH = 6), the efficacy of chitosan can be reduced at the site of action. Hence, a chemical alteration of chitosan was employed to fabricate a water-soluble derivative of Cs. In this study, the NPs were fabricated using hydrophilic biopolymers such as TMC, TMC-cys (TCs) and CMD to design efficient and safe drug delivery systems for the posterior segment of the eye.[42] The solubility of TMC-NPs may also be decreased as a consequence of a high degree of methylation (DQ%), which results in a high level of O-methylation. The beneficial approach of combining TMC and cys to fabricate TMC-cys conjugate in preparing desirable derivatives was used in this study to improve the solubility of fabricated NPs and minimize the formation of agglomerates.[43, 44] Conjugation of polymers with the thiol group is the most common method used in the manufacture of mucoadhesive delivery systems.[45] Endocytosis is the dominant mechanism in the adsorption of nanoparticles with a size of <100 nm. The rate of spherical NP internalization is affected by size, shape, surface charge, composition, and surface hydrophilicity. Non-phagocytic cells absorb the highest number of spherical nanoparticles with sizes between 20 and 50 nm.[46] By labeling NPs with Cy5, a qualitative assessment of their number can be obtained by evaluating the intensity of the staining seen through the confocal microscope to compare the cell uptake of the NPs. An increase in the red color intensity in the staining in the NPs-treated group, as compared to the control, could be due to better cellular uptake of NPs by Y79 cells. Therefore, the intensity of the red color that occurs after the labelling can be considered as a direct criterion for assessing the cellular uptake of NPs. As shown in Figure 4, to prove the presence of NPs in the cytoplasm, the cell nucleus was stained with DAPI. Flow cytometry was also utilized in order to provide a qualitative evaluation of the difference in cellular uptake between the two formulations of NPs. As can be seen in Figure 5, the cellular uptake of thiolated chitosan NPs by Y79 cells was better,

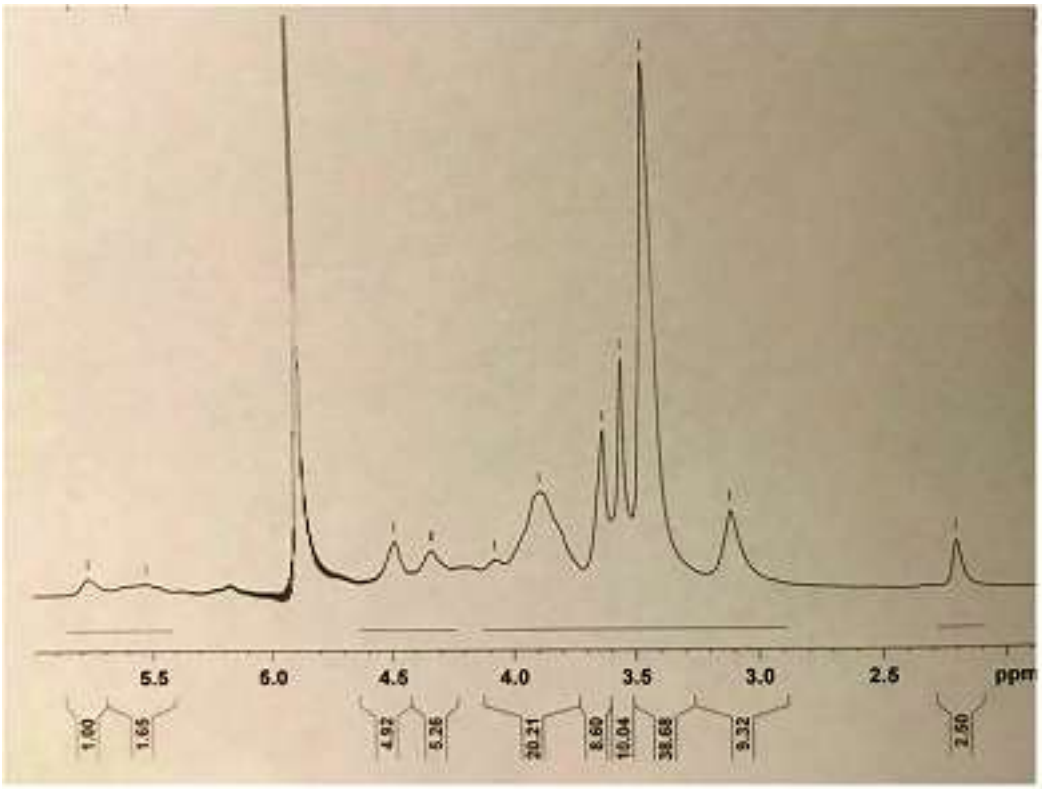

Figure 1. FT-IR spectra of Cs, TMC, and TCs.

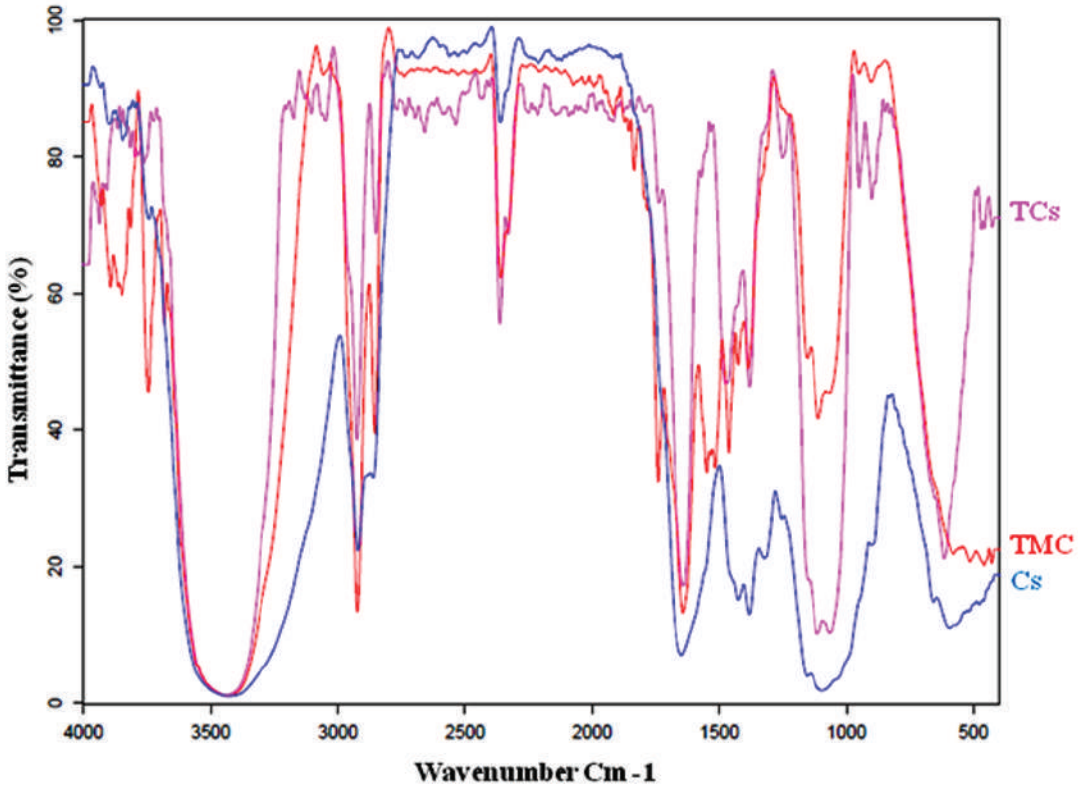

Figure 2. ^{1}H-NMR spectrum of TMC in D2O.

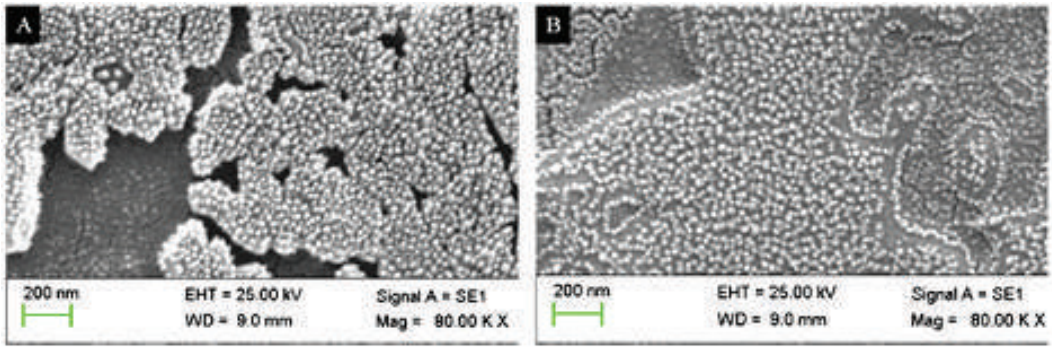

Figure 3. SEM images of CMD-TMC-NPs (A) and CMD-TCs-NPs (B).

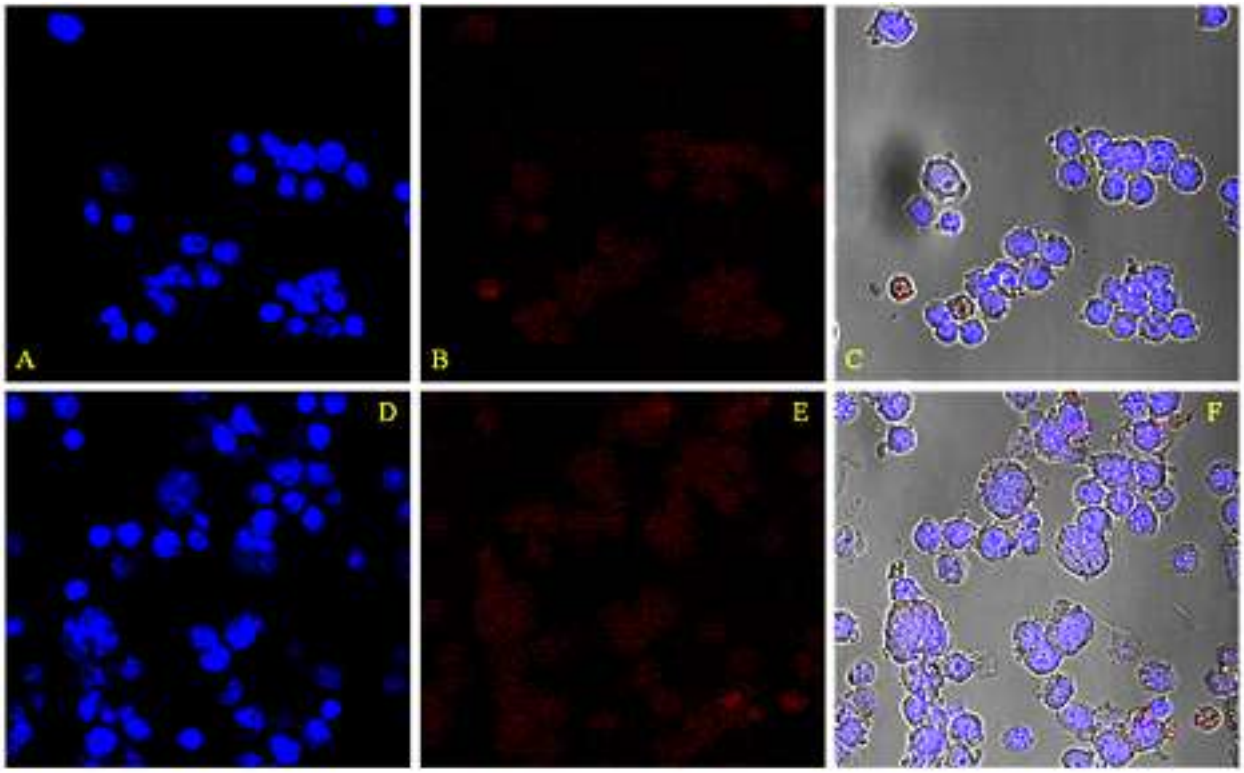

Figure 4. Intracellular localization of CMD-TMC-NPs (A–C) and CMD-TCs-NPs (D–F) in Y79 cells by Cy5-labeled NPs. Labeled NPs appear in red in the confocal microscopy fluorescence images.

which could be due to greater bioadhesion of TCs (TMC-cys) nanoparticles owing to the TMC combination with the thiol group.

In this research, TCs adhesion properties were founded by electrostatic interactions with cysteine. When the NPs are intravitreally injected, they must be able to cross the vitreous barrier to reach their destination. The vitreous body is a polyanionic gel-like mass which is made up of collagen fibers and glycosaminoglycan.[47] Pitkänen et al showed that the major obstacle to nonviral gene delivery systems is the vitreous.[48] Peeters et al.[49] also stated that only PEGylated particles <500 nm are able to have unrestricted movement through the vitreous. Later, it was declared that cationic liposomes with zeta potentials below +20 mV were allowed to defuse efficiently into the murine retina, while liposomes with zeta potential value above +20 mV were completely trapped in the vitreous humor.[50, 51]

The drug bioavailability is dependent on the route of drug administration into the eye.

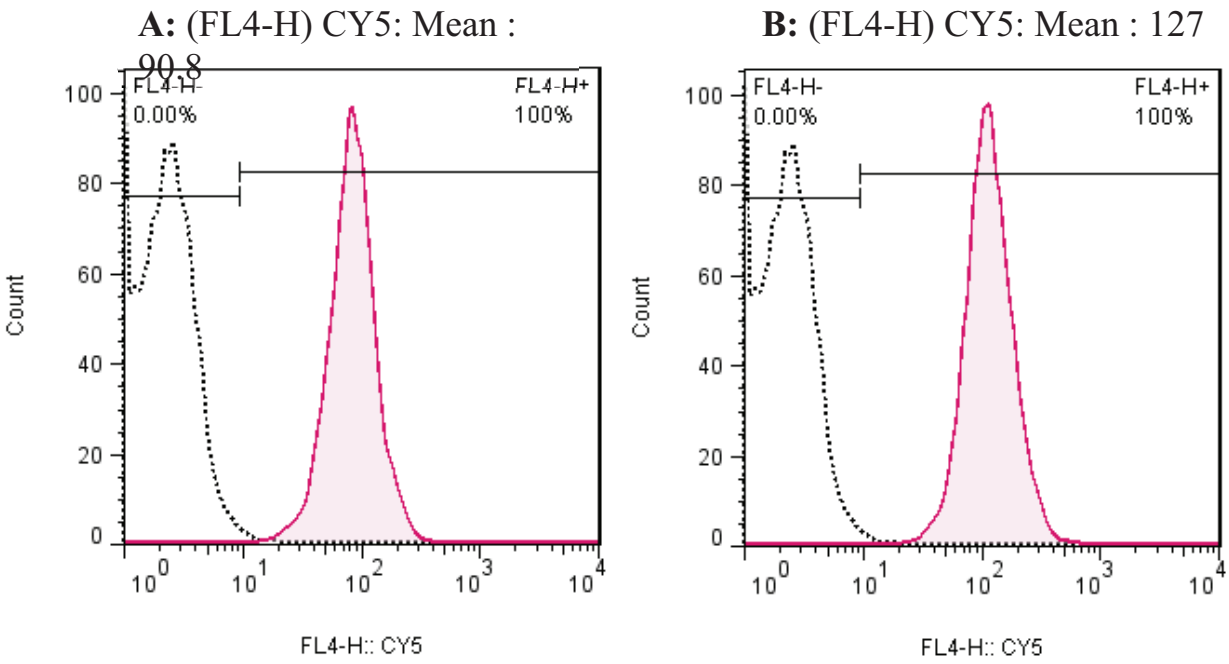

Figure 5. Flow cytometry analysis of cellular uptake of Cy5-labeled (A) CMD-TMC-NPs and (B) CMD-TCs-NPs in Y79 cells after 2 hr incubation time.

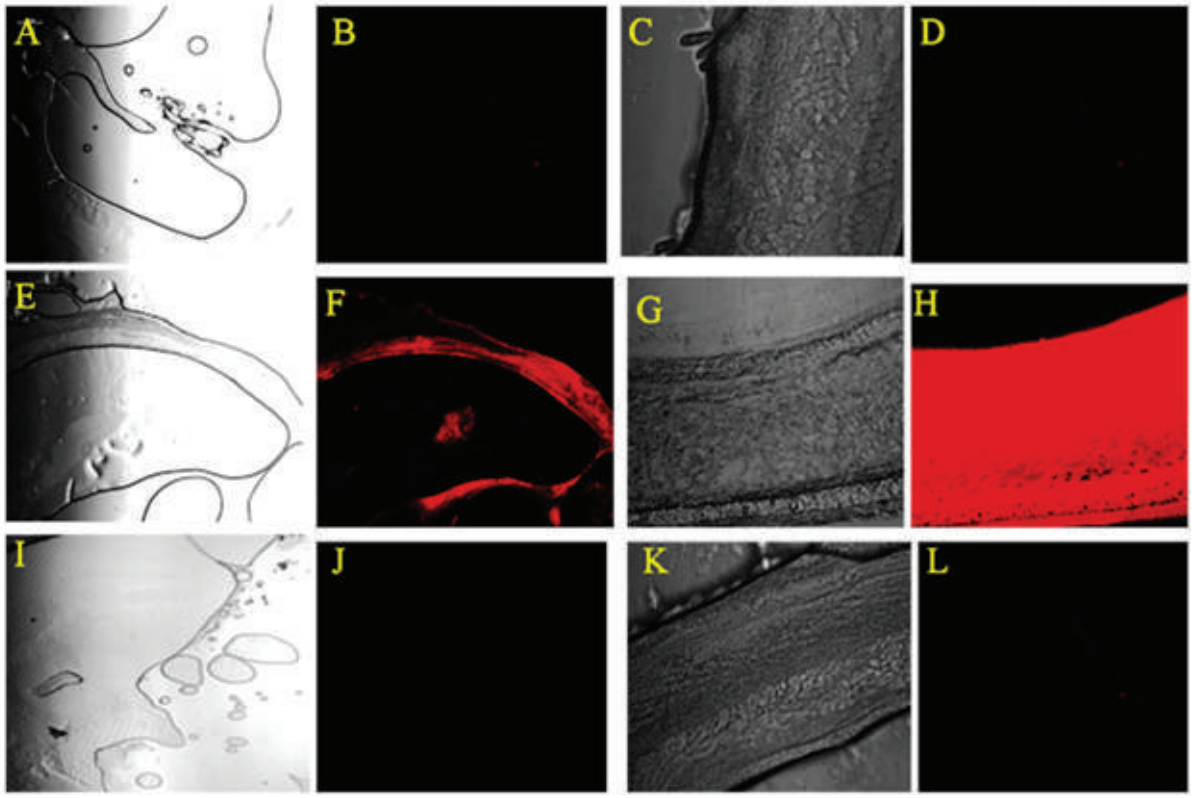

Figure 6. Confocal microscopy of the retinoblastoma and retina at 24 hr after intravitreal injection of CY5-labeled NPs into the vitreous cavity of rat with retinoblastoma. (A–E) Control group; untreated retinoblastoma (A) and untreated retina (C). (E–H) Eyes injected with Cy5-labeled CMD-TCs-NPs. The Cy5-labeled CMD-TCs-NPs diffused to the tumor mass (F) and through the retinal layers (H). (I–L) Eyes injected with Cy5-labeled CMD-TMC-NPs. Cy5-labeled CMD-TMC-NPs are entirely trapped in the vitreous and are not able to reach the retina even after 24 hr.

Effectiveness of systematically administrated drug vehicles for ocular posterior segment drug delivery is limited by different factors including the wide drug distribution to the off-target sites and the presence of the blood–retinal barrier.[52] Therefore, in this study, in order to achieve maximum bioavailability, IVT injection of nanoparticles has been used. CMD-TMC and CMD-TCs nanoparticles with identical sizes and diverse surface charges were employed to examine the connection between their diffusion rates and their composition. Confocal imaging was used to track real-time diffusion in the vitreous cavity of the injected Cy5-labelled nanoparticles. By comparing the images of the CMD-TMC-NPs, CMD-TCS-NPs, and the control groups, the Cy5 signal of labeled NPs was determined, and the variations of fluorescence intensity in the confocal images illustrated the distribution of Cy5-labelled NPs [Figure 6]. Two biocopolymers (TMC and TCs) could self-assemble into NPs with identical sizes and various surface charges. TCs could self-assemble into 34 nm NPs and with +11mV surface charges, while TMC NPs assembled into 42 nm NPs with a +29 mV zeta potential. The difference in the surface charges between TMC and TCs NPs may result in different diffusion rates of NPs after the IVT injection. In the two polymer confocal images of Figure 6, TCs with the 11 ± 2.27 mV surface charges displayed the most noticeable alterations in fluorescence signals (red color). The results of this study indicated that the surface charge of nanoparticles might perform a negative or positive role in influencing the retinal penetration of intravitreally injected NPs. This investigation also proved that vitreous with anionic properties is a weak barrier for the movement of NPs with zeta potentials +11 ± 2.27mV, but vitreous can remarkably limit TMC-diffusion with zeta potentials of +29 ± 4.31mV in vivo [Figure 6]. TMC-NPs with zeta potentials of +29 ± 4.31 mV are completely immobilized in the vitreous via electrostatic interactions with negatively charged hyaluronic acid and collagen fibers. As shown in Figure 6, methylated chitosan nanoparticles are completely trapped in the vitreous and are unable to reach the retina even after 24 hr. Thus, a powerfully positive charge (+29 ± 4.31 mV) on the particle surface has a remarkable negative impact on diffusion after IVT injection.

Through comparing the fluorescence changes in the eye injected with TCs or TMC, the results illustrated in Figure 6 indicate that the appropriate surface charges on the particle surface (i.e., +11 ± 2.27 mV) improved the diffusion efficacy of the particles after IVT injection. Accordingly, surface improving of the NPs with the thiol group in CMD-TCs-NPs boosts the transfection efficacy of the NPs through the development of intra-chain disulphide bonds within the complex. After the success of this elementary step, we plan to use nanoparticle-based CMD-TCs as a controlled drug delivery system for anticancer drugs for retinoblastoma treatment.

In conclusion, an effort to facilitate the application of more potent medicine for the local chemotherapy of retinoblastoma to ensure minimization of local and systemic adverse effects, we embarked on the current study. One challenge that is evident in delivering the relevant medicine to the posterior of the eye is the ability of the medicine to break through the vitreous cavity. Nanoparticles have been determined to be a viable alternative in targeting specific areas for medication due to their ability to adsorb and diffuse medication in specific areas locally. Our study has revealed that appropriate surface charges (preferably +11 ± 2.27 mV) on the surface of nanoparticles NPs that were manufactured with different chitosan derivatives may boost their diffusion after IVT injection. A positive charge adversely affects the rate of vitreous diffusion of NPs. This research showed that when NPs were intravitreally injected, the surface, charge of NPs is the most significant limiting factor in their penetration through the vitreous. The cationic bio-polymer with appropriate surface charges is able to reach the retina and diffuse through the retinal layers. The ionic gelation technique was efficient in synthesizing a biocompatible polymeric nanosystem for drug delivery into the posterior segment of the eye. The current study demonstrated increased ocular bioavailability of CMD-TCs-NPs relative to CMD-TMC-NPs in retinoblastoma containing rat eyes.

Financial Support and Sponsorship

This research was funded by Tehran University of Medical Sciences, Tehran, Iran.

Conflicts of Interest

The authors report no conflicts of interest in this work.

REFERENCES

1. Lawrence MS, Miller JW. Ocular tissue permeabilities. *Int Ophthalmol Clin* 2004;44:53–61.
2. Cheruvu NP, Amrite AC, Kompella UB. Effect of eye pigmentation on transscleral drug delivery. *Invest Ophthalmol Vis Sci* 2008;49:333–341.
3. Kennedy BG, Mangini NJ. P-glycoprotein expression in human retinal pigment epithelium. *Mol Vis* 2002;8:422–430.
4. Le Goff MM, Bishop PN. Adult vitreous structure and postnatal changes. *Eye* 2008;22:1214–1222.
5. Mains J, Wilson CG. The vitreous humor as a barrier to nanoparticle distribution. *J Ocul Pharmacol Ther* 2013;29:143–150.
6. Pershing S, Bakri SJ, Moshfeghi DM. Ocular hypertension and intraocular pressure asymmetry after intravitreal injection of anti-vascular endothelial growth factor agents. *Ophthalmic Surg Lasers Imaging Retina* 2013;44:460–464.
7. Ghasemi Falavarjani K, Nguyen QD. Adverse events and complications associated with intravitreal injection of anti-VEGF agents: a review of literature. *Eye* 2013;27:787–794.
8. Kumar A, Sehra SV, Thirumalesh MB, Gogia V. Secondary rhegmatogenous retinal detachment following intravitreal bevacizumab in patients with vitreous hemorrhage or tractional retinal detachment secondary to Eales' disease. *Graefes Arch Clin Exp Ophthalmol* 2012;250:685–690.
9. Al-Halafi AM. Nanocarriers of nanotechnology in retinal diseases. *Saudi J Ophthalmol* 2014;28:304–309.
10. Yasin MN, Svirskis D, Seyfoddin A, Rupenthal ID. Implants for drug delivery to the posterior segment of the eye: a focus on stimuli-responsive and tunable release systems. *J Control Release* 2014;196:208–221.
11. Rawas-Qalaji M, Williams CA. Advances in ocular drug delivery. *Curr Eye Res* 2012;37:345–356.
12. Rowe-Rendleman CL, Durazo SA, Kompella UB, Rittenhouse KD, Di Polo A, Weiner AL, et al. Drug and gene delivery to the back of the eye: from bench to bedside. *Invest Ophthalmol Vis Sci* 2014;55:2714.
13. Kritchenkov AS, Andranovits S, Skorik YA. Chitosan and its derivatives: vectors in gene therapy. *Russ Chem Rev* 2017;86:231–239.
14. Tiwari S, Bahadur P. Modified hyaluronic acid based materials for biomedical applications. *Int J Biol Macromol* 2019;121:556–571.
15. Poshina DN, Raik SV, Poshin AN, Skorik YA. Accessibility of chitin and chitosan in enzymatic hydrolysis: a review. *Polym Degrad Stab* 2018;156:269–278.
16. Berezin AS, Lomkova EA, Skorik YA. Chitosan conjugates with biologically active compounds: design strategies, properties, and targeted drug delivery. *Russ Chem Bull* 2012;61:781–795.
17. Pettignano A, Charlot A, Fleury E. Carboxyl-functionalized derivatives of carboxymethyl cellulose: towards advanced biomedical applications. *Polym Rev* 2019;59:510–560.
18. Fernando IPS, Kim D, Nah JW, Jeon YJ. Advances in functionalizing fucoidans and alginates (bio) polymers by structural modifications: a review. *Chem Eng J* 2019;355:33–48.
19. Siafaka PI, Titopoulou A, Koukaras EN, Kostoglou M, Koutris E, Karavas E, Bikiaris DN. Chitosan derivatives as effective nanocarriers for ocular release of timolol drug. *Int J Pharm* 2015;495:249–264.
20. Rassu G, Gavini E, Jonassen H, Zambito Y, Fogli S, Breschi MC, Giunchedi P. New chitosan derivatives for the preparation of rokitamycin loaded microspheres designed for ocular or nasal administration. *J Pharm Sci* 2009;98:4852–4865.
21. Bongiovì F, Di Prima G, Palumbo FS, Licciardi M, Pitarresi G, Giammona G. Hyaluronic acid-based micelles as ocular platform to modulate the loading, release, and corneal permeation of corticosteroids. *Macromol Biosci* 2017;17:1700261.
22. Zambito Y, Di Colo G. Thiolated quaternary ammonium-chitosan conjugates for enhanced precorneal retention, transcorneal permeation and intraocular absorption of dexamethasone. *Eur J Pharm Biopharm* 2010;75:194–199.
23. Hume LR, Lee HK, Benedetti L, Sanzgiri YD, Topp EM, Stella VJ. Ocular sustained delivery of prednisolone using hyaluronic acid benzyl ester films. *Int J Pharm* 1994;111:295–298.
24. Xu Q, Boylan NJ, Suk JS, Wang Y-Y, Nance EA, Yang J-C, et al. Nanoparticle diffusion in, and microrheology of, the bovine vitreous ex vivo. *J Control Release* 2013;167:76–84.
25. Koo H, Moon H, Han H, Na JH, Huh MS, Park JH, et al. The movement of self-assembled amphiphilic polymeric nanoparticles in the vitreous and retina after intravitreal injection. *Biomaterials* 2012;33:3485–3493.
26. Xu Q, Boylan NJ, Suk JS, Wang YY, Nance EA, Yang JC, et al. Nanoparticle diffusion in, and microrheology of, the bovine vitreous ex vivo. *J Control Release* 2013;167:76–84.
27. Koo H, Moon H, Han H, Na JH, Huh MS, Park JH, et al. The movement of self-assembled amphiphilic polymeric nanoparticles in the vitreous and retina after intravitreal injection. *Biomaterials* 2012;33:3485–3493.
28. Sieval AB, Thanou M, Kotze´ AF, Verhoef JC, Brussee J, Junginger HE. NMR preparation characterization of highly substituted N-trimethyl chitosan chloride. *Carbohydr Polym* 1998;36:157–165.
29. Snyman D, Hamman JH, Kotze JS, Rolling JE, Kotze AF. The relationship between the absulote molecular weight and the degree of quaternization of N-trimethy chitosan chloride. *Carbohydr Polym* 2002;50:145–150.
30. Margit DH, Constantia EK, Bernkop-Schnürch A. In vitro evaluation of the viscoelastic properties of chitosan–thioglycolic acid conjugates. *Eur J Pharm Biopharm* 2003;55:185–190.
31. Roldo M, Hornof M, Caliceti P, danBernkop-Schnurch A. Mucoadhesive thiolated chitosans as platforms for oral controlled drug delivery: synthesis an in vitro evaluation. *Eur J Pharm Biopharm* 2004;57:115–121.
32. Tekie FSM, Kiani M, Zakerian A, Pilevarian F, Assali A, Soleimani M, et al. Nano polyelectrolyte complexes

of carboxymethyl dextran and chitosan to improve chitosan-mediated delivery of miR-145, *Carbohydr Polym* 2017;159:66–75.

33. Lanlan L, Jiawei G, Yuquan W, Xiaoxing X, Hui T, Jin L, et al. A broad-spectrum ROS-eliminating material for prevention of inflammation and drug-induced organ toxicity. *Adv Sci* 2018;5:1800781.
34. Zhigang X, Shiying L, Yuejun K, Mingfeng W. Glutathione- and pH-responsive nonporous silica prodrug nanoparticles for controlled release and cancer therapy. *Nanoscale* 2015;7:5859–5868.
35. Chevez-Barrios P, Hurwitz MY, Louie K, Marcus KT, Holcombe VN, Schafer P, et al. Metastatic and nonmetastatic models of retinoblastoma. *Am J Pathol* 2000;4:1405–1412.
36. De Britto D, Celi Goy R, CampanaFilho SP, Assis OBG. Quaternary salts of chitosan: history, antimicrobial features, and prospects. *Int J Carbohydr Chem* 2011;2011:312539.
37. Fang L, LijieW, Jingjing Z, Wenqiang T, Yuan Ch, Fang D, et al. Preparation and characterization of quaternized chitosan derivatives and assessment of their antioxidant activity. *Molecules* 2018;23:516.
38. Zhu X, Su M, Tang S, Wang L, Liang X, Meng F, et al. Synthesis of thiolated chitosan and preparation nanoparticles with sodium alginate for ocular drug delivery. *Mol Vis* 2012;18:1973–1982.
39. Maciel MVOB, Almeida AR, Machado MH, de MeloA PZ, da Rosa CG, de Freitas DZ, et al. *Syzygium aromaticum* L. (clove) essential oil as a reducing agent for the green synthesis of silver nanoparticles. *Open J Appl Sci* 2019;9:45–54.
40. Irimia T, Ghica M, Popa L, Anuta V, Arsene AL, Dinu-Pîrvu CE. Strategies for improving ocular drug bioavailability and corneal wound healing with chitosan-based delivery systems. *Polymers* 2018;10:1221.
41. Felt O, Furrer P, Mayer J, Plazonnet B, Buri P, Gurny R. Topical use of chitosan in ophthalmology: tolerance assessment and evaluation of precorneal retention. *Int J Pharm* 1999;180:185–193.
42. Bernkop-Schnurch A, Hornof M, Zoidl T. Thiolatedpolymers-thiomers: synthesis and in vitro evaluation of chitosan-2-iminothiolane conjugates. *Int J Pharm* 2003;260:229–237.
43. Bernkop-Schnürch A. Thiomers: a new generation of mucoadhesive polymers. *Adv Drug Deliv Rev* 2005;57:1569–1582.
44. Shin JM, Song SH, Vijayakameswara Rao N, Lee ES, Ko H, Park JH. A carboxymethyl dextran-based polymeric conjugate as the antigen carrier for cancer immunotherapy. *Biomater Res* 2018;22:21.
45. Vasic K, Knez Ž, Konstantinova EA, Kokorin AI, Gyergyek S, Leitgeb M. Structural and magnetic characteristics of carboxymethyl dextran coated magnetic nanoparticles: from characterization to immobilization application. *React Funct Polym* 2020;148:104481.
46. Kulkarni AD, Patel HM, Surana SJ, Vanjari YH, Belgamwar VS, Pardeshi CV. N,N,N-Trimethyl chitosan: an advanced polymer with myriad of opportunities in nanomedicine. *Carbohydr Polym* 2017;157:875–902.
47. Foroozandeh P, Abdul Aziz A. Insight into cellular uptake and intracellular trafficking of nanoparticles. *Nanoscale* 2018;13:339.
48. Käsdorf BT, Arends F, Lieleg O. Diffusion regulation in the vitreous humor. *Biophys J* 2015;109:2171–2181.
49. Pitkänen L, Ruponen M, Nieminen J, Urtti A. Vitreous is a barrier in nonviral gene transfer by cationic lipids and polymers. *Pharm Res* 2003;20:576–583.
50. Peeters L, Sanders NN, Braeckmans K, Boussery K, de Voorde JV, Smedt SCD, et al. Vitreous: a barrier to nonviral ocular gene Therapy. *Invest Ophthalmol Vis Sci* 2005;46:3553–3561.
51. Lee J, Goh U, Lee HJ, Kim J, Jeong M. Effective retinal penetration of lipophilic and lipid-conjugated hydrophilic agents delivered by engineered liposomes. *Mol Pharm* 2017;14:423–430.
52. Ravar F, Saadat E, Gholami M, Dehghankelishadi P, Mahdavi M, Azami S. Hyaluronic acid-coated liposomes for targeted delivery of paclitaxel, in-vitro characterization and in-vivo evaluation. *J Control Release* 2016;10:10–22.
53. Kompella UB, Amrite AC, Pacha Ravi R, Durazo SA. Nanomedicines for back of the eye drug delivery, gene delivery, and imaging. *Prog Retin Eye Res* 2013;36:172–198.

Original Article

Development of a Spatio-temporal Contrast Sensitivity Test for Clinical Use

Marcelo Fernandes Costa[1,2], PhD; Leonardo Dutra Henriques[1], PhD; Otávio Côrrea Pinho[1], BPsy

[1]Laboratório da Visão, Departamento de Psicologia Experimental, Instituto de Psicologia, Universidade de São Paulo, São Paulo, Brazil
[2]Núcleo de Neurociências Aplicada, Universidade de São Paulo, São Paulo, Brazil

ORCID:
Marcelo Fernandes Costa: https://orcid.org/0000-0002-3944-8457

Abstract

Purpose: We developed a contrast sensitivity test that considers an integrative approach of spatial and temporal frequencies to evaluate the psychophysical channels in processing two-dimensional stimulus for clinical use. Our new procedure provides a more efficient isolation of the magnocellular and parvocellular visual pathways supporting spatiotemporal contrast sensitivity processing.

Methods: We evaluated 36 participants of both sexes aged 18–30 years with 20/20 or better best-corrected visual acuity. Two spatial frequencies (0.5 cycles per degree [cpd] and 10 cpd), being in one of the three temporal frequencies (0.5 cycle per second [cps], 7.5 cps, and 15 cps), were presented in a high-resolution gamma corrected monitor. A two-alternative forced-choice procedure was conducted, and the staircase method was used to calculate the contrast sensitivity. Reliability was assessed using a retest procedure within a month (±5 days) under the same conditions.

Results: Results showed statistical significance in 0.5 cpd and 10 cpd spatial frequencies for 0.5 cps (F = 77.36; $p < 0.001$), 7.5 cps (F = 778.37; $p < 0.001$), and 15 cps (F = 827.23; $p < 0.001$) with a very high (η^2 = 0.89) effect size. No statistical differences were found between the first and second sessions for all spatial frequencies. For reliability, a significantly high correlation and high internal consistency were found in all spatiotemporal conditions. The limits were calculated for normality.

Conclusion: We developed an approach to investigate the spatiotemporal integration of contrast sensitivity designed for clinical purposes. The relative contribution of the low spatial frequencies/high temporal frequencies and the high spatial frequencies/low temporal frequencies of the psychophysical channels can also be evaluated separately.

Keywords: Clinical Psychophysics; Drifting Grating; Dynamic Contrast Sensitivity; Primary Visual Pathway; Spatial Vision

J Ophthalmic Vis Res 2022; 17 (1): 69–77

INTRODUCTION

The evaluation of visual functions has improved in the last three decades with the development of visual tests for visual acuity (VA),[1–6] contrast sensitivity (CS),[7–12] color vision (CV),[13–16] motion perception (MP),[17–20] and stereopsis (ST),[21–26] among others. Despite these developments and multiple studies showing that visual functions other than VA provide diagnosis for subclinical and early impairments in visual function,[27–38] ophthalmology and visual sciences associated with optometry and orthoptic clinical practice have been preferentially using VA as a measurement of visual function.

The clear advantage of CS over VA measurements is the more detailed description of spatial vision, since symptomatic changes can occur in CS with VA within normal limits.[39, 40] Further, the test for VA is a measurement of the spatial separation function mediated by the parvocellular (PC) pathway, while CS measurements carry information mediated by the PC and magnocellular (MC) pathways.[41–45] Since both pathways can be measured by a CS function, it is an obvious clinical test with more resources for diagnosis of visual impairments.

Clinical assessment of CS is mainly performed using charts such as Pelli-Robson and Functional Acuity Contrast Test (FACT).[43, 46] Both methodologies have significant limitations. The Pelli-Robson chart is based on a recognition VA test; however, it has a fixed low spatial frequency in the overall chart, and the contrast steps are based on three letters, which could lead to a learning effect after only a few uses. Another problem related to the Pelli-Robson chart is the need to read letters, which reduces testing potential for young children. The FACT is composed of five spatial frequencies and nine contrast levels. One important problem is that almost all participants with normal vision can see the last contrast level for middle frequencies, inserting a roof effect to reduce the sensitivity of the test. They were unable to see more than half of the contrast levels for low and high spatial frequencies. Furthermore, the suprathreshold contrast levels were also fixed, reducing the precision of sensitivity measurement. Despite these problems, these methods have been successfully used to measure CS in clinical settings.

Some studies have proposed alternative methods to isolate the contribution of the PC and MC pathways for psychophysical measurements of CS with relative success.[47] However, they were designed to identify the psychophysical signature of the PC and MC pathways, and they took a long time to be completed (about one and a half hour), which made them unviable for clinical purposes.

Considering the above, we purposed a new CS test which intends to deal with chart measurement problems, and aimed to make the test user-friendly. The use of the same test for children and adults can make data comparable for development follow-ups, including a dynamic variable that amplifies the differences between PC and MC pathways. The possibility of isolating visual pathways is mandatory because many ocular and cerebral diseases affect these pathways differently. Our experience in the study of the traditional CS measurements in mercury,[30, 48–50] diabetes mellitus type 2,[51, 52] multiple sclerosis,[53] and Leber's Ocular Hereditary Neuropathy[54–56] motivated us to develop a CS test with greater efficiency in isolating PC and MC pathways for clinical testing.

METHODS

Participants

We evaluated 36 participants (17 men and 19 women) with a best-corrected VA of 20/20 or

Correspondence to:

Marcelo Fernandes Costa, PhD. Departamento de Psicologia Experimental, Instituto de Psicologia, Universidade de São Paulo, Av. Prof. Mello Moraes, 1721 Butantã, São Paulo, SP 05508-030, Brazil.
E-mail: costamf@usp.br

Received 22-04-2020; Accepted 11-03-2021

Access this article online

Website: https://knepublishing.com/index.php/JOVR

DOI: 10.18502/jovr.v17i1.10172

How to cite this article: Costa MF, Henriques LD, Pinho OC. Development of a Spatio-temporal Contrast Sensitivity Test for Clinical Use. J Ophthalmic Vis Res 2022;17:69–77.

better, measured using the ETDRS–Tumbling E chart (Xenônio Rep. Prod., São Paulo, Brazil). The exclusion criteria were absence of ophthalmologic complaints and/or diabetes mellitus, rheumatoid arthritis, systemic arterial hypertension, any other known systemic diseases, smokers, and the presence of dichromacy or anomalous trichromacy using the 38 plates version of the Ishihara pseudoisochromatic plates (Kanehara Trade Inc., Tokyo, Japan).

The participants, aged between 18 and 30 years (M = 22.6; SD = 3.7) were undergraduate and graduate students of the Institute of Psychology of the University of São Paulo. This study was approved by the local ethics committee via the approval number 66767317.5.0000.5561. All participants provided written consent for the inclusion of material about themselves and acknowledged that they could not be identified, as we ensured complete anonymity. The study followed the principles of the 1964 Declaration of Helsinki and its revised version.

Equipment and Stimulus

CS functions were also measured psychophysically with the software PSYCHO for Windows v2.36 (Cambridge Research) using a Sony Trinitron 19 in. (GFD-420). The monitor was driven by a Cambridge Research VSG 2/4 graphics board with a refresh rate of 100 Hz non-interlaced and an 800 × 600 resolution.

The stimuli used were horizontal sinusoidal gratings with an average luminance of 10 fL, that is, 34.4 cd/m^2, measured using an Optical OP200-E photometer (Cambridge Research) and a visual angle of 4°. The luminance output of the screen was calibrated using a luminance meter (LS-110, Konica Minolta Sensing, Inc., Osaka, Japan). Screen uniformity was checked at maximum output. The contrast of the sinusoidal grating is defined as a Michelson contrast:

$$C = \frac{L_{\max} - L_{\min}}{L_{\max} + L_{\min}},$$

where L_{max} is the maximum and L_{min} is the minimum luminance consisting of a dimensional value. Gratings of 0.5 cycles per degree (cpd) and 10 cpd drifted rightward and leftward at temporal frequencies of 0.5, 7.5, and 15 cycles per second (cps). Testing was conducted in a dark room with the participants positioned 1 m away from the video monitor.

Procedure

Participants were sat in a comfortable chair 1 m away from the monitor screen and were instructed to keep their eye fixed on a small black cross centered on the screen. Head stabilization was not performed. Ophthalmological patches (Oftan, AMP, São Paulo, Brazil) were used to cover one randomly chosen eye.

At the beginning of the experiment, the participant was adapted to a gray mean luminance in the dark for 5 min. The stimulation consisted of a drifting grating with a randomly chosen spatial frequency presented by 1000 ms, followed by 3000 ms for the response in a two-alternative forced-choice (2-AFC) procedure, pressing a specific keyboard key for the right (m) and left (z) based on their perception of the grating's drifting side [Figure 1].

A psychophysical staircase procedure with a dynamic step size was used to determine the threshold. The staircase began with a high contrast level (70 ± 10 randomly chosen), which changed the luminance to the mean luminance background. The change depended on the participant's response: the grating contrast approached the background mean luminance every time there was a correct response and moved away from it when there was an incorrect response. The dynamic step consisted of a 50% reduction of the contrast level between the stimulus and background luminance. After the second reversal, the reduction changed to 12.5% between the stimulus level and background luminance. The contrast improvement always changed in increments of 25%. After seven staircase reversals, the program automatically calculated the contrast thresholds as the average luminance corresponding to the last five reversals. All testing procedures, including the adaptation time, lasted approximately 20 min.

For all spatial frequencies, the contrast thresholds were converted to CS according to the following equation:

$$S = \frac{1}{Ct},$$

where *Ct* is the contrast threshold. To define the CS function, the CS for each spatial frequency was plotted.

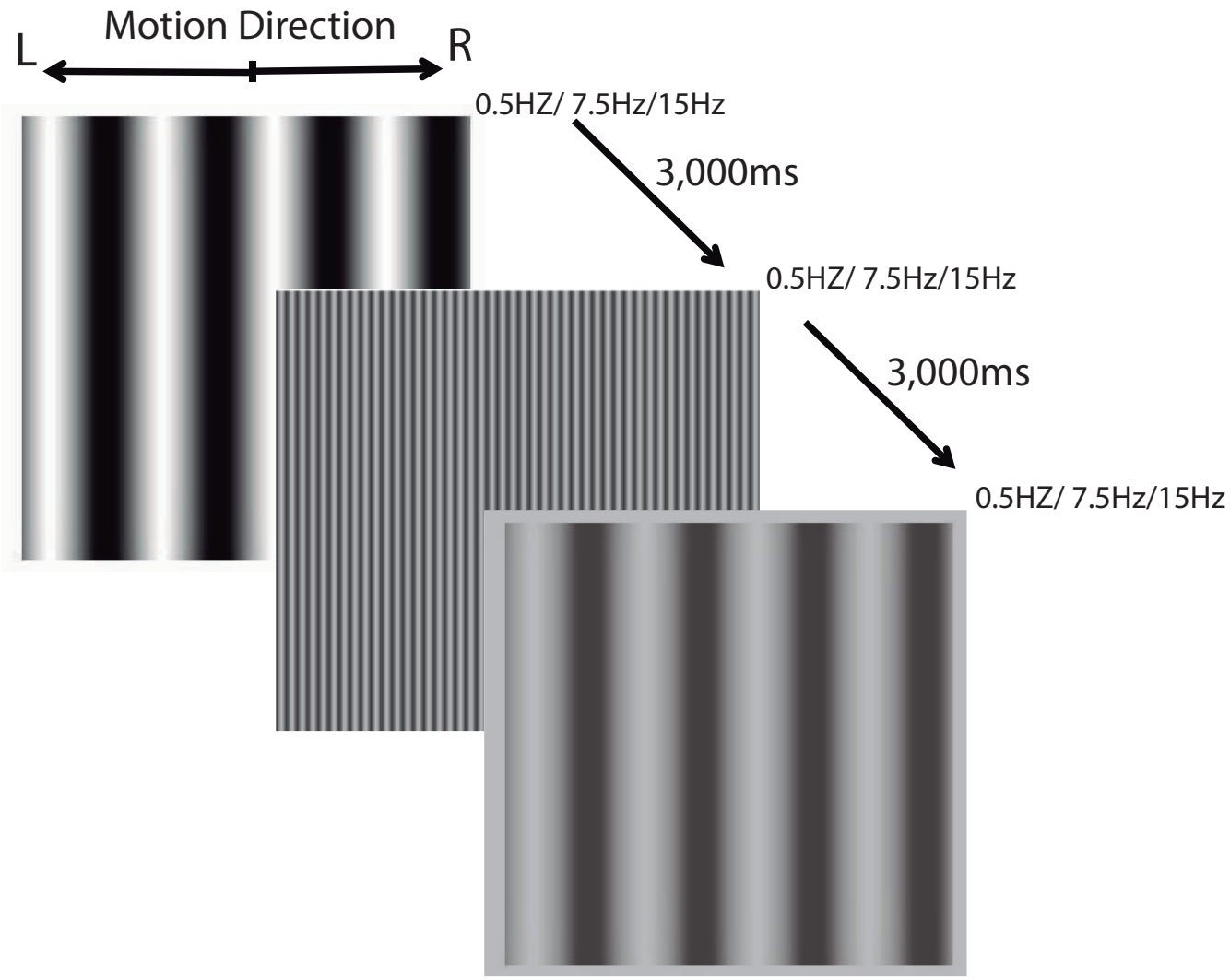

Figure 1. The illustrative timeline of the testing session. A spatial frequency randomly chosen was presented by 1 s, moving rightward or leftward in an also randomly chosen temporal frequency. The patient had up to 3 s to judge the movement of the grating in a two-AFC procedure.

Test reliability was estimated by comparing CS measurements in a test–retest design. The retest of the CS measurements was performed in all participants with a mean interval of one month (±5 days) between the first and second measurements. The retests were also performed monocularly in the same eye and under the conditions of the first test.

Statistical Analysis

Statistical analyses were performed using Statistica v.6.0.4, (StatSoft Inc., Tulsa, OK, USA, 2001). A complete descriptive analysis was performed. The normal distribution was checked by the Shapiro–Wilk and Kolmogorov–Smirnoff tests. A repeated-measures ANOVA was used to evaluate the statistical differences between spatial frequencies, drift velocity, and test–retest conditions. The correlation was calculated using the Pearson's product moment correlation test. No significant differences ($p < 0.05$) were observed between the conditions. The effect size, which is a quantitative measure of the magnitude of the experiment effect, was assessed using Cohen's *d* classification, that is, $d = 0.2$ was considered a "small" effect size, $d = 0.5$ represented a "medium" effect size, $d = 0.8$ a "large" effect size, and $d = 1.4$ a "huge effect" size.[57] The interpretation of the effect size was that if the means of the two groups do not differ by 0.2 or more SD, the difference could be considered trivial, even if it is statistically significant.

RESULTS

All participants successfully completed both the first and second sessions. The CS measured in the first and second experimental sessions is described in detail in Table 1.

Considering the spatial frequencies of the grating, statistically significant results were found between 0.5 cpd and 10 cpd for 0.5 cps (F = 77.36; $p < 0.001$), 7.5 cps (F = 778.37; $p < 0.001$), and 15 cps (F = 827.23; $p < 0.001$) in the first and second sessions. The calculated effect size was considered to be very high ($\eta^2 = 0.89$). No statistical difference was found between the first and second sessions for all spatial frequencies for 0.5 cps (F = 0.11; p = 0.73), 7.5 cps (F = 0.06; p = 0.93), and 15 cps (F = 0.24; p = 0.63). The results are shown in Figure 2.

Reliability was assessed using Pearson's correlation, and the results are shown in Figure 3. A significantly high correlation was found in 0.5 cpd for 0.5 cps (r = 0.988; $p < 0.001$), 7.5 cps (r = 0.919; $p < 0.001$), and 15 cps (r = 0.985; $p < 0.001$), and in 10 cpd for 0.5 cps (r = 0.989; $p < 0.001$), 7.5 cps (r = 0.972; $p < 0.001$), and 15 cps (r = 0.980; $p < 0.001$).

Internal consistency was assessed using Cronbach's alpha coefficient. A high internal consistency was obtained for 0.5 cpd (α = 0.8449) with high item-total correlation for 0.5 cps (r = 0.880), 7.5 cps (r = 0.836), and 15 cps (r = 0.894). Similarly, a high item-total correlation was also observed for 10 cpd (α = 0.8963) to 0.5 cps (r = 0.997), 7.5 cps (r = 0.994), and 15 cps (r = 0.979).

Based on the tolerance limits, we calculated the boundaries of the CS normality range for clinical purposes. Tolerance limits were calculated considering the mean value (X) and with a factor (k) multiplied by the standard deviation (SD).[58] The k factor can be chosen considering the percentage of the population covered (90%, 95%, or 99%) and the significance level of 0.90, 0.95, or 0.99, according to the number of participants. For our number of participants, we used the value 2.03, in which we covered 95% of the population with a p-value of 0.95. The tolerance limits are presented in the rightmost columns of Table 1.

DISCUSSION

Clinical evaluation of CS has been improved in ophthalmological clinics[8, 9] and it is a good step forward in understanding the spatial vision of their patients, as VA is a one-dimensional evaluation and CS is a two-dimensional test, since contrast is added to each spatial frequency measured. In our study, we included one more dimension by adding temporal modulation, which is a significant improvement, considering that objects in our visual environment are frequently moving. Using this more complex approach to investigate spatial vision, we can potentially be able to help our patients more efficiently and conduct more informative studies about visual and ophthalmological diseases and about the visual impairment suffered.

The robustness of our CS test was addressed by calculating the validity and reliability of the measurement. Validity was assessed by measuring the Pearson's correlation coefficients of the first and second measurements. We had a high correlation coefficient for both low (0.5 cpd) and high (10 cpd) spatial frequencies, regardless of the temporal frequency used. Since both the first and second measurements were highly correlated, this suggested that the influence of external variables had a low impact on the results obtained. Further, the reliability was considered high, suggesting that the reliability of our test was strong.

We also compared the mean contrast sensitivities of the first and second measurements. The absence of statistical significance in the same spatial frequencies compared to the first and second testing sessions and the statistical difference between the temporal frequencies within the first and the second testing sessions corroborate that our new CS test is robust.

An additional advantage of our measurement is the possibility of isolating the MC and PC visual pathways that contribute to CS. Using the amplitude of extracellular synaptic potential recordings for different Michelson contrast levels, retinal cells that project to the MC layer of the lateral geniculate nucleus (LGN) showed a logarithmic curve, in which huge improvements in amplitude responses occurred with small contrast increments. For the retinal ganglion cells projecting to the PC layer of the LGN, a linear curve was modeled with a small increase in amplitude response with a moderate increase in contrast levels.[41] The psychophysical correlates of these visual pathways were obtained using a pedestal paradigm.[47] MC-inferred responses were related to high temporal frequencies and PC-inferred responses related

Table 1. Descriptive data from the first and second contrast sensitivity measurements

Spatial frequency	First measurement			Second measurement		
	0.5 cps	7.5 cps	15 cps	0.5 cps	7.5 cps	15 cps
0.5 cpd	174.2 (32.5)	332.6 (78.6)	163.2 (37.4)	174.8 (32,2)	332.6 (56.9)	167.2 (33.4)
10 cpd	113.7 (43.7)	76.2 (25.4)	34.7 (7.8)	117.7 (41.3)	77.7 (25.9)	35.2 (6.9)

cpd, cyle per degree; cps, cycle per second

Table 2. Tolerance limits of contrast sensitivity for normality ranges

Spatial frequency	Tolerance limits		
	0.5 cps	7.5 cps	15 cps
0.5 cpd			
Upper	240.3	492.2	239.1
Lower	108.2	173	87.3
10 cpd			
Upper	202.5	127.9	50.5
Lower	24.8	24.6	18.8

cpd, cyle per degree; cps, cycle per second

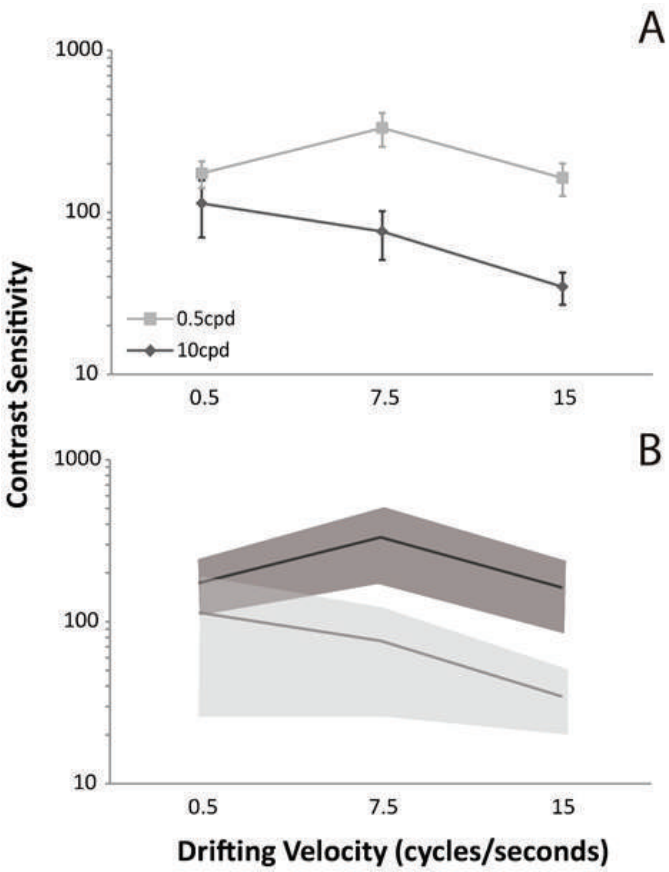

Figure 2. The psychophysical CS signature for the low (0.5 cpd) and high (10 cpd) spatial frequency. (A) The mean and standard deviation of the spatiotemporal interaction. (B) The normality range to be used for clinical purposes. In both panels, it is evident that the middle and high temporal frequencies are more discriminable areas to isolate the MC and PC contribution in the CS.

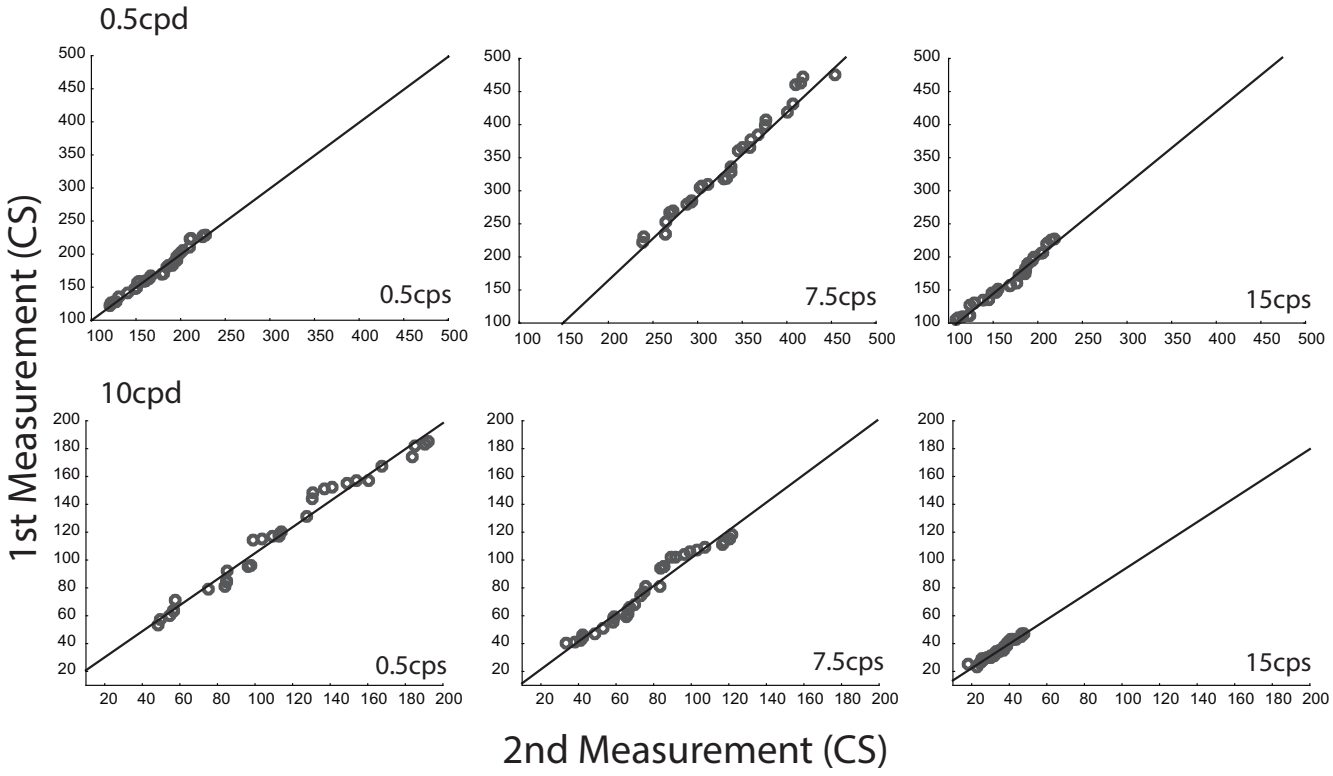

Figure 3. Correlations between the first and second measurements for reliability purposes. A strong correlation is evident for both low and high spatial frequencies in all temporal frequencies.

to low temporal frequencies. According to the spatial profile, low spatial frequencies were related to the MC-inferred pathway and the PC-inferred pathway related to high spatial frequencies.[45] The results obtained in our test are in line with earlier studies since the high spatial frequency with a low temporal modulation had better CS than the results for the middle or high temporal frequencies. On the other hand, better CS was obtained for the middle and high temporal modulations for low spatial frequencies.

Furthermore, we found a significantly different signature of CS spatiotemporal integration. For the low spatial frequency, there was a reduction in CS as the temporal frequency increased in an almost linear fashion. For the high spatial frequency, the curve had an inverted U-shape, in which there was an increase in CS as the temporal frequency increased from 0.5 to 7.5 Hz and then, there was an inversion of the relation since the CS reduced as the temporal frequency increased from 7.5 to 15 Hz. The different signatures of the MC- and PC-CS measured psychophysically have two important implications. First, the test was successful in isolating the MC and PC contributions of the measured spatiotemporal CS. Second, the difference in the CS shape has an important contribution for diagnostic purposes, adding resolution to the CS measurement.

The isolation of MC and PC pathways has a huge clinical significance because many ophthalmological and neurological diseases affect these visual pathways differently. Visual impairment related to reading problems in children with learning difficulties and dyslexia has been related to the reduction of CS at low spatial frequencies, suggesting an MC pathway failure.[32] MP, also an MC pathway function, is impaired in children with Down's Syndrome[34] and strabismic amblyopia.[28, 59] We believe that our test improves the MC- and PC-mediated CS measurements because it integrates spatial and temporal proprieties in one measurement.

Considering the significant clinical applications, we calculated the normality range for clinical purposes. Of course, there are some restrictions on the use of normal ranges, as we calculated based on the age of our sample. For children and

elderly patients, additional measurements should be performed in future studies.

In summary, we developed a test to investigate the spatiotemporal integration of CS, designed for clinical purposes. The relative contribution of the low spatial frequencies/high temporal frequencies, and the high spatial frequencies/low temporal frequencies of the psychophysical channels can also be evaluated separately. The validation and replicability were highly successful, and tolerance limits were calculated to define the normality ranges.

Acknowledgments

The authors would like to thank all the students at the Psychology Institute, University of São Paulo, who voluntarily participated in the experiments.

Financial Support and Sponsorship

This research was supported by grants from FAPESP (Projeto Tematico # 2014/26818-2 to Dora Fix Ventura and Marcelo Fernandes Costa); CNPq #401153/2009-6 to M.F.C.; M.F.C. is CNPq research fellow.

Conflicts of Interest

The authors declare that they have no conflict of interest.

REFERENCES

1. Ferris FL 3rd, Kassoff A, Bresnick GH, Bailey I. New visual acuity charts for clinical research. *Am J Ophthalmol* 1982;94:91–96.
2. Adoh TO, Woodhouse JM. The Cardiff acuity test used for measuring visual acuity development in toddlers. *Vision Res* 1994;34:555–560.
3. Bach M. The Freiburg Visual Acuity Test – variability unchanged by post-hoc re-analysis. *Graef Arch Clin Exp* 2007;245:965–971.
4. Bastawrous A, Rono HK, Livingstone IA, Weiss HA, Jordan S, Kuper H, et al. Development and validation of a smartphone-based visual acuity test (Peek Acuity) for clinical practice and community-based fieldwork. *JAMA Ophthalmol* 2015;133:930–937.
5. Becker R, Teichler G, Graf M. Comparison of visual acuity measured using Landolt-C and ETDRS charts in healthy subjects and patients with various eye diseases. *Klin Monatsbl Augenh* 2011;228:864–867.
6. Manny RE, Hussein M, Gwiazda J, Marsh-Tootle W. Repeatability of ETDRS visual acuity in children. *Invest Ophth Vis Sci* 2003;44:3294–3300.
7. Ginsburg AP. A new contrast sensitivity vision test chart. *Am J Optom Physiol Opt* 1984;61:403–407.
8. Adams RJ, Mercer ME, Courage ML, Vanhofvanduin J. A new technique to measure contrast sensitivity in human infants. *Optometry Vision Sci* 1992;69:440–446.
9. Alexander KR, McAnany JJ. Determinants of contrast sensitivity for the Tumbling E and Landolt C. *Optometry Vision Sci* 2010;87:28–36.
10. Alexander KR, Xie W, Derlacki DJ. Visual acuity and contrast sensitivity for individual Sloan letters. *Vis Res* 1997;37:813–819.
11. Choi AJ, Nivison-Smith L, Phu J, Zangerl B, Khuu SK, Jones BW, et al. Contrast sensitivity isocontours of the central visual field. *Sci Rep* 2019;9:11603.
12. Dakin SC, Turnbull PR. Similar contrast sensitivity functions measured using psychophysics and optokinetic nystagmus. *Sci Rep* 2016;6:34514.
13. Atchison DA, Bowman KJ, Vingrys AJ. Quantitative scoring methods for D15 panel tests in the diagnosis of congenital color-vision deficiencies. *Optometry Vision Sci* 1991;68:41–48.
14. Bailey JE, Neitz M, Tait DM, Neitz J. Evaluation of an updated HRR color vision test. *Visual Neurosci* 2004;21:431–436.
15. Birch J. Clinical use of the City University Test (2nd Edition). *Ophthalmic Physiol Opt* 1997;17:466–472.
16. Reffin JP, Astell S, Mollon JD. Trials of a computer-controlled color-vision test that preserves the advantages of pseudoisochromatic plates. In: Drum B, Moreland JD, Serra A, editors. Colour vision deficiencies X. Dordrecht: Springer; 1991. 69–76 p.
17. Armstrong V, Maurer D, Lewis TL. Sensitivity to first- and second-order motion and form in children and adults. *Vis Res* 2009;49:2774–2781.
18. Borghuis BG, Tadin D, Lankheet MJM, Lappin JS, van de Grind WA. Temporal limits of visual motion processing: psychophysics and neurophysiology. *Vision* 2019;3:5.
19. Hollants-Gilhuijs MA, Ruijter JM, Spekreijse H. Visual half-field development in children: detection of motion-defined forms. *Vis Res* 1998;38:651–657.
20. Manny RE, Fern KD. Motion coherence in infants. *Vis Res* 1990;30:1319–1329.
21. Birch E, Petrig B. FPL and VEP measures of fusion, stereopsis and stereoacuity in normal infants. *Vis Res* 1996;36:1321–1327.
22. Earle DC. Perception of glass pattern structure with stereopsis. *Perception* 1985;14:545–552.
23. Langley K, Fleet DJ, Hibbard PB. Stereopsis from contrast envelopes. *Vis Res* 1999;39:2313–2324.
24. Norman JF, Norman HF, Craft AE, Walton CL, Bartholomew AN, Burton CL, et al. Stereopsis and aging. *Vis Res* 2008;48:2456–2465.
25. Shea SL, Fox R, Aslin RN, Dumais ST. Assessment of stereopsis in human infants. *Invest Ophth Vis Sci* 1980;19:1400–1404.
26. Wilcox LM, Harris JM, McKee SP. The role of binocular stereopsis in monoptic depth perception. *Vis Res* 2007;47:2367–2377.
27. Costa M, Oliveira A, Santana C, Ventura D, Zatz M. Red-green color vision impairment in Duchenne muscular dystrophy. *Neuromuscular Disord* 2007;17:815.

28. Costa MF, Cunha G, de Oliveira Marques JP, Castelo-Branco M. Strabismic amblyopia disrupts the hemispheric asymmetry for spatial stimuli in cortical visual processing. *Br J Vis Impair* 2016;34:141–150.
29. Costa MF, Moreira SM, Hamer RD, Ventura DF. Effects of age and optical blur on real depth stereoacuity. *Ophthalmic Physiol Opt* 2010;30:660–666.
30. Costa MF, Tomaz S, de Souza JM, Silveira LC, Ventura DF. Electrophysiological evidence for impairment of contrast sensitivity in mercury vapor occupational intoxication. *Environ Res* 2008;107:132–138.
31. da Costa MF, Paranhos A, Lottenberg CL, Castro LC, Ventura DF. Psychophysical measurements of luminance contrast sensitivity and color discrimination with transparent and blue-light filter intraocular lenses. *Ophthalmol Ther* 2017;6:301–312.
32. Cormack FK, Tovee M, Ballard C. Contrast sensitivity and visual acuity in patients with Alzheimer's disease. *Int J Geriatr Psychiatry* 2000;15:614–620.
33. Croningolomb A, Sugiura R, Corkin S, Growdon JH. Incomplete achromatopsia in Alzheimers disease. *Neurobiol Aging* 1993;14:471–477.
34. Del Viva MM, Tozzi A, Bargagna S, Cioni G. Motion perception deficit in Down Syndrome. *Neuropsychologia* 2015;75:214–220.
35. Aaen-Stockdale C, Hess RF. The amblyopic deficit for global motion is spatial scale invariant. *Vis Res* 2008;48:1965–1971.
36. Acheson JF, Cassidy L, Grunfeld EA, Shallo-Hoffman JA, Bronstein AM. Elevated visual motion detection thresholds in adults with acquired ophthalmoplegia. *Br J Ophthalmol* 2001;85:1447–1449.
37. Boets B, Wouters J, van Wieringen A, Ghesquiere P. Coherent motion detection in preschool children at family risk for dyslexia. *Vis Res* 2006;46:527–535.
38. Ezzati A, Khadjevand F, Zandvakili A, Abbassian A. Higher-level motion detection deficit in Parkinson's disease. *Brain Res* 2010;1320:143–151.
39. Ginsburg AP. Contrast sensitivity and functional vision. *Int Ophthalmol Clin* 2003;43:5–15.
40. Amesbury EC, Schallhorn SC. Contrast sensitivity and limits of vision. *Int Ophthalmol Clin* 2003;43:31–42.
41. Kaplan E, Shapley RM. The primate retina contains two types of ganglion cells, with high and low contrast sensitivity. *Proc Natl Acad Sci USA* 1986;83:2755–2757.
42. Keri S, Benedek G. Visual contrast sensitivity alterations in inferred magnocellular pathways and anomalous perceptual experiences in people at high-risk for psychosis. *Vis Neurosci* 2007;24:183–189.
43. Pelli DG, Bex P. Measuring contrast sensitivity. *Vis Res* 2013;90:10–14.
44. Alexander KR, Barnes CS, Fishman GA, Pokorny J, Smith VC. Contrast sensitivity deficits in inferred magnocellular and parvocellular pathways in retinitis pigmentosa. *Invest Ophthalmol Vis Sci* 2004;45:4510–4519.
45. Costa MF. Clinical psychophysical assessment of the ON- and OFF-systems of the magnocellular and parvocellular visual pathways. *Neurosci Med* 2011;2:330–340.
46. Onal S, Yenice O, Cakir S, Temel A. FACT contrast sensitivity as a diagnostic tool in glaucoma: FACT contrast sensitivity in glaucoma. *Int Ophthalmol* 2008;28:407–412.
47. Smith VC, Sun VCW, Pokorny J. Pulse and steady-pedestal contrast discrimination: effect of spatial parameters. *Vis Res* 2001;41:2079–2088.
48. Canto-Pereira LHM, Lago M, Costa MF, Rodrigues AR, Saito CA, Silveira LCL, et al. Visual impairment on dentists related to occupational mercury exposure. *Environ Toxicol Pharmacol* 2005;19:517–522.
49. Feitosa-Santana C, Barboni MT, Oiwa NN, Paramei GV, Simoes AL, da Costa MF, et al. Irreversible color vision losses in patients with chronic mercury vapor intoxication. *Vis Neurosci* 2008;25:487–491.
50. Ventura DF, Simoes AL, Tomaz S, Costa MF, Lago M, Costa MTV, et al. Colour vision and contrast sensitivity losses of mercury intoxicated industry workers in Brazil. *Environ Toxicol Pharmacol* 2005;19:523–529.
51. Feitosa-Santana C, Oiwa NN, Paramei GV, Bimler D, Costa MF, Lago M, et al. Color space distortions in patients with type 2 diabetes mellitus. *Vis Neurosci* 2006;23:663–668.
52. Feitosa-Santana C, Paramei GV, Nishi M, Gualtieri M, Costa MF, Ventura DF. Color vision impairment in type 2 diabetes assessed by the D-15d test and the Cambridge Colour Test. *Ophthalmic Physiol Opt* 2010;30:717–723.
53. Moura AL, Teixeira RA, Oiwa NN, Costa MF, Feitosa-Santana C, Callegaro D, et al. Chromatic discrimination losses in multiple sclerosis patients with and without optic neuritis using the Cambridge Colour Test. *Vis Neurosci* 2008;25:463–468.
54. Gualtieri M, Bandeira M, Hamer RD, Costa MF, Oliveira AG, Moura AL, et al. Psychophysical analysis of contrast processing segregated into magnocellular and parvocellular systems in asymptomatic carriers of 11778 Leber's hereditary optic neuropathy. *Vis Neurosci* 2008;25:469–474.
55. Ventura DF, Gualtieri M, Oliveira AG, Costa MF, Quiros P, Sadun F, et al. Male prevalence of acquired color vision defects in asymptomatic carriers of Leber's hereditary optic neuropathy. *Invest Ophth Vis Sci* 2007;48:2362–2370.
56. Ventura DF, Quiros P, Carelli V, Salomao SR, Gualtieri M, Oliveira AG, et al. Chromatic and luminance contrast sensitivities in asymptomatic carriers from a large Brazilian pedigree of 11778 Leber hereditary optic neuropathy. *Invest Ophth Vis Sci* 2005;46:4809–4814.
57. Cohen J. Quantitative methods in psychology. *Psychol Bull* 1992;112:155–159.
58. Dixon WJ, Massey FJ. Introduction to statistical analysis. 3rd ed. New York, NY: McGraw-Hill; 1969.
59. Aaen-Stockdale C, Ledgeway T, Hess RF. Second-order optic flow deficits in amblyopia. *Invest Ophth Vis Sci* 2007;48:5532–5538.

Original Article

Prevalence and Burden of Refractive Errors at National and Sub-national Levels in Iran

Seyed Farzad Mohammadi[1], MD- FICO; Farshad Farzadfar[2], MD; Parinaz Mehdi Pour[2], MS
Elham Ashrafi[1], PhD; Alireza Lashay[1], MD; Bahram Mohajer[2], MD; Mohsen Asadi Lari[3], MD

[1]Translational Ophthalmology Research Center, Farabi Eye Hospital, Tehran University of Medical Sciences, Tehran, Iran
[2]Non-Communicable Diseases Research Center, Endocrinology and Metabolism Research Institute, Tehran University of Medical Sciences, Tehran, Iran
[3]Department of Epidemiology, School of Public Health, Iran University of Medical Sciences, Tehran, Iran

ORCID:
Seyed-Farzad Mohammadi:0000-0002-9209-3034
Elham Ashrafi:0000-0001-8640-0168

Abstract

Purpose: To estimate the prevalence, burden of refractive errors and their associated trend from 1990 to 2018 and geographic inequalities in Iran.

Methods: Data regarding the epidemiology of refractive errors was extracted from three different sources: systematic review of published literature, data from visual school screening programs, and data from Iran's national health survey (NHS). The pool of all available data on refractive errors as well as demographic, location, and socioeconomic status covariates were fitted in spatio-temporal and Gaussian process regression models to predict the prevalence of refractive errors from the years 1990 to 2018 in 31 provinces grouped by age and sex in order to calculate years lived with disability (YLDs).

Results: In 2018, the age-adjusted prevalence of refractive errors was 16.32% (95% uncertainty interval [UI]: 12.44–21.48%) in both sexes, 17.98% (95% UI: 13.74–23.61%) in women, and 14.66% (95% UI: 11.14–19.36%) in men. The prevalence of refractive errors reveals that it increases with age. Refractive errors contributed to 441.41 and 348.38 YLDs in men and women, respectively. The age-standardized prevalence growth was 31.30% in females and 24.32% in males from the years 1990 to 2018. Significant geographical heterogeneity was observed. The age-standardized YLDs rates of refractive errors represent an increasing trend of 28.9% increase from 1990 to 2018.

Conclusion: Over 28 years, the prevalence of refractive errors increased significantly. Women tend to have higher rates of prevalence. The prevalence increased in older ages. Border provinces had the lowest prevalence. Age-standardized YLDs rates of refractive errors increased by about 30%.

Keywords: Burden; Disability-adjusted Life Years; Iran; Prevalence; Refractive Errors

J Ophthalmic Vis Res 2022; 17 (1): 78–88

INTRODUCTION

Refractive errors are recognized as approximately half of the causes of visual impairment (VI) and the second leading cause of functional blindness.[1] It impinges on patients' quality of life through functional, psychosomatic, and cosmetic issues while also causing economic burden.[2] Refractive errors are listed among one of the four non-fatal disorders classified in the 20 top causes of disability-adjusted life years (DALYs).[3] Since refractive disorders mostly initiate early in life, remarkable morbidity assessed by years of living with disability (YLDs) is associated more with this eye disorder as compared to other ocular diseases.[3] Compared to other causes of VI, refractive errors in most cases is easily treatable by prescribing glasses which is one of the most cost-effective interventions in eye care. If left uncorrected, refractive errors can affect performance, reduce employability, and productivity, and compromise the entire life of patients.[2–5]

Uncorrected refractive disorders relative to the total DALYs increased by 42% globally when compared to 1990,[6] and refractive disorders were responsible for the loss of healthy life of approximately 44.8 years per 100,000 population globally with an increasing trend and with an advance in age from 40 years onward.[7, 8] The Eastern Mediterranean region has the second-highest DALY recorded from refractive errors among world regions. This is the consequence of a higher prevalence (188.7; 95% uncertainty interval [UI]: 125.3–276.9%) of refractive error in addition to the suboptimal implementation of prevention/treatment options. Therefore, cost-effective prevention programs are recommended to address this epidemiological priority.[6] Refraction/accommodation (functional) disorders in Iran accounted for 0.42% DALY in 1990 and 0.47% in 2010, where the associated costs and issues were greater than that of other causes of VI, namely cataract, glaucoma, and macular degeneration.[9]

Providing reliable evidence and situational analysis is required for promoting good health practices. Global Burden of Disease (GBD) 2017 has presented estimates for the economic and social burden of refractive errors; which, however, lack subnational estimates and comprehensive inclusion of the present national surveys data in Iran.

This study aims to estimate the incidence, prevalence, burden, and trend of refractive errors during the period of 1990 to 2018 at the national and sub-national levels in Iran.

METHODS

Data Sources

This research represents secondary data analysis on three data sources; the systematic review of published literature, data from the Ministry of Health and Medical Education (MoHME) screening programs, and Iran's National Health Survey (NHS) data [Figure 1]. A detailed explanation of the search strategy and cleaning process of all data sources is presented in a supplementary document.[10]

Systematic review

Published literature between January 1980 and December 2018 present in Medline (PubMed), ISI Web of Science, Scopus, Iranian Digital databases of SID (http://www.sid.ir), Barakat knowledge network system (http://health.barakatkns.com), and in the national ophthalmic literature database by Noor Ophthalmology Research Center (http://iraneyedoc.com) were all searched.

Correspondence to:

Elham Ashrafi, PhD. Translational Ophthalmology Research Center, Farabi Eye Hospital, Tehran University of Medical Sciences, Qazvin Square, Tehran 1336616351, Iran.
E-mail: eashrafi@sina.tums.ac.ir

Received 29-05-2021; Accepted 21-09-2021

Access this article online

Website: https://knepublishing.com/index.php/JOVR

DOI: 10.18502/jovr.v17i1.10173

How to cite this article: Mohammadi SF, Farzadfar F, Pour PM, Ashrafi E, Lashay A, Mohajer B, Lari MA. Prevalence and Burden of Refractive Errors at National and Sub-national Levels in Iran. J Ophthalmic Vis Res 2022;17:78–88.

Additionally, the abstract books of the Iranian ophthalmology annual congresses from the years 2008 through 2010 were screened and included only if the inclusion criteria was satisfied. A detailed explanation of the study selection criteria and critical appraisal is described in the protocol paper.[10] A crosswalk method was applied in extracting the pertinent data where cases related to myopia/hyperopia/astigmatism were combined to those of refractive error and modified the rural/urban scope. A total of 146 data points from 10 provinces were extracted from the systematic review and included in the analysis [Table 1].

Refractive error screening programs

Unpublished official data for the prevalence of refractive errors occurring in the years 2007, 2010, and 2012 were gathered from screening programs performed in the elementary schools of all the provinces. A total of 1156 data points were extracted [Table 1].

National Health Survey

The National Health Survey (NHS) includes two self-reporting questions about spectacles use ("Do you use glasses?") and spectacles need ("Do you need glasses to see clearly?") in all age groups and provinces in the years 1990 and 2000. After an adjustment of the NHS data by MoHME/Systematic Review Data while using a crosswalk method and adjusting for missing data, a total of 1488 data points were generated [Table 1].

Statistical Analysis

A total number of 2790 data points were included from the above data sources. We aimed to estimate the prevalence of refractive errors for different age groups, between the two sexes, at national level, and in 31 provinces, from the years 1990 to 2018. Generalized Linear Mixed Model (GLMM) was applied to impute missing values of these age-sex-location-time combinations. In this model, we predicted the prevalence of refractive errors with fixed covariates, including years of schooling, wealth indices, urbanization ratios, as well as the random effects of the location of the provinces. Urbanization ratios and population data were retrieved from the national censuses, which were conducted by the Statistical Center of Iran (SCI). To calculate other covariates in the statistical models, we used Household Expenditure and Income surveys from the years 1990 to 2018, which were also conducted by the SCI. The second step after applying the GLMM was the application of an age-spatio-temporal (AST) model capturing all variations for time, location (province), and age groups of residuals from the first model. In the AST model, we assumed that there were unmeasured variations in residuals that were derived from GLMM. To estimate these variations, we weighted adjacent years, provinces, and ages by three matrices and used neighboring elements of the matrix that had more correlation with each other where this measure decreased by increasing their distances. The weighted residuals were then added back to GLMM predictions and final estimates of prevalence were produced. In order to have robust estimates with certainty, using estimated rates, we employed Gaussian Process Regression (GPR) which is a Bayesian technique. It defines a flexible model with hierarchical priors for its parameters and it also has a mean and covariance function. In this study, these functions were defined in the AST model and the Matérn function, respectively. Gaussian Process Regression (GPR) samples were drawn from the posterior distribution by using the Markov Chain Monte Carlo method and we calculated the median for the final estimates of prevalence and 2.5 and 97.5 percentiles for its uncertainty.[10]

The data collected from the 2018 record of the national population in Iran was used as the standard population in a direct age-standardized analysis to facilitate the statistical comparisons between provinces.

Since refractive errors do not have fatal consequences, DALYs were considered equal to YLDs, which were estimated by multiplying the prevalence by the reported disability weight for refractive errors in the GBD study, and the duration of symptoms.

RESULTS

Prevalence of Refractive Errors

At national level, in the year 2018, the age-adjusted prevalence of refractive errors was estimated at

Table 1. Data source specifications.

Source	Sex	Age (yr)	Province	Year	Coverage	Number of data point
Systematic Review	Male/female	All ages	10	1999–2014	Sub-national	146 (5.23%)
Ministry of Health	Male/female	7–15	31	2007, 2010, 2012	National/sub-national	1156 (37.6%)
National Health Survey	Male/female	All ages	31	1990, 2000	National	1049 (41.43%)

Table 2. Prevalence of refractive errors by sex and age group in year 2018.

Age group (yr)	Sex	Prevalence	Lower limit	Upper limit
0–6	Female	1.25	1.1	1.41
0–6	Male	1.01	0.9	1.13
7–11	Female	4.26	3.04	5.97
7–11	Male	3.33	2.34	4.75
12–14	Female	7.6	5.56	10.39
12–14	Male	6.1	4.42	8.42
15–17	Female	7.31	5.22	10.27
15–17	Male	5.58	3.91	7.95
18–24	Female	12.32	9.62	15.75
18–24	Male	9.48	7.17	12.54
25–34	Female	11.42	8.69	14.98
25–34	Male	8.53	6.57	11.05
35–44	Female	16.35	12.96	20.66
35–44	Male	13.1	10.12	17.02
45–54	Female	27.16	21.51	34.23
45–54	Male	25.62	19.56	33.56
55–64	Female	30.71	24.55	38.45
55–64	Male	23.12	18.1	29.6
65–74	Female	32	24.99	40.95
65–74	Male	26.43	21.05	33.17
75–84	Female	36.22	26.91	48.93
75–84	Male	27.94	20.57	38.14
85	Female	29.22	20.72	41.31
85	Male	25.75	19	34.95

16.32% (95% UI: 12.44%, 21.48%). It is 17.98% (95% UI: 13.74–23.61%) in women and 14.66% (95% UI: 11.14–19.36%) in men. The age-standardized prevalence increased by 31.30% in females and 24.32% in males during the years 1990 to 2018.

The prevalence of refractive errors showed an increasing trend with age in both sexes, with the highest prevalence among women older than 85 years with a prevalence of 29.22% (95% UI: 20.72–41.31%) in 2018. The highest rise is seen in ages 35 to 44 years [Table 2; Figures 2 & 3].

Geographic Distribution of Refractive Errors

The age-standardized prevalence of refractive errors in different provinces is reported in Figure 4. Provinces heterogeneity was observed

Table 3. Age-standardized DALYs per 100,000 in different years and sex.

Year	Male	Female
1990	144.95	177.86
1995	172.69	213.64
2000	205.87	257.28
2005	255.14	319.81
2010	302.38	381.64
2018	348.38	441.41

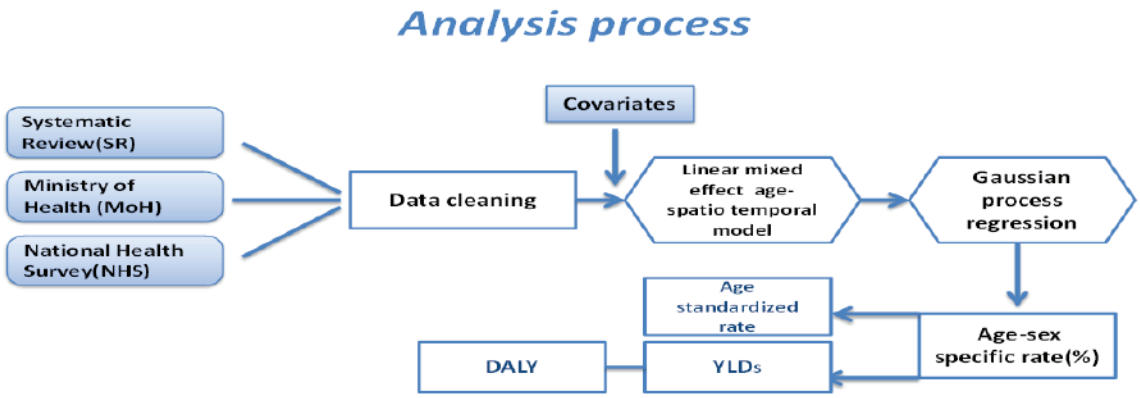

Figure 1. Analysis process for YLDs calculation. DALY, disability-adjusted life years; YLD, years lived with disability.

consistently during the study period. The highest age-standardized prevalence recorded in 2018 was 20.4% in North Khorasan while the lowest was discovered in Tehran with a prevalence of 13.8%. Country provinces located at the borders tend to have lower levels of refractive errors while central provinces showed higher levels, particularly in recent years. The data also show a negative association with the wealth index (*r*: 0.6; *P*: 0.032).

The Burden of Refractive Errors (Per 100,000)

Refractive errors contributed to 441.41 and 348.38 YLDs in men and women, respectively. The YLDs in 2018 in age and gender groups are summarized in Table 3. The highest number of years of life lost was seen in women over 85 years with 499.55 YLDs.

Nationally, the age-standardized YLDs rates of refractive errors reveal an increasing trend of 28.9% during this period [Figure 5].

DISCUSSION

This study represented a national first effort to collect data from multiple sources at the individual level to estimate the prevalence of refractive errors over an extended period in Iran. It revealed that a total of 13 million Iranian citizens are affected by refractive errors. Similar to the global patterns, advancing age, female gender, and lower socioeconomic status were identified as risk factors.[6, 11]

Refractive error prevalence carries an inherent "age-related" feature; where it was determined through the study that the possibility of developing some kind of refractive error increases with age. While in viewing the data of the decade one age category a prevalence of under 10% refractive error was noticed in 2018 throughout the country, it increased to approximately 17% in the ninth decade age category. Several phenomena may explain this, juvenile myopia generally commences before 6 years of age and continues to occur and increase in severity up to 16 years or more. In later years, keratoconus incidence in the second and third decades contributes modestly to increased refractive error. In later years especially where people approach their 40s, presbyopia and latent hyperopia may develop and manifest in patients. The incidence of the presbyopia

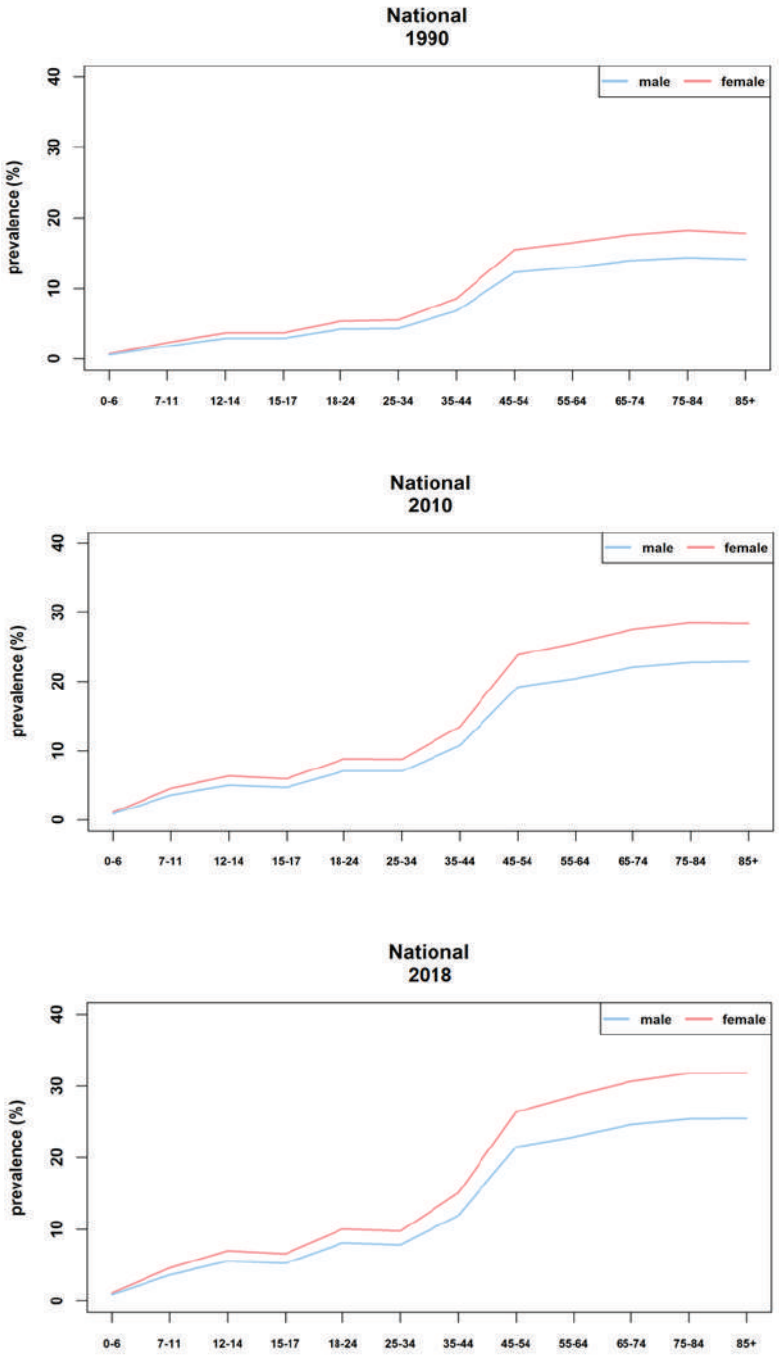

Figure 2. Refractive errors prevalence at national level by sex and age group from 1990 to 2018.

and hyperopia conditions fluctuates to a higher level during the middle aged category of the population which is clearly reflected in the study diagrams. Decoupling of lenticular astigmatism (from corneal astigmatism) and emergence of nuclear sclerosis may also contribute to the age-related changes. The latter should explain the trend in the >70 years (index myopia) category. Diabetes mellitus is another source for incidental refractive error in the middle to older ages as it may induce refractive index shifts in the crystalline lens.

The increasing trend in the prevalence of refractive errors is consistent with other reports in

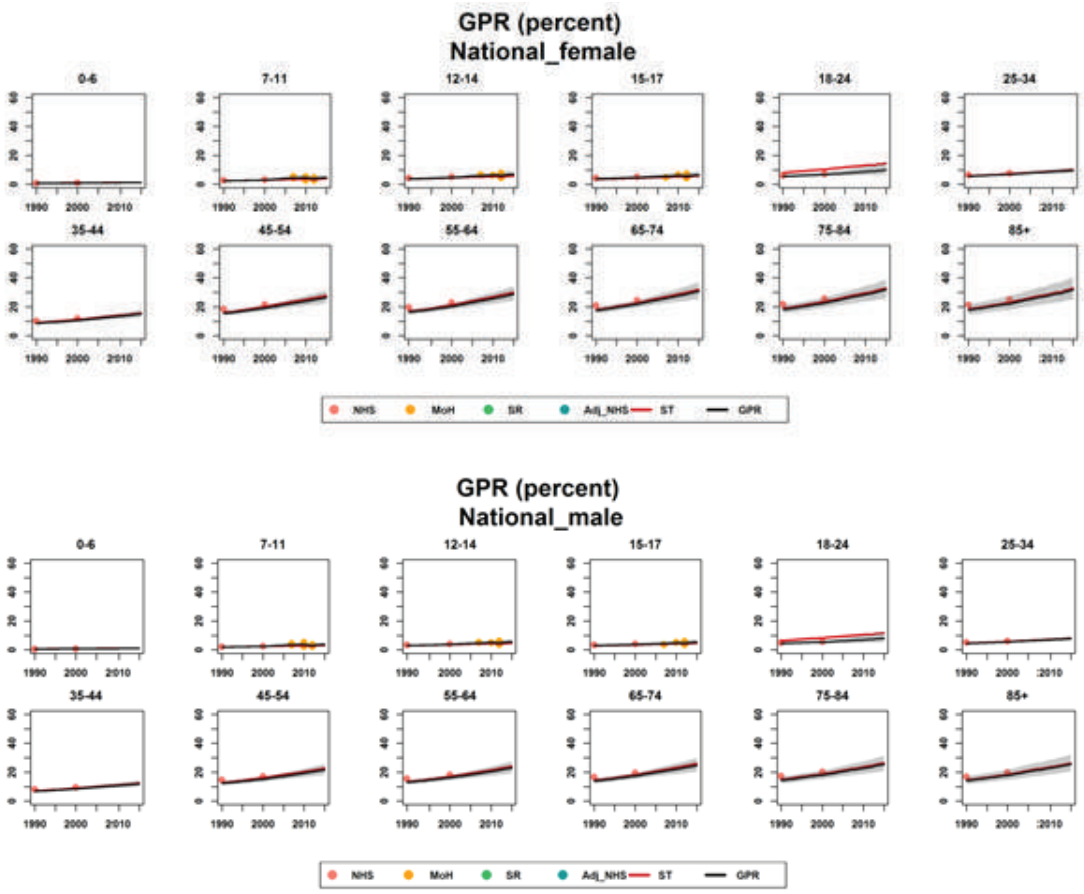

Figure 3. Trend of refractive errors prevalence at national level by sex and age groups from 1990 to 2018.

the world and region.[6, 11] However, our prevalence estimates in Iran are lower as compared with corresponding figures in the region. In addition, relative to global estimates, refractive errors prevalence estimated in Iran reflects a more positive outcome.[11]

It is known that the world is experiencing a pandemic of refractive errors.[12] In 2010, about 28% of the world's population was affected by short-sightedness. This is predicted to rise to 34% by 2020 and then to approximately 50% by 2050.[13] The aging population has many more people with refractive errors (demographic transition). Presbyopia and manifest hyperopia are the two major contributors in older ages. The myopia epidemic, on the other hand, may be caused by epidemiologic transition factors; daily habits that encompass the use of digital, sight-intensive, and night and near vision-oriented activities may affect the state of vision in molecularly vulnerable people where they may become more prone to myopia. Many ecological studies suggested a correlation between indoor and nightlife activities with the prevalence of myopia and its related severity.[14–16] In addition, lifestyle changes involving the execution of more intense visual tasks such as using a computer or a smartphone led to glasses being prescribed even for patients diagnosed with minimal myopia. An increase in the prevalence of refractive errors in Iran may be attributed to lifestyle changes due to technological advancements and behavioral factors relating to specific age groups. The initial and progressive pace of juvenile myopia in recent years were both attributed to near-work activities and digital life. Cohort studies have proven the axial growth in the eyes in the global population.[17] The COVID-19 pandemic due to the lifestyle restrictions has exacerbated the use of digital apparatus and the need for indoor entertainment where now there are frequent studies revealing more myopia incidence and progression.[18] However, it should also be mentioned that based on particular studies this phenomenon seems to not be consistent

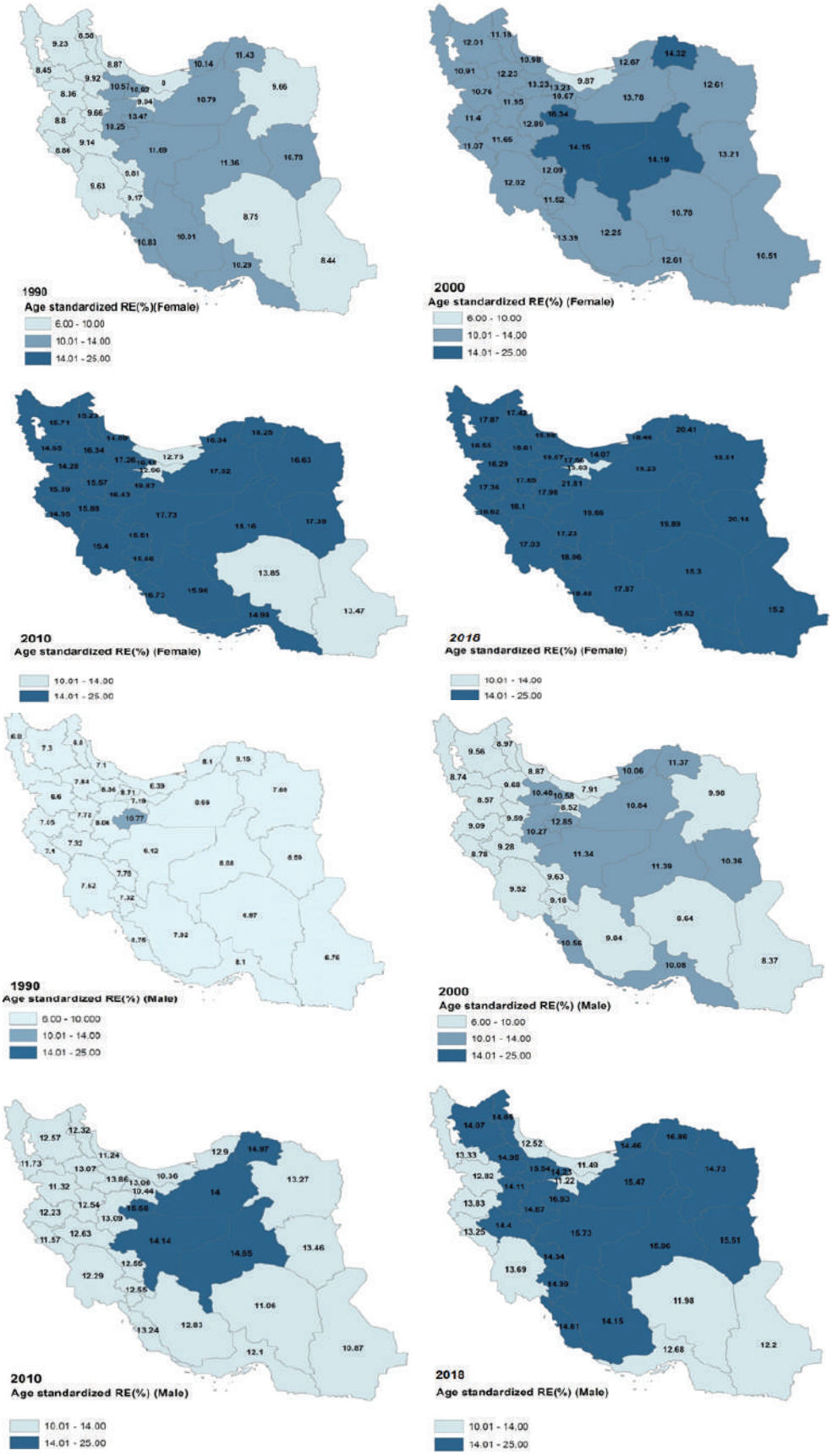

Figure 4. Geographic distribution of age-standardized prevalence in different years (a: Females, b: Males).

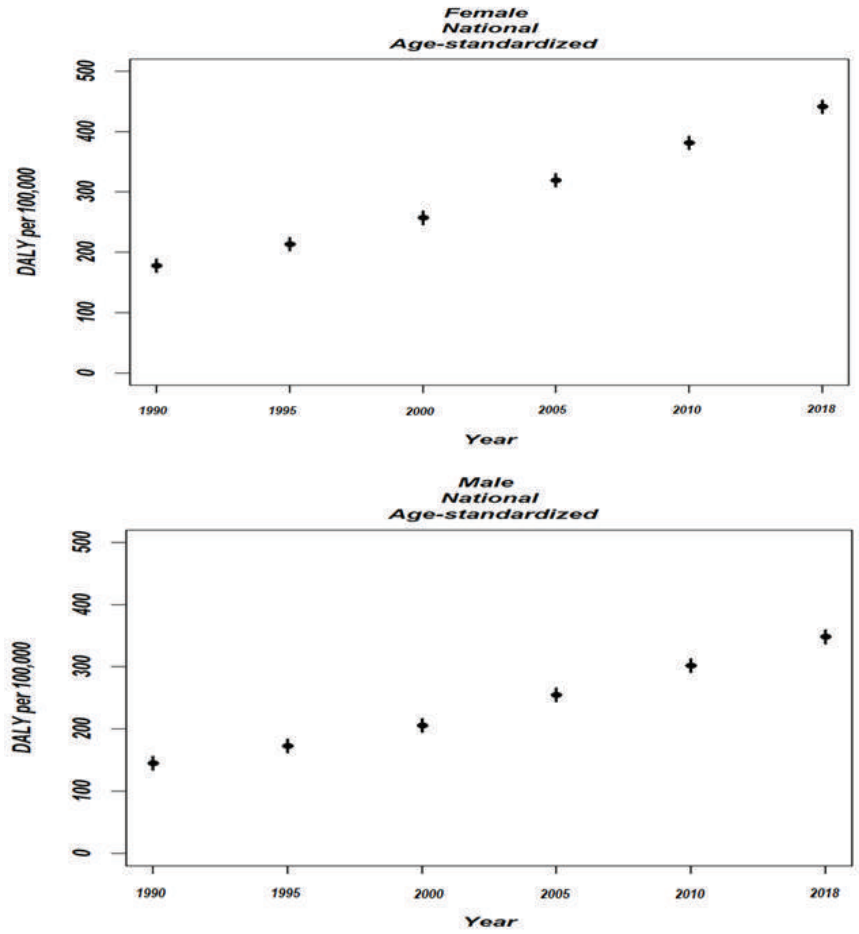

Figure 5. Age-adjusted DALYs (YLDs) per 100,000 at national level by sex from 1990 to 2018.

among all races, Asians being the most sensitive while Africans seem unsusceptible.[11] The age-standardized prevalence estimates of refractive error in our study from the years 1990 to 2018 translate into >100% rise which mostly follows the trend of juvenile myopia.[13, 19]

The authors of the current study would like to indicate the challenge experienced in the conducting the assignment of the disability index for VI to refractive errors. Refractive errors are highly heterogeneous and their severity is divergent. Although some refractive errors are essentially a variation of normality, others are so disabling that without correction they constitute clear handicap and "functional" blindness. As a result of our analysis, we recommend that the approach to addressing the global burden of this disease needs major improvement in this regard including cost estimation and social attribution of the disability.

DALYs attributed to refractive disorders increased 52% worldwide as compared to 1990 and increased by 82% in Iran.[9] Our study showed a higher prevalence and DALY as compared to Institute for Health Metrics and Evaluation (IHME). This might be due to the nature of IHME estimation and imputation of missing data by neighboring data because of security and insufficient evidences from Iran in prior years. Imputation from neighboring countries' evidence may constitute another source of disparity.

In our study, it was revealed that the prevalence of refractive errors in central provinces which generally possess better socioeconomic status (better education and more indoor occupations) is higher than those of the marginal provinces. Prior studies on the prevalence of refractive errors have already confirmed higher myopia prevalence in environments that possess more advanced levels of education, income, and professional occupations.[20] Modern careers tend to be

associated with sight-intensive work. In several epidemiological studies[21–26] as a consequence of the mentioned trends, increased attention is now directed to addressing unmet refractive error correction and control of myopia conditions.

In summary, the challenging data extraction process in our current study proved useful in determining the prevalence of the refractive errors phenomena in Iran. This study has provided the required evidence in determining the associated burden (economic and social) of these conditions and the basis for the recommendation to the respective health authorities about the necessity to address these issues. Over a span of 28 years, the prevalence of refractive errors has increased significantly in Iran by 16.32% (the age-standardized prevalence growth was 31.30% in females and 24.32% in males from the years 1990 to 2018). Prevalence in females was 3.5% higher than that of males. The prevalence rates increased in older ages. Significant geographical heterogeneity was observed where border provinces possessed a lower prevalence of refractive errors. The age-standardized YLDs rates of refractive errors showed an increasing trend of 28.9% during the period. Lifestyle changes and behavioral adaptions due to technological advancements and other social restrictions continues to perpetuate the onslaught of myopia and other VI issues globally, which further emphasizes the need to manage diagnoses, their prevention and treatment of these related issues.

Financial Support and Sponsorship

This work was partially supported by the Tehran University of Medical Sciences under Grant number 24423.

Conflicts of Interest

There are no conflicts of interest.

REFERENCES

1. Naidoo KS, Leasher J, Bourne RR, Flaxman SR, Jonas JB, Keeffe J, et al. Global vision impairment and blindness due to uncorrected refractive error, 1990–2010. *Optom Vis Sci* 2016;93:227–234.
2. Kandel H, Khadka J, Goggin M, Pesudovs K. Impact refractive error on quality of life: a qualitative study. *Clin Exp Ophthalmol* 2017;45:677–688.
3. WHO. The global burden of disease: 2004 update [Internet]. Geneva: World Health Organization; 2008 [cited 2015 September 1]. Available from: http://www.who.int/healthinfo/global_burden_disease/GBD_report_2004update_full.pdf.Accessed June 25, 2019.
4. Holden BA. Blindness and poverty: a tragic combination. *Clin Exp Optom* 2007;90:401–403.
5. Tahhan N, Papas E, Fricke TR, Frick KD, Holden BA. Utility and uncorrected refractive error. *Ophthalmology* 2013;120:1736–1744.
6. Lou L, Yao C, Jin Y, Perez V, Ye J. Global patterns in health burden of uncorrected refractive error. *Invest Ophthalmol Vis Sci* 2016;57:6271–6277.
7. Murray CJ, Barber RM, Foreman KJ, Ozgoren AA, Abd-Allah F, Abera SF, et al. Global, regional, and national disability-adjusted life years (DALYs) for 306 diseases and injuries and healthy life expectancy (HALE) for 188 countries, 1990-2013: quantifying the epidemiological transition. *Lancet* 2015;386:2145–2191.
8. Pascolini D, Mariotti SP. Global estimates of visual impairment: 2010. *Br J Ophthalmol* 2012;96:614–618.
9. Hatef E, Mohammadi SF, Alinia C, Ashrafi E, Mohammadi S-M, Lashay A, et al. National burden of eye diseases in Iran, 1990-2010; findings from the global burden of diseases study 2010. *Middle East Afr J Ophthalmol* 2016;23:89–95.
10. Ashrafi E, Mohammadi SF, Fotouhi A, Lashay A, Asadi-lari M, Mahdavi A, et al. National and sub-national burden of visual impairment in Iran 1990-2013; study protocol. *Arch Iran Med* 2014;17:810–815.
11. Hashemi H, Fotouhi A, Yekta A, Pakzad R, Ostadimoghaddam H, Khabazkhoob M. Global and regional estimates of prevalence of refractive errors: systematic review and meta-analysis. *J Curr Ophthalmol* 2017;30:3–22.
12. Dolgin E. The myopia boom. *Nature* 2015;519:276–278.
13. Holden BA, Fricke TR, Wilson DA, Jong M, Naidoo KS, Sankaridurg P, et al. Global prevalence of myopia and high myopia and temporal trends from 2000 through 2050. *Ophthalmology* 2016;123:1036–1042.
14. Ono K, Hiratsuka Y, Murakami A. Global inequality in eye health: country-level analysis from the global burden of disease study. *Am J Public Health* 2010;100:1784–1788.
15. Rahi JS, Cumberland PM, Peckham CS. Myopia over the life course: prevalence and early life influences in the 1958 British birth cohort. *Ophthalmology* 2011;118:797–804.
16. Huang HW, Teh Chang DS, Chang Wu P. The association between near work activities and myopia in children—a systematic review and meta-analysis. *PLoS One* 2015;10:e0140419.
17. French AN, Morgan IG, Mitchell P, Rose KA. Risk factors for incident myopia in Australian schoolchildren: the Sydney Adolescent Vascular and Eye Study. *Ophthalmology* 2013;120:2100–2108.
18. Zhang X, Cheung SSL, Chan HN, Zhang Y, Wang YM, Yip BH, et al. Myopia incidence and lifestyle changes among school children during the COVID-19 pandemic: a population-based prospective study. *Br J Ophthalmol* 2021;bjophthalmol-2021-319307.
19. The impact of myopia and high myopia. Report of the Joint World Health Organization–Brien Holden Vision

Institute Global Scientific Meeting on Myopia. University of New South Wales, Sydney, Australia, March 16–18, 2015. Geneva: World Health Organization; 2017 [cited 2019 June 25]. Available from: https://www.who.int/blindness/causes/MyopiaReportforWeb.pdf.

20. Foster PJ, Jiang Y. Epidemiology of myopia. *Eye* 2014;28:202–208.
21. Wu PC, Tsai CL, Hu CH, Yang YH. Effects of outdoor activities on myopia among rural school children in Taiwan. *Ophthalmic Epidemiol* 2010;17:338–342.
22. Deng L, Gwiazda J, Thorn F. Children's refractions and visual activities in the school year and summer. *Optom Vis Sci* 2010;87:406–413.
23. Dirani M, Tong L, Gazzard G. Outdoor activity and myopia in Singapore teenage children. *Br J Ophthalmol* 2009;93:997–1000.
24. Rose KA, Morgan IG Ip J. Outdoor activity reduces the prevalence of myopia in children. *Ophthalmology* 2008;115:1279–1285.
25. Jones LAS, Sinnott LT, Mutti DO, Mitchell GL, Moeschberger ML, Zadnik K. Parental history of myopia, sports and outdoor activities, and future myopia. *Invest Ophthalmol Vis Sci* 2007;48:3524–3532.
26. Onal S, Toker E, Akingol Z. Refractive errors of medical students in Turkey: one year follow-up of refraction and biometry. *Optom Vis Sci* 2007;84:175–180.

Review Article

Penetrating Keratoplasty versus Deep Anterior Lamellar Keratoplasty for Keratoconus: A Systematic Review and Meta-analysis

Majid Shams[1], MD; Ali Sharifi[1], MD; Zahra Akbari[2], MD; Ali Maghsoudlou[3], MD; Mohammad Reza Tajali[2], MD

[1]*Department of Ophthalmology, Shafa Hospital, Kerman University of Medical Sciences, Kerman, Iran*
[2]*Student Research Committee, Kerman University of Medical Sciences, Kerman, Iran*
[3]*Noor Eye Hospital, Tehran, Iran*

ORCID:
Majid Shams: https://orcid.org/0000-0003-4315-0749
Zahra Akbari: https://orcid.org/0000-0002-3315-8977

Abstract

Keratoconus is the most common form of primary corneal thinning. Different methods have been suggested to deal with the condition, including glasses, contact lenses, and surgical interventions, like penetrating keratoplasty (PKP) and deep anterior lamellar keratoplasty (DALK), well-known methods of the latter. This study was conducted to compare the outcomes and side effects of the two mentioned keratoplasty techniques. First, we systematically reviewed all original articles studies on PubMed, Scopus, Web of Science, and Embase. Then, the extracted data were pooled and meta-analyzed on each of the intended outcomes. A total of 30 studies were included in which PKP was more commonly performed compared to DALK. We found that adverse outcomes consisting of cataracts, graft rejection, graft failure, High-IOP, and corneal infection, were all more common findings in the PKP groups compared to the DALK groups. However, only for the high-IOP, cataracts, and graft rejection, the analysis of the extracted results demonstrated statistical significance. Overall, the DALK groups demonstrated significantly better results when considering the improvement levels by measuring the Endothelial Cell Count (ECC) and Spherical Equivalent (SE). In addition, though statistically insignificant, the Central Corneal Thickness(CCT), Best Corrected Visual Acuity(BCVA), Topographic Cylinder(TC), Refractive Cylinder values were greater in the PKP groups. Based on our study and with its limitations in mind, we can conclude that DALK can be a relatively safer and more effective procedure. Though, a larger number of high-standard randomized clinical trials still need to be conveyed for more definite conclusions.

Keywords: Corneal Transplant; Deep Anterior Lamellar Keratoplasty; Keratoconus; Penetrating Keratoplasty

J Ophthalmic Vis Res 2022; 17 (1): 89–107

INTRODUCTION

Keratoconus defined as bilateral[1, 2] and asymmetrical[3, 4] degeneration of the cornea is the most common form of primary corneal thinning. Local thinning of the cornea caused by keratoconus leads to corneal protrusion and then severe myopia and irregular astigmatism.[2, 5]

Different methods have been utilized to treat this condition, including prescribing glasses and contact lenses for the early stages[5, 6] and keratoplasty for the advanced stages of the disease.[6] Keratoconus is the most common pathology requiring corneal transplants in most ophthalmology centers worldwide. Similarly, based on available data, keratoconus is also the most common eye pathology requiring corneal transplant in Iran.[8, 9] According to one study, approximately 10–20% of keratoconus cases end up requiring standard penetrating keratoplasty (PKP). If the corneal cone's size, the severity of the keratoconus or corneal hydrops limits the possibility of utilizing contact lenses to treat the condition, keratoplasty should be performed.[10] Despite the popular use and high success rates of PKP, there is always a 20% risk that the host develops an immune reaction to the graft, of which 85% is due to the endothelial cell rejection. Approximately 2.5% of graft rejections lead to graft failure.[11, 12]

Some studies have also shown that in PKP cases, the number of endothelial cells decreases by 4.2% each year. This decline may continue until 5–10 years after the transplantation.[13] Other PKP complications include expulsive hemorrhage, endophthalmitis, synechiae of the iris to the angle or point of incision of the graft, side effects of long-term corticosteroids use, and predisposition to traumatic injuries.[14]

In the recent decade, the rate of performing the lamellar keratoplasty (LK) procedure has increased.[15] Potential immunological incompatibilities after the insult, leading to complications including graft rejection, are of considerable importance, therefore, the injured corneal layers are removed, and the healthy tissue is preserved.[16] Deep anterior lamellar keratoplasty (DALK) is a type of LK that reconnects the stroma to the Descemet's membrane in cases whose stroma might be in danger of loss.[17] This technique prevents the recipient's endothelium replacement with the donor's and mitigates the risk of endothelial induced rejection. However, the risk of rejection will not be completely eliminated due to the remaining epithelial layer.[18, 19]

Although the LK is rapidly becoming the method of choice in corneal transplant, some studies have compared DALK with PKP to determine the more appropriate option for treating keratoconus.[20] Considering the importance of the subject and that very few comprehensive studies have evaluated and compared both techniques in keratoconus cases, our study aims to conduct a systematic review to compare the outcomes and side effects of these two techniques.

METHODS

We completed our systematic review in accordance with the Preferred Reporting Items for Systematic Reviews and Meta-Analyses (PRISMA) guidelines (http://www.prisma-statement.org/).[21]

For this systematic review, we searched PubMed, Scopus, Embase, Web of Science databases for articles published up to the end of May 2021.

Inclusion and Exclusion Criteria

All English comparative studies on adults including clinical trials, retrospective and prospective cohort studies on keratoconus treated with DALK and PKP were used in the data assessment. We excluded all editorials, conferences, commentaries,

Correspondence to:

Zahra Akbari, MD Candidate. Kerman University of Medical Sciences, Faculty of Medicine, Kerman 7616913555, Iran.
E-mail: Zahraakbari75@yahoo.com

Received 05-03-2021; Accepted 11-11-2021

Access this article online

Website: https://knepublishing.com/index.php/JOVR

DOI: 10.18502/jovr.v17i1.10174

How to cite this article: Shams M, Sharifi A, Akbari Z, Maghsoudlou A, Tajali MR. Penetrating Keratoplasty versus Deep Anterior Lamellar Keratoplasty for Keratoconus: A Systematic Review and Meta-analysis. J Ophthalmic Vis Res 2022;17:89–107.

letter to editors, and reviews. In addition, non-English studies, case reports, case–controls, noncomparative studies, and those evaluating DALK and PKP effects without a focus on keratoconus were excluded. There were no limitations regarding the sex of the evaluated cases. However, only studies which evaluated adults were included.

Search Strategy

We conducted a thorough manual search on the Web of Science, Embase, PubMed, and Scopus, considering the publications up to May 2021. The searched queries are delineated below:

SCOPUS and Web of Science

TITLE-ABS-KEY (compar* AND (lamell* AND penet*) AND keratocon*) AND (LIMIT-TO (DOCTYPE , "ar")) AND (LIMIT-TO (LANGUAGE , "English"))

Pubmed

compar*[tiab] AND (lamell*[tiab] AND penet*[tiab]) AND keratocon*[tiab] Filters: Clinical Study, Clinical Trial, Comparative Study, Controlled Clinical Trial, Evaluation Study, Multicenter Study, Observational Study, Pragmatic Clinical Trial, Randomized Controlled Trial, English

Embase

compar*:ti,ab,kw AND lamell*:ti,ab,kw AND penet*:ti,ab,kw AND keratocon*:ti,ab,kw AND ('case study'/de OR 'clinical trial'/de OR 'cohort analysis'/de OR 'comparative effectiveness'/de OR 'comparative study'/de OR 'controlled clinical trial'/de OR 'controlled study'/de OR 'cross sectional study'/de OR 'intervention study'/de OR 'major clinical study'/de OR 'observational study'/de OR 'prospective study'/de OR 'randomized controlled trial'/de OR 'randomized controlled trial topic'/de OR 'retrospective study'/de) AND 'article'/it

Evaluating Recovered Evidence

After completing the search, two reviewers separately removed duplicated findings via Endnote version 20. A manual check for duplication was also performed to ensure none existed. Subsequently, two authors performed initial evaluations of titles and abstracts of the recovered evidence. After recovering all the available articles in the second phase, they were then evaluated by the research team.

Data Extraction

Two authors independently extracted data from the articles according to the following criteria:

- Included study's first author
- The year the study was published
- Study type
- Country of origin
- Patients' age and sex
- Duration of follow-up
- Corneal infection rates
- Graft rejection rates (the rate of the rejection episodes seen in cases)
- Graft failure rates
- Cataract rates
- High-intraocular pressure (IOP; also known as ocular hypertension; an eye pressure of >21 mm Hg) rates
- Mean and standard deviation (SD) of best-corrected visual acuity (BCVA) in LogMAR scale (defined as the highest score on the Snellen chart when wearing either a visual aiding device, like glasses or contact lenses)
- Refractive (RC) and topographic cylinder (TC; defined as refractive power of the cylindrical lenses and the mapping the anterior curvature of the cornea, respectively)
- Central corneal thickness (CCT; defined as the thickness of the cornea measured by optical low coherence reflectometry)
- Endothelial cell count (ECC; estimation of corneal endothelial reserve by corneal endothelial photography)
- Spherical equivalent (an estimate of the eyes' refractive error calculated by merging the nearsightedness or farsightedness and cylindrical astigmatism components)

All the mentioned values were included based on the last known follow-up of each study. Finally, the extracted data were reviewed and double-checked by the senior author.

Quality Assessment

The quality of the included studies was evaluated independently by two authors using the critical appraisal tool, provided by The Joanna Briggs Institute, containing 13, 12, and 8 items for assessing RCTs, cohort, and cross-sectional studies, respectively.

Data Analysis

For quantitative outcomes, the mean differences and SD, and the risk-ratio for qualitative outcomes were determined and analyzed. Methods of meta-analysis and random-effects models were used to combine the results using the 14th edition of the STATA software. Furthermore, heterogeneity between the studies was determined by employing the I^2 test. The *p*-value was set at <0.05 for the significance level.

RESULTS

We identified 1129 articles in the systematic search of resources. After reviewing the titles and abstracts, 1079 articles were excluded from the study of which 347 were duplications. After reviewing the full-text of the articles, 20 were put aside again. Finally, 30 articles were included into this meta-analysis. The information of the selected articles is shown in Figure 1.

Among the 30 articles chosen, 25 were cohort (retrospective or prospective), 3 were cross-sectionals, and 2 were randomized-clinical trials. Information about each study is shown in Table 1.

Quality Assessment

Based on the Joanna Briggs Institute's critical appraisal tool, the three cross-sectional studies scored within a range of 6–8 out of a possible 8. The two randomized-clinical trials scored 10 out of a possible 13. In addition, the 25 cohort studies within a range of 9–11 out of a possible 12.

Meta-Analysis Results

Central corneal thickness (CCT)

In nine of the studies, the mean and SD of central corneal thickness after PKP and DALK was reported. A total of 271 eyes were treated with PKP and 316 eyes with DALK. The mean age of the cases treated with PKP and DALK was 31.56 and 30.72, respectively. Furthermore, the follow-up duration was 24.87 and 20.81 months for PKP and DALK, respectively. Heterogeneity between the studies was significant (I2 = 85.9%, *p*-value < 0.001). According to the meta-analysis results with the help of the random-effects model, integrated mean differences (mean PKP – mean DALK) for the central corneal thickness were measured as –0.10 (pooled MD = –0.10, 95% CI: –0.57 – 0.37, *p*-value = 0.671). Figure 2 shows the forest plot of the meta-analysis.

Spherical equivalent (SE)

In 16 studies, the mean and SD of the spherical equivalent identified after PKP and DALK was reported. A total of 2552 eyes were treated with PKP, and 1105 eyes were treated with DALK. The mean age of cases treated with PKP and DALK was 29.2 and 28.39 years, respectively. The duration of the follow-up was 35.36 months for PKP and 27.33 months for DALK cases. Heterogeneity was statistically significant (I2 = 80.4%, *p*-value < 0.001). Integrated mean differences (mean PKP – mean DALK) of PKP and DALK for the spherical equivalent was 0.32 (pooled MD = 0.32, 95% CI; 0.10 – 0.54, *p*-value = 0.004). Figure 3 illustrates the forest plot of the meta-analysis results.

Best-corrected visual acuity (BCVA)

Eighteen studies reported the mean and SD of BCVA after both PKP and DALK. A total of 3301 eyes were treated with PKP and 1388 eyes with DALK. The mean age of cases treated with PKP and DALK was 30.54 and 28.14 years, respectively. Duration of follow-up was 29.71 months for PKP and 27.60 months for DALK cases. Heterogeneity was statistically significant (I2 = 65.1%, *p*-value < 0.001). Integrated mean differences (mean PKP – mean DALK) for the BCVA was measured as –0.01 (pooled MD = –0.01, 95% CI; –0. 61 – 0.13, *p*-value = 0.869). Figure 4 illustrates the forest plot of the meta-analysis.

Topographic cylinder

The mean and SD of the topographic cylinder occurring after PKP and DALK was reported in

Table 1. Data related to evaluated studies

Author	Design	Year	Country	Sample size PKP	Sample size DALK	Mean age in PKP	Mean age in DALK	Follow-up PKP (month)	Follow-up DALK (month)	PKP Sex Male	PKP Sex Female	DALK Sex Male	DALK Sex Female	Main value evaluated
Abdelaal et al[23]	Retrospective cohort	2021	Saudi Arabia	15	21									Graft Rejection
Abu Eta et al[24]	Retrospective cohort	2020	Israel	21	32									High-IOP
Akdemir et al[25]	Retrospective cohort	2012	Turkey	30	30	28.07	29.67	12.58	12.58	16	14	14	16	BCVA
Alzahrani et al[26]	Retrospective cohort	2018	UK	21	16	30.14	32.56	13.95	14.87	14	7	11	5	BCVA, CCT
Amayem et al[27]	Retrospective cohort	2012	Saudi Arabia	30	47	26.5	24.3	24	24					Refractive Cylinder, SE
Bahar et al[28]	Retrospective cohort	2008	Canada	20	17	42.2	32.5	53.2	17	11	9	11	6	Endothelial Cell Count, Infection Rate, Graft Rejection, Topographic Cylinder
Cohen et al[29]	Retrospective cohort	2010	USA	30	11	35.4	45.5	21.9	22.5	21	9	8	3	Cataract Frequency, High-IOP, Graft Rejection, Refractive Cylinder, SE, BCVA
Donoso et al[30]	Retrospective cohort	2015	Chile	49	90	31.7	28.3	48.6	36.8					High-IOP, ECC, Infection Rate, Graft Rejection, Topographic and Refractive Cylinder, CCT
Funnell et al[31]	Cohort	2006	UK	20	20	32	28	12	12	14	6	11	9	High-IOP, Graft Rejection, Graft Failure, Topographic Cylinder

Table 1. Data related to evaluated studies

Author	Design	Year	Country	Sample size PKP	Sample size DALK	Mean age in PKP	Mean age in DALK	Follow-up PKP (month)	Follow-up DALK (month)	PKP Sex Male	PKP Sex Female	DALK Sex Male	DALK Sex Female	Main value evaluated
Godefrooij et al[32]	Retrospective cohort	2016	Netherlands	736	297	38.07	35.65			499	237	204	93	BCVA
Hamdi et al[33]	Cross-sectional	2017	Egypt	12	24	26.95	23.79			9	3	14	10	Topographic and Refractive Cylinder, SE, BCVA
Huang et al[34]	Retrospective cohort	2015	China	79	68	24.3	24.1	93.1	93.5	50	29	40	28	Topographic and Refractive Cylinder, SE, BCVA
Jafarinasab et al[35]	Cross-sectional	2011	Iran	45	23	29.8	27.2	31.4	29.2					Topographic Cylinder, SE, BCVA
Janiszewska-Bil et al[36]	Cohort	2021	Poland	40	50	28.4	28.6	12	12	24	16	28	22	High-IOP, ECC, Topographic Cylinder, CCT, BCVA
Javadi et al[37]	Randomized clinical trial	2010	Iran	35	42	30.89	26.91	24.6	22	28	7	29	13	Graft Rejection, Topographic Cylinder, CCT, SE, BCVA
Jones et al[38]	Retrospective cohort	2009	UK	1917	455									Graft Rejection, Graft Failure, SE, BCVA
Kasbekar et al[39]	Cohort	2014	UK	3124	1086			60	60					Infection rate, Graft Rejection, Graft Failure
Khattak et al[40]	Retrospective cohort	2018	Saudi Arabia	99	108	28.9	27.8	29.3	28.1	59	40	67	41	High-IOP, ECC, Cataracts, Infection rate, Graft Rejection, Graft Failure, Topographic and Refractive Cylinder, SE, BCVA

Table 1. Data related to evaluated studies

Author	Design	Year	Country	Sample size PKP	Sample size DALK	Mean age in PKP	Mean age in DALK	Follow-up PKP (month)	Follow-up DALK (month)	PKP Sex Male	PKP Sex Female	DALK Sex Male	DALK Sex Female	Main value evaluated
Kim et al[41]	Retrospective cohort	2011	Korea	38	19	26.2	25.3	51.7	22.6	25	13	17	2	SE
Koytak et al [42]	Retrospective cohort	2011	Turkey	39	44	36.24	34.54	24	24	24	15	26	18	ECC, CCT
Kubaloglu et al [43]	Cohort	2011	Turkey	24	20	30.2	25.6	6	6			112	95	Topographic and Refractive Cylinder, SE, CCT, BCVA
Macintyre et al [44]	Retrospective cohort	2014	Australia	42	31	32.3	29.2	53.7	51.8	22	20	19	12	Cataracts, Graft Rejection, Graft Failure, Refractive Cylinder, BCVA
Motlagh et al [45]	Cross-sectional	2012	Iran	57	49			35	30.3					SE, BCVA
Oh et al [46]	Retrospective cohort	2013	Korea	5	11	27.4	28	45	30	3	2	7	4	ECC, Refractive and Topographic Cylinder, CCT, SE, BCVA
Pedrotti et al [47]	Retrospective cohort	2016	Italy	16	16	34.1	35.9			7	9	7	9	Graft Rejection, Graft Failure, Topographic and REfractive Cylinder, CCT, SE, BCVA
Sogutlu Sari et al [48]	Cohort	2012	Turkey	75	99	28.44	27.59	25.53	21.54					Graft Rejection, Refractive Cylinder, SE, BCVA

Table 1. Data related to evaluated studies

Author	Design	Year	Country	Sample size PKP	Sample size DALK	Mean age in PKP	Mean age in DALK	Follow-up PKP (month)	Follow-up DALK (month)	PKP Sex Male	PKP Sex Female	DALK Sex Male	DALK Sex Female	Main value evaluated
Watson et al [49]	Retrospective cohort	2004	UK	22	25	33.9	32.6	55	28	14	8	17	8	Infection, Graft Rejection , Graft Failure,
Yüksel et al [50]	Clinical trial	2017	Turkey	38	38	35.3	34.9	12	12	15	23	10	28	High-IOP, Graft Rejection, Topographic Cylinder, SE, BCVA
Zhang et al [51]	Retrospective cohort	2013	China	52	75	21.9	20.6	60.2	46.9	45	7	55	20	High-IOP, Cataracts, Graft Rejection, Topographic Cylinder, SE
Ziaei et al [52]	Retrospective cohort	2019	New Zealand	42	27	35	36.1			25	17	12	15	CCT

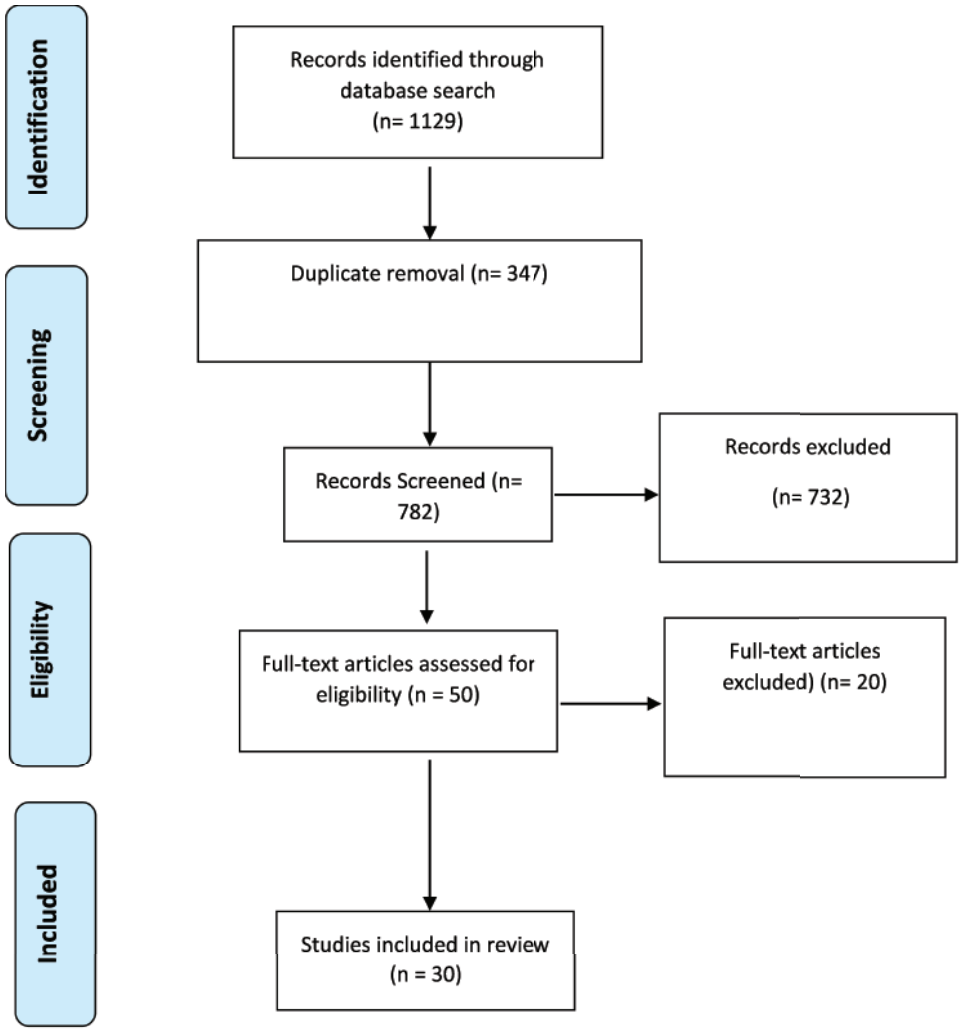

Figure 1. Diagram of the studies evaluation.

14 studies. A total of 534 eyes underwent PKP and 602 underwent DALK. The mean age of cases treated with PKP and DALK was 30.00 and 28.01 years, respectively. Follow-up for PKP and DALK groups was 35.61 and 28.79 months, respectively. Heterogeneity was statistically significant (I2 = 69.8%, *p*-value < 0.001). Integrated mean differences (mean PKP – mean DALK) for the topographic cylinder was 0.11 (pooled MD = 0.11.95% CI; –0.12 – 0.34, *p*-value = 0.359). Figure 5 shows the forest plot of the meta-analysis.

Refractive cylinder

The mean and SD of refractive cylinder occurring after PKP and DALK was reported in 11 studies. A total of 439 eyes underwent PKP and 525 underwent DALK. The mean age of cases treated with PKP and DALK was 29.65 and 29.09 years, respectively. Follow-up for PKP and DALK groups was 38.57 and 34.91 months, respectively. Heterogeneity was statistically significant (I2 = 52%, *p*-value = 0.022). Integrated mean differences (mean PKP – mean DALK) for the refractive cylinder was 0.08 (pooled MD = 0.27, 95% CI; –0.12 – 0.28, *p*-value = 0.428). Figure 6 shows the forest plot of the meta-analysis.

High IOP

High IOP occurring after PKP and DALK appeared in eight studies. A total of 349 eyes were treated with PKP, and 424 were treated with DALK. The mean age of cases treated with PKP and DALK was

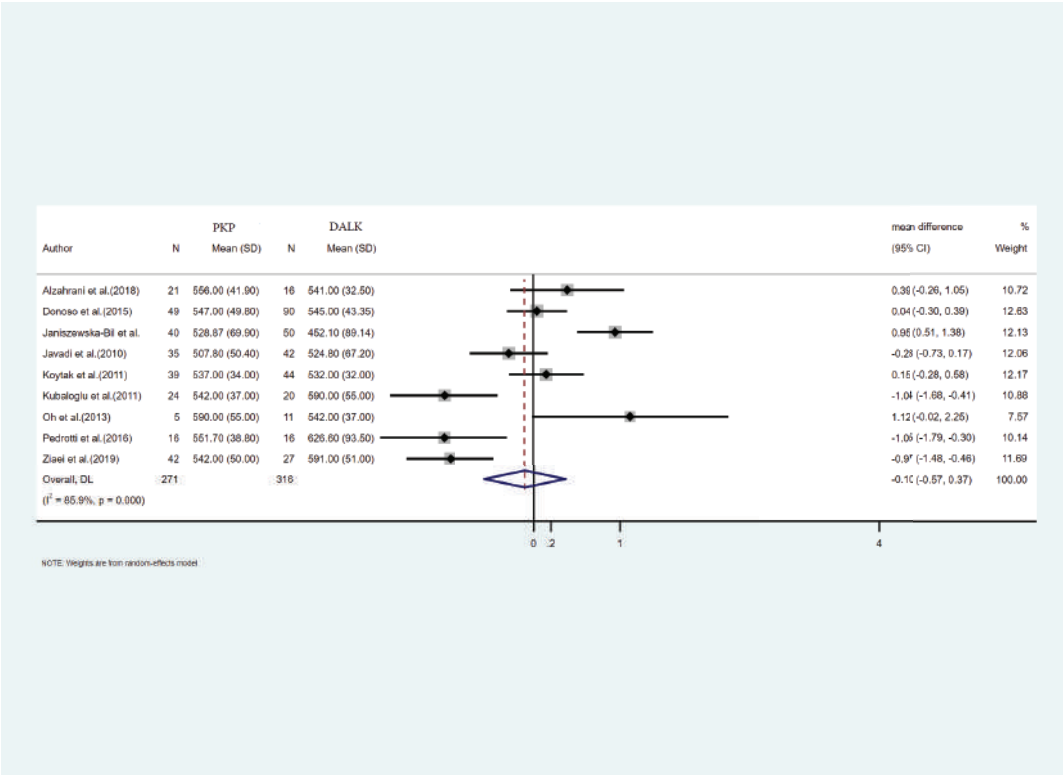

Figure 2. Results of meta-analysis for central corneal thickness.

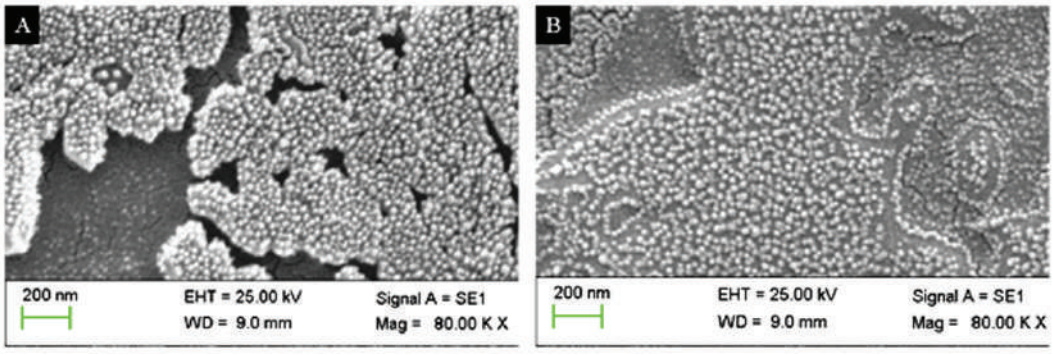

Figure 3. Results of the meta-analysis of the spherical equivalent.

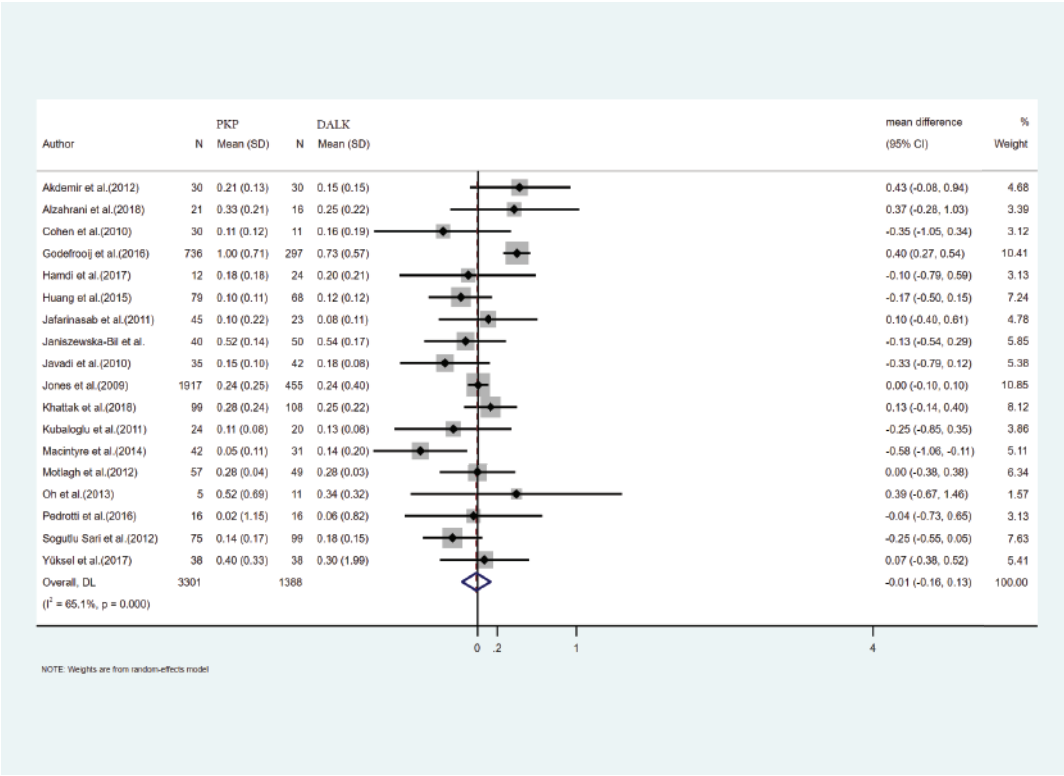

Figure 4. Results of the meta-analysis of the best-corrected visual acuity.

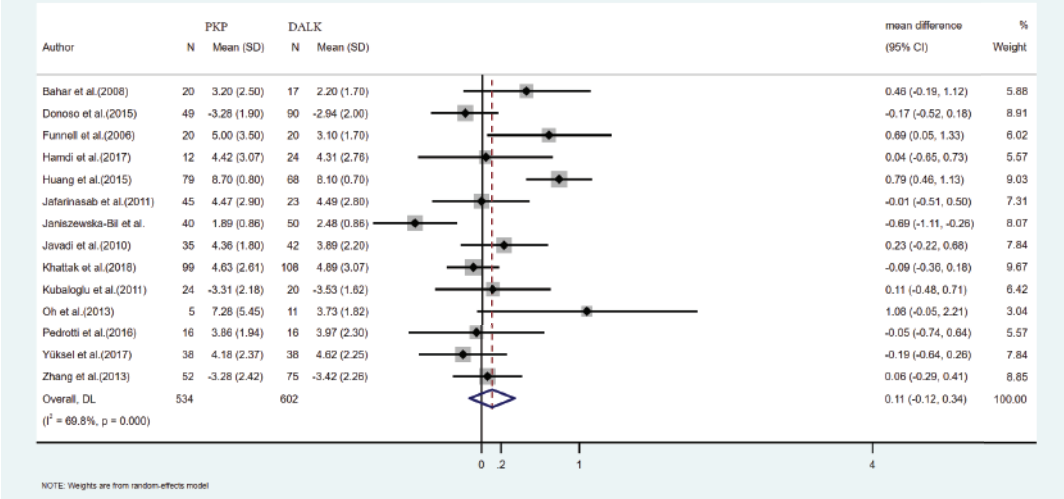

Figure 5. Results of the meta-analysis of the topographic cylinder.

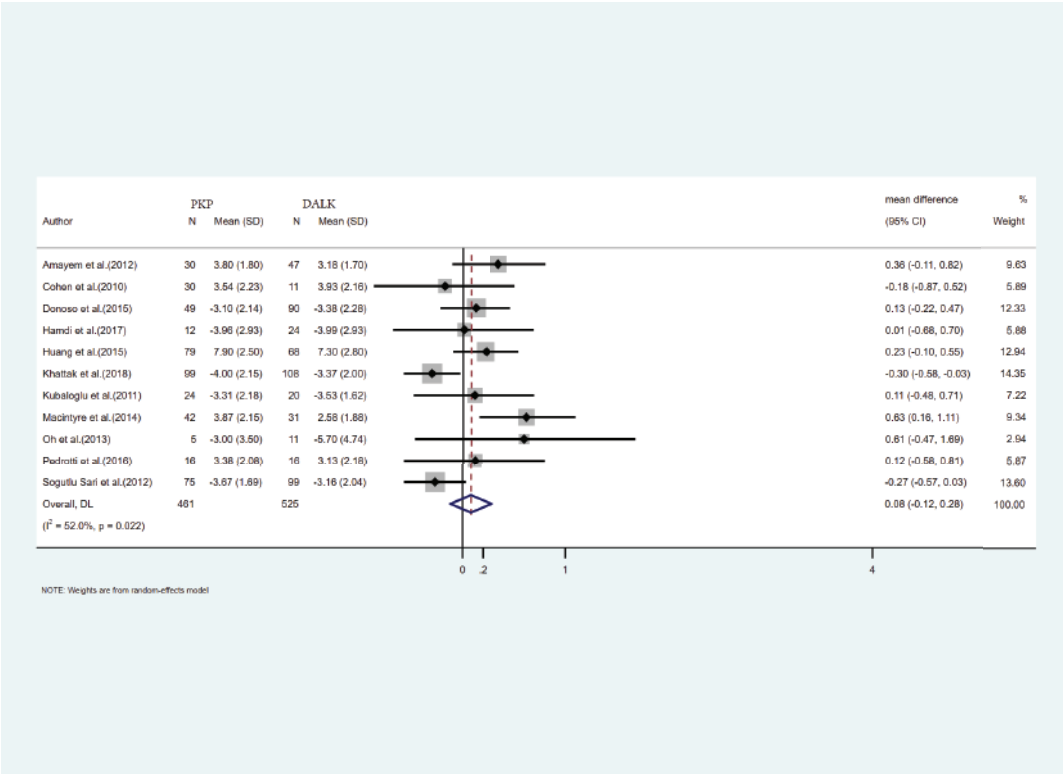

Figure 6. Results of the meta-analysis of the refractive cylinder.

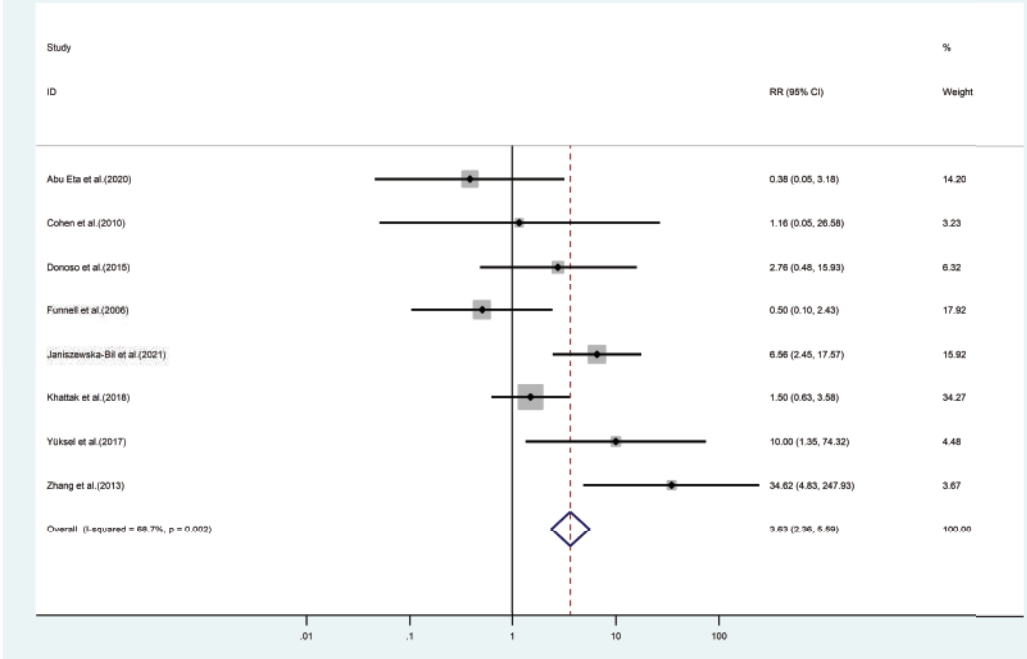

Figure 7. Results of the meta-analysis of the high IOP.

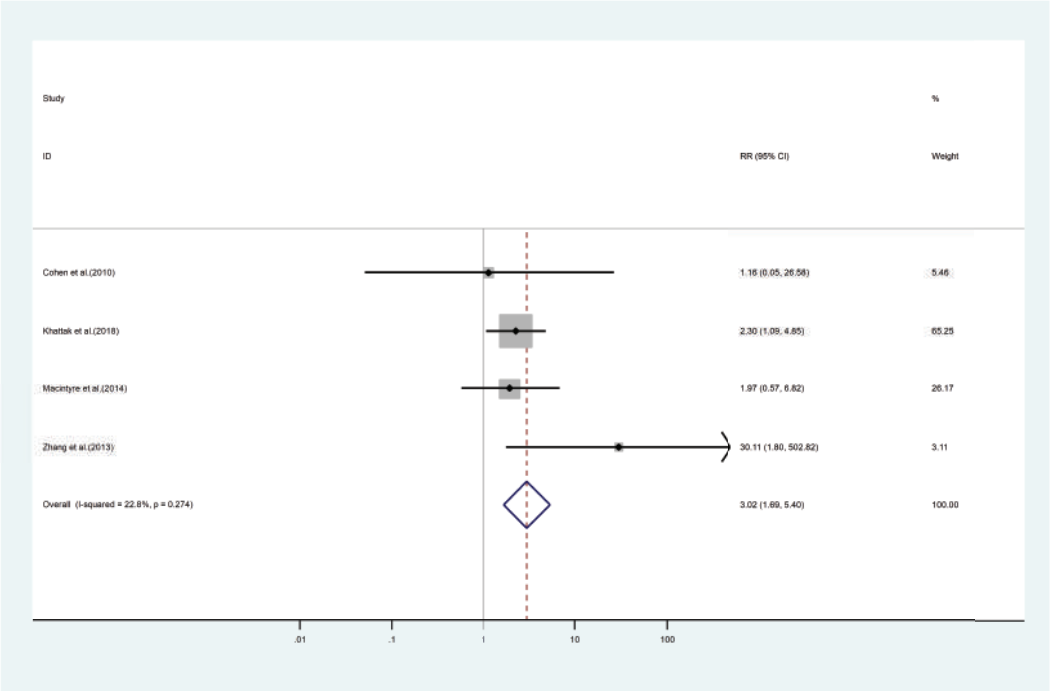

Figure 8. Results of the meta-analysis of the cataract.

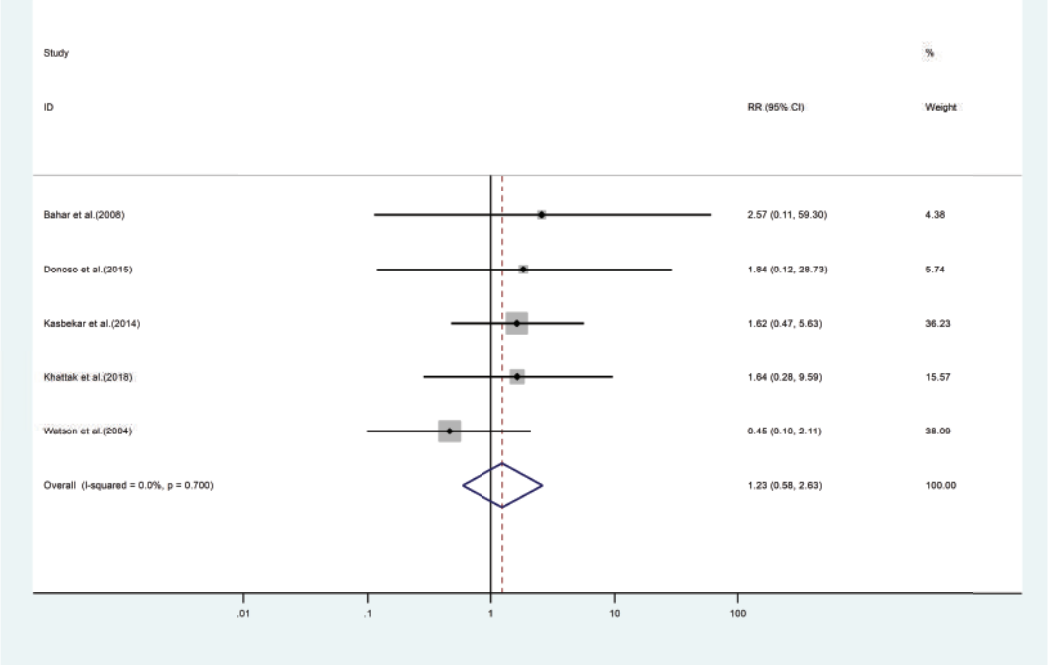

Figure 9. Results of the meta-analysis of the corneal infection.

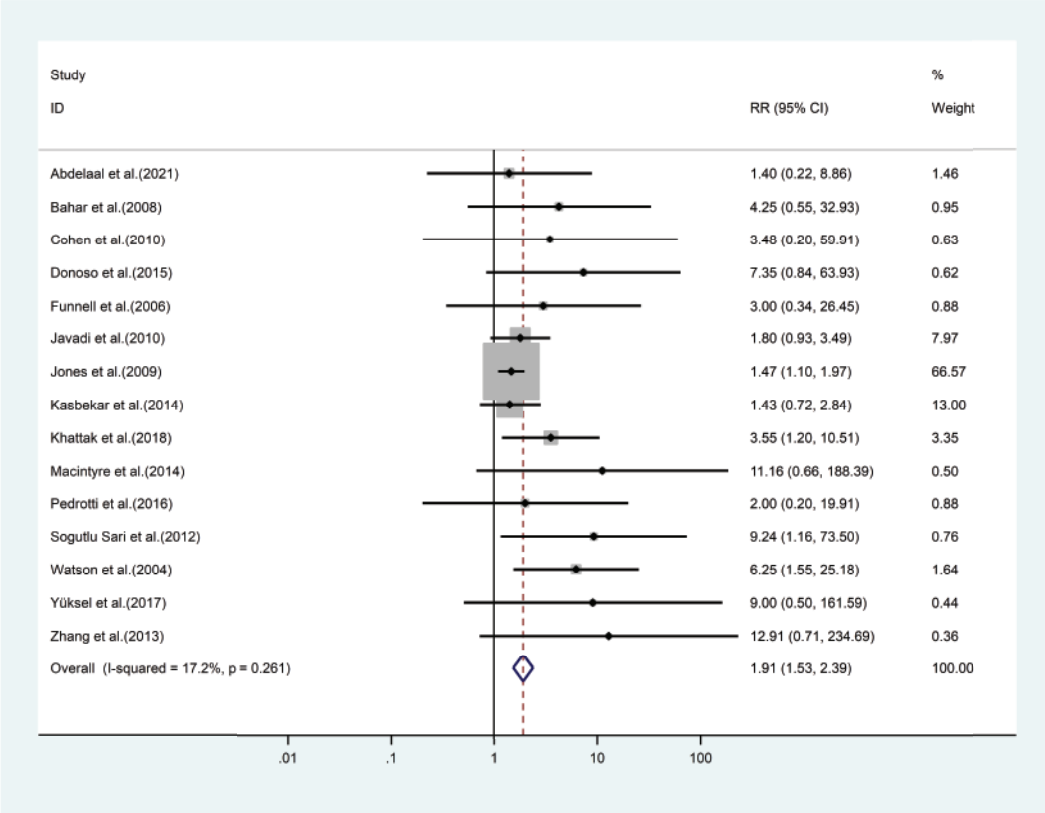

Figure 10. Results of the meta-analysis of the graft rejection.

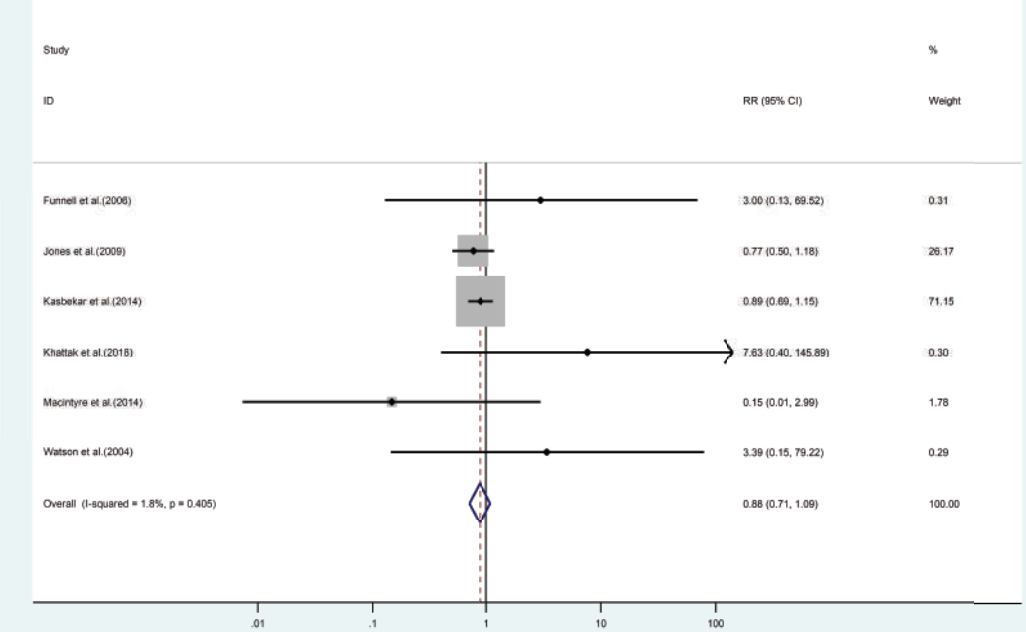

Figure 11. Graft failure meta-analysis results.

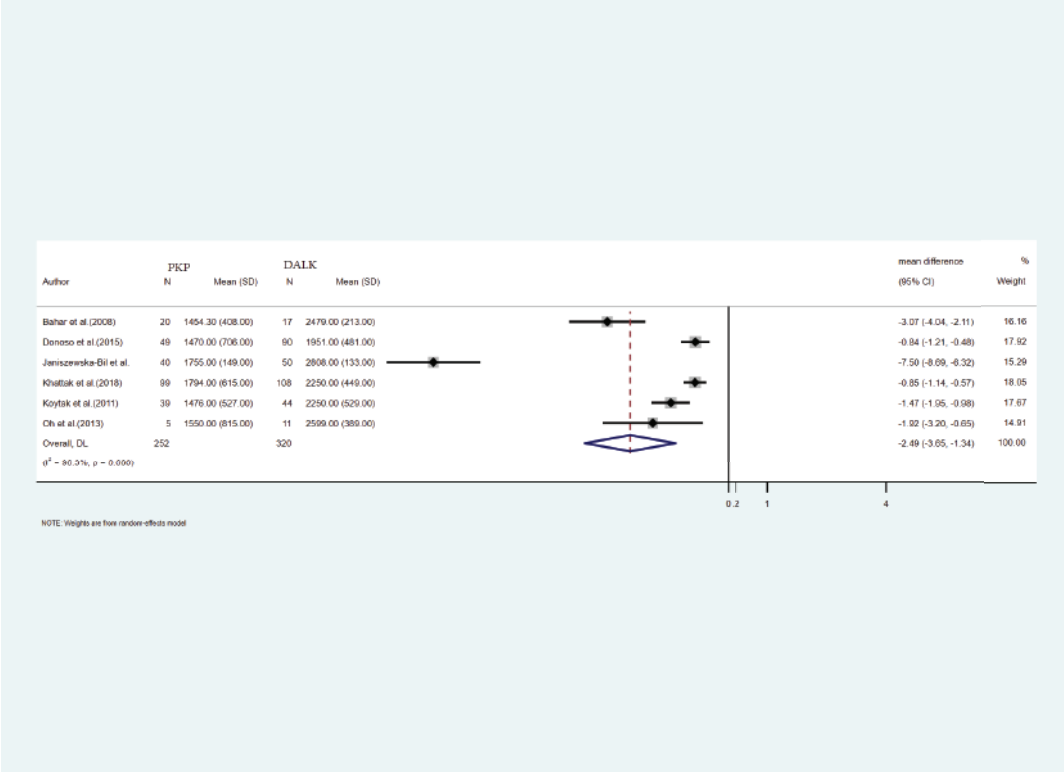

Figure 12. Endothelial cell count meta-analysis results.

30.51 and 30.52 years, respectively. The duration of follow-up for the PKP cases was 28 and 24.32 months for the DALK cases. Heterogeneity was statistically significant (I2 = 68.7, p-value = 0.002). The random-effects model showed the PKP group's high IOP risk ratio as 3.63 times that of the DALK group (pooled HR = 3.63, 95% CI; 2.36 – 5.59, *p*-value = 0.018). Forest's plot is presented in Figure 7.

Cataract

In six studies reporting cataract occurring after PKP and DALK, 223 eyes were treated with PKP and 225 eyes with DALK. The mean age of cases was 29.62 years for PKP and 30.77 years for DALK. Follow-up period was 41.27 months for PKP and 37.32 months for DALK cases. Heterogeneity was not statistically significant (I2 = 22.8, *p*-value = 0.274). The risk ratio of cataract incidence in the PKP group was 3.02 times that of the DALK group (pooled HR = 3.02, 95% CI; 1.69 – 5.40, *p*-value = 0.62). Figure 8 presents the forest plot of the meta-analysis.

Corneal infection

Corneal infection manifesting after PKP and DALK was reported in five studies. A total of 3314 eyes were treated with PKP and 1326 eyes were treated with DALK. The mean age of cases treated with the PKP and DALK method was 34.17 and 30.3 years, respectively. The duration of the cases' follow-up in the PKP and the DALK groups was 49.22 and 33.98 months. Heterogeneity was not statistically significant (Q-value = 0.24, df = 2, (I2 = 0.000, *p*-value = 0.7). The risk ratio of corneal infection incidence in the PKP group was measured at 1.23 times that of the DALK group (pooled HR = 1.23, 95% CI; 0.58 – 2.63, *p*-value = 0.700). Figure 9 illustrates the forest plot of the meta-analysis.

Graft rejection

Graft rejection occurring after PKP and DALK was observed in 15 studies. A total of 5554 eyes were treated with PKP and 2134 eyes with DALK. The mean age of cases undergoing PKP was 32.25 and 30.81 years for DALK. PKP cases were followed-up for 38 months and the DALK cases for

29.88 months. Heterogeneity was not statistically significant (I2 = 17.2, *p*-value = 0.261). The graft rejection risk ratio of PKP to DALK was 1.91 (pooled HR = 2.33, 95% CI; 1.69 – 3.22, *p*-value = 0.179). Figure 10 presents the forest plot.

Graft failure

Six studies discussed graft failure presenting after PKP and DALK. A total of 5224 eyes were treated with PKP and 1725 were treated with DALK. The mean age of cases treated with PKP and DALK was 31.77 and 29.4 years, respectively. Follow-up for the PKP group was 42 months and 35.98 months for the DALK group. Heterogeneity was not statistically significant (I2 = 1.8, *p*-value = 0.405). The risk ratio of the graft failure incidence in the PKP group was 0.88 of the DALK group (pooled HR = 0.88, 95% CI; 0.71 – 1.09, *p*-value = 0.98). In Figure 11, a related forest plot is illustrated.

Endothelial cell count

The mean and SD of endothelial cell count presenting after PKP and DALK was reported in six studies. A total of 252 eyes underwent PKP and 320 underwent DALK. The mean age of cases treated with PKP and DALK was 32.47 and 29.95 years, respectively. Follow-up for PKP and DALK groups was 35.35 and 24.65 months, respectively. Heterogeneity was statistically significant (I2 = 96.3%, *p*-value < 0.001). Integrated mean differences (mean PKP – mean DALK) for the endothelial cell count was –2.49 (pooled MD = –2.49 95% CI; –3.65 – –1.34, *p*-value = 0.000). Figure 12 shows the forest plot of the meta-analysis.

DISCUSSION

In this study, a total of 6773 cases of PKP and 2891 cases of DALK were documented and reviewed. In those studies, where differences in sex were evaluated, the male cases were subjected to more interventions in both the PKP and DALK procedures than the female cases. The mean age for PKP and DALK categories was 30.97 and 29.80 years, respectively. Furthermore, the cases were followed-up in the PKP and DALK groups for 34.99 and 28.59 months, respectively.

CCT in the DALK group was 10% greater overall than registered in the PKP group, which was not statistically significant. The study by Liu et al[53] could not find statistical significance regarding the differences in this value when comparing the two groups.

The SE value in the PKP group was 32% higher overall, which was also statistically significant. This finding may be due to the tighter suturing in DALK. Henein et al[54] and Liu et al[53] did not find any statistical significance when comparing the value between the two groups. However, the study by Song et al[55] found this value to be significantly more improved in the DALK group.

BCVA measured in the DALK group insignificantly demonstrated to be 1% better as compared to the PKP group. However, the study by Henein et al[54] revealed statistical significance in favor of the PKP group. In Song et al[55] and Liu et al[53], this value was not statistically significant.

Regarding the topographic cylinder, the PKP group showed insignificantly greater results (about 11%). Furthermore, neither of the studies by Henein et al[54] nor Song et al[55] demonstrated statistical significance.

The PKP group demonstrated insignificantly greater results on the refractive cylinder values than the DALK group (8% overall). Henein et al[54] demonstrated significance in the improvement of the RC in the DALK group. Song et al,[55] however, found no statistical significance in the differences of RC between the two groups.

The ECC was 2.49 score unique higher in the DALK group as compared to the PKP group. Consistent with the study by Liu et al,[53] this finding also turned out to be statistically significant. In the study by Henein et al,[54] the ECC values were not statistically significant between the two groups. DALK involved the inner portion of the cornea less often than PKP. The procedure is also less invasive.

Cataracts (38 vs 12 cases), graft rejection (413 vs 80 cases), graft failure (286 vs 105 cases), High-IOP (73 vs 30 cases), and corneal infection (22 vs 11 cases) were all more common findings in the PKP groups as compared to the DALK groups. Except for the high IOP, cataract and graft rejection the remaining complications were not statistically significant when we compared the results of the two groups.

Graft failure, consistent with our study, was not statistically significant in the studies by Henein et al[54] and Liu et al.[53] In addition, High IOP was significantly more common in the PKP group

when compared in the study by Liu et al.[53] Furthermore, in prior review studies by Henein et al,[54] Song et al,[55] and Liu et al,[53] the DALK groups suffered significantly fewer graft rejection episodes. Furthermore, consistent with our study, Liu et al[53] found statistical significance regarding the number of post-op cataracts occurring in the PKP group.

SUMMARY

Despite the results favoring the DALK procedure and its utility in most of the evaluated outcomes, we cannot definitively conclude that the procedure is more eventful compared to PKP. This remark is primarily due to the small sample size, study design variability, and mismatched follow-up durations leading to, in some incidences, significant heterogeneity that could not be addressed via met-regression or sensitivity analyses. Therefore, we believe that any conclusions from the comparisons must be taken with a grain of salt. Ultimately, we believe that to increase the validity of a possible meta-analysis, future randomized controlled trials need to be conducted with consistently matching follow-up durations and timing between the sessions.

Limitations

Our study's limitation was that we did not include other types of lamellar keratoplasty techniques due to the low number of available cases. Furthermore, formulas used to convert the domains to the SD might not be as accurate as desired, which can be due to statistical limitations.

Financial Support and Sponsorship

Nil.

Conflicts of Interest

The authors do not have any conflicts of interest.

REFERENCES

1. Zadnik K, Barr JT, Gordon MO, Edrington TB. Biomicroscopic signs and disease severity in keratoconus. Collaborative Longitudinal Evaluation of Keratoconus (CLEK) Study Group. *Cornea* 1996;15:139–146.
2. Kennedy RH, Bourne WM, Dyer JA. A 48-year clinical and epidemiologic study of keratoconus. *Am J Ophthalmol* 1986;101:267–273.
3. Zadnik K, Steger-May K, Fink BA, Joslin CE, Nichols JJ, Rosenstiel CE, et al. Between-eye asymmetry in keratoconus. *Cornea* 2002;21:671–679.
4. Chopra I, Jain AK. Between eye asymmetry in keratoconus in an Indian population. *Clin Exp Optom* 2005;88:146–152.
5. Rabinowitz YS. Keratoconus. *Surv Ophthalmol* 1998;42:297–319.
6. Bilgin LK, Yılmaz S, Araz B, Yüksel SB, Sezen T. 30 years of contact lens prescribing for keratoconic patients in Turkey. *Cont Lens Anterior Eye* 2009;32:16–21.
7. Gordon MO, Steger-May K, Szczotka-Flynn L, Riley C, Joslin CE, Weissman BA, et al. Baseline factors predictive of incident penetrating keratoplasty in keratoconus. *Am J Ophthalmol* 2006;142:923–930.
8. Fallahi Motlagh B, Javadi MA, Jafari Nasab MR, Rabbanikhah Z, Anisian A, Souri H. Corneal transplantation in patients with keratoconus. *Iran J Ophthalmol* 2003;16:9–19. [In Persian]
9. Javadi MA, Mohammadi MJ, Mirdehghan SA, Sajjadi SH. A comparison between donor-recipient corneal size and its effect on the ultimate refractive error induced in keratoconus. *Cornea* 1993;12:401–405.
10. Brierly SC, Izquierdo Jr L, Mannis MJ. Penetrating keratoplasty for keratoconus. *Cornea* 2000;19:329–332.
11. Kirkness CM, Ficker LA, Steele AD, Rice NS. The success of penetrating keratoplasty for keratoconus. *Eye* 1990;4:673–688.
12. Lim L, Pesudovs K, Coster DJ. Penetrating keratoplasty for keratoconus: visual outcome and success. *Ophthalmology* 2000;107:1125–1131.
13. Colin J, Velou S. Current surgical options for keratoconus. *J Cataract Refract Surg* 2003;29:379–386.
14. Agarwal Rk. Deep lamellar keratoplasty, an alternative to penetrating keratoplasty. *Br J Ophthalmol* 1997;81:178–179.
15. Croasdale CR, Barney E, Warner EJ. Eye bank tissue utilization between endothelial keratoplasty and penetrating keratoplasty. *Cornea* 2013;32:280–284.
16. Cassidy D, Beltz J, Jhanji V, Loughnan MS. Recent advances in corneal transplantation for keratoconus. *Clin Exp Optom* 2013;96:165–172.
17. Weed KH, McGhee CN, MacEwen CJ. Atypical unilateral superior keratoconus in young males. *Cont Lens Anterior Eye* 2005;28:177–179.
18. MacIntyre R, Chow SP, Chan E, Poon A. Long-term outcomes of deep anterior lamellar keratoplasty versus penetrating keratoplasty in Australian keratoconus patients. *Cornea* 2014;33:6–9.
19. Van Dooren B, Mulder PG, Nieuwendaal CP, Beekhuis WH, Melles GR. Endothelial cell density after posterior lamellar keratoplasty (Melles techniques): 3 years follow-up. *Am J Ophthalmol* 2004;138:211–217.
20. Shimazaki J, Shimmura S, Ishioka M, Tsubota K. Randomized clinical trial of deep lamellar keratoplasty vs penetrating keratoplasty. *Am J Ophthalmol* 2002;134:159–165.
21. Moher D, Liberati A, Tetzlaff J, Altman DG, Prisma Group. Preferred reporting items for systematic reviews

and meta-analyses: the PRISMA statement. *PLoS Med* 2009;6:e1000097.

22. Joanna Briggs Institute. The Joanna Briggs Institute Critical Appraisal tools for use in JBI systematic reviews checklist for prevalence studies [Internet]. Adelaide, Australia: Joanna Briggs Institute; 2017. Available from: http://joannabriggs.org/research/critical-appraisaltools.html
23. Abdelaal AM, Alqassimi AH, Malak M, Hijazi HT, Hadrawi M, Khan MA. Indications of keratoplasty and outcomes of deep anterior lamellar keratoplasty compared to penetrating keratoplasty. *Cureus* 2021;13:e13825.
24. Busool Abu Eta Y, Tomkins-Netzer O, Mimouni M, Hamed Azzam S, Shehadeh Mashour R. Predicting factors of ocular hypertension following keratoplasty: Indications versus the procedure. *Eur J Ophthalmol* 2021;31:1749–1753.
25. Akdemir MO, Kandemir B, Sayman IB, Selvi C, Dogan OK. Comparison of contrast sensitivity and visual acuity between deep anterior lamellar keratoplasty and penetrating keratoplasty in patients with keratoconus. *Int J Ophthalmol* 2012;5:737–741.
26. Alzahrani K, Dardin SF, Carley F, Brahma A, Morley D, Hillarby MC. Corneal clarity measurements in patients with keratoconus undergoing either penetrating or deep anterior lamellar keratoplasty. *Clin Ophthalmol* 2018;12:577–585.
27. Amayem AF, Hamdi IM, Hamdi MM. Refractive and visual outcomes of penetrating keratoplasty versus deep anterior lamellar keratoplasty with hydrodissection for treatment of keratoconus. *Cornea* 2013;32:e2–e5.
28. Bahar I, Kaiserman I, Srinivasan S, Ya-Ping J, Slomovic AR, Rootman DS. Comparison of three different techniques of corneal transplantation for keratoconus. *Am J Ophthalmol* 2008;146:905–912.e1.
29. Cohen AW, Goins KM, Sutphin JE, Wandling GR, Wagoner MD. Penetrating keratoplasty versus deep anterior lamellar keratoplasty for the treatment of keratoconus. *Int Ophthalmol* 2010;30:675–681.
30. Donoso R, Díaz C, Villavicencio P. Comparative study of keratoconus between Anwar's deep anterior lamellar keratoplasty versus converted penetrating keratoplasty. *Arch Soc Esp Oftalmol* 2015;90:257–263.
31. Funnell CL, Ball J, Noble BA. Comparative cohort study of the outcomes of deep lamellar keratoplasty and penetrating keratoplasty for keratoconus. *Eye* 2006;20:527–532.
32. Godefrooij DA, Gans R, Imhof SM, Wisse RP. Trends in penetrating and anterior lamellar corneal grafting techniques for keratoconus: a national registry study. *Acta Ophthalmol* 2016;94:489–493.
33. Hamdi IM, Hamdi MM. Quality of vision after deep anterior lamellar keratoplasty (fluid dissection) compared to penetrating keratoplasty for the treatment of keratoconus. *J Ophthalmol* 2017;2017:4507989.
34. Huang T, Hu Y, Gui M, Hou C, Zhang H. Comparison of refractive outcomes in three corneal transplantation techniques for keratoconus. *Graefes Arch Clin Exp Ophthalmol* 2015;253:1947–1953.
35. Jafarinasab MR, Feizi S, Javadi MA, Hashemloo A. Graft biomechanical properties after penetrating keratoplasty versus deep anterior lamellar keratoplasty. *Curr Eye Res* 2011;36:417–421.
36. Janiszewska-Bil D, Czarnota-Nowakowska B, Krysik K, Lyssek-Boron A, Dobrowolski D, Grabarek BO, et al. Comparison of long-term outcomes of the lamellar and penetrating keratoplasty approaches in patients with keratoconus. *J Clin Med* 2021;10:2421.
37. Javadi MA, Feizi S, Yazdani S, Mirbabaee F. Deep anterior lamellar keratoplasty versus penetrating keratoplasty for keratoconus: a clinical trial. *Cornea* 2010;29:365–371.
38. Jones MN, Armitage WJ, Ayliffe W, Larkin DF, Kaye SB. Penetrating and deep anterior lamellar keratoplasty for keratoconus: a comparison of graft outcomes in the United kingdom. *Invest Ophthalmol Vis Sci* 2009;50:5625–5629.
39. Kasbekar SA, Jones MN, Ahmad S, Larkin DF, Kaye SB. Corneal transplant surgery for keratoconus and the effect of surgeon experience on deep anterior lamellar keratoplasty outcomes. *Am J Ophthalmol* 2014;158:1239–1246.
40. Khattak A, Nakhli FR, Al-Arfaj KM, Cheema AA. Comparison of outcomes and complications of deep anterior lamellar keratoplasty and penetrating keratoplasty performed in a large group of patients with keratoconus. *Int Ophthalmol* 2018;38:985–992.
41. Kim KH, Choi SH, Ahn K, Chung ES, Chung TY. Comparison of refractive changes after deep anterior lamellar keratoplasty and penetrating keratoplasty for keratoconus. *Jpn J Ophthalmol* 2011;55:93–97.
42. Koytak A, Kubaloglu A, Sari ES, Atakan M, Culfa S, Ozerturk Y. Changes in central macular thickness after uncomplicated corneal transplantation for keratoconus: penetrating keratoplasty versus deep anterior lamellar keratoplasty. *Cornea* 2011;30:1318–1321.
43. Kubaloglu A, Coskun E, Sari ES, Gunes AS, Cinar Y, Piñero DP, et al. Comparison of astigmatic keratotomy results in deep anterior lamellar keratoplasty and penetrating keratoplasty in keratoconus. *Am J Ophthalmol* 2011;151:637–643.e1.
44. Macintyre R, Chow SP, Chan E, Poon A. Long-term outcomes of deep anterior lamellar keratoplasty versus penetrating keratoplasty in Australian keratoconus patients. *Cornea* 2014;33:6–9.
45. Motlagh BF, Sedghipoor MR, Abroon G, Sadigh AL. Outcomes of penetrating keratoplasty and deep anterior lamellar keratoplasty for keratoconus in a university teaching hospital. *Iran J Ophthalmol* 2012;24:52–56.
46. Oh BL, Kim MK, Wee WR. Comparison of clinical outcomes of same-size grafting between deep anterior lamellar keratoplasty and penetrating keratoplasty for keratoconus. *Korean J Ophthalmol* 2013;27:322–330.
47. Pedrotti E, Passilongo M, Fasolo A, Ficial S, Ferrari S, Marchini G. Refractive outcomes of penetrating keratoplasty and deep anterior lamellar keratoplasty in fellow eyes for keratoconus. *Int Ophthalmol* 2017;37:911–919.
48. Sögütlü Sari E, Kubaloglu A, Ünal M, Piñero Llorens D, Koytak A, Ofluoglu AN, et al. Penetrating keratoplasty versus deep anterior lamellar keratoplasty: comparison of optical and visual quality outcomes. *Br J Ophthalmol* 2012;96:1063–1067.
49. Watson SL, Ramsay A, Dart JK, Bunce C, Craig E. Comparison of deep lamellar keratoplasty and penetrating

keratoplasty in patients with keratoconus. *Ophthalmology* 2004;111:1676–1682.

50. Yüksel B, Kandemir B, Uzunel UD, Çelik O, Ceylan S, Küsbeci T. Comparison of visual and topographic outcomes of deep-anterior lamellar keratoplasty and penetrating keratoplasty in keratoconus. *Int J Ophthalmol* 2017;10:385–390.
51. Zhang YM, Wu SQ, Yao YF. Long-term comparison of full-bed deep anterior lamellar keratoplasty and penetrating keratoplasty in treating keratoconus. *J Zhejiang Univ Sci B* 2013;14:438–450.
52. Ziaei M, Vellara HR, Gokul A, Ali NQ, McGhee CNJ, Patel DV. Comparison of corneal biomechanical properties following penetrating keratoplasty and deep anterior lamellar keratoplasty for keratoconus. *Clin Exp Ophthalmol* 2020;48:174–182.
53. Liu H, Chen Y, Wang P, Li B, Wang W, Su Y, et al. Efficacy and safety of deep anterior lamellar keratoplasty vs. penetrating keratoplasty for keratoconus: a meta-analysis. *PLoS ONE* 2015;10:e0113332.
54. Henein C, Nanavaty MA. Systematic review comparing penetrating keratoplasty and deep anterior lamellar keratoplasty for management of keratoconus. *Cont Lens Anterior Eye* 2017;40:3–14.
55. Song Y, Zhang J, Pan Z. Systematic review and meta-analysis of clinical outcomes of penetrating keratoplasty versus deep anterior lamellar keratoplasty for keratoconus. *Exp Clin Transplant* 2020;18:417–428.

Review Article

Update on Management of Non-proliferative Diabetic Retinopathy without Diabetic Macular Edema; Is There a Paradigm Shift?

Amir Arabi[1,2], MD, MPH; Ramin Tadayoni[3], MD, PhD; Hamid Ahmadieh[1,4], MD; Toktam Shahraki[1,5], MD Homayoun Nikkhah[1,2], MD

[1]*Ophthalmic Research Center, Research Institute for Ophthalmology and Vision Science, Shahid Beheshti University of Medical Sciences, Tehran, Iran*
[2]*Department of Ophthalmology, Torfeh Medical Center, Shahid Beheshti University of Medical Sciences, Tehran, Iran*
[3]*Université de Paris, Ophthalmology Department, AP-HP, Lariboisière, Saint Louis and Fondation Adolphe de Rothschild Hospitals, Paris, France*
[4]*Department of Ophthalmology, Labbafinejad Medical Center, Shahid Beheshti University of Medical Sciences, Tehran, Iran*
[5]*Department of Ophthalmology, Imam Hossein Medical Center, Shahid Beheshti University of Medical Sciences, Tehran, Iran*

ORCID:
Amir Arabi: https://orcid.org/0000-0002-6523-7533
Homayoun Nikkhah: https://orcid.org/0000-0002-2414-4661

Abstract

Diabetic retinopathy (DR) is the major cause of visual impairment and blindness in the working-age population. Conventional management for nonproliferative diabetic retinopathy (NPDR) without diabetic macular edema (DME) is derived from the findings of the Early Treatment Diabetic Retinopathy Study (ETDRS). Although the ETDRS protocol basically includes observation, selected cases of severe NPDR may undergo scatter laser photocoagulation. Post-hoc analysis of recent trials has shown that patients with NPDR receiving intravitreal anti-vascular endothelial growth factor (anti-VEGF) for DME would experience improvement in the DR severity scale (DRSS). In addition, recent randomized trials (PANORAMA and Protocol W) have revealed that early intervention with intravitreal aflibercept in eyes with moderately severe to severe NPDR is associated with significant improvement in DRSS and reduced vision-threatening complications of DR. Based on recent studies, it seems that the therapeutic approach to NPDR may undergo a substantial change and a paradigm shift toward considering early intervention with the administration of intravitreal anti-VEGF injections. However, the long-term results and the duration of adherence to anti-VEGF therapy for eyes with NPDR are not yet defined. It is also not apparent whether improvement in DRSS is a true disease modification. Studies showed that DRSS improvement is not associated with retinal reperfusion. In addition, DRCR.net Protocol W showed no visual acuity benefit with the early intravitreal aflibercept injection in moderate to severe NPDR as compared with performing observation plus intravitreal aflibercept applied only after progression to proliferative DR or vision-impairing DME. The cost–benefit ratio is also a challenge. Herein, we look at different aspects of early anti-VEGF application and discuss its pros and cons in the process of treating NPDR.

Keywords: Diabetic Macular Edema; Management; Nonproliferative Diabetic Retinopathy; Paradigm Shift

J Ophthalmic Vis Res 2022; 17 (1): 108–117

INTRODUCTION

According to the recent report of the International Diabetes Federation (IDF), about 400 million people live with diabetes mellitus (DM) worldwide; this prevalence is estimated to approach 600 million individuals by 2035.[1] One of the most common microvascular complications of DM is diabetic retinopathy (DR), which is reported to be the leading cause of visual impairment in the working-age population.[2, 3] Diabetic retinopathy is classically categorized into two types: nonproliferative diabetic retinopathy (NPDR) and proliferative diabetic retinopathy (PDR). Diabetic macular edema (DME) is another important manifestation of DR, which may be experienced across all DR severity stages. While approaches to the patients with PDR or DME is straightforward, the therapeutic approach to NPDR patients with no DME has not been well established.

Conventional management for NPDR without DME, which is derived from the findings of the Early Treatment Diabetic Retinopathy Study (ETDRS)[4] includes observation for mild and moderate NPDR. Most cases of severe NPDR are also followed closely; however, selected cases may undergo scatter laser photocoagulation. Post-hoc analysis of recent trials has shown that patients with NPDR receiving intravitreal anti-vascular endothelial growth factor (anti-VEGF) drugs for DME would experience amelioration in the DR severity scale (DRSS).[5, 6] In addition, more recent randomized controlled trials (PANORAMA study and DRCR.net Protocol W) have revealed that early intervention with intravitreal injection of aflibercept in eyes with moderately severe to severe NPDR may be associated with significant improvement in DRSS and reduced vision-threatening complications although the effect on visual acuity has not been significantly different compared to proper follow-up with timely treatment of complications.[7, 8] Based on recent studies, the therapeutic approach toward treating NPDR may undergo a significant change and paradigm shift to early intervention with intravitreal anti-VEGF injections that may substitute the conventional approach. However, the long-term results of anti-VEGF therapy for eyes with NPDR are not yet determined, and it is not clear how durable this approach will be and whether it is connected with enhanced visual functions and improved quality of life (QoL). The cost–benefit ratio is also a challenge that needs to be addressed. Herein, we review the different aspects of NPDR management and the early application of anti-VEGF therapy.

Management of NPDR Without DME

Management of NPDR patients without DME involves all interventions that prevent occurrence of vision-threatening complications including PDR and DME. This goal can be achieved by both systemic and ocular interventions.

Systemic management

Glycemic control

Control of hyperglycemia remains the basis of care in diabetic patients. Intensive glycemic control evaluated in two landmark trials, the Diabetes Control and Complications Trial (DCCT) and the UK Prospective Diabetes Study (UKPDS), assisted in reducing the risk of developing retinopathy and slowing the DR progression in both type 1 and type 2 DM[9, 10] These results have been supported in other studies.[11, 13] As an observation in the DCCT and UKPDS, the people in the early intensive glycemic control group had a significantly lower risk for long-term retinopathy progression and microvascular disorders regardless of the glycemic condition in the later course of the diabetes.[14, 15] The American Diabetes Association (ADA)

Correspondence to:

Homayoun Nikkhah, MD. Ophthalmic Research Center, Research Institute for Ophthalmology and Vision Science, Shahid Beheshti University of Medical Sciences, No. 23, Paidarfdard St., Boostan 9 St., Pasadaran Ave., Tehran 16666, Iran.
E-mail: h.nikkhah52@gmail.com

Received 13-08-2021; Accepted 11-11-2021

Access this article online

Website: https://knepublishing.com/index.php/JOVR

DOI: 10.18502/jovr.v17i1.10175

How to cite this article: Arabi A, Tadayoni R, Ahmadieh H, Shahraki T, Nikkhah H. Update on Management of Non-proliferative Diabetic Retinopathy without Diabetic Macular Edema; Is There a Paradigm Shift? . J Ophthalmic Vis Res 2022;17:108–117.

recommends a hemoglobin A1c (HbA1c) of <7%, with the recommendation of adjustment on an individual basis to avoid probable complications, such as hypoglycemia.[16]

Blood pressure control

Several studies have investigated the role of blood pressure regulation in the incidence and progression of DR. Some of these studies have demonstrated a positive effect from the intensive control of blood pressure, whereas no beneficial effect on the incidence and progression of DR has been observed in others.[17–20] Generally, blood pressure control has been recommended as a principal part of the standard care in diabetic patients, primarily because of its known beneficial effect on macro-vascular complications of DM rather than for its effect on DR.[21] However, blood pressure control may also reduce the damage to endothelial cells, through which slowing of DR progression may be achieved.[22] The available evidence does not support the idea that blood pressure control alone can inhibit or slow the progression of DR.[23]

Control of hyperlipidemia

The effects of dyslipidemia on DR incidence and progression have been controversial. In a new meta-analysis, no significant difference in lipid profile was observed between patients with and without DR.[24] However, Sankara Nethralaya Diabetic Retinopathy Epidemiology and Molecular Genetic Study (SN-DREAMS II) reported a threefold increase in the risk of DR progression to PDR stage in patients with higher triglycerides levels.[25] The ACCORD Eye Study has confirmed that fenofibrate benefits patients with DR.[26] Furthermore, the FIELD study confirmed that fenofibrate could prevent the progression of DR independent of serum lipids' levels.[27] It is postulated that the role of fenofibrate is more effective via iron chelation rather than hyperlipidemia treatment. Given the role of iron in retinal damages via oxidative pathways, iron chelation with fenofibrate may play a protective role in reducing retinal damage in DR.[28] In the Collaborative Atorvastatin Diabetes Study and the Heart Protection Study, the progression of DR did not differ between patients treated with statins and those who received placebo.[29, 30]

Miscellaneous systemic risk factors

Anemia is considered a risk factor of the microvascular complications of diabetic patients.[31, 32] Some studies have suggested that lower hemoglobin levels may be linked to progression of DR.[33, 34] Dietary modification, regular monitoring of anemia, and treatment with supplements may stop the progression of DR.[35]

A meta-analysis has revealed an association between vitamin D deficiency and increased risk of DR in type 2 DM.[36] Recently, it has been postulated that vitamin D3 exerts protective effects against retinal cell apoptosis and vascular damage in DR patients via an anti-inflammatory mechanism.[37]

A new meta-analysis discovered that the risk of DR was greater in smokers with type 1 diabetes; while in those patients who suffered with type 2 diabetes, the risk of PDR significantly decreased in smokers in comparison with nonsmokers.[38] In the Wisconsin Epidemiologic Study of Diabetic Retinopathy (WESDR), smoking was not significantly associated with the progression of DR in a 4-year and 10-year follow-up period.[39] Although the relationship between smoking and progression of DR remains inconclusive, there is evidence that suggests that smoking encourages macro-vascular complications associated with DM. As a result, it is recommended that patients who suffer with DM be strongly advised to cease smoking.

Ophthalmic management

Laser photocoagulation for NPDR

As DR reaches proliferative stage, retinal photocoagulation is applied to preserve the vision. This indication was derived from the presentation of two landmark studies, Diabetic Retinopathy Study (DRS) and ETDRS, where the findings convinced ophthalmologists to reach consensus on laser photocoagulation as a gold standard procedure for high-risk PDR (HRPDR).[40] Nevertheless, the question remains: Can retinal photocoagulation for patients with nonproliferative stages of DR decrease the risk of visual impairment by preventing the progression to PDR stage?

Patients with either PDR in at least one eye or severe NPDR in both eyes were included

in the DRS.[41] One eye of each patient was randomly assigned to laser photocoagulation and the second eye was considered as the control group. The two-year risk of severe visual loss in eyes with severe NPDR was 3.2% and 2.8% in the control and laser photocoagulation groups, respectively. The four-year rates were 12.8% and 4.3%, respectively. Although the researchers found that 50% of the eyes with severe NPDR who were in the control group developed new vessels in one year, after considering the small risk of severe visual loss in the control group and the possible side effects of laser photocoagulation they did not recommend laser photocoagulation for all NPDR patients. Nevertheless, the DRS offered laser photocoagulation in NPDR eyes in some instances: one eye of a patient with severe NPDR in both eyes, presence of severe retinal ischemia, when the patient was pregnant or there was coexisting disorders such as renal failure that might accelerate the course of DR.[40]

The ETDRS remains the only study addressing the question of the suitable time for starting laser photocoagulation.[4] Patients with moderate to severe NPDR or early PDR were included. Early photocoagulation was randomly performed in one eye of each patient and the other eye was assigned to deferred photocoagulation. In the latter, patients underwent laser therapy when high-risk PDR was detected. In the deferred photocoagulation group who had severe NPDR, the rate of PDR development was 51%, 71%, and 79% in the first-, third-, and fifth-year visits, respectively.[4] Compared to deferred photocoagulation, early photocoagulation decreased progression to high-risk PDR by 25% and 50% with full scatter and mild scatter photocoagulation, respectively.[4] However, the rate at the five-year visit determined that severe visual loss was low and comparable among the study groups (2.6% and 3.7% in early and deferral photocoagulation groups, respectively).[4]

A recent survey built a Markov model to explore whether it would be cost-effective either to apply panretinal photocoagulation (PRP) at the NPDR stage or to wait until HRPDR developed.[43] They found that earlier PRP at the severe NPDR stage was less costly and more effective than administering PRP to patients with high-risk PDR. It meant that fewer patients in the earlier PRP group progressed to more advanced stages of DR.

The most common complications of PRP are decreased visual field and exacerbation of macular edema.[44, 45] Fong et al have reported that visual field defects may occur in almost half of the treated patients, and the incidence is correlated with the intensity of the laser therapy.[46] A recent study based on optical coherence tomography angiography (OCT-A) has reported that in laser-treated severe NPDR eyes, ocular blood flow is significantly reduced, which may be associated with decreased visual acuity in these patients.[47]

Anti-VEGF for NPDR

Intravitreal anti-VEGF therapy for NPDR is an evolving concept. Clinical data show that VEGF contributes to the pathogenesis of both NPDR and PDR.[48, 49] According to the results of retrospective studies, anti-VEGF treatment can improve the DRSS and reduce the rate of PDR development.[50]

Utilization of anti-VEGF in NPDR with DME

RISE and RIDE were two phase-III, double-blind randomized clinical trials of intravitreal ranibizumab versus sham in patients with DME. In an exploratory analysis of RISE and RIDE trials, among the eyes with baseline ETDRS severity level of 53 (severe NPDR) or less, monthly intravitreal ranibizumab injection administered for 24 months was associated with a ≥2-step improvement in DRSS in 47% of eyes, as compared to 6.8% in the sham group ($P < 0.001$).[5] Furthermore, it has been noted that the cumulative probability of DR progression was 34% in the sham-treated patients and 11.2–11.5% in the ranibizumab-treated patients by month 24.[5] In addition, it has been reported that intravitreal ranibizumab in patients of RISE and RIDE trials slowed the progression of retinal non-perfused areas.[51]

Similarly, in the VIVID-DME and VISTA-DME trials, a significantly greater proportion of patients treated with aflibercept (week 100: 34.9%) compared with those treated with laser (13%) achieved a ≥2 step DRSS improvement ($P < 0.0001$).[52] In addition, the proportion of patients who developed PDR was significantly less in those who received intravitreal aflibercept as compared with the sham-treated group (week 100: 2.2% vs 9.1%, $P < 0.0001$).[52]

DRCR.net Protocol T compared the efficacy of intravitreal aflibercept, ranibizumab, and bevacizumab in the treatment of DME. Based on a post hoc analysis of the Protocol T,

25%, 22% and 31% of NPDR eyes receiving aflibercept, bevacizumab, and ranibizumab for DME demonstrated improvement in DRSS at two-year follow-up, respectively.[53] There were no statistically significant differences among the three commercially available anti-VEGFs in terms of inducing the regression of DR.

Utilization of anti-VEGF in NPDR without DME

The PANORAMA study was the first randomized clinical trial evaluating the role of intravitreal aflibercept on DRSS and incidence of vision-threatening complications (PDR and/or anterior segment neovascularization) and center-involved (CI) DME in patients with moderately severe to severe NPDR without DME. In this phase-3 clinical trial, 402 patients were randomly assigned to sham versus aflibercept administered every 8 weeks after 5 monthly loading doses versus aflibercept administered every 16 weeks after 3 monthly loading doses. At two-year follow-up, the proportion of eyes with 2-step or more improvement in DRSS was 12.8%, 62.2%, and 50% in the sham group, every 16 weeks aflibercept group and every 8 weeks (converted to pro re nata [PRN] in the second year) aflibercept group, respectively ($P < 0.001$ for both).[7] Furthermore, the proportion of eyes that developed vision-threatening complications and/or CI-DME were 50.4%, 16.3%, and 18.7% in the sham group, every 16 weeks and every 8 weeks aflibercept groups, respectively ($P < 0.001$ for both comparisons).

DRCR.net Protocol W is a phase-3 randomized clinical trial evaluating the role of intravitreal aflibercept (injected at baseline, months 1, 2, and 4; and after that every four months through to two years) versus sham in reducing vision-threatening complications in eyes with moderate to severe NPDR.[8] While the primary endpoint was recently reported at two years, the patients will be followed-up to four years. The two-year risk of developing CI-DME with decreased visual acuity or PDR was 16.3% and 43.5% in the aflibercept and sham groups, respectively (adjusted hazard ratio, 0.32 [97.5% confidence interval {CI}, 0.21–0.5; $P < 0.001$]). DRSS improved ≥2-steps from baseline to year 2 in 44.8% and 13.7% of eyes receiving aflibercept and sham, respectively (adjusted odds ratio, 5.91 [97.5% CI, 3.19–10.95; $P < 0.001$]).

Monte Carlo simulation of a real-world cohort of treatment-naive patients with NPDR from the IBM® Explorys® database suggested that severe NPDR treatment with anti-VEGF would significantly decrease the probability of progression to PDR by 51.7% at the five-year follow-up period. Furthermore, the incidences of sustained blindness in severe NPDR patients were reduced with anti-VEGF therapy by 57.7% over a 10-year follow-up period.[54]

The phase-2 BOULEVARD trial compared the efficacy of Faricimab, a bispecific antibody, inhibiting both VEGF-A and angiopoietin-2, with ranibizumab in the treatment of patients with DME.[55] At the six-month follow-up period, among the patients who were treatment-naïve, 2-steps or greater improvement in the DRSS was achieved in 12.2%, 27.7%, and 38.6% of eyes in the 0.3 mg ranibizumab, 1.5 mg Faricimab, and 6 mg Faricimab groups, respectively.[55]

DISCUSSION

Conventional management of NPDR without DME included observation along with controlling the systemic condition. The ETDRS showed that in one year, 26% of eyes with moderately severe NPDR and 52% of eyes with severe NPDR in the deferred photocoagulation group would progress to PDR, a vision-threatening complication of DR. The rate of progression to PDR reached 66% and 75–81% at the five-year follow-up period.[42] Recently, there has been increasing evidence that anti-VEGF treatments would improve DRSS and decrease the risk of vision-threatening complications such as PDR and DME,[7, 8] raising an important question: Is it recommended to target the DR at the nonproliferative stage by administering intravitreal anti-VEGF injections to prevent the disease progression and reduce the risk of vision threatening complications? There are pros and cons for this evolving approach.

Pros of Using Anti-VEGF in NPDR Without DME

There is increasing evidence in favor of administering intravitreal anti-VEGF injection in nonproliferative stages of DR without DME. The PANORAMA study showed that intravitreal aflibercept reduces the risk of vision-threatening complications by 77% and 83% in every 16 weeks and every 8 weeks (PRN in the second year)

groups, respectively, as compared with the sham group at 100 weeks.[7] At the end of the second year, data were also emphasized in the DRCR.net W protocol, where the risk of vision-threatening complications was 16.3% and 43.5% for the aflibercept and the sham groups, respectively.[8]

Extension of non-perfusion areas is the major pathology in DR. Diabetic retinopathy leads to upregulation of VEGF and contributes to further progression of non-perfusion areas as a vicious cycle. It was demonstrated that anti-VEGF therapy slows the development and progression of retinal non-perfusion in patients with DME.[51] However, a small interventional cohort with short term follow-up showed that anti-VEGF induced improvement of DRSS could occur without any retinal reperfusion.[56]

Epidemiological studies have shown that DR has an adverse effect on the quality of life (QoL). A recent longitudinal and observational study showed that QoL significantly decreases with aggravation of DR severity from mild NPDR to PDR.[57] Furthermore, a cross-sectional study showed that vision-related functional burden is significantly greater in patients with severe NPDR or PDR versus those with no retinopathy.[58]

Longitudinal population-based studies have shown that more advanced DR at diagnosis is associated with higher risk of developing sustained blindness.[59] Kaplan-Meier's analysis of a recent epidemiological study has shown that eyes with moderate NPDR, severe NPDR, and PDR were 2.6, 3.6, and 4 times, respectively, more likely to develop sustained blindness, as compared to eyes with mild NPDR, after two years of follow-up.[59]

Cons of Using Anti-VEGF in NPDR Without DME

At the end of two-year follow-up in the PANORAMA study, 49.6% of eyes in the sham group did not develop vision-threatening complications and/or CI-DME.[7] This shows that nearly half of the patients who have NPDR will not progress to PDR or develop DME despite not receiving any intraocular injection.

Some complications have been reported regarding the use of intravitreal anti-VEGF injections. Common complications are the incidence of floaters and the rise of IOP.[60, 61] The most devastating complication is infectious endophthalmitis. The prevalence of endophthalmitis following intravitreal injections is estimated to be 0.01–0.26%.[62]

It is not clear whether intravitreal anti-VEGF for severe NPDR can be associated with enhanced visual function and improved QoL. DRCR.net Protocol W, during a two-year period, showed no visual benefit of the preventive intravitreal aflibercept treatment in eyes with moderate to severe NPDR as compared with those eyes that underwent observation plus aflibercept which was administered only after progression to PDR or vision-impairing CI-DME. The mean change of visual acuity was –0.9 and –2.0 ETDRS letters in aflibercept and sham groups, respectively (P = 0.47).[8]

The long-term real-world benefits of anti-VEGF therapy for eyes with NPDR are not yet determined. It is not clear how durable the treatment is and how long the patients should receive anti-VEGF treatment. In the second year of the PANORAMA study, those patients who initially received aflibercept every eight weeks transitioned to PRN. Concomitantly the rate of 2-steps or more improvement in DRSS reduced from 79.9% to 50%.[7] Furthermore, in the RISE/RIDE open label extension (OLE) study, nearly 40% of eyes that did not receive any more ranibizumab injections during the OLE experienced 2-steps or more worsening in the DRSS.[63]

It is not apparent whether improvement in the DRSS following intravitreal injections of anti-VEGFs is a true disease modification. In a case series by Couturier et al, no reflow of vessels or reperfusion of capillary bed was found in non-perfusion areas using ultra-widefield (UWF) fluorescein angiography (FA) and swept-source widefield (SS-WF) OCT-A in eyes with DR after 3 anti-VEGF injections.[64] In addition, Bonnin et al showed that after administering anti-VEGF injections in DR eyes, the improvement in the DRSS score based on color fundus photograph could occur without retinal reperfusion on UWF FA.[65] In an OLE of RISE/RIDE study, it was shown that patients with anti-VEGF injection induced moderate NPDR were more prone to DR progression compared to patients with moderate NPDR at enrollment who were randomized to the sham group.[63]

The cost–benefit ratio is also a challenge that needs to be addressed. Answering this question requires more time and further studies.

Possible Effects of VEGF-independent Drugs on NPDR Course

Inhibition of the VEGF independent pathways may also affect the course of DR. There is some evidence that angiopoietin/Tie2 and Rho-associated kinase (ROCK) play an influential role in retinal perfusion. Inhibition of angiopoietin 2 may enhance the effects of VEGF inhibition in improving the DRSS.[55]

Expression of Rho-associated kinase (ROCK) is increased in diabetic eyes and activation of ROCK-1 induces focal retinal vasoconstriction and subsequent retinal ischemia.[66, 67] An in vivo study showed that fasudil (a specific ROCK inhibitor) decreased vasoconstriction, improved retinal flow, and could potentially reduce the retinal ischemia.[67] Intravitreal ripasudil also decreased the retinal non-perfusion areas and improved retinal blood flow in a murine model of retinal vein occlusion.[68] Ahmadieh et al reported that a combination of intravitreal bevacizumab and fasudil in eyes with persistent DME and macular ischemia was associated with significantly more visual improvement as compared with solely administering intravitreal bevacizumab. This significant visual improvement could be due to improved perfusion induced by the ROCK inhibitor.[69] Further research is needed to determine the role of ROCK inhibitors in ameliorating diabetes-induced retinal microvascular damage and improving DRSS.

SUMMARY

The concept of slowing the progressive course of DR and preventing the vision-threatening complications of this potentially blinding disease may represent the initial sign of a paradigm shift from the observation, which has been the standard care for patients with NPDR to a new strategy comprising intravitreal anti-VEGF injections. However, there is not enough evidence supporting this paradigm shift at present. A new classification may help improving the management of NPDR based on recent progress in understanding of the pathophysiology and advances in treatment of DR and addresses the need to possible paradigm shift in the future.

Financial Support and Sponsorship

The authors declare that they did not receive any fund for the current manuscript or any research relevant to the present study.

Conflicts of Interest

The authors have no conflicts of interest to declare.

REFERENCES

1. Gao HX, Regier EE, Close KL. International Diabetes Federation World Diabetes Congress 2015. *J Diabetes* 2016;8:300–302.
2. Shaw JE, Sicree RA, Zimmet PZ. Global estimates of the prevalence of diabetes for 2010 and 2030. *Diabetes Res Clin Pract* 2010;87:4–14.
3. Klein R, Lee KE, Knudtson MD, Gangnon RE, Klein BE. Changes in visual impairment prevalence by period of diagnosis of diabetes: the Wisconsin Epidemiologic Study of Diabetic Retinopathy. *Ophthalmology* 2009;116:1937–1942.
4. Early Treatment Diabetic Retinopathy Study Research Group. Early photocoagulation for diabetic retinopathy. ETDRS report number 9. *Ophthalmology* 1991;98:766–785.
5. Ip MS, Domalpally A, Hopkins JJ, Wong P, Ehrlich JS. Long-term effects of ranibizumab on diabetic retinopathy severity and progression. *Arch Ophthalmol* 2012;130:1145–1152.
6. Mitchell P, McAllister I, Larsen M, Staurenghi G, Korobelnik JF, Boyer DS, et al. Evaluating the impact of intravitreal aflibercept on diabetic retinopathy progression in the VIVID-DME and VISTA-DME studies. *Ophthalmol Retina* 2018;2:988–996.
7. Brown DM, Wykoff CC, Boyer D, Heier JS, Clark WL, Emanuelli A, et al. Evaluation of intravitreal aflibercept for the treatment of severe nonproliferative diabetic retinopathy: results from the PANORAMA randomized clinical trial. *JAMA Ophthalmol* 2021;139:1–10.
8. Maturi RK, Glassman AR, Josic K, Antoszyk AN, Blodi BA, Jampol LM, et al. Effect of intravitreous anti-vascular endothelial growth factor vs sham treatment for prevention of vision-threatening complications of diabetic retinopathy: the protocol W randomized clinical trial. *JAMA Ophthalmol* 2021;139:701–712.
9. Diabetes Control and Complications Trial Research Group. Effect of intensive diabetes treatment on the development and progression of long-term complications in adolescents with insulin-dependent diabetes mellitus: Diabetes Control and Complications Trial. *J Pediatr* 1994;125:177–188.
10. Stratton IM, Kohner EM, Aldington SJ, Turner RC, Holman RR, Manley SE, et al. UKPDS 50: risk factors for incidence and progression of retinopathy in Type II diabetes over 6 years from diagnosis. *Diabetologia* 2001;44:156–163.

11. Shichiri M, Kishikawa H, Ohkubo Y, Wake N. Long-term results of the Kumamoto Study on optimal diabetes control in type 2 diabetic patients. *Diabetes Care* 2000;23:B21–B29.
12. Wang PH, Lau J, Chalmers TC. Meta-analysis of effects of intensive blood-glucose control on late complications of type I diabetes. *Lancet* 1993;341:1306–1309.
13. Ohkubo Y, Kishikawa H, Araki E, Miyata T, Isami S, Motoyoshi S, et al. Intensive insulin therapy prevents the progression of diabetic microvascular complications in Japanese patients with non-insulin-dependent diabetes mellitus: a randomized prospective 6-year study. *Diabetes Res Clin Pract* 1995;28:103–117.
14. Drzewoski J, Kasznicki J, Trojanowski Z. The role of "metabolic memory" in the natural history of diabetes mellitus. *Pol Arch Med Wewn* 2009;119:493–500.
15. Holman RR, Paul SK, Bethel MA, Matthews DR, Neil HA. 10-year follow-up of intensive glucose control in type 2 diabetes. *N Engl J Med* 2008;359:1577–1589.
16. American Diabetes Association. Standards of medical care in diabetes-2014. *Diabetes Care* 2014;37:S14–S80.
17. UK Prospective Diabetes Study Group. Tight blood pressure control and risk of macrovascular and microvascular complications in type 2 diabetes: UKPDS 38. *BMJ* 1998;317:703–713.
18. Schrier RW, Estacio RO, Jeffers B. Appropriate blood pressure control in NIDDM (ABCD) trial. *Diabetologia* 1996;39:1646–1654.
19. Klein R, Klein BE, Moss SE, Cruickshanks KJ. The Wisconsin Epidemiologic Study of Diabetic Retinopathy: XVII. The 14-year incidence and progression of diabetic retinopathy and associated risk factors in type 1 diabetes. *Ophthalmology* 1998;105:1801–1815.
20. Estacio RO, Jeffers BW, Gifford N, Schrier RW. Effect of blood pressure control on diabetic microvascular complications in patients with hypertension and type 2 diabetes. *Diabetes Care* 2000;23:B54–B64.
21. Hansson L, Zanchetti A, Carruthers SG, Dahlof B, Elmfeldt D, Julius S, et al. Effects of intensive blood-pressure lowering and low-dose aspirin in patients with hypertension: principal results of the Hypertension Optimal Treatment (HOT) randomised trial. HOT Study Group. *Lancet* 1998;351:1755–1762.
22. Raum P, Lamparter J, Ponto KA, Peto T, Hoehn R, Schulz A, et al. Prevalence and cardiovascular associations of diabetic retinopathy and maculopathy: results from the Gutenberg Health Study. *PLoS One* 2015;10:e0127188.
23. Do DV, Wang X, Vedula SS, Marrone M, Sleilati G, Hawkins BS, et al. Blood pressure control for diabetic retinopathy. *Cochrane Database Syst Rev* 2015;1:CD006127.
24. Zhou Y, Wang C, Shi K, Yin X. Relationship between dyslipidemia and diabetic retinopathy: a systematic review and meta-analysis. *Medicine* 2018;97:e12283.
25. Srinivasan S, Raman R, Kulothungan V, Swaminathan G, Sharma T. Influence of serum lipids on the incidence and progression of diabetic retinopathy and macular oedema: Sankara Nethralaya Diabetic Retinopathy Epidemiology and Molecular genetics Study-II. *Clin Exp Ophthalmol* 2017;45:894–900.
26. Chew EY, Davis MD, Danis RP, Lovato JF, Perdue LH, Greven C, et al. The effects of medical management on the progression of diabetic retinopathy in persons with type 2 diabetes: the Action to Control Cardiovascular Risk in Diabetes (ACCORD) Eye Study. *Ophthalmology* 2014;121:2443–2451.
27. Keech AC, Mitchell P, Summanen PA, O'Day J, Davis TM, Moffitt MS, et al. Effect of fenofibrate on the need for laser treatment for diabetic retinopathy (FIELD study): a randomised controlled trial. *Lancet* 2007;370:1687–1697.
28. Mandala A, Armstrong A, Girresch B, Zhu J, Chilakala A, Chavalmane S, et al. Fenofibrate prevents iron induced activation of canonical Wnt/ß-catenin and oxidative stress signaling in the retina. *NPJ Aging Mech Dis* 2020;6:12.
29. Colhoun HM, Betteridge DJ, Durrington PN, Hitman GA, Neil HA, Livingstone SJ, et al. Primary prevention of cardiovascular disease with atorvastatin in type 2 diabetes in the Collaborative Atorvastatin Diabetes Study (CARDS): multicentre randomised placebo-controlled trial. *Lancet* 2004;364:685–696.
30. Collins R, Armitage J, Parish S, Sleigh P, Peto R. MRC/BHF Heart Protection Study of cholesterol-lowering with simvastatin in 5963 people with diabetes: a randomised placebo-controlled trial. *Lancet* 2003;361:2005–2016.
31. Hosseini MS, Rostami Z, Saadat A, Saadatmand SM, Naeimi E. Anemia and microvascular complications in patients with type 2 diabetes mellitus. *Nephrourol Mon* 2014;6:e19976.
32. Thomas M, Tsalamandris C, MacIsaac R, Jerums G. Anaemia in diabetes: an emerging complication of microvascular disease. *Curr Diabetes Rev* 2005;1:107–126.
33. Traveset A, Rubinat E, Ortega E, Alcubierre N, Vazquez B, Hernandez M, et al. Lower hemoglobin concentration is associated with retinal ischemia and the severity of diabetic retinopathy in type 2 diabetes. *J Diabetes Res* 2016;2016:3674946.
34. Ranil PK, Raman R, Rachepalli SR, Pal SS, Kulothungan V, Lakshmipathy P, et al. Anemia and diabetic retinopathy in type 2 diabetes mellitus. *J Assoc Physicians India* 2010;58:91–94.
35. Idiculla J, Nithyanandam S, Joseph M, Christeena J. Anemia as a risk factor for diabetic retinopathy (dr) with special reference to nutritional etiology. *Diabetes* 2018;67:591.
36. Luo BA, Gao F, Qin LL. The association between vitamin D deficiency and diabetic retinopathy in type 2 diabetes: a meta-analysis of observational studies. *Nutrients* 2017;9:307.
37. Lu L, Lu Q, Chen W, Li J, Li C, Zheng Z. Vitamin D3 protects against diabetic retinopathy by inhibiting high-glucose-induced activation of the ROS/TXNIP/NLRP3 inflammasome pathway. *J Diabetes Res* 2018;2018:8193523.
38. Cai X, Chen Y, Yang W, Gao X, Han X, Ji L. The association of smoking and risk of diabetic retinopathy in patients with type 1 and type 2 diabetes: a meta-analysis. *Endocrine* 2018;62:299–306.
39. Moss SE, Klein R, Klein BE. Cigarette smoking and ten-year progression of diabetic retinopathy. *Ophthalmology* 1996;103:1438–1442.
40. Moutray T, Evans JR, Lois N, Armstrong DJ, Peto T, Azuara-Blanco A. Different lasers and techniques for proliferative diabetic retinopathy. *Cochrane Database Syst Rev* 2018;3:Cd012314.

41. The Diabetic Retinopathy Study Research Group. Indications for photocoagulation treatment of diabetic retinopathy: Diabetic Retinopathy Study Report no. 14. *Int Ophthalmol Clin* 1987;27:239–253.
42. Early Treatment Diabetic Retinopathy Study Research Group. Fundus photographic risk factors for progression of diabetic retinopathy. ETDRS report number 12. *Ophthalmology* 1991;98:823–833.
43. Mistry H, Auguste P, Lois N, Waugh N. Diabetic retinopathy and the use of laser photocoagulation: is it cost-effective to treat early? *BMJ Open Ophthalmol* 2017;2:e000021.
44. Royle P, Mistry H, Auguste P, Shyangdan D, Freeman K, Lois N, et al. Pan-retinal photocoagulation and other forms of laser treatment and drug therapies for non-proliferative diabetic retinopathy: systematic review and economic evaluation. *Health Technol Assess* 2015;19:v–xxviii, 1–247.
45. El Rami H, Barham R, Sun JK, Silva PS. Evidence-based treatment of diabetic retinopathy. *Semin Ophthalmol* 2017;32:67–74.
46. Fong DS, Girach A, Boney A. Visual side effects of successful scatter laser photocoagulation surgery for proliferative diabetic retinopathy: a literature review. *Retina* 2007;27:816–824.
47. Iwase T, Kobayashi M, Yamamoto K, Ra E, Terasaki H. Effects of photocoagulation on ocular blood flow in patients with severe non-proliferative diabetic retinopathy. *PLoS One* 2017;12:e0174427.
48. Aiello LP, Avery RL, Arrigg PG, Keyt BA, Jampel HD, Shah ST, et al. Vascular endothelial growth factor in ocular fluid of patients with diabetic retinopathy and other retinal disorders. *N Engl J Med* 1994;331:1480–1487.
49. Adamis AP, Miller JW, Bernal MT, D'Amico DJ, Folkman J, Yeo TK, et al. Increased vascular endothelial growth factor levels in the vitreous of eyes with proliferative diabetic retinopathy. *Am J Ophthalmol* 1994;118:445–450.
50. Zhao Y, Singh RP. The role of anti-vascular endothelial growth factor (anti-VEGF) in the management of proliferative diabetic retinopathy. *Drugs Context* 2018;7:212532.
51. Campochiaro PA, Wykoff CC, Shapiro H, Rubio RG, Ehrlich JS. Neutralization of vascular endothelial growth factor slows progression of retinal nonperfusion in patients with diabetic macular edema. *Ophthalmology* 2014;121:1783–1789.
52. Mitchell P, McAllister I, Larsen M, Staurenghi G, Korobelnik JF, Boyer DS, et al. Evaluating the impact of intravitreal aflibercept on diabetic retinopathy progression in the VIVID-DME and VISTA-DME studies. *Ophthalmol Retina* 2018;2:988–996.
53. Bressler SB, Liu D, Glassman AR, Blodi BA, Castellarin AA, Jampol LM, et al. Change in diabetic retinopathy through 2 years: secondary analysis of a randomized clinical trial comparing aflibercept, bevacizumab, and ranibizumab. *JAMA Ophthalmol* 2017;135:558–568.
54. Lim JI. Long-term clinical impact of intravitreal anti-VEGF therapy for severe non-proliferative diabetic retinopathy (NPDR): analyses through a discrete event simulation model. Association for Research in Vision and Ophthalmology Annual Meeting; May 6, 2021; virtual meeting.
55. Sahni J, Patel SS, Dugel PU, Khanani AM, Jhaveri CD, Wykoff CC, et al. Simultaneous inhibition of angiopoietin-2 and vascular endothelial growth factor-A with faricimab in diabetic macular edema: BOULEVARD phase 2 randomized trial. *Ophthalmology* 2019;126:1155–1170.
56. Bonnin S, Dupas B, Lavia C, Erginay A, Dhundass M, Couturier A, et al. Anti-vascular endothelial growth factor therapy can improve diabetic retinopathy score without change in retinal perfusion. *Retina* 2019;39:426–434.
57. Yadav P, Singh SV, Nada M, Dahiya M. Impact of severity of diabetic retinopathy on quality of life in type 2 Indian diabetic patients. *Int J Community Med Public Health* 2021;8:207–211.
58. Willis JR, Doan QV, Gleeson M, Haskova Z, Ramulu P, Morse L, et al. Vision-related functional burden of diabetic retinopathy across severity levels in the United States. *JAMA Ophthalmol* 2017;135:926–932.
59. Wykoff CC, Khurana RN, Nguyen QD, Kelly SP, Lum F, Hall R, et al. Risk of blindness among patients with diabetes and newly diagnosed diabetic retinopathy. *Diabetes Care* 2021;44:748–756.
60. Wu L, Martinez-Castellanos MA, Quiroz-Mercado H, Arevalo JF, Berrocal MH, Farah ME, et al. Twelve-month safety of intravitreal injections of bevacizumab (Avastin): results of the Pan-American Collaborative Retina Study Group (PACORES). *Graefes Arch Clin Exp Ophthalmol* 2008;246:81–87.
61. Shikari H, Silva PS, Sun JK. Complications of intravitreal injections in patients with diabetes. *Semin Ophthalmol* 2014;29:276–289.
62. Menchini F, Toneatto G, Miele A, Donati S, Lanzetta P, Virgili G. Antibiotic prophylaxis for preventing endophthalmitis after intravitreal injection: a systematic review. *Eye* 2018;32:1423–1431.
63. Goldberg RA. What happens to diabetic retinopathy severity scores with less aggressive treatment? A post hoc analysis of the RISE and RIDE open label extension study. Paper presented at: the American Society of Retina Specialists Annual Meeting; July 29, 2019; Chicago, IL.
64. Couturier A, Rey PA, Erginay A, Lavia C, Bonnin S, Dupas B, et al. Widefield oct-angiography and fluorescein angiography assessments of nonperfusion in diabetic retinopathy and edema treated with anti-vascular endothelial growth factor. *Ophthalmology* 2019;126:1685–1694.
65. Bonnin S, Dupas B, Lavia C, Erginay A, Dhundass M, Couturier A, et al. Anti-vascular endothelial growth factor therapy can improve diabetic retinopathy score without change in retinal perfusion. *Retina* 2019;39:426–434.
66. Arita R, Hata Y, Nakao S, Kita T, Miura M, Kawahara S, et al. Rho kinase inhibition by fasudil ameliorates diabetes-induced microvascular damage. *Diabetes* 2009;58:215–226.
67. Rothschild PR, Salah S, Berdugo M, Gélizé E, Delaunay K, Naud MC, et al. ROCK-1 mediates diabetes-induced retinal pigment epithelial and endothelial cell blebbing: contribution to diabetic retinopathy. *Sci Rep* 2017;7:8834.
68. Hida Y, Nakamura S, Nishinaka A, Inoue Y, Shimazawa M, Hara H. Effects of ripasudil, a ROCK inhibitor, on retinal edema and nonperfusion area in a retinal vein occlusion murine model. *J Pharmacol Sci* 2018;137:129–136.

69. Ahmadieh H, Nourinia R, Hafezi-Moghadam A, Sabbaghi H, Nakao S, Zandi S, et al. Intravitreal injection of a Rho-kinase inhibitor (fasudil) combined with bevacizumab versus bevacizumab monotherapy for diabetic macular oedema: a pilot randomized clinical trial. *Br J Ophthalmol* 2019;103:922–927.

Review Article

Orbital Inflammation Caused by Aminobisphosphonates

J Gonzalez Barlatay, MD; C Pagano Boza, MD; GV Hernandez Gauna, MD; JE Premoli, MD

Division of Orbital and Ophthalmic Plastic Surgery, Hospital Italiano de Buenos Aires, Argentina

ORCID:

J Gonzalez Barlatay: http://orcid.org/0000-0002-3412-359X

Abstract

The aim of this review was to describe orbital inflammation secondary to aminobisphosphonates by analyzing demographic data, clinical presentation, and treatment of the disease. This is a narrative literature review. The search was performed using databases such as Ovid/MEDLINE and COCHRANE. The searches were limited to papers in the English language. We found 43 cases of orbital inflammation due to aminobisphosphonates. Zoledronate was the drug most associated with orbital side effects. Clinical presentation was evident by unilateral involvement (89%), palpebral edema (88%), conjunctival congestion (81%), chemosis (79%), ocular pain (77%), ocular motility impairment (65%), proptosis (56%), and blurred vision (39%). It can affect both eyes (11%) and is accompanied by anterior uveitis (23%). Orbital inflammation secondary to aminobisphosphonates is a severe side effect. Clinically, it cannot be distinguished from idiopathic inflammation of the orbit. Therefore, it is important to rule out previous drug exposure. Timely treatment is vital to expect a favorable outcome, with systemic corticosteroids being the treatment of choice.

Keywords: Alendronate; Bisphosphonates; Dacryoadenitis; Myositis; Pamidronate; Zoledronate

J Ophthalmic Vis Res 2022; 17 (1): 118–122

INTRODUCTION

Bisphosphonate group of drugs are widely used in diseases such as osteoporosis, Paget's disease, osteoclastic bone metastases, and multiple myeloma. These drugs have a high affinity for bone tissue, where they combine with hydroxyapatite crystals to inhibit bone resorption. As a result, untoward bone events decrease, and pain is relieved. Among the well-known adverse effects, the possibility of triggering an acute systemic inflammatory phase response, characterized by fever, pain, nausea, and fatigue within the first 72 hr after administration occurs in approximately 40–50% of the patients.[1] Symptoms are usually transient and resolve spontaneously. However, in several cases, they may be treated with analgesic and antipyretic drugs. The clinical presentation is accompanied by a decrease in the lymphocyte

Correspondence to:

J Gonzalez Barlatay, MD. Peron 4190, Ciudad Autónoma de Buenos Aires, Argentina.
Email: joaquingonzalezbarlatay@gmail.com

Received 06-05-2020; Accepted 01-08-2021

Access this article online

Website: https://knepublishing.com/index.php/JOVR

DOI: 10.18502/jovr.v17i1.10176

How to cite this article: Barlatay JG, Boza CP, Gauna GVH, Premoli JE. Orbital Inflammation Caused by Aminobisphosphonates. J Ophthalmic Vis Res 2022;17:118–122.

count and an increase in pro-inflammatory markers, such as IL-6, IFN-γ, and TNF-α.[2–5]

Ocular adverse effects related to bisphosphonates have also been reported. The most frequent complications are conjunctivitis, anterior uveitis, episcleritis, and scleritis.[6] Orbital inflammation indicates its clinical severity. It can range from minimal congestion to severe inflammation with visual impairment if not promptly diagnosed and treated in time. Clinically, it cannot be differentiated from idiopathic orbital inflammation. The aim of this study was to perform a literature review on orbital inflammation secondary to bisphosphonates to increase the knowledge of rare adverse effects and determine the best management methods.

METHODS

The search was performed using databases such as Ovid/MEDLINE and COCHRANE, using English language restriction in the electronic searches for papers. We searched electronic databases in August 2020. The keywords used for the search were: bisphosphonates, OR orbital inflammation, OR myositis, OR ocular side effects, OR ocular adverse effects, and OR ocular inflammation. At the same time, the search was performed by changing the word bisphosphonate with aminobiphosphonates, zoledronate, ibandronate, alendronate, and pamidronate.

Selection Criteria

All the papers that described orbital inflammation due to aminobisphosphonates were included. Patients with intraocular side effects that did not involve the orbit were excluded. A database with demographic data, type of drug, disease onset time, clinical characteristics, and treatment of choice was created.

The study was approved by the Institutional Review Board at the *Instituto Universitario del Hospital Italiano de Buenos Aires* and adhered to the tenets of the Declaration of Helsinki.

RESULTS

A total of 43 cases of orbital inflammation due to aminobisphosphonates were found in 26 articles published in Ovid/MEDLINE and COCHRANE, including case reports and reviews.[7–33] The first article on this topic was published in 1999[7] and the last one in 2019.[33] Demographic data of the patients are summarized in Table 1. Zoledronate was the drug most associated with orbital side effects. The clinical presentations are summarized in Table 2. Unilateral involvement occurred in 89% of the patients. Symptoms and signs included palpebral edema (88%), conjunctival congestion (81%), chemosis (79%), ocular pain (77%), ocular motility impairment (65%), proptosis (56%), and blurred vision (39%). Only two cases had complications, one had a severe reduction in visual acuity due to anterior ischemic optic neuritis (AION),[13] and other reported recurrent orbital inflammation without visual impairment.[30]

A total of 27 patients stopped treatment with bisphosphonates due to orbital inflammation, three patients continued treatment despite orbital involvement, and no severe complications were reported.

DISCUSSION

Orbital inflammation caused by bisphosphonates is a rare adverse drug reaction. To date, only 43 case reports have been published worldwide.[7–33] The route of administration seems to be associated with latency time for the onset of symptoms. The patients treated with oral alendronate started showing signs and symptoms between 15 and 21 days after treatment, while the patients treated with intravenous pamidronate and zoledronate presented them 3 days later. Zoledronate is the bisphosphonate most frequently associated with this reaction when compared with others, and it can be related to it being the most frequently used for its effectiveness in the treatment of osteoporosis. The risk of suffering this acute response and its severity is higher after the first intravenous administration and occur less frequently with fewer symptoms in subsequent administrations. The Horizon trial reported an incidence of orbital inflammation associated with the administration of 30% intravenous zoledronate with the first dose, 7% with the second, and 3% with the third dose.[34] Unilateral orbital inflammation was most frequent (89%), but it may be bilateral (11%). Clinical signs and symptoms included palpebral edema (88%), conjunctival congestion (81%), chemosis (79%), ocular pain (77%), ocular motility impairment (65%), proptosis (56%), and blurred vision (39%).

Table 1. Patients' demographic data

Total patients	43
Age (yr), mean ± SD	65.39 ± 9.1
Sex	Female 60% (*n* = 26)
	Male 40% (*n* = 17)
Reason for aminobisphosphonates use	Osteoporosis 56% (*n* = 24)
	Metastasis 21% (*n* = 9)
Type of aminobisphosphonates	Zoledronate 67% (*n* = 29)
	Alendronate 14% (*n* = 6)
	Pamidronate 12% (*n* = 5)
	Risedronate 7% (*n* = 3)

SD, standard deviation

Table 2. Clinical presentation and treatment

Clinical presentation	Unilateral 89% (*n* = 38)
	Palpebral edema 88% (*n* = 38)
	Conjunctival congestion 81% (*n* = 35)
	Chemosis 79% (*n* = 34)
	Ocular pain 77% (*n* = 33)
	Motility impairment 65% (*n* = 28)
	Proptosis 56% (*n* = 24)
	Blurred vision 39% (*n* = 17)
Complications	AION 2.32% (*n* = 1)
Type of treatment	Systemic corticoid 72% (*n* = 31)
	Oral Prednisolone alone 48.83% (*n* = 21)
	Methylprednisolone EV + Oral Prednisolone 23.25% (*n* = 10)
	Solve spontaneously 11.63% (*n* = 5)
	Without data 9.30 (*n* = 4)
	NSAIDs 4.65 % (*n* = 2)
	Topic Prednisolone 2.23% (*n* = 1)

AION, anterior ischemic optic neuritis; NSAIDs, nonsteroids anti-inflammatory drugs

Moreover, 23% of the cases were associated with anterior uveitis. On the contrary, this sign may not be associated with idiopathic orbital inflammation; for that reason, when anterior uveitis develops, physicians may exclude bisphosphonate administration. It is typically non-axial, due to the different structures that could be involved, such as lacrimal gland, extraocular muscles, or intraorbital fat, alone or together. The decrease in visual acuity can be multifactorial. Among the causes, we found corneal keratitis, either because of proptosis or lagophthalmos, dacryoadenitis, due to a decrease in the production of tears; and anterior or posterior uveitis is associated with compressive or ischemic optic neuropathy. A 68-year-old male with metastatic prostate cancer was reported to experience severe complications. He consulted the physician two weeks after the onset of ocular pain and redness. He had visual acuity and visual field deficits because of an AION. Ischemia may have been caused by orbital or ocular inflammation contiguously affecting the posterior ciliary arteries

that supply the optic disc, creating local small-vessel vasculitis. This highlights the importance of applying the timely treatment once symptoms have started.[13]

The mechanism by which these drugs produce inflammation could be related to the presence of a nitrogenous group that rapidly activates monocytes and a subtype of T-cells called gamma-delta, in both *in vitro*[35–38] and *in vivo* conditions.[1, 39] This activation leads to the release of cytokines and inflammatory mediators that produce an acute inflammatory response. Local inflammation is followed by an acute phase of systemic inflammatory response with the presence of symptoms such as fever, pain, nausea, and fatigue in 25% of the patients. It is worth mentioning that all patients who developed a bilateral orbital condition (11%) also had systemic symptoms.

Currently, oral systemic corticosteroids alone or following an intravenous corticosteroid cycle are the treatment of choice, with excellent results in 72% of the patients.[31] The response was effective in all cases; symptoms and CT scan or MRI findings showed complete resolution when the treatment was started seasonally. Delays in treatment are associated with an increased risk of complications.[13] Only a few cases resolve spontaneously or with nonsteroidal anti-inflammatory drugs (NSAIDs), limiting the current information to suggest this type of therapeutic decision. For this reason, these two options may only be considered in mild inflammation without the risk of visual impairment, or in patients with contraindications to corticosteroid treatment.

It has not yet been proven that the treatment of orbital inflammation requires stopping the use of bisphosphonates. Although most of the studies reported the suspension of the antiresorptive drug as treatment, the three cases published that continued with the bisphosphonate but associated with systemic steroids resolved the orbital inflammation without complications.

Thus, we recommend that in the event of mild symptoms of orbital compromise without risk of visual impairment, bisphosphonate treatment could be continued in conjunction with anti-inflammatory treatment. However, in severe orbital inflammation with visual threat or optic neuropathy, bisphosphonates should be discontinued.

SUMMARY

Orbital inflammation caused by aminobisphosphonates is rather infrequent; however, ophthalmologists must recognize this adverse effect secondary to the drug. This condition must be ruled out when orbital inflammation, with or without anterior uveitis is present. Patients' knowledge of the use of these drugs is key to diagnosis. The treatment of choice is the administration of systemic corticosteroids, which are effective in suppressing the inflammatory response with complete resolution when started appropriately. Delayed treatment may be associated with a poor prognosis.

Financial Support and Sponsorship

Nil.

Conflicts of Interest

There are no conflicts of interest.

REFERENCES

1. Olson K, Van Poznak C. Significance and impact of bisphosphonate-induced acute phase responses. *J Oncol Pharm Pract* 2007;13:223–229.
2. Thiébaud D, Sauty A, Burckhardt P, Leuenberger P, Sitzler L, Green JR, et al. An in vitro and in vivo study of cytokines in the acute-phase response associated with bisphosphonates. *Calcif Tissue Int* 1997;61:386–392.
3. Buckler HM, Mercer SJ, Davison, Hollis S, Richardson P, Anderson D. Evaluation of adverse experiences related to pamidronate infusion in Paget's disease of bone. *Ann Rheum Dis* 1998:57;572–572.
4. Dicuonzo G, Vincenzi B, Santini D, Avvisati G, Rocci L, Battistoni F, et al. Fever after zoledronic acid administration is due to increase in TNF-α and IL-6. *J Interferon Cytokine Res* 2003;23:649–654.
5. Reid IR, Gamble GD, Mesenbrink P, Lakatos P, Black DM. Characterization of and risk factors for the acute-phase response after zoledronic acid. *J Clin Endocrinol Metab* 2010;95:4380–4387.
6. Macarol V, Fraunfelder FT. Pamidronate disodium and possible ocular adverse drug reactions. *Am J Ophthalmol* 1994;118:220–224.
7. Mbekeani JN, Slamovits TL, Schwartz BH, Sauer HL. Ocular inflammation associated with alendronate therapy. *Arch Ophthalmol* 1999;117:837–838.
8. Ryan PJ, Sampath R. Idiopathic orbital inflammation following intravenous pamidronate. *Rheumatology* 2001;40:956–957.

9. Subramanian PS, Kerrison JB, Calvert PC, Miller NR. Orbital inflammatory disease after pamidronate treatment for metastatic prostate cancer. *Arch Ophthalmol* 2003;121:1335–1336.
10. Benderson D, Karakunnel J, Kathuria S, Badros A. Scleritis complicating zoledronic acid infusion. *Clin Lymphoma Myeloma* 2006;7:145–147.
11. Phillips PM, Newman SA. Orbital inflammatory disease after intravenous infusion of zoledronate for treatment of metastatic renal cell carcinoma. *Arch Ophthalmol* 2008;126:137–139.
12. Sharma NS, Ooi J-L, Masselos K, Hooper MJ, Francis IC. Zoledronic acid infusion and orbital inflammatory disease. *N Engl J Med* 2008;359:1410–1411.
13. Seth A, Anderson DP, Albiani DA, Barton JJS. Orbital inflammation and optic neuropathy with zoledronic acid for metastatic prostate cancer. *Can J Ophthalmol* 2009;44:467–468.
14. Procianoy F, Procianoy E. Orbital inflammatory disease secondary to a single-dose administration of zoledronic acid for treatment of postmenopausal osteoporosis. *Osteoporos Int* 2010;21:1057–1058.
15. Yang EB, Birkholz ES, Lee AG. Another case of bisphosphonate-induced orbital inflammation. *J Neuroophthalmol* 2010:30:94–95.
16. Missotten G, Verheezen Y. Orbital inflammation after use of zoledronic acid for metastasized prostate carcinoma. *Bull Soc Belge Ophtalmol* 2010;315:23–24.
17. Yeo J, Jafer AK. Zolendronate associated inflammatory orbital disease. *NZ Med J* 2010;1323:50–52.
18. Kaur H, Uy C, Kelly J, Moses AM. Orbital inflammatory disease in a patient treated with zoledronate. *Endocr Pract* 2011;17:e101–e103.
19. Ortiz-Perez S, Fernandez E, Molina JJ, Sanchez-Dalmau B, Navarro M, Corretger X, et al. Two cases of drug-induced orbital inflammatory disease. *Orbit* 2011;30:37–39.
20. Peterson JD, Bedrossian EH. Bisphosphonate-associated orbital inflammation—a case report and review. *Orbit* 2012;31:119–123.
21. Rahimy E, Law SK. Orbital inflammation after zoledronate infusion: an emerging complication. *Can J Ophthalmol* 2013;48:e11–e12.
22. Schwab P, Harmon D, Bruno R, Fraunfelder FW, Kim DH. A 55-year-old woman with orbital inflammation. *Arthritis Care Res* 2012;64:1776–1782.
23. Böni C, Kordic H, Chaloupka K. Bisphosphonate-associated orbital inflammatory disease and uveitis anterior - a case report and review. *Klin Monbl Augenheilkd* 2013;230:367–369.
24. Lefebvre DR, Mandeville JT, Yonekawa Y, Arroyo JG, Torun N, Freitag SK. A case series and review of bisphosphonate-associated orbital inflammation. *Ocul Immunol Inflamm* 2014;25:1–6.
25. Vora MM, Rodgers IR, Uretsky S. Nitrogen bisphosphonate-induced orbital inflammatory disease. *Ophthalmic Plast Reconstr Surg* 2014;30:e84–e85.
26. Pirbhai A, Rajak SN, Goold LA, Cunneen TS, Wilcsek G, Martin P, et al. Bisphosphonate-induced orbital inflammation: a case series and review. *Orbit* 2015;34:331–335.
27. Gonzalez Barlatay J, Hernandez Gauna G, Premoli J, Luis VR, Jorge PE. Orbital inflammation caused by bisphosphonates case report and literature review. *IJOO* 2016;2:148–151.
28. Muruganandam M, Sandhu H. Orbital inflammation secondary to zoledronic acid, a rare presentation. *J Clin Rheumatol* 2016;22:384.
29. Umunakwe OC, Herren D, Kim SJ, Kohanim S. Diffuse ocular and orbital inflammation after zoledronate infusion-case report and review of the literature. *Digit J Ophthalmol* 2017;23:18–21.
30. Tan M, Kalin-Hajdu E, Narayan R, Wong SW, Martin TG. Zoledronic acid-induced orbital inflammation in a patient with multiple myeloma. *J Oncol Pharm Pract* 2019;25:1253–1257.
31. Chehade LK, Curragh D, Selva D. Bisphosphonate-induced orbital inflammation: more common than once thought? *Osteoporos Int* 2019;30:1117–1120.
32. Herrera I, Kam Y, Whittaker TJ, Champion M, Ajlan RS. Bisphosphonate-induced orbital inflammation in a patient on chronic immunosuppressive therapy. *BMC Ophthalmol* 2019;19:51.
33. Keren S, Leibovitch I, Ben Cnaan R, Neudorfer M, Fogel O, Greenman Y, et al. Aminobisphosphonate-associated orbital and ocular inflammatory disease. *Acta Ophthalmol* 2019;97:e792–e799.
34. Black DM, Delmas PD, Eastell R, Reid IR, Boonen S, Cauley JA, et al. Once-yearly zoledronic acid for treatment of postmenopausal osteoporosis. *N Engl J Med* 2007;356:1809–1822.
35. Kunzmann V, Bauer E, Feurle J, Weissinger F, Tony HP, Wilhelm M. Stimulation of γδ T cells by aminobisphosphonates and induction of antiplasma cell activity in multiple myeloma. *Blood* 2000;96:384–392.
36. Gober H-J, Kistowska M, Angman L, Jenö P, Mori L, De Libero G. Human T cell receptor γδ cells recognize endogenous mevalonate metabolites in tumor cells. *J Exp Med* 2003;197:163–168.
37. Roelofs AJ, Jauhiainen M, Mönkkönen H, Rogers MJ, Mönkkönen J, Thompson K. Peripheral blood monocytes are responsible for γδ T cell activation induced by zoledronic acid through accumulation of IPP/DMAPP. *Br J Haematology* 2009;144:245–250.
38. Thompson K, Keech F, McLernon DJ, Vinod K, May RJ, Simpson WG, et al. Fluvastatin does not prevent the acute-phase response to intravenous zoledronic acid in post-menopausal women. *Bone* 2011;49:140–145.
39. Kunzmann V, Bauer E, Wilhelm M. γ/δ T-cell stimulation by pamidronate. *N Engl J Med* 1999;340:737–738.

Perspective

Herpes Zoster Ophthalmicus: A Devastating Disease Coming Back with Vengeance or Finding Its Nemesis?

Michael Tsatsos[1], PhD, FEBOS-CR, MRCOphth; Ioannis Athanasiadis[2], MD, MRCSEd(Ophth)
Athina Myrou[3], MD, PhD; George M Saleh[4], FRCS, FRCOPhth; Nikolaos Ziakas[1], MD, PhD

[1]Department of Ophthalmology, Aristotle University of Thessaloniki, Thessaloniki, Greece
[2]Moorfields Eye Hospital, NHS Foundation Trust at Bedford Eye Clinic, Bedford, UK
[3]1st Propeudeutic Internal Medicine Department, AHEPA University Hospital, Thessaloniki, Greece
[4]National Institute for Health Research Biomedical Research Centre at Moorfields Eye Hospital and the UCL Institute of Ophthalmology, London, UK

ORCID:
Michael Tsatsos: http://orcid.org/0000-0003-1280-4113
Ioannis Athanasiadis: http://orcid.org/0000-0002-6236-7540

Abstract

Herpes zoster ophthalmicus is a frequent, painful, and debilitating condition caused by the reactivation of the varicella-zoster virus alongside the ophthalmic branch of the trigeminal nerve. Twenty-five percent of adults will develop the disease during their lifetime with the risk increasing to one in two over the age of 50. Herpes zoster ophthalmicus presents with a plethora of ocular manifestations ranging from the characteristic rash in the distribution of the ophthalmic branch of the fifth cranial nerve to more severe keratouveitis, disciform keratitis, and even retinal necrosis. Up to 20% of affected patients develop post-herpetic neuralgia which can persist for years after the acute episode, resulting in potentially devastating consequences for the patient's social, financial, and professional circumstances, as well as their quality of life and daily activities. Shingles prevention studies indicated that the herpes zoster vaccine markedly reduces the burden of the disease, as well as the incidence of both infection and post-herpetic neuralgia. Here we review the vaccinations available for herpes zoster, the reasons behind their limited adoption so far, as well as the future perspectives and challenges associated with this debilitating disease in the era of herpes zoster vaccination and coronavirus disease pandemic.

Keywords: Eye; Herpes Zoster; Immunity; Vaccine

J Ophthalmic Vis Res 2022; 17 (1): 123–129

INTRODUCTION

The varicella zoster virus (VZV) is a highly contagious alpha-herpesvirus that causes two separate diseases in humans: varicella (chickenpox) and herpes zoster (HZ, shingles). Varicella is the primary disease and leads to latency of the virus, primarily in peripheral autonomic ganglia including dorsal root ganglia, cranial nerve ganglia such as the trigeminal

Correspondence to:
Ioannis Athanasiadis, MD, MRCSEd(Ophth). Moorfields at Bedford Eye Clinic, Bedford Hospital NHS Trust, Kempston Road, Bedford MK42 9DJ, England.
E-mail: athana1972@yahoo.com

Received: 29-08-2021 Accepted: 18-11-2021

Access this article online

Website: https://knepublishing.com/index.php/JOVR

DOI: 10.18502/jovr.v17i1.10177

How to cite this article: Tsatsos M, Athanasiadis I, Myrou A, Saleh GM, Ziakas N. Herpes Zoster Ophthalmicus: A Devastating Disease Coming Back with Vengeance or Finding Its Nemesis? . J Ophthalmic Vis Res 2022;17:123–129.

ganglion, and autonomic ganglia such as in the enteric nervous system.[1–3]

Herpes zoster is the secondary disease that results from reactivation of the dormant virus, even decades after the initial infection, either spontaneously or secondary to a number of triggering factors. This usually appears as painful or pruritic cutaneous vesicules that occurs in a certain dermatomal distribution pattern, either on the face or on the back [Figure 1]. This viral reactivation occurs mostly with increasing age due to reduced immunity in this population. Triggering factors that can reactivate the virus also involve immunosuppression from disease or drugs, injury, X-ray irradiation, infection, and malignancy. Approximately one in three people will be affected by HZ during their life.[1–3]

Varicella zoster virus-related diseases can lead to serious ocular morbidity, which can range from asymptomatic corneal scars to severe sight impairment and in more advanced cases painful blind eyes. An important and potentially devastating complication of shingles, post-herpetic neuralgia, can persist long after the resolution of the rash and can significantly affect patient's quality of life, especially in the population over the age of 60 where other ocular and systemic comorbidities may be present as well. The economic impact of such a debilitating disease cannot be overlooked; loss of working hours, time off work, patient's frequent need of home care and the chronicity of symptoms, and thus treatment, add further financial burden to an already overstretched healthcare system worldwide.[4] Several treatments exist for herpes zoster, but to be successful need to be applied early on the course of the disease. This in turn led to the development of prevention strategies with vaccines.[1, 5]

Reasons for Limited Introduction of VZV Vaccinations

Although the health and economic benefits associated with prevention of HZ infections are obvious, the introduction of varicella prophylaxis through vaccination has been a matter of controversy. Effective vaccines against varicella and HZ are available; however, there are healthcare systems that are reluctant to introduce routine vaccination because modelling studies have predicted that the reduction in varicella would lead to an increased incidence of HZ cases.[2] The question as to whether the varicella vaccine results to a higher incidence of shingles remains controversial but has gained popularity through the theory of reduced immune response boosting compared to the actual disease. However, this notion is not widely accepted by the scientific community.[1]

Whilst the incidence of zoster is increasing in the United States, this rise began before the varicella vaccine was introduced. Zoster is also increasing in areas where the varicella vaccine is not being used, and this appears to be multifactorial including increased identification of zoster, an aging population, and the ever growing number of immunocompromised patients including those on biological treatments to control a range of diseases.[1]

Cost-effectiveness of HZ vaccine has been previously shown to be favorable and comparable to vaccinations for other diseases, however, the adult coverage remains lower than expected.[6]

The COVID-19 pandemic has led to circular type of governmental measures in an attempt to restrict its distribution in the community. Thus, a number of HZ patients that would seek help from either primary or secondary care, were reluctant to visit their physician in the midst of the pandemic.[7]With the high penetrance of the Delta COVID-19 variant seen in most countries some sort of restriction of movement is here to stay for longer than initially expected, making the case for prevention of any disease a lot more favorable than before.[8]

The Shingles Prevention Study, a randomized, placebo-controlled trial, assessed burden of illness and post-herpetic neuralgia (PHN) incidence in >38,000 people aged ≥60 years who received the live attenuated zoster vaccine or a placebo. Compared with placebo, vaccination significantly reduced the severity of HZ cases as well as the incidence of HZ and PHN. The conclusion was that prophylactic vaccination can positively affect the incidence and course of HZ disease and result in an overall improvement of the patient's quality of life.[5]

Available Vaccinations

Nowadays there are two vaccines available for the prevention of HZ, the live attenuated Zostavax® vaccine (ZVX) first released in 2006 and the

newer adjuvanted HZ subunit Shingrix vaccine (HZsu) becoming available almost a decade later, in 2017.[9]

In 2008, the Advisory Committee on the Immunization Practices (ACIP) of the United States Centers for Disease Control and Prevention (CDC) recommended the routine vaccination with ZVX for all persons older than 60 years with a dose of the vaccine. Those who report a previous episode of zoster as well as people with chronic medical conditions (e.g., diabetes mellitus) could also be vaccinated. There was no need to consider history of varicella (chickenpox) or to conduct serologic testing for varicella immunity before routine administration of zoster vaccine. Zostavax® vaccine vaccination at that time was not recommended for people who have received varicella vaccine (VV) in the past.

However, there was no need to ask about VV history before administering ZVX as those eligible, that have received the VV previously, would have been very few. The specific vaccine was introduced toward the end of the previous decade and very few adults were since then eligible for this. Hence, almost all persons in the age group recommended to have ZVX in 2008 would not have received the VV.

Accordingly, the 2018 ACIP recommendation was that HZsu may be used in adults aged ≥50 years, irrespective of previously receiving varicella vaccine or ZVX. Also screening for a history of chickenpox (varicella) was not required and adults previously affected by herpes zoster should also receive the vaccine as the disease can recur.[10, 11]

The live attenuated vaccine (ZVX) Zostavax® (Merck and Co.) is associated with protection against shingles and PHN in half or more of individuals over 60 years old. Such protection however, wanes over time, starting as early as the first year following immunization and essentially disappearing after eight years. The use of boosters is not recommended in the case of Zostavax®. The safe use of Zostavax® is also not guaranteed in immunocompromised persons due to the higher risk of serious VZV infections.[1] Injection site reactions such as pain, swelling, and erythema occur in >45% of vaccinated people. Headache and more serious adverse events, including hypersensitivity reactions range from uncommon to rare.[12]

In an attempt to find an alternative vaccine offering better protection and ensuring the safety of the immunocompromised patients, a new vaccine, Shingrix, was developed (Glaxo Smith Kline). *This* is a non-live "subunit" recombinant vaccine (HZ/su), made of a truncated form of the VZV glycoprotein E surface antigen, combined with the AS01B Adjuvant System, which enhances the immune response to VZV.[1, 3, 13] The vaccine requires two doses, two to six months apart and provides about 97% protection to healthy persons up to the age of 70 when immunized. It also provides protection against the difficult-to-treat PHN.[1]

HZ/su offers 97% protection against HZ in those aged 50 years or older, including 87% efficacy in those 80 years or older, indicating that the efficacy of HZ/su is not greatly affected by the vaccinated individual's age.[14] It is currently being tested for safety and immunogenicity in immunocompromised patients. The most challenging aspect of Shingrix is that is associated with a higher incidence of side effects for the first few days after immunization, such as local skin reactions at the injection site, fever, and malaise. Serious adverse effects are relatively rare.[1]

Disadvantages and Benefits of Available Vaccinations

Advantages and disadvantages of available vaccination are summarized in Table 1. The live attenuated zoster vaccine boosts VZV-specific cell-mediated immunity in older vaccinated individuals, thereby explaining the efficacy of the vaccine. Despite this, efficacy against HZ is limited to 51% in those vaccinated aged 60 years or older, and decreases as the age at the time of vaccination increases. In addition, the protection by ZVX falls significantly 6–8 years after vaccination. The magnitude and duration of protection have been confirmed by effectiveness studies.[14]

ZOE-50 and ZOE-70 studies concluded that the recombinant zoster vaccine reduced the incidence of HZ by over 90% and PHN by at least 89% in all studied age groups for at least four years after vaccination. Local and systemic reactions were of mild to moderate intensity and transient in nature. The overall safety profile of the vaccine was clinically acceptable.[3]

The public health impact of *Shingrix* vaccination was assessed in a mathematical model, suggesting that in the US, using this vaccine in those ≥50

years of age could prevent 11 to 15 million cases of herpes zoster and 1.6 to 2.1 million cases of PHN. Overall, *Shingrix* recombinant vaccine has a clinically acceptable safety profile and a high efficacy against herpes zoster in adults 50 years of age or older.[3]

Thirty percent of the unvaccinated adults will develop HZ during their life; increasing to 50% in people ≥85 years old. Ophthalmologists worldwide are well aware of the serious HZ-related ophthalmic complications. However, as shown in a large population cohort in Korea, HZ increases the risk of stroke and myocardial infarction, especially in those relatively young who are at less risk for atherosclerosis.[13] Vaccination with *Shingrix* could therefore reduce the incidence and associated costs of herpes zoster and its complications.[3]

Another important aspect of Shingrix vaccine that is of outmost significance during the pandemic is that it has been postulated that Shingrix vaccine may help body's immune system against other infections including 2019 coronavirus disease (COVID-19).[15]

In view of the health challenges caused by the COVID-19 pandemic and its resultant pressure on healthcare systems worldwide and restriction of movement even for elective health visits, any benefit offered would be welcomed. This synergistic and additive beneficial effect could offer added value if possibly the HZ vaccine is given before the COVID-19 vaccine so as to get the maximum benefit.

Future Perspectives

Herpes zoster ophthalmicus is associated with serious sequelae locally and systemically that have severe effects on the patients' quality of life and even lifespan. HZO can lead to complications ranging from periocular and conjunctival involvement to the devastating results of multiple ocular and extraocular manifestations [Figure 2]. Visual compromise can occur in severe and recurrent cases; and cases refractory to treatment are not an uncommon encounter to the anterior segment specialist.[16] Whether vaccination can offer a viable solution to help limit the extent of herpes zoster-related complications needs further scientific evaluation so that to better elucidate exactly what the role of vaccination will be; even if this means that herpes zoster ophthalmic disease could become an essentially subspecialist condition requiring referral to tertiary centers. In order to reach the desirable objective, we feel that collaboration with other specialties, such as otorhinolaryngology and neurology, while dealing with the various HZ manifestations is very desirable and could benefit our patients globally.

Recently, following the COVID-19 pandemic, there was special interest shifted on the relation between HZV and Severe Acute Respiratory Syndrome Coronavirus 2 (SARS-CoV-2), and their respective immunization methods. There were reports that vaccination against COVID-19 as well as the disease itself could lead to reactivation of VZV and recurrence of HZV disease in different dermatomes. This could affect both immunocompetent individuals without risk factors or comorbidity that would contribute to the development of HZ disease and immunocompromised patients with autoimmune inflammatory diseases.[17] Similar observations have been previously made in patients suffering from COVID-19, with an increase in HZ cases during the COVID-19 pandemic, which suggests an association between these diseases.[18] Although this correlation is not well-established, this is a field which will definitely attract attention in the future. Indeed, there are already studies underway looking into the association and measuring the effect of the Shingrix vaccine on the immune system and whether that has any effect on the ability to fight off other infections such as COVID-19.[15] With the accumulation of further data, more definite conclusions can be drawn, and strategies can develop to reduce treatment burdens for patients and the healthcare systems overall.

We are now developing the tools which will allow us to take action in preventing the extent and complications of this potentially debilitating, sight threatening or even life threatening disease. The efficacy of Shingrix has been shown to be higher than the previously available vaccine, reaching levels of 97.2% and 91.3% in adults 50 and 70 years, respectively, whereas the live attenuated virus vaccine (Zostavax) has reached around 55% of efficacy.[13]

In summary, pediatric/adolescent vaccination against varicella zoster has not been described although an increasing number of infections have been described for both herpes simplex as well as herpes zoster in adolescents and young adults.[19, 20] Adult vaccinations prevent

Table 1. Risks and benefits of zoster vaccination

Attributes/Vaccine	Adantages	Disadvantages	Risks/Side effects
ZOSTAVAX	No boosters required Protection against Herpes Zoster and Post-Herpetic Neuralgia	Efficacy against Herpes Zoster limited to 51% in vaccinees ≥60 years of age Efficacy lower as the age at the time of vaccination increases The protection provided by Zoster Vaccine declines significantly at 6–8 years after vaccination	Injection site reactions Erythema Pain Swelling Pruritus Warmth Hematoma Headache Hypersensitivity reactions (including anaphylactic reactions, fever, rash, and lymphadenopathy at the injection site)
SHINGRIX	Protection against Herpes Zoster and Post-Herpetic Neuralgia Reduces incidence of Herpes Zoster by over 90% and post-herpetic neuralgia by at least 89% Efficacy was sustained over at least 4 years after vaccination	Two doses required	Mild to moderate and transient injection site and systemic reactions Fever Malaise Myalgia

Figure 1. Herpes zoster ophthalmicus with typical dermatomal distribution on the face along the first and second branch of the trigeminal nerve.

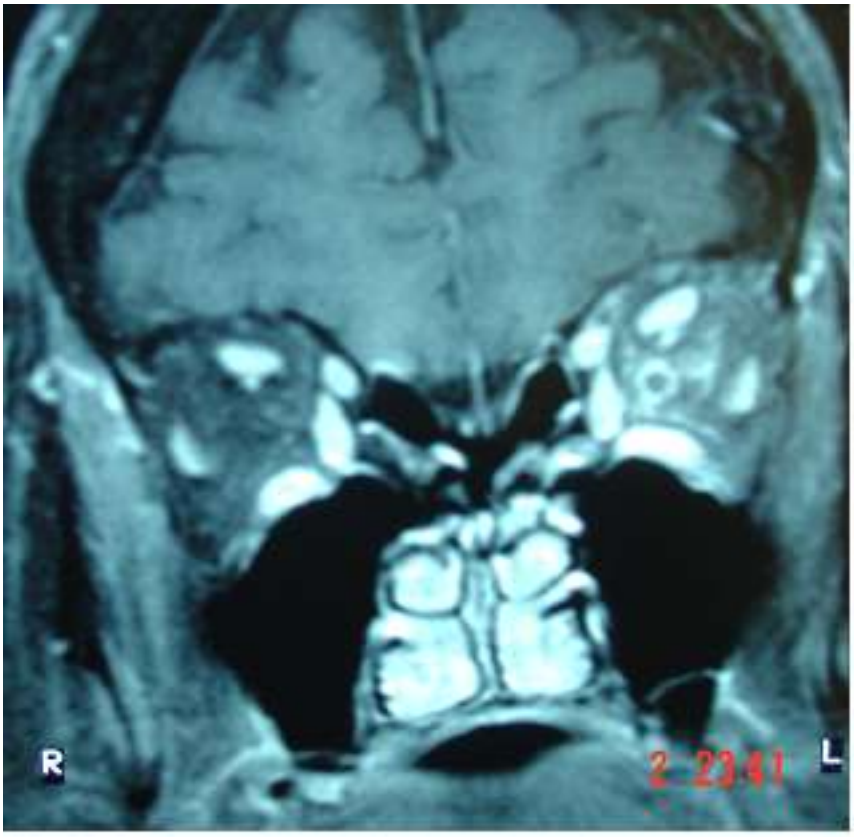

Figure 2. MRI scan depicting characteristic and rare Optic perineuritis resulting from orbital involvement in a patient with Herpes zoster ophthalmicus. Enlargement of extraocular muscles is also obvious on the left side.

morbidity, disability and death and have favorable cost-effectiveness profiles. Efforts to increase the implementation of vaccination in adults and addressing barriers to implementation are needed.[5, 6]

Acknowledgements

George M Saleh was supported by the National Institute for Health Research (NIHR) Biomedical Research Centre based at Moorfields Eye Hospital NHS Foundation Trust and UCL Institute of Ophthalmology. The views expressed are those of the author(s) and not necessarily those of the NHS, the NIHR or the Department of Health.

Declaration of patient consent

The authors certify that they have obtained all appropriate patient consent forms. In the form the patient has given her consent for her images and other clinical information to be reported in the journal. The patient understand that her name and initial will not be published and due efforts will be made to conceal her identity, but anonymity cannot be guaranteed.

Financial Support and Sponsorship

Nil.

Conflicts of Interest

The authors do not have any conflicts of interest. Informed consent allowing the use of face photos for research, publication and teaching has been obtained alongside departmental guidelines.

REFERENCES

1. Kennedy PGE, Gershon AA. Clinical features of Varicella-Zoster virus infection. *Viruses* 2018;10:E609.
2. Wutzler P, Casabona G, Cnops J, Akpo EIH, Safadi MAP. Herpes zoster in the context of varicella vaccination - an equation with several variables. *Vaccine* 2018;36:7072–7082.

3. Lecrenier N, Beukelaers P, Colindres R, Curran D, De Kesel C, De Saegher JP et al. Development of adjuvanted recombinant zoster vaccine and its implications for shingles prevention. *Expert Rev Vaccines* 2018;17:619–634.
4. Harvey M, Prosser LA, Rose AM, Ortega-Sanchez IR, Harpaz R. Aggregate health and economic burden of herpes zoster in the United States: illustrative example of a pain condition. *Pain* 2020;161:361–368.
5. Johnson RW, Bouhassira D, Kassianos G, Leplège A, Schmader KE, Weinke T. The impact of herpes zoster and post-herpetic neuralgia on quality-of-life. *BMC Med* 2010;8:37.
6. Leidner AJ, Murthy N, Chesson HW, Biggerstaff M, Stoecker C, Harris AM et al. Cost-effectiveness of adult vaccinations: a systematic review. *Vaccine* 2019;37:226–234.
7. Stephenson E, Butt DA, Gronsbell J, Ji C, O'Neill B, Crampton N, et al. Changes in the top 25 reasons for primary care visits during the COVID-19 pandemic in a high-COVID region of Canada. *PLoS One* 2021;16:e0255992.
8. Kannan S, Shaik Syed Ali P, Sheeza A. Evolving biothreat of variant SARS-CoV-2 - molecular properties, virulence and epidemiology. *Eur Rev Med Pharmacol Sci* 2021;25:4405–4412.
9. Good CB, Parekh N, Hernandez I. Avoiding rash decisions about zoster vaccination: insights from cost-effectiveness evidence. *BMC Med* 2018;16:238.
10. Harpaz R, Ortega-Sanchez IR, Seward JF, Advisory Committee on Immunization Practices (ACIP) Centers for Disease Control and Prevention (CDC). Prevention of herpes zoster: recommendations of the Advisory Committee on Immunization Practices (ACIP). *MMWR Recomm Rep* 2008;57:1–30.
11. Dooling KL, Guo A, Patel M, Lee GM, Moore M, Belongia EA, et al. Recommendations of the Advisory Committee on Immunization Practices for Use of Herpes Zoster Vaccines. *MMWR Morb Mortal Wkly Rep* 2018;67:103–108.
12. Shapiro M, Kvern B, Watson P, Guenther L, McElhaney J, McGeer A. Update on herpes zoster vaccination: a family practitioner's guide. *Can Fam Physician* 2011;57:1127–1131.
13. Galvis V, Tello A, Carre?o NI, Berrospi RD, Ni?o CA, Rey JJ. Herpes Zoster vaccination: an urgent priority. *Cornea* 2018;37:e57–e58.
14. Weinberg A, Kroehl ME, Johnson MJ, Hammes A, Reinhold D, Lang N, et al. Comparative immune responses to licensed Herpes Zoster vaccines. *J Infect Dis* 2018;218:S81–S87.
15. ClinicalTrials.gov. Training the innate immune system against SARS-CoV-2 (COVID-19) using the Shingrix vaccine in nursing home residents (NH-Shingrix) [Internet]; 2020 Aug 21 [cited 2021 August 2021]. Available from: https://clinicaltrials.gov/ct2/show/results/NCT04523246
16. Athanasiadis I, Konstantinidis A, Papaioannou A, Ioannis Kyprianou I, Georgiadis N. A case of Herpes Zoster Ophthalmicus associated with multiple ocular and extraocular manifestations. *Neuro-Ophthalmology* 2008;32:75–79.
17. Psichogiou M, Samarkos M, Mikos N, Hatzakis A. Reactivation of Varicella Zoster Virus after vaccination for SARS-CoV-2. *Vaccines* 2021;9:572.
18. Maia CMF, Marques NP, de Lucena EHG, de Rezende LF, Martelli DRB, Martelli-J?nior H. Increased number of Herpes Zoster cases in Brazil related to the COVID-19 pandemic. *Int J Infect Dis* 2021;104:732–733.
19. Tsatsos M, MacGregor C, Athanasiadis I, Moschos MM, Hossain P, Anderson D. Herpes simplex virus keratitis: an update of the pathogenesis and current treatment with oral and topical antiviral agents. *Clin Exp Ophthalmol* 2016;44:824–837.
20. Tsatsos M, MacGregor C, Athanasiadis I, Moschos MM, Jameel S, Hossain P et al. Herpes simplex virus keratitis: an update of the pathogenesis and current treatment with oral and topical antiviral agents - comment. *Clin Exp Ophthalmol* 2017;45:932.

Case Report

Treatment of Choroidal Metastasis from Epidermal Growth Factor Mutant Non-Small Cell Lung Cancer with First-line Osimertinib Therapy

Anderson N. Vu[1], MD; Urmi V. Mehta[1,2] BS; Paul Israelsen[1], MD; Sai-Hong Ignatius Ou[3,4], MD, PhD Andrew W. Browne[1,4,5,6], MD, PhD

[1]*Gavin Herbert Eye Institute, Department of Ophthalmology, University of California Irvine, Irvine, CA, USA*
[2]*Western University of Health Sciences, Pomona, CA, USA*
[3]*Chao Family Comprehensive Cancer Center, Division of Hematology-Medical Oncology, Department of Internal Medicine, University of California Irvine, Orange, CA, USA*
[4]*School of Medicine, University of California Irvine, Irvine, CA, USA*
[5]*Institute for Clinical and Translational Sciences, University of California Irvine, Irvine, CA, USA*
[6]*Department of Biomedical Engineering, Henry Samueli School of Engineering, University of California Irvine, Irvine, CA, USA*

ORCID:

Anderson N. Vu: https://orcid.org/0000-0003-0820-0536

Abstract

Purpose: To illustrate the regression of a metastatic lesion through ophthalmic imaging and correlating findings with standard chest imaging and treatment with osimertinib, an oral chemotherapy agent specific to Epidermal Growth Factor Receptor + Non-small Cell Lung Cancer (EGFR+ NSCLC).

Case Report: A 63-year-old Asian male presented to ophthalmology with a complaint of left blurry vision. Initial ophthalmic exam revealed a choroidal lesion and imaging results highlighted a spiculated lung mass with brain and bony metastases. Osimertinib was chosen for its specificity and ability to cross the blood–brain barrier. Follow-up ophthalmic and radiographic imaging were repeated over the course of treatment.

Conclusion: After the initiation of osimertinib, ophthalmic and computed tomography imaging highlighted the regression of the ocular metastatic disease and primary malignancy, respectively.

Osimertinib is an effective first-line treatment of EGFR+ NSCLC and corresponding metastatic sites. Additionally, ophthalmic imaging can be used to monitor general response to chemotherapy agents when ocular metastasis is identified.

Keywords: Carcinoma; Choroidal Neoplasm; Multimodal Imaging; Neoplasm Metastasis; Non-small Cell Lung; Osimertinib

J Ophthalmic Vis Res 2022; 17 (1): 130–134

INTRODUCTION

The choroidal vasculature underlying the retina is the most common site for intraocular metastasis.[1] Visual disturbances may sometimes be the first presenting sign of metastatic disease to the eye. The most common malignancies to metastasize to the choroid are breast, lung, and gastrointestinal tract.[1] Once malignancy is suspected in the eye, prompt characterization is needed to determine therapy targeting the primary lesion and its dissemination. Osimertinib is an irreversible third-generation Epidermal Growth Factor Receptor Tyrosine Kinase Inhibitor (EGFR-TKI) that targets EGFR-TKI sensitizing and T790M resistance mutations and is the standard of care as first-line treatment of Epidermal Growth Factor Receptor + Non-small Cell Lung Cancer (EGFR+ NSCLC).[2–4] We present a case of choroidal metastasis from a primary pulmonary malignancy with full characterization and follow-up using ophthalmic imaging as a clinical endpoint for treatment response to osimertinib.

CASE REPORT

A 63-year-old Asian male presented to ophthalmology clinic with complaint of central blurry vision of the left eye. Past medical history revealed well-controlled type II diabetes mellitus and no past ocular history. Best-corrected visual acuity in both eyes was 20/20, however, the patient reported blurry vision in the left eye. Pupillary responses, confrontational visual field testing, and intraocular pressure were normal.

Initial slit-lamp examination was unremarkable. On detailed funduscopy of the left eye, a non-pigmented choroidal lesion was noted superior to the macula [Figure 1a] with subretinal fluid extending from the tumor into the subfoveal space [Figures 1b & 2a]. Fundus examination of the right eye was normal. Autofluorescence imaging of the left eye showed hyperfluorescence with a mixed or speckled pattern overlying the subretinal lesion [Figure 1b]. Optical coherence tomography (OCT) highlighted an abnormal foveal contour with subretinal fluid in the affected eye [Figure 2a]. B-scan ultrasound on the same visit demonstrated a 6.6 × 6.1 × 2.1 mm lesion in the left eye with heterogenous echogenicity [Figure 2b]. Screening computed tomography of the chest, abdomen, and pelvis highlighted a large 5.0 × 4.3 cm spiculated mass with central necrosis encasing the pulmonary vessels in the right upper lobe of the lung [Figure 3b]. In addition to the mass, enlarged lower paratracheal lymph nodes, lesions on the L4 spinous process, T1 vertebral body, and left adrenal nodule were noted and suspect of metastases.

Histological examination from fine needle aspiration of the lung mass and right lower paratracheal lymph node highlighted atypical cells and adenocarcinoma, respectively. Subsequent positive immunohistochemical staining with NapsinA, TTF- 1, BER-EP4, CK7, and Ki67 confirmed a malignancy of pulmonary origin. Positron emission tomography with Fluorodeoxyglucose (PET-FDG) revealed a right upper lobe pulmonary mass with extension into the right suprahilar region [Figure 3a], right paratracheal and mediastinal lymph node metastases, a 14-mm adrenal nodule, as well as T1 vertebral body, posterior iliac, and left acetabular bony metastases. MRI findings demonstrated a 4-mm enhancement in the left superior frontal gyrus suspect of brain metastases without significant mass effect. Due to the patient's "never- smoking" status, chances of finding a targetable driver mutation were high, and therefore, initiation of chemotherapy was withheld until sequencing was complete. Patient was then started on denosumab 120 mg every four weeks.

Two months after presentation, further ophthalmic work-up revealed gravitated subretinal fluid and decreased acuity of the affected eye (20/60). B-scan ultrasound highlighted an

Correspondence to:

Anderson N. Vu, MD. 837 Health Sciences Rd. Room 2216 Bench #1, Irvine, CA 92617, USA.
Email: andersnv@hs.uci.edu

Received 09-02-2021; Accepted 11-11-2021

Access this article online

Website: https://knepublishing.com/index.php/JOVR

DOI: 10.18502/jovr.v17i1.10178

How to cite this article: Vu AN, Mehta UV, Israelsen P, Ignatius Ou A-H, Browne AW. Treatment of Choroidal Metastasis from Epidermal Growth Factor Mutant Non-Small Cell Lung Cancer with First-line Osimertinib Therapy . J Ophthalmic Vis Res 2022;17:130–134.

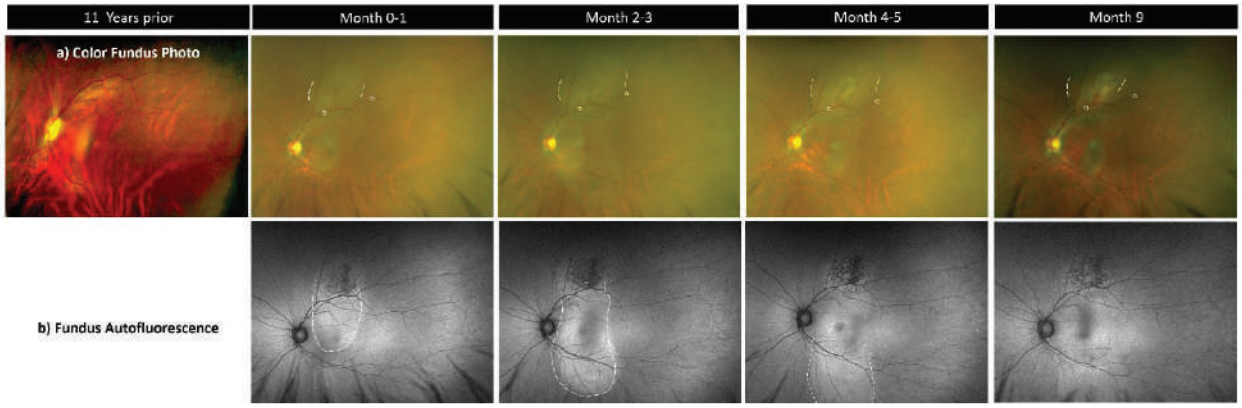

Figure 1. (a) Color fundus photography showing lateral boundaries (dotted lines) of tumor above fovea. White circles are the same bifurcation of vessels in each image. (b) Autofluorescence showing speckled pattern and extent of subretinal fluid (dotted lines).

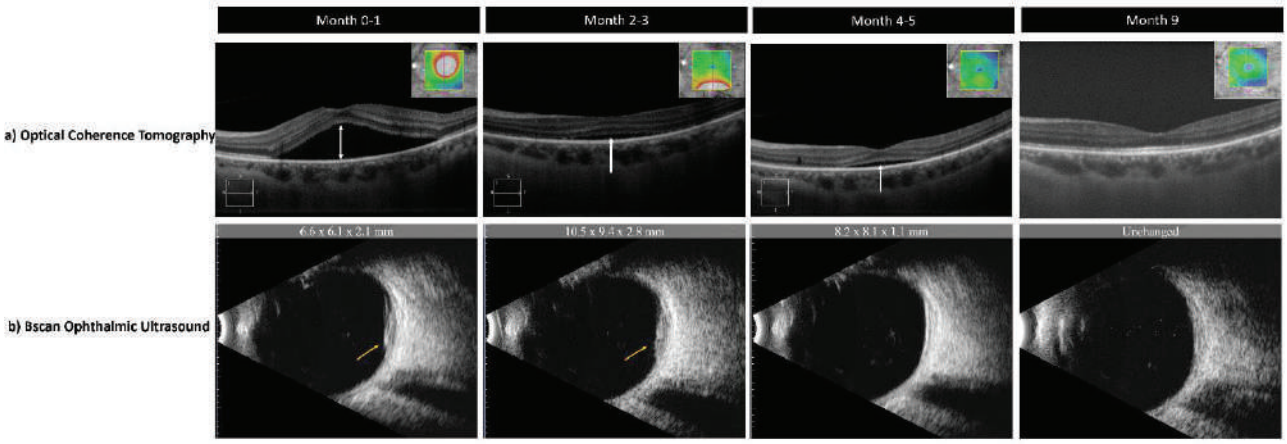

Figure 2. (a) Optical coherence tomography showing resolving subretinal fluid and flattening of retina. (b) Bscan ophthalmic ultrasound showing regression of metastatic lesion.

enlarged growth at 10.5 × 9.4 × 2.8 mm, with OCT showing worsening subfoveal fluid. Next-generation sequencing of the malignancy showed an EGFR pathogenic mutation variant. Patient subsequently began osimertinib 80 mg daily and denied targeted radiation therapy.

One month later, the patient's pin-hole acuity improved to 20/40, with color fundus photography showing an amelanotic choroidal lesion with subretinal fluid that had not grown, B-scan ultrasound showed a smaller mass (8.2 × 8.1 × 1.1 mm), and OCT revealed a flat lesion with decreasing subretinal fluid. A brain MRI highlighted resolution of the left frontal enhancement, while CT scans demonstrated interval decreases of lesions in the right upper lobe of the lung and some bony metastases, though Lesions in the T4 vertebral body and left acetabulum were unchanged.

Patient also exhibited a new 8-mm enhancement of the right hepatic lobe, not seen in earlier imaging. Intravenous chemotherapy was withheld as the interval change was markedly improved with osimertinib therapy alone.

Approximately nine months after diagnosis and daily treatment with oral osimertinib, patient was seen with resolving visual symptoms. Visual acuity of the left eye was correctable to 20/30. Fundus examination and B-scan ultrasound showed a grossly flat retina with no detectable mass and resolved subretinal fluid. OCT also demonstrated similar results. Most recent CT scan showed improved interval changes in the right lung mass and paratracheal lymph nodes, as well as a sclerotic appearance of the bony metastases and hypoattenuation of the previously noted liver enhancement.

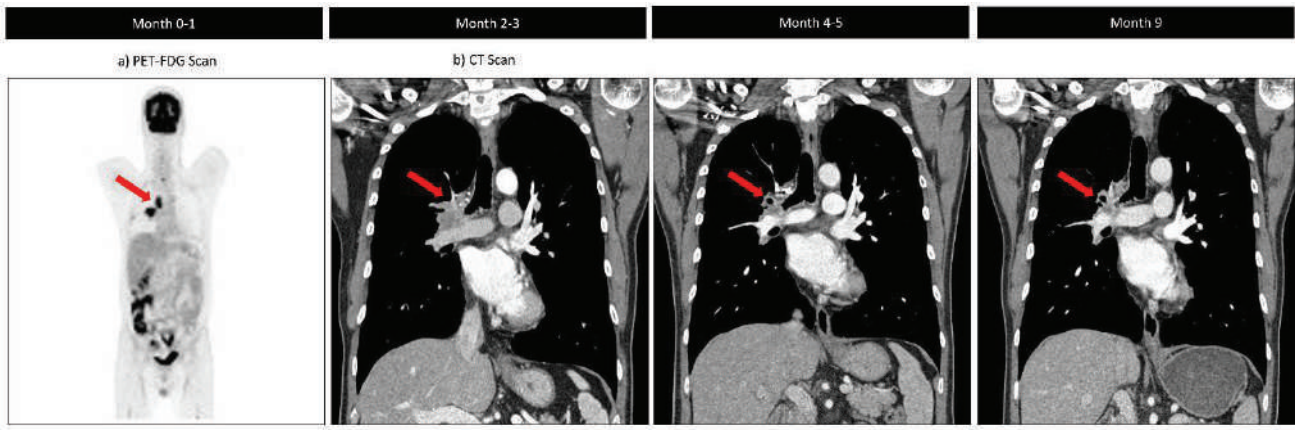

Figure 3. Positron emission and computed tomography showing primary epidermal growth factor receptor + non-small cell lung carcinoma. Osimertinib initiated after two to three month time point.

DISCUSSION

Although ocular metastases are infrequent in lung cancer patients, ocular metastasis of pulmonary adenocarcinoma is less common, as adenocarcinoma spreads to the liver and adrenal glands more commonly.[5] Additionally, the presence of choroidal metastasis may occur in up to 8.4% of primary cases of EGFR + NSCLC.[6] The mean age of diagnosing uveal metastasis is 60 years and blurry or disturbed visual acuity is the most common presenting symptom.[1, 7, 8] In addition to blurry vision, the patient did report mild fatigue and weight loss. Past studies have shown that choroidal metastasis (CM) has a yellow–white discoloration and is highly associated with subretinal fluid.[1] Furthermore, the association of subretinal fluid and CM occurs in approximately 28.4% of patients.[8] If these features are identified, it should initiate prompt investigation for a primary source. In the past, uveal metastasis in lung cancer generally carried a poor prognosis with mean time to death after discovery of 18.4 months in older patients (age 61–80).[7] However, molecular profiling has recently led to improved treatment regimens, where osimertinib has shown increased median overall survival (38.6 months) compared to other EGFR-TKIs gefitinib and erlotinib (31.8 months) in treatment naïve NSCLC.[9] Combinations of both systemic and external beam radiotherapies for CM previously showed lower regrowth rates,[10, 11] but therapies targeting driver mutations spare patients from ophthalmic adverse reactions to therapy, including radiation keratopathy, iris neovascularization and glaucoma, accelerated cataract formation, and optic neuropathy.[12]

Here, we present an informative depiction of the regression of ocular metastasis, where biopsy and next-generation sequencing directed the selection of osimertinib treatment due to its efficacy with EGFR-variant pulmonary adenocarcinoma and ability to penetrate the blood–brain barrier.[3, 4] This case adds to the growing body of evidence highlighting the utilization of molecular profiling to optimally treat choroidal metastasis of EGFR + NSCLC.[13–15] However, in comparison to the some cases of ocular metastases treated with osimertinib, first- or second-generation TKIs were not attempted as first-line, as sequencing led to a more advantageous treatment plan that would spare adverse reactions to intravenous chemotherapy and targeted radiation.[14, 15] Additionally, we comprehensively correlate ophthalmic and systemic radiographic imaging over the time course of treatment to highlight visual symptomatic improvement alongside mass regression that was not described in earlier cases. However, our case also confirms prior experience in the field, where ophthalmic imaging offered a real-time, low-cost, and noninvasive monitoring of ocular metastasis and therapeutic response to newer agents like osimertinib.[13–15]

Ethics approval

This case report was conducted in accordance with the Declaration of Helsinki, data collection and evaluation were conducted in accordance with the

Health Insurance Portability and Accountability Act (HIPAA).

Consent to Participate

Informed consent was obtained from all individual participants included in the study. Consent for publication was obtained according to the ICMJE Recommendations for Protection of Research Participants. The participant has consented to the submission of the case report to the journal.

Financial Support and Sponsorship

Nil.

Conflicts of Interest

There are no conflicts of interest.

REFERENCES

1. Shields CL, Shields JA, Gross NE, Schwartz GP, Lally SE. Survey of 520 eyes with uveal metastases. *Ophthalmology* 1997;104:1265–1276.
2. Yver A. Osimertinib (AZD9291)-a science-driven, collaborative approach to rapid drug design and development. *Ann Oncol* 2016;27:1165– 1170.
3. Gao Z, Wang W, Gu A, Lu J, Huang A, Xiong L, et al. Analysis of the clinical effect of osimertinib on 90 cases with advanced lung adenocarcinoma. *Transl Lung Cancer Res* 2020;9:1464–1471.
4. Wang N, Zhang Y, Mi Y, Deng H, Chen G, Tang Z, et al. Osimertinib for EGFR-mutant lung cancer with central nervous system metastases: a meta-analysis and systematic review. *Ann Palliat Med* 2020;9:80.
5. Milovanovic I, Stjepanovic M, Mitrovic D. Distribution patterns of the metastases of the lung carcinoma in relation to histological type of the primary tumor: an autopsy study. *Ann Thorac Med* 2017;12:191–198.
6. Bouchez C, Pluvy J, Soussi G, Nguenang M, Brosseau S, Tourne M, et al. Epidermal growth factor receptor-mutant non-small cell lung Cancer and Choroidal metastases: long-term outcome and response to epidermal growth factor receptor tyrosine kinase inhibitors. *BMC Cancer* 2020;20:1186.
7. Shields CL, Acaba-Berrocal LA, Selzer EB, Mayro EL, Newman JH, Malik K, et al. Uveal metastasis-based on patient age in 1,111 patients. *Retina* 2018;40:1.
8. Konstantinidis L, Rospond-Kubiak I, Zeolite I, Heimann H, Groenewald C, Coupland SE, et al. Management of patients with uveal metastases at the Liverpool Ocular Oncology Centre. *Br J Ophthalmol* 2014;98:92–98.
9. Ramalingam SS, Vansteenkiste J, Planchard D, Cho BC, Gray JE, Ohe Y, et al. Overall survival with osimertinib in untreated, EGFR-mutated advanced NSCLC. *N Engl J Med* 2020;382:41–50.
10. Jardel P, Sauerwein W, Olivier T, Bensoussan E, Maschi C, Lanza F, et al. Management of choroidal metastases. *Cancer Treat Rev* 2014;40:1119–1128.
11. Shah SU, Mashayekhi A, Shields CL, Walia HS, Hubbard GB 3rd, Zhang J, et al. Uveal metastasis from lung cancer: Clinical features, treatment, and outcome in 194 patients. *Ophthalmology* 2014;121:352–357.
12. Ramos MS, Echegaray JJ, Kuhn-Asif S, Wilkinson A, Yuan A, Singh AD, et al. Animal models of radiation retinopathy – From teletherapy to brachytherapy. *Exp Eye Res* 2019;181:240–251.
13. Mariachiara M, Celeste R, Federico F, Nicole B, Antonio C. Choroidal metastasis from non-small-cell lung cancer responsive to Osimertinib: a case report: efficacy of a third-generation epidermal growth factor tyrosine kinase inhibitor. *Int Ophthalmol* 2018;38:2669–2675.
14. Keshwani K, Roelofs KA, Hay G, Lewis R, Plowman N. Treating choroidal metastases and improving vision with osimertinib in EGFR T790M-mutated lung adenocarcinoma: a case report and review of the literature. *Ocul Oncol Pathol* 2021;7:26–30.
15. Dall'Olio FG, Ruatta C, Melotti B, Sperandi F, Ciardella AP, Ardizzoni A. Response to osimertinib in choroidal metastases from EGFRmt T790M-positive non-small cell lung adenocarcinoma. J Thorac Oncol 2017;12:e165–e167.

Case Report

Coats'-like Response Associated with Linear Scleroderma

Hassan Behboudi[1], MD; Habib Zayeni[2], MD; Asghar Haji-Abbasi[2], MD; Zahra Moravvej[1], MD Ebrahim Azaripour[1], MD; Yousef Alizadeh[1], MD; Reza Soltani-Moghadam[1], MD

[1]*Eye Research Center, Department of Eye, Amiralmomenin Hospital, School of Medicine, Guilan University of Medical Sciences, Rasht, Iran*

[2]*Rheumatology Research Center, Razi Hospital, School of Medicine, Guilan University of Medical Sciences, Rasht, Iran*

ORCID:

Hassan Behboudi: https://orcid.org/0000-0001-9149-9270

Abstract

Purpose: To present a case of linear scleroderma known as "en coup de sabre" associated with Coats'- like response.

Case Report: A 12-year-old boy presented with subacute painless vision loss in the ipsilateral side of the patient's en coup de sabre lesion. Ocular examination revealed vitreous hemorrhage with severe exudation of the posterior pole and telangiectatic vessels. Fundus fluorescein angiography indicated multiple vascular beadings and fusiform aneurysms with leakage which was consistent with a Coats'-like response. The patient was subsequently treated with intravitreal bevacizumab and targeted retinal photocoagulation. Twelve months' follow-up showed marked resolution of macular exudation with significant visual improvement.

Conclusion: Physicians should be aware of the possible ophthalmic disorders accompanying en coup de sabre and careful ophthalmologic examinations should be performed in these patients. As presented in the current case, treatment with intravitreal anti-VEGF agents and laser photocoagulation may be a beneficial option for patients with coats'-like response.

Keywords: Bevcizumab; Coat's Disease; Craniofacial; En Coup de Sabre; Scleroderma

J Ophthalmic Vis Res 2022; 17 (1): 135–139

INTRODUCTION

Linear scleroderma known as "en coup de sabre" (ECDS) is a form of localized scleroderma.[1] The disorder presents with localized facial atrophy of the skin and the underlying tissue particularly in the frontoparietal area.[1] En coup de sabre has been associated with a number of periocular and ocular manifestations. Periocular manifestations include enophthalmos and extraocular muscles and eyelids involvement. Ocular findings such as

Correspondence to:

Hassan Behboudi, MD. Eye Research Center, Department of Eye, Amiralmomenin Hospital, 17 Shahrivar St., Rasht, Guilan 41396-37459, Iran.
E-mail: Behboudi@gums.ac.ir

Received 04-06-2020; Accepted 23-11-2021

Access this article online

Website: https://knepublishing.com/index.php/JOVR

DOI: 10.18502/jovr.v17i1.10179

How to cite this article: Behboudi H, Zayeni H, Haji-Abbasi A, Moravvej Z, Azaripour E, Alizadeh Y, Soltani-Moghadam R. Coats'-like Response Associated with Linear Scleroderma. J Ophthalmic Vis Res 2022;17:135–139.

corneal alterations, cataract, iritis, and iris atrophy have also been reported.[2, 3] We report a case of ECDS presenting with decreased vision in the ipsilateral eye diagnosed as a Coats'-like response.

CASE REPORT

A 12-year-old boy noticed painless vision loss in his left eye several days before. There was no history of visual disturbances and no family history of significant ocular disorders. He did not report any previous trauma and prior use of any medication. On physical examination, linear depressed scarring of the cutaneous and subcutaneous tissue of the left frontoparietal area was noted. This atrophic band of skin extended from the left eyebrow to the frontoparietal scalp [Figure 1]. His best-corrected visual acuity (BCVA) was 20/20 in the right eye and 20/200 in the left eye. The size of pupils was normal and there was no afferent pupillary defect. Ocular motility was within normal range. The intraocular pressure by applanation tonometry was 14 mmHg in both eyes. On slit lamp examination, the anterior segment was normal in both eyes. Funduscopy of the left eye showed vitreous hemorrhage with severe exudation in the posterior pole and telangiectatic vessels and saccular aneurysms in the mid-peripheral and peripheral retina. The optic disc was normal. The right fundus examination was unremarkable. Para-clinical evaluations with spectral-domain optical coherence tomography (SD-OCT) and fundus fluorescein angiography (FFA) were performed. SD-OCT of the left macula revealed intraretinal fluid and marked exudates [Figure 2]. FFA demonstrated vascular tortuosity and multiple beading and fusiform aneurysms with distinct leakage in the mid-peripheral and peripheral regions. Areas of capillary nonperfusion with no neovascularization were noted. The fundus findings were compatible with Coats'-like response. Corresponding rheumatologic consultation diagnosed his atrophic skin lesion as "en coup de sabre" (ECDS) a form of craniofacial linear scleroderma. Further examinations did not show any neurological signs or systemic involvement of scleroderma. Laboratory tests for antinuclear, anti-centromer, and Scl70 antibodies, erythrocyte sedimentation rate, and blood composition were normal.

The patient was scheduled for three monthly intravitreal injections of 1.25 mg/0.05 ml bevacizumab. On follow-up examinations, there was a significant decrease in macular exudation and vitreous hemorrhage. Targeted laser photocoagulation was performed over the abnormal retinal vasculature. Macular SD-OCT demonstrated significant reduction of intraretinal fluid and exudates [Figure 3]. At 12-month follow-up examination, BCVA improved to 20/25 in the left eye. Fundus examination and repeated FFA showed moderate resolution of vascular beading and tortuosity with no evidence of peripheral neovascularization [Figure 4]. The patient was scheduled for ophthalmic visits every three months. After one year of follow-up, we noted a loss of visual acuity (BCVA: 20/32) and moderate recurrence of macular edema and exudation. The patient was subsequently treated with one session of intravitreal injection of 1.25 mg/0.05 ml bevacizumab. He is currently under routine ophthalmic and rheumatologic observation.

DISCUSSION

Craniofacial linear scleroderma known as "en coup de sabre" (ECDS) presents with contraction and stiffness of the frontal or parieto-frontal area forming a depressed lesion in the skin and subcutaneous tissue.[1] Various etiologies including trauma, radiotherapy, and autoimmunity have been proposed.[4] En coup de sabre usually affects children in the first decade and is predominantly seen in females.[5] Ocular manifestations is not common in localized scleroderma, however, it has been reported to occur in 14% of the patients with ECDS.[3] Eyelid and adnexal involvement are the most common periocular abnormalities. Also, anterior segment inflammation is reported as the most frequent ocular manifestation.[3]

In the present case, a boy with ECDS presented with ipsilateral vision loss. The specific clinical picture and FFA were in favor of a Coats'-like response which refers to a fundus with the similar clinical appearance of Coats' disease in the setting of other ocular or systemic disorders. Coats disease is defined as idiopathic retinal light bulb telangiectasias with intraretinal and/or subretinal exudation without appreciable retinal or vitreal traction.[6] The pathogenesis is believed to be related to the breakdown of blood–retinal barrier due to changes at the endothelial level and the presence of abnormal pericytes.[7]

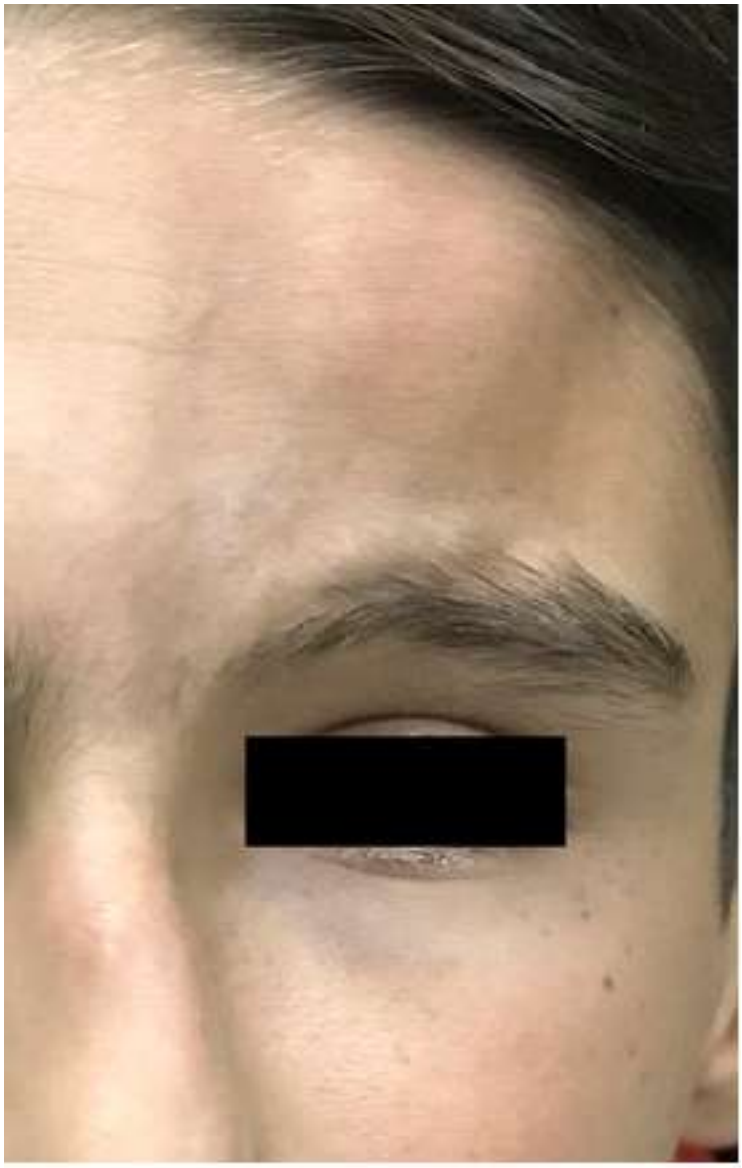

Figure 1. Photograph of the patient showing depressed left forehead skin lesion (en coup de sabre).

To the best of our knowledge, there have been only five previous reports of this Coats'-like response in patients with ECDS.[8–12] One of them resulted in exudative retinal detachment and severe vision loss in early childhood.[8] Unlike previous reports, our patient regained nearly normal vision following appropriate treatment. We believe that treatment with intravitreal anti-VEGF agents and/or laser photocoagulation may be beneficial for patients with Coats' like response. This treatment may halt or at least delay progression of the retinal abnormalities.

It is of value to mention progressive hemifacial atrophy (Parry–Romberg syndrome) which is a hemifacial atrophy mainly below the forehead with an unknown etiology.[13] Overlapping features of ECDS and ipsilateral hemifacial atrophy have been described in literature and it is thought that they may lie on the same spectrum.[13] Coats'-like response has been reported in a number of cases with progressive hemifacial atrophy.[14] The exact cause of this association remains undetermined; however, several theories have been suggested regarding the pathogenesis of scleroderma. The subclinical occlusive vasculitis can be caused by an inflammatory process with a probable autoimmune basis.[15] Vascular abnormalities such as endothelial cells loss, increased vascular permeability, and defective angiogenesis have been recognized in linear

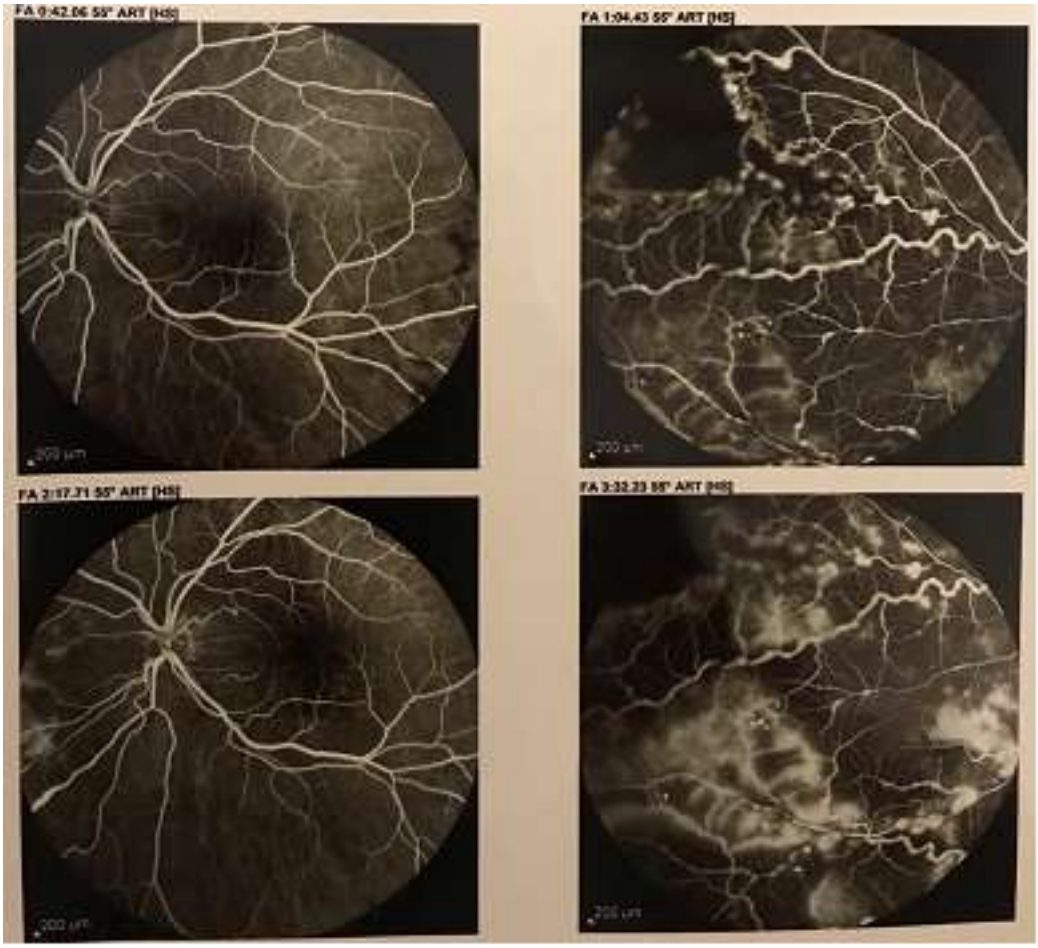

Figure 2. Fundus fluorescein angiography. Vascular tortuosity and fusiform aneurysms with leakage and non-perfusion areas in the mid-peripheral and peripheral regions.

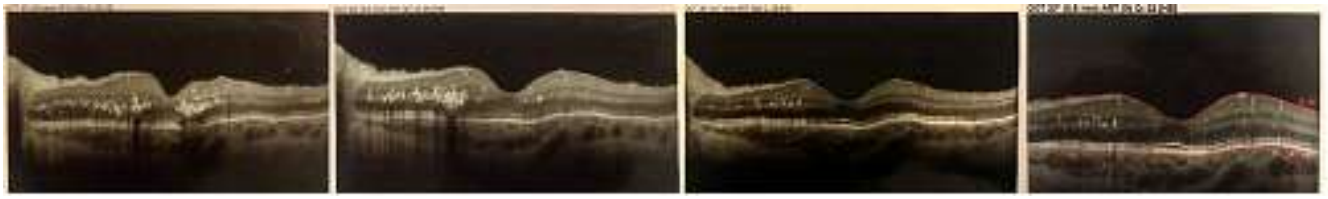

Figure 3. Macular optical coherence tomography at baseline, 3-month, 8-month, and 12-month visits (from left to right).

scleroderma.[16] It is hypothesized that systemic endothelial cell injury leads to the production of IFNα and subsequent tissue hypoxia and expression of VEGF.[15] Intracranial vascular abnormalities have also been reported in patients with linear scleroderma. Gunness et al described an ipsilateral brain cavernoma in a patient with localized scleroderma on the frontal side of scalp.[17]

We presume that the vascular, inflammatory, and immunological processes involved may explain the vascular telangiectasia, dilatation, and leakage observed in Coats'-like response. Previous literature and the present case suggest that eyes as well as brain can be affected by linear scleroderma, which is commonly known as a limited skin disorder. Accordingly, we advise routine ophthalmologic examination including dilated funduscopy every three to four months in the first three years of presentation in patients with ECDS. Also, those presenting with visual complaints should be examined promptly. Pediatricians, dermatologists, and rheumatologists should be aware of the

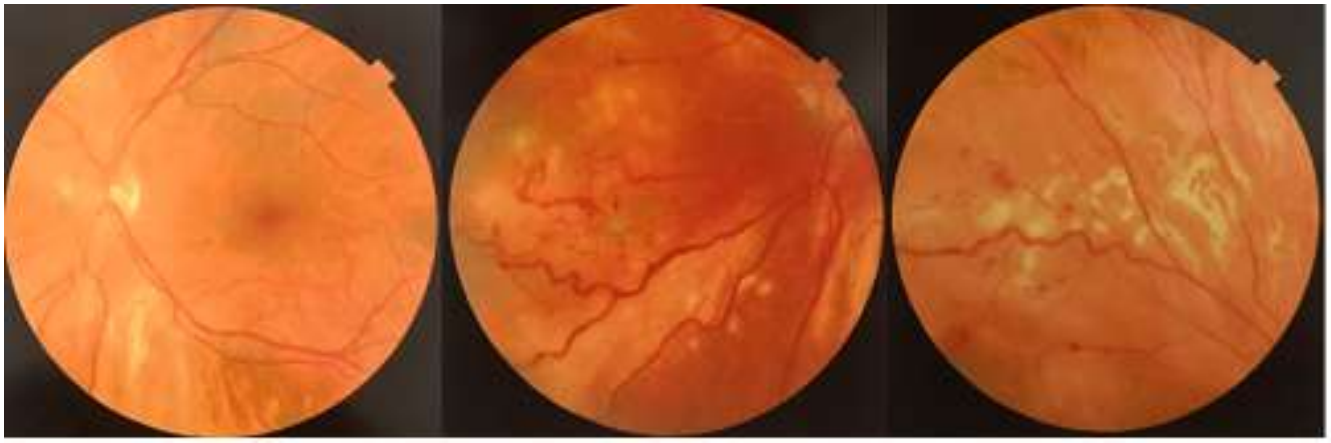

Figure 4. Fundus photograph at 12-month, showing reduced vascular tortuosity and beading.

possible ophthalmic disorders associated with ECDS.

Financial Support and Sponsorship

Nil.

Conflicts of Interest

There are no conflicts of interest.

REFERENCES

1. Careta MF, Romiti R. Localized scleroderma: clinical spectrum and therapeutic update. *An Bras Dermatol* 2015;90:62–73.
2. Segal P, Jablonska S, Mrzyglod S. Ocular changes in linear scleroderma. *Am J Ophthalmol* 1961;51:807–813.
3. Zannin ME, Martini G, Athreya BH, Russo R, Higgins G, Vittadello F, et al. Ocular involvement in children with localised scleroderma: a multi-centre study. *Br J Ophthalmol* 2007;91:1311–1314.
4. Peña-Romero AG, García-Romero MT. Diagnosis and management of linear scleroderma in children. *Curr Opin Pediatr* 2019;31:482–490.
5. Orozco-Covarrubias L, Guzman-Meza A, Ridaura-Sanz C, Carrasco Daza D, Sosa-de-Martinez C, Ruiz-Maldonado R. Scleroderma 'en coup de sabre'and progressive facial hemiatrophy. Is it possible to differentiate them? *J Eur Acad Dermatol Venereol* 2002;16:361–366.
6. Sen M, Shields CL, Honavar SG, Shields JA. Coats disease: an overview of classification, management and outcomes. *Indian J Ophthalmol* 2019;67:763.
7. Recchia FM, Capone A. Coats' disease. In: Reynolds J, Olitsky S, editors. Pediatric retina. Berlin, Heidelberg: Springer; c2011. 235–243 p.
8. Fledelius HC, Danielsen PL, Ullman S. Ophthalmic findings in linear scleroderma manifesting as facial en coup de sabre. *Eye* 2018;32:1688.
9. George MK, Bernardino CR, Huang JJ. Coats-like response in linear en coup de sabre scleroderma. *Retin Cases Brief Rep* 2011;5:275–278.
10. Holl-Wieden A, Klink T, Klink J, Warmuth-Metz M, Girschick H. Linear scleroderma 'en coup de sabre'associated with cerebral and ocular vasculitis. *Scand J Rheumatol* 2006;35:402–404.
11. Lenassi E, Vassallo G, Kehdi E, Chieng AS, Ashworth JL. Craniofacial linear scleroderma associated with retinal telangiectasia and exudative retinal detachment. *J AAPOS* 2017;21:251–254.
12. Neki A, Sharma A. Ipsilateral Coat's reaction in the eye of a child withen coup de sabre morphoea-a case report. *Indian J Ophthalmol* 1992;40:115.
13. El-Kehdy J, Abbas O, Rubeiz N. A review of Parry-Romberg syndrome. *J Am Acad Dermatol* 2012;67:769–784.
14. Bucher F, Fricke J, Neugebauer A, Cursiefen C, Heindl LM. Ophthalmological manifestations of Parry-Romberg syndrome. *Surv Ophthalmol* 2016;61:693–701.
15. Fleming JN, Nash RA, Mahoney WM, Schwartz SM. Is scleroderma a vasculopathy? *Curr Rheumatol Rep* 2009;11:103–110.
16. Zulian F, Vallongo C, Woo P, Russo R, Ruperto N, Harper J, et al. Localized scleroderma in childhood is not just a skin disease. *Arthritis Rheum* 2005;52:2873–2881.
17. Gunness VRN, Munoz D, González-López P, Alshafai N, Mikhalkova A, Spears J. Ipsilateral brain cavernoma under scleroderma plaque: a case report. *Pan Afr Med J* 2019;32:13.

Case Report

Peripapillary Capillary Network in Methanol Induced Optic Neuropathy

Kiana Hassanpour[1,2], MD, MPH; Negin Mohammadi[1], MD; Hamideh Sabbaghi[3,4], PhD; Alireza Amirabadi[1], MD Mohammad Pakravan[1], MD

[1]*Ophthalmic Research Center, Research Institute for Ophthalmology and Vision Science, Shahid Beheshti University of Medical Sciences, Tehran, Iran*
[2]*Department of Ophthalmology, Imam Hossein Hospital, Shahid Beheshti University of Medical Sciences, Tehran, Iran*
[3]*Ophthalmic Epidemiology Research Center, Research Institute for Ophthalmology and Vision Science, Shahid Beheshti University of Medical Sciences, Tehran, Iran*
[4]*Department of Optometry, School of Rehabilitation, Shahid Beheshti University of Medical Sciences, Tehran, Iran*

ORCID:
Mohammad Pakravan: https://orcid.org/0000-0002-5421-0359
Kiana Hassanpour: https://orcid.org/0000-0002-1788-7352

Abstract

Purpose: To present the optical coherence tomography angiography (OCT-A) findings of the radial peripapillary capillary (RPC) network in an individual with severe bilateral methanol-induced toxic optic neuropathy (MTON) in comparison to a normal subject and a patient with retinitis pigmentosa.

Case Report: A 35-year-old man with severe bilateral MTON was referred to the neuro-ophthalmology clinic at the Labbafinejad Medical Center. The Angio Vue OCT 3D set of 4.5 × 4.5 mm was used to measure the disc and peripapillary vessel density. Two subjects were examined with the same protocol as controls to determine the effect on the RPC vessel density in multiple scenarios. One of the controls was a healthy individual with the prerequisite matches of age and sex while the second one was a known retinitis pigmentosa (RP) patient. RPC density was measured as 37.7 in the patient with MTON, 46.9 in the RP patient, and 54.7 in the healthy control.

Conclusion: The reduction in the RPC vessel density in a patient with MTON compared to that of a healthy individual and also a patient with RP may be due to the loss of capillaries secondary to the loss of nerve fibers and ganglion cells. Moreover, MTON can be considered an optic neuropathy with direct mitochondrial damage to the endothelial cells of the capillaries.

Keywords: Methanol-induced Toxic Optic Neuropathy; Optical Coherence Tomography Angiography; Radial Peripapillary Capillary Network

J Ophthalmic Vis Res 2022; 17 (1): 140–145

INTRODUCTION

Methanol poisoning could be caused by drinking homemade alcoholic beverages.[1] Patients who survive this life-threatening condition may also suffer other morbidities including methanol-induced toxic optic neuropathy (MTON).[2] Formic Acid, a metabolite of methanol can result in acute retinal ganglion cells injury and edema of the optic nerve. The presence of the intraretinal fluid revealed in the optical coherence tomography (OCT) reports could present an argument for the role of vessel injury as one of the plausible culprits in the pathophysiology of the disease, MTON. Nurieva et al showed a progressive and chronic loss of those axons that survived after methanol poisoning which supports the aforementioned hypothesis.[3] Due to the rarity of these cases, studies are scarce and the exact mechanism behind the progressive axonal loss remains unknown.

To examine retinal vascularity in MTON, fluorescein angiography (FA) is not always feasible because of the concurrent poor general status and high prevalence of renal insufficiency in these patients. Optical coherence tomography angiography (OCT-A) as a noninvasive novel technique for visualization of vascular flow is viable and provides high-resolution images of both retinal and radial peripapillary capillaries.[4] In this report, we present the OCT-A findings of the radial peripapillary capillary (RPC) network in an individual with severe bilateral MTON.

CASE REPORT

A 35-year-old man with the chief complaint of bilateral decreased visual acuity following the ingestion of a homemade alcoholic beverage two weeks prior was referred to us. He had been in a coma for two days and had undergone hemodialysis twice during the acute phase. He had previously received the protocol suggested by the author (MP) that included erythropoietin and intravenous steroid.[2, 6] Visual loss was detected after the improvement of consciousness. When we first saw him, visual acuity was counting fingers at 30 cm in the right eye and no light perception (NLP) in the left eye. Trace afferent pupillary defect was detected in the left eye. The anterior segment slit-lamp biomicroscopy and Goldmann applanation tonometry results were normal. In the funduscopy, the optic nerves were mildly swollen. Macula and retinal periphery tests were normal bilaterally. The perimetry test was not possible to execute.

The OCT-A was performed using XR Avanti Angio Vue OCTA (Optovue Inc., Fermont, CA, USA). The Angio Vue OCT 3D set of 4.5× 4.5 mm was used to measure disc and peripapillary vessel density. For vessel analysis, a slab between the outer limit of the retinal nerve fiber layer (RNFL) and the internal limiting membrane was made. Two regions of interest (ROI) were defined for measuring vessel density within the area occupied by the vessels. Two elliptical contour lines were used first for defining the disc area which was determined manually and second for corresponding to a peripapillary area with a width of 0.75 mm from the first elliptical line. Two subjects were examined with the same protocol as controls. One of the controls was a healthy individual with the matching prerequisites of age and sex while the second one was a known patient with a history of retinitis pigmentosa (RP), which started from early adulthood and visual acuity of counting fingers at 4 m in both eyes. In examination of the RP patient, it was revealed that he had optic pallor in both eyes as well as arterial narrowing, diffuse retinal degeneration, and peripheral bone spicules.

Capillary peripapillary vessel density was 37.7% in the MTON patient, 46.9% in the RP patient, and 54.7% in the healthy control. Figure 1 shows the OCT-A images of all three cases. In the MTON case, measurements of the OCT-A Angio Vue vessel analysis were all lower, as compared to that of the

Correspondence to:

Mohammad Pakravan, MD. Department of Ophthalmology, Labbafinejad Medical Center, Paidarfard St., Boostan 9 St., Pasdaran, Tehran 16666Iran.
E-mail: Mohpakravan@gmail.com

Received 21-01-2020; Accepted 22-09-2021

Access this article online

Website: https://knepublishing.com/index.php/JOVR

DOI: 10.18502/jovr.v17i1.10180

How to cite this article: Hassanpour K, Mohammadi N, Sabbaghi H, Amirabadi A, Pakravan M. Peripapillary Capillary Network in Methanol Induced Optic Neuropathy . J Ophthalmic Vis Res 2022;17:140–145.

Table 1. Peripapillary OCT-A parameter in MTON, RP, and healthy control

Variables		MTON vessel density (%)		RP vessel density (%)		Healthy control vessel density (%)	
		Capillaries	All	Capillaries	All	Capillaries	All
Whole image	OD	38.4	45.5	45.7	49.5	50.1	56.5
	OS	37.1	43.6	44.7	48	49.9	56.6
Inside disc	OD	39.4	51	39.7	50	45.2	54.7
	OS	34.6	44.5	44.4	53.2	47.0	57.8
Peripapillary	OD	37.7	44.9	46.9	50.2	54.7	60.6
	OS	36	43.3	42.3	45.1	54.1	60.5
Superior hemifield	OD	36.5	44.2	46.9	50.2	54.8	60.9
	OS	39.1	46	39.7	41.9	53.5	61.2
Inferior hemifield	OD	39	45.5	47	50.1	54.5	60.2
	OS	32.7	41.3	45.1	48.5	54.8	59.7
Nasal	OD	34		47		52	
	OS	32		47		63	
Temporal	OD	51		52		54	
	OS	27		41		47	

MTON, methanol-induced toxic optic neuropathy; RP, retinitis pigmentosa

controls [Table 1]. Peripapillary OCT in the patient with MTON revealed an average RNFL thickness of 148 microns in the right eye and 140 microns in the left eye.

DISCUSSION

In this case report, we described the findings of the peripapillary OCT-A in a case of MTON. We discovered the reduction in the RPC vessel density two weeks after the MTON situation was compared to a healthy individual and also to a patient with optic pallor secondary to RP. The possible mechanism explaining the reduced vascular density may be the loss of capillaries secondary to the loss of nerve fibers and ganglion cells.[5] Loss of RNFL and the ganglion cell layer (GCL) happens as a result of two separate mechanisms. Formic acid which is a toxic metabolite produced after methanol ingestion directly enters the ganglion cells and causes severe structural and functional damage. Ganglion cell damage then results in nerve fiber loss. Moreover, the edema subsequent to RNFL damage may cause a compartment syndrome.[6]

Various studies investigating OCT-A in different optic neuropathies reported a reduction of peripapillary vessel density, for example, in non-arteritic anterior ischemic optic neuropathy (NAION),[7] optic neuritis,[8] optic atrophy secondary to retinal dystrophies,[9] thyroid eye disease,[10] vitamin deficiency,[11] or Leber hereditary optic neuropathy (LHON).[12] Two possible mechanisms may explain peripapillary vessel density reduction in different optic neuropathies. First, any diseases causing axonal loss leads to reduced metabolic need in the RNFL layer and consequently reduces capillaries through autoregulatory mechanisms.[5] The next mechanism is the direct injury of the capillaries by the acquired disease. While the former is thought to be more prominent in vessel dropouts, the latter can also be highlighted in optic neuropathies with mitochondrial damages such as with LHON which can also have a direct adverse impact on vascular endothelial and vascular smooth muscle cells viability.[13]

Examining both eyes of the patient, the eye with more severe visual loss showed lower vessel density in all four quadrants. RNFL thickness cannot be a reliable measure in the acute phase,

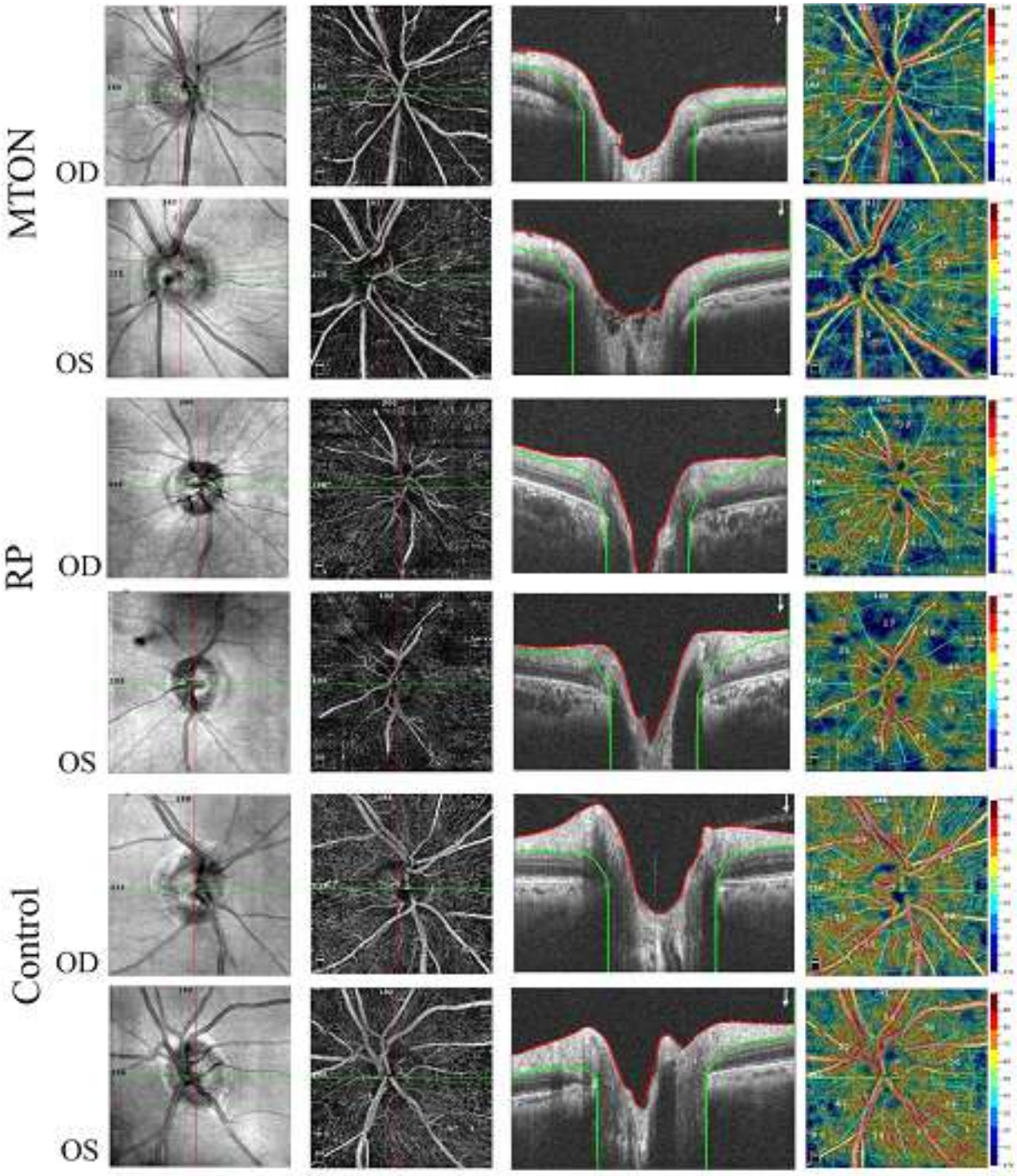

Figure 1. Peripapillary OCT-A images in MTON compared to RP and a healthy individual. From left to right, SLO images, En-face OCT-A (ILM-NFL), corresponding B-scan, vessel density map in MTON, RP patient, and a healthy control. Vessel density analysis has been done between two slabs shown in B-scans.

however, the thickness was slightly higher in the right eye (148 and 140 in the right and left eyes, respectively). Previous reports confirmed the accordance of peripapillary vessel dropout and RNFL loss in different acute and chronic optic neuropathies including glaucoma and non-arteritic ischemic optic neuropathy (NAION),[8, 14] so lower temporal vessel density can indicate higher axonal damage in this important area.

In MTON, formate toxicity inhibits the mitochondrial function through inhibition of the cytochrome oxidase system. Production of

reactive oxygen species and toxic aldehydes exacerbate mitochondrial damage.[15] Therefore, MTON can be considered an optic neuropathy with both direct mitochondrial damage of endothelial cells of capillaries and secondary autoregulatory reduction of peripapillary vessels. Another striking finding in our patient was the lower vessel density in the temporal quadrant of the NLP eye; this finding could strengthen the hypothesis of direct mitochondrial damage of the vessels in the event of methanol poisoning. RNFLs of the papillomacular bundle which is directly responsible for central visual acuity contain more vulnerable and smaller fibers. Previous studies confirmed the order of RNFL involvement in Leber hereditary optic neuropathy (LHON), a disease of mitochondrial involvement, first affects the temporal quadrant and lastly the nasal quadrant.[16]

In RP, vascular damage is the early event and optic neuropathy can be considered as a secondary event resulting from peripapillary vessel attenuation and photoreceptor degeneration.[9] In our RP patient, optic pallor was obvious, yet the vessel density was higher in all quadrants as compared to the MTON patient. Although the lower RP vessel density compares to the MTON in only one case which might not be conclusive, it could imply that both mechanisms are connected in MTON. In other words, RNFL, GCL, and vascular endothelial cell destruction together accentuate the damage of vessels and these could explain why RPC vessel dropout is more severe in MTON.

OCT-A is a safe and fast method to evaluate retinal vessels in survivors of methanol poisoning in whom FA may be contradicted. Spaide et al comparing FA and OCT-A in 12 patients with different optic neuropathies concluded OCT-A outperforms FA in the visualization of the precapillary network.[17] Moreover, the quantitative measurement of ONH vessels is possible with OCT-A rather than FA. Nevertheless, many patients with NLP cannot be evaluated by OCT-A as a result of poor fixation.

In conclusion, MTON as a rare and devastating optic neuropathy can be further evaluated by OCT-A. Our report demonstrated a reduction in RPC vessel density for the first time. Future studies are needed to confirm our findings in a series of patients.

Acknowledgment

This article is taken from the disease registry, titled “The Iranian National Registry of Inherited Retinal Dystrophy (IRDReg®)” and code number of IR.SBMU.ORC.REC.1396.15 from the ethic committee, that was supported by the deputy of research and technology in Shahid Beheshti University of Medical Sciences (http://dregistry.sbmu.ac.ir).

Financial Support and Sponsorship

Nil.

Conflicts of Interest

There are no conflicts of interest.

REFERENCES

1. Massoumi G, Saberi K, Eizadi-Mood N, Shamsi M, Alavi M, Morteza A. Methanol poisoning in Iran, from 2000 to 2009. *Drug Chem Toxicol* 2012;35:330–333.
2. Pakravan M, Sanjari N. Erythropoietin treatment for methanol optic neuropathy. *J Neuroophthalmol* 2012;32:325–328.
3. Nurieva O, Diblik P, Kuthan P, Sklenka P, Meliska M, Bydzovsky J, et al. Progressive chronic retinal axonal loss following acute methanol-induced optic neuropathy: four-year prospective cohort study. *Am J Ophthalmol* 2018;191:100–115.
4. Akil H, Falavarjani KG, Sadda SR, Sadun AA. Optical coherence tomography angiography of the optic disc; an overview. *J Ophthal Vis Res* 2017;12:98.
5. Falavarjani KG, Tian JJ, Akil H, Garcia GA, Sadda SR, Sadun AA. Swept-source optical coherence tomography angiography of the optic disk in optic neuropathy. *Retina* 2016;36:S168–S77.
6. Pakravan M, Esfandiari H, Sanjari N, Ghahari E. Erythropoietin as an adjunctive treatment for methanol-induced toxic optic neuropathy. *Am J Drug Alcohol Abuse* 2016;42:633–639.
7. Sharma S, Ang M, Najjar RP, Sng C, Cheung CY, Rukmini AV, et al. Optical coherence tomography angiography in acute non-arteritic anterior ischaemic optic neuropathy. *Br J Ophthalmol* 2017;101:1045–1051.
8. Chen JJ, AbouChehade JE, Iezzi Jr R, Leavitt JA, Kardon RH. Optical coherence angiographic demonstration of retinal changes from chronic optic neuropathies. *Neuroophthalmology* 2017;41:76–83.
9. Mastropasqua R, Borrelli E, Agnifili L, Toto L, Di Antonio L, Senatore A, et al. Radial peripapillary capillary network in patients with retinitis pigmentosa: an optical coherence tomography angiography study. *Front Neurol* 2017;8:572.

10. Zhang T, Xiao W, Ye H, Chen R, Mao Y, Yang H. Peripapillary and macular vessel density in dysthyroid optic neuropathy: an optical coherence tomography angiography study. *Invest Ophthalmol Vis Sci* 2019;60:1863–1869.
11. Pellegrini F, Prosdocimo G, Papayannis A, Cirone D. Optical coherence tomography angiography findings in deficiency optic neuropathy. *Neuroophthalmology* 2019;43:401–406.
12. Takayama K, Ito Y, Kaneko H, Kataoka K, Ra E, Terasaki H. Optical coherence tomography angiography in Leber hereditary optic neuropathy. *Acta Ophthalmol* 2017;95:e344–e345.
13. Chiong M, Cartes-Saavedra B, Norambuena-Soto I, Mondaca-Ruff D, Morales PE, García-Miguel M, et al. Mitochondrial metabolism and the control of vascular smooth muscle cell proliferation. *Front Cell Dev Biol* 2014;2:72.
14. Jia Y, Wei E, Wang X, Zhang X, Morrison JC, Parikh M, et al. Optical coherence tomography angiography of optic disc perfusion in glaucoma. *Ophthalmology* 2014;121:1322–1332.
15. Liesivuori J, Savolainen H. Methanol and formic acid toxicity: biochemical mechanisms. *Pharmacol Toxicol* 1991;69:157–163.
16. Pan BX, Ross-Cisneros FN, Carelli V, Rue KS, Salomao SR, Moraes-Filho MN, et al. Mathematically modeling the involvement of axons in Leber's hereditary optic neuropathy. *Invest Ophthalmol Vis Sci* 2012;53:7608–7617.
17. Spaide RF, Klancnik JM, Cooney MJ. Retinal vascular layers imaged by fluorescein angiography and optical coherence tomography angiography. *JAMA Ophthalmol* 2015;133:45–50.

Case Report

Tubercular Osteomyelitis of the Orbit Presenting as Periorbital Cellulitis

Shruti Bhattacharya, MBBS; Usha K Raina, MD; Shantanu K Gupta, MS; Manisha Mishra, MS; Varun Saini, MS Brajesh Kumar, MBBS

Department of Ophthalmology, Guru Nanak Eye Centre, Maulana Azad Medical College, New Delhi, India

Abstract

Purpose: Osteomyelitis of the orbital bones presenting as an orbital cellulitis is a rare form of extrapulmonary tuberculosis (TB). We report a rare case of tubercular osteomyelitis of the orbital bones presenting as a periorbital cellulitis.

Case Report: A seven-year-old female child presented to our tertiary eye care center with swelling involving the right eyelids and the right cheek for two months. She had been provisionally diagnosed elsewhere as pre-septal cellulitis and had been given oral antibiotics. We clinically diagnosed her as orbital cellulitis, but her non-responsiveness to intravenous antibiotics prompted us to get a contrast enhanced computed tomography (CECT) of the orbit and paranasal sinuses, which was suggestive of tubercular etiology. However, the patient had no foci for TB elsewhere. We used a relatively new, but rapid test, called Cartridge-based Nucleic Acid Amplification Test (CBNAAT) on the pus aspirate which was positive for TB. Thereafter, the patient was started on anti-tubercular treatment to which she responded wonderfully.

Conclusion: A high index of suspicion should be kept for TB infection in cases of orbital cellulitis with unusual clinical behavior in an endemic region such as India.

Keywords: Orbital Tuberculosis; Periorbital Cellulitis; Tubercular Osteomyelitis

J Ophthalmic Vis Res 2022; 17 (1): 146–149

INTRODUCTION

Tuberculosis (TB) is a major cause of morbidity and mortality in developing nations. It is a multisystem infectious disease caused by Mycobacterium TB. TB may be pulmonary or extrapulmonary depending on whether lungs are the primary site of infection or not.

Ocular tuberculosis (OTB) is a manifestation of extrapulmonary TB. It is considered rare even in endemic areas. OTB may be primary or secondary. When the eye is the initial portal of entry of the bacteria, it is considered a primary ocular TB. In secondary ocular TB, the involvement of the eye is due to spread from hematogenous route or

Correspondence to:

Manisha Mishra, MS. Guru Nanak Eye Centre, Maulana Azad Medical College Campus, Bahadur Shah Zafar Marg, New Delhi 110002, India.
E-mail: manisha.mishra4266@gmail.com

Received 28-08-2019; Accepted 22-05-2020

Access this article online

Website: https://knepublishing.com/index.php/JOVR

DOI: 10.18502/jovr.v17i1.10181

How to cite this article: Bhattacharya S, Raina UK, Gupta SK, Mishra M, Saini V, Kumar B. Tubercular Osteomyelitis of the Orbit Presenting as Periorbital Cellulitis . J Ophthalmic Vis Res 2022;17:146–149.

from adjacent structures.[1] Ocular TB may have myriad presentations depending upon the site of infection as well as the severity. However, uveal involvement is more common because of its high blood supply.[2, 3]

Orbital TB is more commonly seen in children with a female predisposition. It is insidious in onset and is usually unilateral.[4] It may present as unilateral proptosis/draining sinus tract/orbital swelling/lid swelling/radiographic features of bony destruction.

We present a rare case of tubercular osteomyelitis of the orbital bones masquerading as periorbital cellulitis.

CASE REPORT

A seven-year-old female child presented to our tertiary eye care center with tender swelling involving the right eye and the right cheek for two months. This was not associated with decrease in vision, discharge, photophobia, or fever.

On examination, the swelling involved the right upper and lower eyelid along with the right upper cheek; it was firm in consistency, tender and warm to touch, erythematous, with negative fluctuation tests, and no pus points or discharging sinuses (as shown in Figures 1A & 1B). Visual acuity was 6/6 in both eyes. Anterior as well as posterior segment examination of the eye were unremarkable. Despite the extensive edema, extraocular movements were full and free. Direct and consensual light reflexes were normal. A note was made of the enlarged submandibular lymph nodes. These were 2 × 2 cm, non-tender, non-conglomerated, firm in consistency, not fixed to the overlying skin. The overlying skin was not red and non-tender. The child was otherwise afebrile and had no other systemic complaints.

Furthermore, the patient was being treated with oral antibiotics (no records brought) at a peripheral center for the past one month before presentation to our center, with a steady increase in the size of the swelling. History elicited from the attendants showed their noncompliance with the prescribed treatment. Thereafter, the child was admitted for a course of intravenous antibiotics, with the provisional diagnosis being orbital cellulitis. However, poor response to intravenous antibiotics even after one week prompted us to investigate further. A contrast enhanced computerized tomography of the orbit and the paranasal sinuses (PNS) was ordered which showed a peripherally enhancing collection in the anterolateral aspect of the right maxillary sinus and zygomatic arch, extending superiorly along the lateral aspect of right orbit, showing lytic erosive changes, along with periosteal thickening and bony sequestration in the zygoma (axial scan shown in Figure 3A & 3B). These radiographic features were suggestive of TB.

The child had no history of fever, night sweats, no previous history of TB, and no history of contact with TB. In addition, the swelling was not like a typical tubercular cold abscess and the lymph nodes were not matted nor fixed to the skin. But in view of high endemicity of TB in our country, it was still kept on top of our differentials.

Except for a raised erythrocyte sedimentation rate (ESR), the complete blood count and liver function tests were unremarkable. The tuberculin sensitivity test (TST) showed 20 mm after 48 hr - however this is nonspecific. Fine needle aspiration cytology (FNAC) was done from the swollen submandibular lymph nodes – it showed necrotic changes but no granuloma or acid fast bacilli (AFB). Sputum as well as gastric aspirate microscopy for AFB showed no evidence of AFB.

Antigravity aspirate of the swelling was done with a 26-gauge needle, under local anesthesia. Around 1 ml of the watery yellowish aspirate was then sent for gram stain, bacterial and fungal cultures, and a relatively new test – the Cartridge-based Nucleic Acid Amplification Test (CBNAAT), also known as the Genexpert test. CBNAAT turned out to be positive, thus confirming the diagnosis of primary tubercular osteomyelitis of the right maxilla; the bacterial and gram stain reports were negative, thus ruling out secondary superinfection. The child was put on a four-drug anti-tubercular treatment (isoniazid [10 mg/kg] rifampicin [15 mg/kg], ethambutol [20 mg/kg], and pyrazinamide [35 mg/kg]) and responded well to the treatment, by complete shrinkage of the swelling within six weeks [Figures 2A & 2B].

DISCUSSION

Tuberculosis (TB) is a major health problem in developing countries. However, even in endemic areas, orbital TB is a rare entity. Orbital TB can be diagnosed using the following criteria: (1)

clinical/radiological or histological evidence of TB from the orbital lesion associated with evidence of TB elsewhere, (2) demonstration of AFB in the orbital lesion, (3) isolation of mycobacteria in culture from biopsied tissue, and (4) demonstration of mycobacterial infection by doing a PCR on the biopsied tissue.[5]

Orbital TB has been clinically classified into five categories: classical periostitis, orbital tuberculoma with no bony destruction, orbital TB with evidence of bony destruction (not classified as classical periostitis), orbital TB as a result of spread from paranasal sinuses and dacryoadenitis. Patients with classical periostitis present with chronic ulceration or discharging sinus in the periorbital region. There may or may not be evidence of bony erosion or sclerosis radiographically. Orbital tuberculoma presents with palpable mass, proptosis, or diplopia. When radiologic evidence of bony destruction, osteolytic changes, or erosion is seen, it is classified as orbital TB with bony destruction. Maxillary sinus is the most commonly involved sinus from which TB can spread to orbit. Such patients usually present with proptosis and dystopia of the globe. Patients with tubercular dacryoadenitis present with a mass in the lacrimal region and regional lymphadenopathy.[5, 6] Osteomyelitis of tubercular origin involving the orbital bones is rare. Mandible is the most common craniofacial bone affected by TB.[7] This condition is usually secondary to a primary tubercular lesion elsewhere, such as the lungs and the abdomen. However, primary involvement of these bones have also been reported.

Our patient presented with swelling involving the right periorbital region extending up to the right cheek. She was given a course of antibiotics to which no response was seen and the patient was investigated for other etiologies including TB. Our differentials at this time were local cellulitis, neoplasia, pseudotumor, easophillic granuloma, and TB, and she was investigated for all of these diagnoses.

Incision and drainage of the swelling was not done because an incision and drainage (I&D) would lead to a persistently discharging sinus in case it was tubercular in etiology.

There was no histopathology evidence of TB but radiologically the lesion was suggestive of TB which was done a week later after no response to intravenous antibiotics. We waited for a week before imaging was done because the history of treatment given to her was very uncompliant and no intravenous antibiotics were given before the patient presented to us.

We did keep in mind other conditions causing lytic changes in the orbit such as neoplastic, inflammatory, and rare causes like eosinophilic granulomas. Our diagnosis of TB was confirmed by CBNAAT test done on the sample from the orbital lesion. Thereafter, the patient was started on anti-tubercular drugs.

We should keep a high index of suspicion for orbital TB in cases like ours especially in endemic areas such as India. The patient should be investigated for the same. However, the diagnosis is often challenging in cases of extrapulmonary TB as the number of TB bacilli is often low in these sites.[8] Although the demonstration of AFB in culture is considered the gold standard for diagnosis, it may take up to six to eight weeks, thus delaying the treatment.[9]

Molecular diagnostics such as nucleic acid amplification test play an important role in cases of extrapulmonary TB. A new breakthrough has been the CBNAAT, also known as the Genexpert test. This test not only detects Mycobacterium DNA but also reveals whether it is sensitive to rifampicin or not, thereby identifying multidrug-resistant TB cases. The main advantage of CBNAAT is the speed and accuracy with which it works. It has been shown to have comparable results with culture (which may take up to six to eight weeks). However, it has its own set of flaws such as high cost, need for a stable electricity supply, replenishment of the cartridges every 18 months, and a stable temperature ceiling.[10]

Interferon gamma release assays can also be used as an aid to diagnosis. These tests are based on the production of interferon gamma by T cells specific to antigens of tubercular bacilli. However, they are less sensitive for detection of latent TB infection.[1]

Radiological features of orbital TB include destruction of bone, most commonly the frontal and sphenoidal bones. There may or may not be associated bony sclerosis, inflammation, abscess formation which may extend to infratemporal fossa. Lacrimal gland involvement may also be seen. Involvement of lateral wall is usually suggestive of hematogenous route of infection while involvement

of medial wall is indicative of spread from adjoining paranasal sinuses. There may be associated pre-septal thickening.[11]

Treatment of tubercular osteomyelitis is mainly done using anti-tubercular drugs. Surgery is indicated in cases with extensive destruction, presence of secondary infection, and intracranial involvement. Our patient was managed medically by anti-tubercular treatment.

To conclude, although orbital TB is rare, it should still be kept in mind while seeing patients with orbital lesions in an endemic country, and new tests such as CBNAAT should be used more frequently because of increased sensitivity and rapid diagnosis.

Financial Support and Sponsorship

Nil.

Conflicts of Interest

There are no conflicts of interest.

REFERENCES

1. Shakrachi FI. Ocular tuberculosis: current perspective. *Clin Ophthalmol* 2015;9:2223–2227.
2. Helm CJ, Holland GN. Ocular tuberculosis. *Surv Ophthalmol* 1993;38:229–256.
3. Varma D, Anand S, Reddy AR, Das A, Watson JP, Currie DC, et al. Tuberculosis: an under-diagnosed aetiological agent in uveitis with an effective treatment. *Eye* 2006;20:1068–1073.
4. Sen DK. Tuberculosis of the orbit and lacrimal gland: a clinical study of 14 cases. *J Pediatr Ophthalmol Strabismus* 1980;17:232–238.
5. Mittala R, Sharma S, Rath S, Barik MR, Tripathy D. Orbital tuberculosis: clinicopathological correlation and diagnosis using PCR in formalin-fixed tissues. *Orbit* 2017;36:264–272.
6. Madge SN, Prabhakaran VC, Shome D, Kim U, Honavar S, Selva D. Orbital tuberculosis: a review of the literature. *Orbit* 2008;27:267–277.
7. Sethi A, Sethi D, Agarwal AK, Nigam S, Gupta A. Tubercular and chronic pyogenic osteomyelitis of cranio-facial bones: a retrospective analysis. *J Laryngol Otol* 2008;122:799–804.
8. Lee JY. Diagnosis and treatment of extra pulmonary tuberculosis. *Tuberc Respir Dis* 2015;78:47–55.
9. Singh KG, Tandon S, Nagdeote ST, Sharma K, Kumar A. Role of CB-NAAT in diagnosing mycobacterial tuberculosis and rifampicin resistance in tubercular peripheral lymphadenopathy. *Int J Med Res Rev* 2017;5:242–246.
10. Sahana KS, Prabhu AS, Saldanha PRM. Usage of Cartridge Based Nucleic Acid Amplification Test (CBNAAT/GeneXpert) test as diagnostic modality for pediatric tuberculosis; case series from Mangalore, South India. *J Clin Tuberc Other Mycobact Dis* 2017;11:7–9.
11. Khalil M, Lindley S, Matouk E. Tuberculosis of the orbit. *Ophthalmology* 1985;92:1624–1627.

Photo Essay

Iatrogenic PVD Following Dilated Fundus Examination: A New Diagnosis or Fluke?

Patrick W Commiskey[1], MD; Gagan Kalra[2], MBBS; Jay Chhablani[1], MD

[1]*University of Pittsburgh Medical Center, Pittsburgh, PA, USA*
[2]*Government Medical College and Hospital, Chandigarh, India*

ORCID:
Patrick W Commiskey: https://orcid.org/0000-0002-3367-3047
Jay Chhablani: https://orcid.org/0000-0003-1772-3558

J Ophthalmic Vis Res 2022; 17 (1): 150–151

PRESENTATION

A 55-year-old woman with high myopia (spherical equivalent –8.25 right eye [OD], –8.50 left eye [OS]) and known history of Sjogren syndrome presented for routine asymptomatic hydroxychloroquine screening. No other relevant past ocular, medical, or family history was noted. Visual acuity was found to be 20/20 in both eyes (OU). Dilated fundus examination (DFE) without indentation was performed using tropicamide and phenylephrine, and ancillary testing was performed. No signs of hydroxychloroquine toxicity, Weiss ring, retinal tears, or peripheral retinal pathology were noted OU. Incidentally, the screening spectral domain optical coherence tomography (SD-OCT) revealed tenuous vitreous attachment to the optic disc OS [Figure 1A].

Two hours after the screening outpatient examination, the patient experienced a new floater OS for which she subsequently presented to the ophthalmology emergency. The on-call ophthalmologist noted a Weiss ring OS without retinal tears or detachments OU. A subsequent SD-OCT scan in the left eye demonstrated a complete posterior vitreous detachment (PVD) [Figure 1B]. The patient was reassured, counselled about the warning symptoms of retinal detachment, and scheduled for a repeat DFE in one week.

DISCUSSION

To the best of our knowledge, this is the first report of completion of an impending PVD following cycloplegic DFE. Accommodation-induced ciliary body contraction, anterior displacement of the lens–iris diaphragm, and axial elongation of the vitreous cavity may be more pronounced in myopic patients.[1] There is a known anatomical relationship between ciliary body contraction and anterior movement of anterior vitreous body and zonules.[2, 3] Anterior zonule movement results in adjacent anterior movement of the vitreous parallel to the sclera at the ora serrata.[4] While it is unclear if this force would translate to posterior vitreous movement, there is an interesting case report of vitreo-macular traction (VMT) following pilocarpine-induced miosis

Correspondence to:
Jay Chhablani, MD. University of Pittsburgh Medical Center, 203 Lothrop St., Pittsburgh, PA 15213, USA.
E-mail: Jay.chhablani@gmail.com

Received 11-06-2020; Accepted 03-12-2021

Access this article online

Website: https://knepublishing.com/index.php/JOVR

DOI: 10.18502/jovr.v17i1.10182

How to cite this article: Commiskey PW, Kalra G, Chhablani J. Iatrogenic PVD Following Dilated Fundus Examination: A New Diagnosis or Fluke? . J Ophthalmic Vis Res 2022;17:150–151.

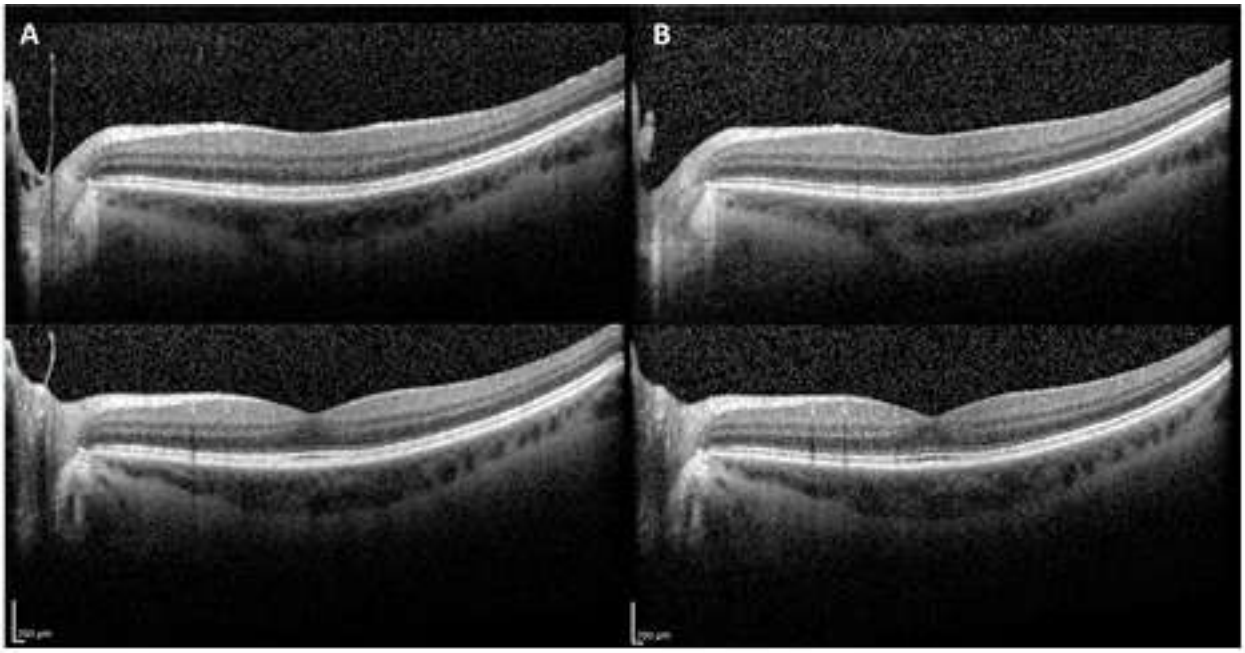

Figure 1. (A) Two optical coherence tomography (OCT) images at the initial visit for a dilated eye exam showed posterior vitreous still attached at the disc margin. (B)Two OCT images at the follow-up visit with new floaters due to posterior vitreous detachment (PVD) 2 hr following the initial exam.

after mydriasis.[5] In a computer animation-based model of accommodation, it was found that during accommodation the vitreous base is pulled forward and the posterior vitreous is pushed backward.[6] Axially, it is during the relaxation of accommodation that the posterior lens capsule moves anteriorly followed by subsequent anterior movement of posterior vitreous causing shearing at the retinal vitreous attachments.[6] Although our report illustrates temporal association of completion of impending PVD following DFE, the precise changes in the posterior hyaloid in response to DFE are still unclear.

Further work could be done to elucidate the relationship between accommodative state and PVD. Wide-field OCT may expand our understanding of peripheral vitreoretinal physiology.

Financial Support and Sponsorship

Nil.

Conflicts of Interest

There are no conflicts of interest.

REFERENCES

1. Culhae HM, Winn B. Dynamic accommodation and myopia. *Invest Ophthalmol Vis Sci* 1999;40:1968–1974.
2. Araki M, Tokoro T, Matsuo C. Movement of the ciliary body associated to accommodation. *Acta Ophthalmol Jpn* 1964;68:1852–1857.
3. Ljubimova F, Eriksson A. Numerical study of the effect of vitreous support on eye accommodation. *Acta Bioeng Biomech* 2005;7:2.
4. Croft MA, Nork TM, McDonald JP, Katz A, Lütjen-Drecoll E, Kaufman PL. Accommodative movements of the vitreous membrane, choroid, and sclera in young and presbyopic human and nonhuman primate eyes. *Invest Ophthalmol Vis Sci* 2013;54:5049–5058.
5. Walker JF, Alvarez MM. Vitreofoveal traction associated with the use of pilocarpine to reverse mydriasis. *Eye* 2007;21:1430–1431.
6. Goldberg DB. Computer-animated model of accommodation and presbyopia. *J Cataract Refract Surg* 2015;41:437–445.

Photo Essay

Pigmentary Retinopathy and Chronic Subretinal Fluid Associated with Pseudoxanthoma Elasticum and Angioid Streaks

Matthew R. Starr, MD; Sophie J. Bakri, MD

Mayo Clinic Department of Ophthalmology, Rochester, MN, USA

J Ophthalmic Vis Res 2022; 17 (1): 152–155

PRESENTATION

We present the ophthalmic findings of a 57-year-old female with pseudoxanthoma elasticum who was initially diagnosed in her 20s after a biopsy of abnormal neck lesions. She began to develop visual problems decades later, but currently has no other related medical problems, including any evidence of coronary artery disease. Our patient complained of bilateral metamorphopsia but with preserved visual acuity of 20/25 in both eyes. In addition to the angioid streaks, the patient also had evidence of pigmentary changes at the posterior pole [Figures 1A–1B]. Optical coherence tomography imaging [Figures 1C–1F] revealed the presence of bilateral subretinal fluid, shaggy photoreceptors, and intraretinal hyperreflective material concentrated within the outer retina that was stable for five years [Figures 1 E & 1F].

DISCUSSION

Angioid streaks are breaks within a weakened Bruch's membrane. They are deep to the neurosensory retina and typically bilateral, irregular, and emanate from the optic disc. Causes include Ehler–Danlos syndrome, Paget's disease, sickle cell, and other hemoglobinopathies, idiopathic, and pseudoxanthoma elasticum.[1] Vision is typically not affected by angioid streaks unless patients develop choroidal neovascularization with resultant macular edema and retinal hemorrhages.[2] Following our patient for 10 years (5 years with spectral domain OCT), she has never had any evidence of a choroidal neovascular complex on fluorescein angiography and thus it was concluded that the subretinal fluid was the result of malfunctioning retinal pigment epithelium due to the pigmentary changes at the posterior pole, a rare finding first described by Zweifel and colleagues in 2011, who concluded the fluid was due to a similar pathophysiology as pattern dystrophy.[3] Clinicians should be aware of the ophthalmic manifestations of pseudoxanthoma elasticum which include angioid streaks which can lead to choroidal neovascularization and severe vision loss but also pigmentary changes at the posterior pole that can lead to chronic subretinal fluid and a milder effect on visual acuity.

Correspondence to:

Sophie J. Bakri, MD. Mayo Clinic, Department of Ophthalmology, 200 First St, Southwest, Rochester 55905, MN, USA.
E-mail: bakri.sophie@mayo.edu

Received 23-07-2019; Accepted 02-04-2021

Access this article online

Website: https://knepublishing.com/index.php/JOVR

DOI: 10.18502/jovr.v17i1.10183

How to cite this article: Starr and Bakri. Pigmentary Retinopathy and Chronic Subretinal Fluid Associated with Pseudoxanthoma Elasticum and Angioid Streaks . J Ophthalmic Vis Res 2022;17:152–155.

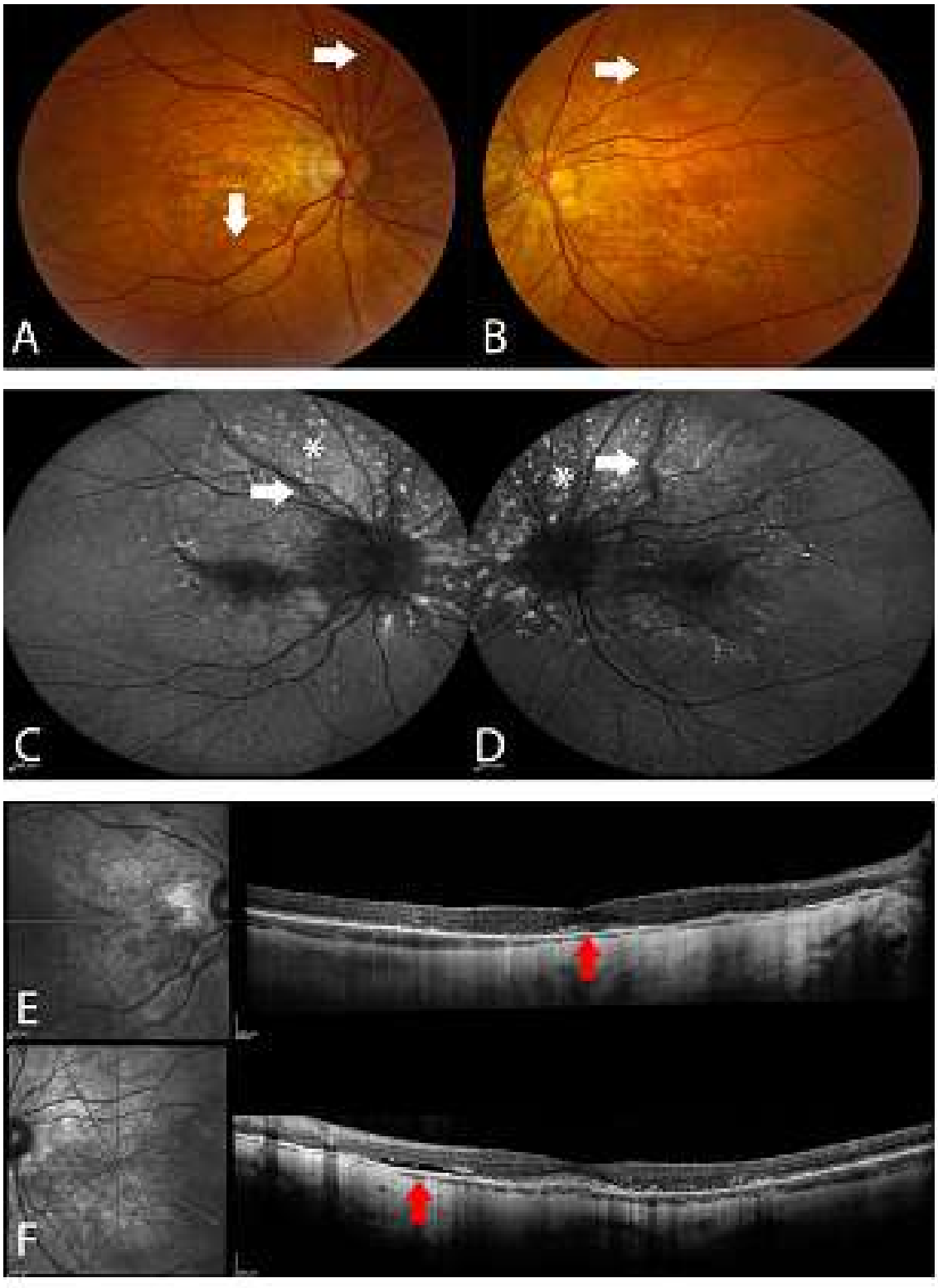

Figure 1. Fundus images (A) with bilateral hyperpigmented lines emanating from the discs, consistent with angioid streaks (white arrows). On FAF (B), the angioid streaks are easily appreciated (white arrows). Also seen are punctate areas of hyper- and hypo-FAF surrounding the disc and within the fovea (asterisks). The hyper-FAF lesions are felt to be accumulations of photoreceptor lipofuscin while the hypo-FAF lesions are thought to be related to subretinal drusenoid deposits. On OCT (C-F), there is evidence of bilateral subretinal fluid (red arrows) consistent with chronic RPE damage that are stable over five years (C & D images taken five years before E & F images).

Financial Support and Sponsorship

Nil.

Conflicts of Interest

There are no conflicts of interest.

REFERENCES

1. Clarkson JG, Altman RD. Angioid streaks. *Surv Ophthalmol* 1982;26:235–246.
2. Nakagawa S, Yamashiro K, Tsujikawa A, Otani A, Tamura H, Ooto S, et al. The time course changes of choroidal neovascularization in angioid streaks. *Retina* 2013;33:825–833.
3. Zweifel SA, Imamura Y, Freund KB, Spaide RF. Multimodal fundus imaging of pseudoxanthoma elasticum. *Retina* 2011;31:482–491.

Letter

Toxic Intraocular Syndrome

Alfredo Amigó, MD, PhD; Paula Martinez-Sorribes MS

Instituto Oftalmológico Amigó, Santa Cruz de Tenerife, Spain

J Ophthalmic Vis Res 2022; 17 (1): 155–156

Over the last three decades, several noninfectious postoperative inflammatory syndromes have been described: toxic anterior segment syndrome (TASS),[1] fibrin syndrome, sterile endophthalmitis, and toxic posterior segment syndrome (TPSS).[2, 3] All have a common toxic origin but none describe all the clinical forms in which toxicity can occur and there are cases of toxicity that do not fit into any of these syndromes. This descriptive limitation can lead to confusion and delay a diagnosis that is essential in the prevention of new cases of ocular toxicity.

The toxic intraocular syndrome (TIOS) that we describe encompasses all forms of toxicity described, referring to any postoperative intraocular inflammation, due to a noninfectious substance, which can occur after any type of intraocular surgery, resulting in toxic damage to any segment of the eye.

Postoperative intraocular toxicity is an underdiagnosed and underreported entity, with a reported frequency ranging from 0.2%[4] to 2.0%,[6] higher than that of infectious endophthalmitis.

The most frequent clinical manifestation of TIOS consists of an early and painless postoperative decrease in vision. The operated segment is usually the most affected, however, there are mixed forms with involvement of both segments,[6, 7] as well as paradoxical forms with inflammatory involvement of the segment opposite to the intervened segment.[8–10] When the anterior segment (AS) is affected, the predominant sign is limbus-to-limbus corneal edema to a variable degree, which may be accompanied by iritis, fibrin bands, hypopyon, and/or pupillary paresis. TASS is a form of TIOS in which the signs and surgery are limited to the AS. When the posterior segment (PS) is involved, the signs are more polymorphic, the vitreous may be clear or with the signs of vitritis, the retina may be intact or be associated with hemorrhages, vasculitis, pigment epithelium lesions, and macular edema. Occasionally, early papillary pallor with optic atrophy may appear. TPSS is a form of TIOS in which after PS surgery the findings are limited to this segment.

Every substance involved in the surgical process has been reported as a cause of operative toxicity. Those related to the cleaning of microcannulated instruments, enzymatic soaps, endotoxins, intraocular dissolutions, denatured viscoelastic, perfluorocarbons, silicone, are among many others.

The most important differential diagnosis is infectious endophthalmitis from which TIOS tends to be differentiated by presenting as a cold and early postoperative inflammation, with decreased vision and no other symptoms. The absence of initial pain, hyperemia, lid edema, or swelling may help to differentiate TIOS from infectious endophthalmitis. Cultures, if taken, will always be negative. The prognosis of TIOS will depend on the type of toxin, its concentration, and time of exposure, ranging from complete spontaneous resolution to irreversible loss of vision or loss of the eyeball.

There is no specific treatment for TIOS with prevention being the best current treatment. Suspecting toxicity, as a possible origin of any postoperative inflammation, is essential in the prevention of new cases given the frequent presentation of TIOS in the form of an outbreak in the following surgical sessions.

Financial Support and Sponsorship

Nil.

Conflicts of Interest

There are no conflicts of interest.

REFERENCES

1. Monson MC, Mamalis N, Olson RJ. Toxic anterior segment inflammation following cataract surgery. *J Cataract Refract Surg* 1992;18:184–189.
2. Charles S. Toxic posterior segment syndrome due to reuse of cannulated tools. Similarities to TASS should be considered. *Retina Today* 2009;July/August:26–27.
3. American Society of Cataract and Refractive Surgery. TPSS registry [Internet]. Fairfax, VA: American Society of Cataract and Refractive Surgery. Available from: https://ascrs.org/tpss-registry
4. Park CY, Lee JK, Chuck RS. Toxic anterior segment syndrome-an updated review. *BMC Ophthalmol* 2018;18:276–284.
5. Hernandez-Bogantes E, Navas A, Naranjo A, Amescua G, Graue-Hernandez E, Flynn Jr H, et al. Toxic anterior segment syndrome: a review. *Surv Ophthalmol* 2019;64:463–476.
6. Nelson M, Tennant MTS, Sivalingam A, Regillo C, Belmont J, Martidis A. Infectious and presumed noninfectious endophthalmitis after intravitreal triamcinolone acetonide injection. *Retina* 2003;23:686–691.
7. Ness T, Feltgen N, Agostini H, Böhringer D, Lubrich B. Toxic vitritis outbreak after intravitreal injection. *Retina* 2010;30:332–338.
8. Andonegui J, Jimenez-Lasanta L, Aliseda D, Lameiro F. Outbreak of toxic anterior segment syndrome after vitreous surgery. *Arch Soc Esp Oftalmol* 2009;84:403–405.
9. Moisseiev E, Barak A. Toxic anterior segment syndrome outbreak after vitrectomy and silicone oil injection. *Eur J Ophthalmol* 2012;22:803–807.
10. Ugurbas SC, Akova YA. Toxic anterior segment syndrome presenting as isolated cystoid macular edema after removal of entrapped ophthalmic ointment. *Cutan Ocul Toxicol* 2010;29:221–223.

Correspondence to:

Alfredo Amigó, PhD. Instituto Oftalmológico Amigó, C/ Bravo Murillo 16, Santa Cruz de Tenerife 38003, Islas Canarias, Spain.
Email: amigo@ioamigo.com

Received 15-04-2020; Accepted 22-02-2021

Access this article online

Website: https://knepublishing.com/index.php/JOVR

DOI: 10.18502/jovr.v17i1.10184

How to cite this article: Amigó A, Martinez-Sorribes P. Toxic Intraocular Syndrome. J Ophthalmic Vis Res 2022;17:155–156.

Erratum

Erratum: Side Effects of Brolucizumab

J Ophthalmic Vis Res 2022; 17 (1): 157–157

In the article titled "Side Effects of Brolucizumab," published on pages 670–675, Issue 4, Volume 16 of *Journal of Ophthalmic and Vision Research*,[1] the name of the second author is written incorrectly as "Saeed Mohammadi" instead of "S. Saeed Mohammadi."

REFERENCES

1. Motevasseli T, Mohammadi S, Abdi F, Freeman WR. Side effects of brolucizumab. *J Ophthalmic Vis Res* 2021;16:670–675.